Universidad de Málaga

Escuela Técnica Superior de Ingeniería de Telecomunicación
Programa de Doctorado en Ingeniería de Telecomunicación

TESIS DOCTORAL

Context-aware Self-Optimization
in Small-Cell Networks

Autor:

ALEJANDRO AGUILAR GARCÍA

Directora:

RAQUEL BARCO MORENO

Julio 2016

UNIVERSIDAD
DE MÁLAGA

AUTOR: Alejandro Aguilar García

http://orcid.org/0000-0002-2270-2260

A mi familia.

Acknowledgements

UNIVERSIDAD DE MÁLAGA

Index

Abstract

Most mobile communications take place at indoor environments, especially in commercial and corporate scenarios. These places normally present coverage and capacity issues due to the poor signal quality, which degrade the end-user Quality of Experience (QoE). In these cases, mobile operators are offering small cells to overcome the indoor issues, being femtocells the main deployed base stations.

Femtocell networks provide significant benefits to mobile operators and their clients. However, the massive integration and the particularities of femtocells, make the maintenance of these infrastructures a challenge for engineers. In this sense, Self-Organizing Networks (SON) techniques play an important role. These techniques are a key feature to intelligently automate network operation, administration and management procedures.

SON mechanisms are based on the analysis of the mobile network alarms, counters and indicators. In parallel, electronics, sensors and software applications evolve rapidly and are everywhere. Thanks to this, valuable context information can be gathered, which properly managed can improve SON techniques performance. Within possible context data, one of the most active topics is the indoor positioning due to the immediate interest on indoor location-based services (LBS).

At indoor commercial and corporate environments, user densities and traffic vary in spatial and temporal domain. These situations lead to degrade cellular network performance, being temporary traffic fluctuations and focused congestions one of the most common issues. Load balancing techniques, which have been identified as a use case in self-optimization paradigm for Long Term Evolution (LTE), can alleviate these congestion problems. This use case has been widely studied in macrocellular networks and outdoor scenarios. However, the particularities of femtocells, the characteristics of indoor scenarios and the influence of users' mobility pattern justify the development of new solutions.

The goal of this PhD thesis is to design and develop novel and automatic solutions for temporary traffic fluctuations and focused network congestion issues in commercial and corporate femtocell environments. For that purpose, the implementation of an efficient management architecture to integrate context data into the mobile network and SON mechanisms is required. Afterwards, an accurate indoor positioning system is developed, as a possible inexpensive solution for context-aware SON. Finally, advanced self-optimization methods to shift users from overloaded cells to other cells with spare resources are designed. These methods tune femtocell configuration parameters based on network information, such as ratio of active users, and context information, such as users' position. All these methods are evaluated in both a dynamic LTE system-level simulator and in a field-trial.

Resumen

La inminente evolución de la red de telefonía móvil se ha visto condicionada a la gran expansión de teléfonos inteligentes y otros dispositivos electrónicos conectados a la misma. Como consecuencia, nuevas tecnologías (LTE – *Long Term Evolution*) son desplegadas sobre las actuales redes móviles, y una gran diversidad de estaciones base (desde macroceldas hasta femtoceldas) se están integrando. Esta nueva situación genera redes móviles heterogéneas (HCN – *Heterogeneous Cellular Networks*) que son muy complejas y difíciles de gestionar por los operadores. Para facilitar esta gestión, es necesario el desarrollo de nuevas técnicas inteligentes de auto-gestión y auto-mantenimiento (SON – *Self-Organizing Networks*) que ayuden a los operador a afrontar la gestión de la red móvil de forma automática y menos costosa. En este sentido, diversos organismos se han encargado de definir una serie de casos de uso de SON para afrontar estos retos.

En la actualidad, el tráfico de la red móvil se concentra básicamente en escenarios de interior (casas, oficinas, centros comerciales), donde es habitual la ausencia de cobertura o una baja calidad de servicio (QoE – *Quality of Experience*). Para solventar estos problemas, el auge de las estaciones de baja potencia y corto alcance es la solución para los operadores. A estos dispositivos se les conoce con el nombre de femtoceldas y ofrecen una serie de particularidades frente a las estaciones base convencionales. Entre sus características, cabe destacar la facilidad y simplicidad para su integración en la red móvil, únicamente es necesario su conexión a Internet (plug and play) para su funcionamiento. Además, debido a la baja complejidad del hardware, presentan una limitación en el número de usuarios a procesar simultáneamente. Esta restricción está entre 1 y 64 usuarios. El despliegue de femtoceldas permite aumentar la cobertura en entornos de interior, mejorar la calidad de la señal, además de aumentar la vida de la batería de los terminales debido a la proximidad entre el terminal y la femtocelda.

La concentración de usuarios en este tipo de entornos es muy dinámica, creando agrupaciones de usuarios en diversos puntos a lo largo del día (reunión en una oficina, evento en un centro comercial, etc.). Ante estas situaciones, el tráfico de la red sufre variaciones temporales y espaciales, lo cual puede ocasionar congestiones en dichas

zonas. Por ello, los operadores se ven obligados a diseñar algoritmos de balance de carga que sean capaces de gestionar y evitar estos problemas, más allá de utilizar técnicas ineficientes como sobredimensionar la red.

Por otro lado, los mecanismos SON hacen uso de parámetros e indicadores proporcionados por la red para, en función de dichos valores, aplicar una nueva configuración de parámetros que mejore el servicio final. Sin embargo, existe información muy valiosa externa a la red del operador y que pueden permitir la mejora de estos mecanismos. La información de contexto o *context-awareness*, es un concepto emergente que cada vez tiene más influencia en las diferentes disciplinas debido a la gran expansión de dispositivos electrónicos en todo el mundo y su permanente conectividad a Internet. Los datos obtenidos por las diversas fuentes proporcionan información de contexto, es decir, parámetros sobre el estado actual de personas, lugares, objetos o dispositivos en un determinado entorno que, procesados de la manera adecuada pueden ofrecer grandes ventajas a los mecanismos SON.

Finalmente, para la integración de todos estos conceptos, se precisa del diseño de una arquitectura de red que sea capaz de gestionar y obtener toda la información necesaria desde las distintas fuentes de contexto y proporcionársela a los mecanismos SON. Esto permite una adaptación de los parámetros de configuración en los elementos de red en entornos de interior más rápida y eficiente. De este modo, se obtiene una red robusta y dinámica frente a cambios bruscos manteniendo unos valores soportados por las políticas del operador y ofreciendo al usuario final una buena calidad de servicio.

Acronyms

3GPP	3rd Generation Partnership Project
LTE	Long Term Evolution
ABP	Area Based Probability
AC	Admission Control
ACM	Adaptive Modulation and Coding
ACU	ACtuator Unit
ADSL	Asymmetrical Digital Subscriber Line
ANDSF	Access Network Discovery and Selection Function
AoA	Angle of Arrival
API	Application Program Interface
ASCII	American Standard Code for Information Interchange
BN	Bayesian Networks
CA	Cell Activity
CAM	Context-aware Module
CAPEX	Capital Expenditures
CBR	Call Blocking Ratio
CDCU	Context Data Collector Unit
CDF	Cumulative Distribution Function
CERP	Cooperative Eigen-Radio Positioning
CQI	Channel Quality Indicator
CR	Cell Reselection
CS	Context service
CSG	Closed Subscriber Group
CSR	Context Service Registering
CST	Cell Status
DCCP	Datagram Congestion Control Protocol
DMRF	Direct Multi-Radio Fusion
DM	Domain Management
DoA	Direction-of-Arrival

DR	Direct Retry
E-UTRAN	Evolved UMTS Terrestrial Radio Access Network
EIA	Extended Indoor A
eNB	eNodeB
EM	Element Manager
EPC	Evolved Packet Core
EPS	Evolved Packet System
FDD	Frequency-Division Duplex
FLC	Fuzzy Logic Controller
FM	Figure of Merit
GPS	Global Positioning System
GSM	Global System for Mobile Communications
HCN	Heterogeneous Cellular Networks
HeNB	Home eNB
HetNets	Heterogeneous Networks
HF	High Frequency
HPLM	Historical Path Loss Maps
HSS	Home Subscriber Server
IM	Integration Module
JCR	Journal Citation Reports
JSON	JavaScript Object Notation
KPI	Key Performance Indicator
LAN	Local Area Network
LBS	Location-based Service
LF	Low Frequency
LIPA	Local IP Access
LNMA	Local Network Manager Agent
LoS	Line of Sight
MCQI	Mean CQI
MDT	Minimization of Drive Test
MEU	MEasurement Unit
MILES	Mobile Indoor Localization Engine for SON
MIMO	Multiple Input Multiple Output
MISO	Multiple Input Single Output
MLB	Mobility Load Balancing
MME	Mobility Management Entity
MSE	Mean Square Error
NCM	Neighbor Cell Maps
NNSF	NAS Node Selection Function
NE	Network Element

UNIVERSIDAD
DE MÁLAGA

NFC	Near Field Communication
NM	Network Management
OAM	Operation, administration and management
OCAS	OAM Context-Aware System
OCU	OAM Coordination Unit
OFDM	Orthogonal Frequency Division Multiplexing
OFDMA	Orthogonal Frequency Division Multiple Access
OPEX	Operational Expenditures
OR	Outage Ratio
P-GW	Packet Data Network Gateway
PCI	Physical Cell Identity
PCRF	Policy and Charging Rules Function
PCS	Proposed Cell Status
PDF	Probability Density Function
PLS	Power Load Sharing
PLUS	Power Load and User Sharing
PRB	Physical Resource Block
PRX	Power Received
PTS	Power Traffic Sharing
PTX	Power Transmitted
PSC	Primary Synchronization Code
PUS	Power User Sharing
QAM	Quadrature Amplitude Modulation
QoE	Quality of Experience
QoS	Quality of Service
QPSK	Quadrature Phase Shift Keying
S-GW	Serving Gateway
SAU	SON Algorithmic Unit
SIPTO	Selected IP Traffic Offload
SPM	Simple Point Matching
SPS	Semipersistent Scheduling
SSID	Service Set IDentifier
RAN	Radio Access Network
RAT	Radio Access Technologies
RD	Reference Distance
REM	Radio Environmental Maps
RF	Radio Frequency
RFID	Radio Frequency IDentification
RRM	Radio Resource Management
RSCP	Received Signal Code Power

UNIVERSIDAD
DE MÁLAGA

RSRP	Reference Signal Received Power
RSSI	Received Signal Strength Indicator
RTD	Round Trip Delay
RxLev	Received Signal Level
SC-FDMA	Single-Carrier Frequency Division Multiple Access
SCTP	Stream Control Transmission Protocol
SIMO	Single Input Multiple Output
SINR	Signal-to-Interference-plus-Noise Ratio
SISO	Single Input Single Output
SON	Self-Organizing Networks
SPM	Simple Point Matching
TCP	Transmission Control Protocol
TDD	Time-Division Duplex
ToF	Time of Flight
UD	Users Distribution
UDP	User Datagram Protocol
UDR	User Dissatisfaction Rate
UDS	United States Dollars
UE	User Equipment
UHF	Ultra High Frequency
UMTS	Universal Mobile Telecommunications System
UR	Utility Function
UWB	Ultra Wide Band
VM	Virtual Maps
WLAN	Wireless Local Area Network
XML	EXtensible Markup Language

UNIVERSIDAD
DE MÁLAGA

Chapter 1

Introduction

This opening chapter aims to introduce the reader to the motivation and the context of this PhD thesis, the research objectives and the structure of the document.

1.1 Motivation

Mobile networks have become a standard infrastructure in human beings life for several services, e.g., voice calls, text messages, video streaming, etc. Furthermore, the requirements posed by the massive expansion of smart-devices and the demand of mobile network services and applications increase the global mobile data traffic (74% of growth in 2015 [1]). Consequently, current mobile network infrastructures are driving towards their limits. In order to overcome these limits, mobile communications have dramatically changed and rapidly evolved. Operators are deploying new mobile technologies, e.g., LTE (*Long Term Evolution*). The LTE technology has been integrated over the already existing mobile infrastructures; GSM (*Global System for Mobile Communications*), UMTS (*Universal Mobile Telecommunications System*), etc., leading to different *Radio Access Technologies* (RAT). Additionally, whilst classical base stations (macrocells) covered areas of tens of kilometers, operators trend to deploy new short-range base stations: *small cells* (e.g., microcells, picocells, femtocells, etc.). These solutions create complex *Heterogeneous Cellular Networks* (HCNs), which partially support the growing demand of clients and applications services.

Mobile communication providers and network engineers have to analyze a huge amount of data in HCNs to assess network performance and to propose the best strategy to solve performance issues. The analysis of these large amounts of information is not a simple task and requires long time and vast resources. That translates into increased capital (CAPEX) and operational expenditures (OPEX) for

the operator. Therefore, the complexity in the operation, administration and management (OAM) of HCNs demands the development of new network self-management techniques. In this sense, key features to intelligently and autonomously automate network management procedures are required. *Self-Organizing Networks* (SON) [2] [3] paradigm is proposed to automatically and cleverly manage mobile cellular network procedures, helping to reduce both, CAPEX and OPEX. SON mechanisms help engineers to reduce time and effort to plan, optimize and troubleshoot cellular networks. Some early studies in this field are [4] [5] [6] [7] [8] [9].

Another challenge for operators is the high number of mobile connections originated at indoor environments, i.e., home, work, shopping malls, etc., especially in commercial and corporate scenarios. Recent market surveys [10] demonstrate that around 80% of all mobile broadband traffic is consumed by users located indoors. These places normally present coverage and capacity issues due to the poor signal quality, which degrade the end-user *Quality of Experience* (QoE). To solve or reduce the impact of these indoor issues, operators are proposing *small cells*. In particular, they are deploying low-cost radio base stations called *femtocells* [11]. These devices are small versions of standard macrocells which have special and specific characteristics (e.g., low-cost, short-range, open/close control access, etc.) compared to other base stations.

Indoor environments present hard and difficult conditions to self-manage these femtocell networks due to the unplanned deployments, cell overlapping, lack of coverage, interference, etc. This fact has stimulated research activity in the field of parameters self-tuning [12] [13] [14] [15] [16] [17]. Additionally, data traffic and local user densities present temporal and spatial concentrations. In these conditions, indoor environments might suffer from serious network problems because most traffic could be located in the same femtocell(s) during short periods. Hence, some femtocells could be overloaded while others are low-loaded. An example of these temporal and spatial variations is easily found in shopping malls, where a temporal spectacle or event could gather many people interested in taking pictures to share them in social networks for a while. A simple solution to support these situations could be to plan the network to offer the maximum expected resources all the time. Nevertheless, this solution would largely increase CAPEX. As a consequence, new SON mechanisms focused on offloading those temporal overloaded femtocells to avoid or solve these situations and to guarantee the end-user QoE are required.

In parallel, software applications and electronic devices evolve rapidly. Smart-devices such as mobile phones are able to provide terminal-centric information thanks to the large number of integrated sensors (accelerometers, barometers, GPS, etc.) and applications. Others like surveillance cameras provide an overview of a place (e.g.,

number of people in a room or restaurant). All of them are able to collect context information in real time and share it with the mobile network with low delay thanks to the high-speed communication infrastructures (optical-fiber, xDSL, etc.). In this sense, this context information from sources out of the mobile networks could provide additional valuable information to SON mechanisms beyond traditional network indicators (i.e., alarms, counters, etc.). Some early studies focused on context-aware SON algorithms are [18] [19] [20] [21].

1.2   Preliminaries

This PhD thesis has been developed within the Ingeniería de Comunicaciones research group (GIC, TIC-102), in the framework of four research lines.

Firstly, the main project supporting this PhD thesis was the MONOLOC project [22]. MONOLOC has focused on the development of an advanced platform for the management of mobile and next-generation heterogeneous networks with indoor user positioning. The project's consortium was composed by leading members of the mobile communication industry: *Alcatel-Lucent* and *Grupo Innovati*; and academia: *University of Málaga* (UMA), *Universidad Carlos III de Madrid* (UC3M) y *Universidad Politécnica de Madrid* (UPM).

The project provided an innovative indoor solution based on the combination of user positioning calculation, self-management of small cells and location-based applications. Its aim was to identify and develop tracking techniques especially for new mobile technologies and use them to the dynamic self-management of the network, being this able to auto-configure, optimize and heal itself. In addition, location-based applications were studied and deployed in live scenarios. In this context, strong and reliable network architectures were developed in order to assure the support to these specifications.

Within MONOLOC project, UMA was responsible for defining the system architecture and for devising location-based SON mechanisms.

Secondly, the GIC has an steady collaboration with a french partner: *École Supérieure d'Ingénieurs en Informatique et Génie des Télécommunications* (ESIGETEL). In this framework, a professor from ESIGETEL has done several stays at UMA and this PhD candidate has also visited ESIGETEL. The result is a joint research on indoor RFID-based positioning systems.

Thirdly, the research in this PhD thesis was also part of a project called "*Técnicas adaptativas de gestión de recurso radio en redes B3G*", funded by Junta de Andalucía

(Proyectos de Investigación de Excelencia), which is related to the development of novel self-optimization techniques, especially focused on the application of reinforcement learning techniques to *Mobility Load Balancing* and *Mobility Robustness Optimization.*

Finally, this PhD thesis has also been related to a project called "*Gestión integral avanzada de funciones SON (Self-Organizing Networks) para redes móviles futuras*", funded by Junta de Andalucía (Proyectos de Investigación de Excelencia), which aims to design advanced coordinated SON mechanisms.

1.3   Research objectives

The aim of this PhD thesis is the design and development of novel SON mechanisms for open access femtocell mobile networks in commercial and corporate indoor scenarios, focusing on the mobility load balancing (MLB) use case. This means, the implementation of algorithms to offload temporary overloaded femtocells to low-loaded femtocells due to the high concentration of users in temporal and spatial domain, avoiding slow adaptive processes. Additionally, some of these methods would be supported by context information in order to improve the network performance.
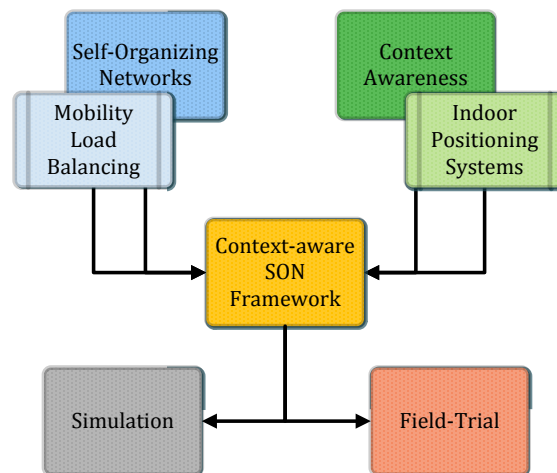
Figure 1.1: Research lines.

To accomplish these goals, three main research lines are studied: 1) a framework and architecture for commercial and corporate environments to integrate context data into the mobile network, 2) a context source focused on the provisioning of indoor positioning and 3) MLB techniques to solve temporary and focused network congestion issues in open access femtocell networks (visual description in Figure 1.1).

Initially, a framework for context-aware SON systems is proposed for commercial and corporate small cell networks. This framework is the base for the implementation of an OAM architecture which integrates and manages context data. It also supports the management of the SON mechanisms. Here, the main objectives are:

- To propose a context-aware SON framework to integrate context data into SON systems.

- To design an OAM architecture to support context-aware SON systems at commercial and corporate small cell networks.

Secondly, an RFID-based (*Radio Frequency IDentification*) indoor positioning system is designed as a context source. The position of the terminals is an example of context information that could be supplied to the SON system to improve its performance. Note that the performance of the SON system would be affected by the accuracy of the indoor positioning system. Here, the main objectives are:

1. To study RFID-based techniques for fusion methods when having multiple antennas in the receiver.

2. To assess the trade-off between the number of active tags and the number of antennas in the receiver.

3. To study techniques for integrating cellular technology information into the RFID-based indoor positioning system.

4. To carry out a radio frequency measurement campaign analyzing both RFID and cellular signals.

Finally, context-aware MLB mechanisms are designed to move terminals from overloaded cells to low-loaded cells. These methods study the singularities of femtocells, the characteristics of indoor environments and the mobility pattern of indoor terminals to achieve their goals. For that purpose, the femtocell transmission power is adjusted in order to force the handover of a terminal from its serving femtocell to a neighboring femtocell. Here, the main objectives are:

1. To design novel SON mechanisms for offloading overloaded open access femtocells at commercial and corporate indoor environments.

2. To mitigate temporal and focused overloaded situations at commercial and corporate indoor scenarios due to the high concentration of users in temporal and spatial domain.

3. To integrate context-aware data into SON algorithms and to assess the benefits of processing that information.

4. To evaluate the impact of indoor positioning system accuracy on location-based SON algorithms.

The evaluation of these systems and methods are demonstrated and assessed in a simulator and in a real testbed.

1.4   Document structure

The organization of this PhD thesis is depicted in Figure 1.2. The first chapter corresponds to this introduction. Chapter 2 provides a brief description of the required technical background to follow the rest of the chapters. This part comprises an introduction to the LTE architecture, the SON paradigm, femtocells and context information. The relationship between each topic is also covered.
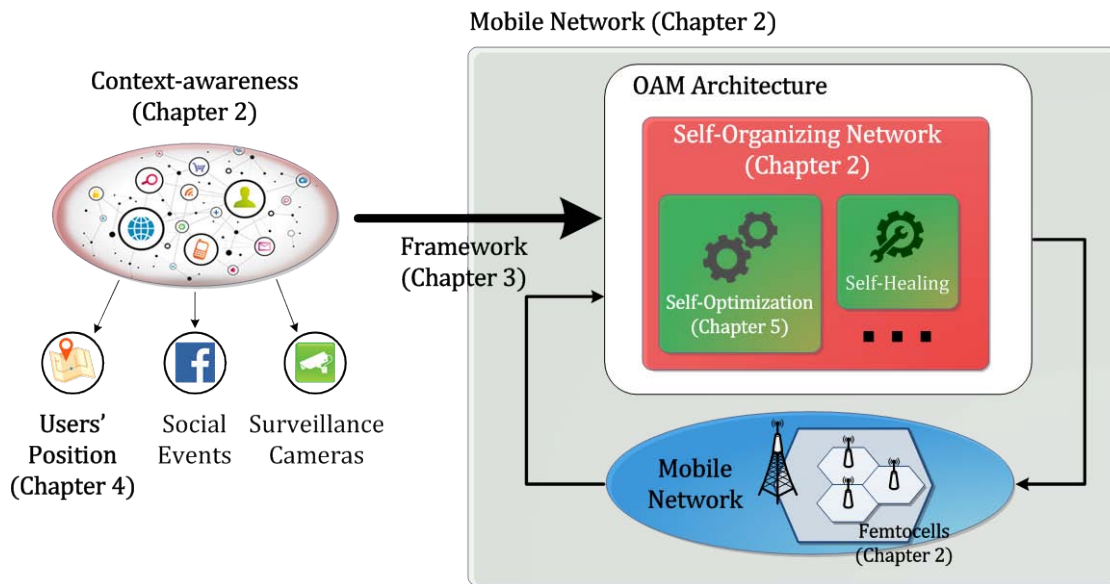
Figure 1.2: Organization of chapters.

Chapter 3 proposes to apply the context-awareness concept to SON mechanisms. Firstly, the context-awareness in SON is introduced. Then, the related work and problem description of this topic are presented. Afterwards, a framework for context-aware SON in indoor environments is proposed. This framework is supported by the designed OAM architecture and the evaluation of a specific use case. Finally, the conclusions and perspectives of this chapter are detailed.

Chapter 4 presents an indoor positioning system as a possible context source for context-aware SON systems. Firstly, this chapter introduces a review of the state-of-the-art regarding indoor positioning systems. Then, the problem description is formulated. Afterwards, the proposed indoor positioning techniques based on multi-antenna RFID system and mobile cellular signal are described. Subsequently, the accuracy of these techniques is evaluated in both simulated and real scenarios. Finally, this chapter includes the conclusions of the study. Additionally, this chapter refers to *Appendix A* and *Appendix B* where the characterization and the signal assessment of RFID and cellular technologies are carried out, respectively.

Chapter 5 develops MLB mechanisms for commercial and corporate LTE femtocells with open access but they could be also adapted to other cellular technologies (UMTS or GSM). Firstly, it introduces MLB use case and the state-of-the-art. Then, it depicts the problem description. Afterwards, MLB methods are designed focusing on femtocell characteristics and context information, in particular the position of the terminals. Subsequently, these systems are evaluated in both a dynamic LTE system-level simulator and in a field-trial. Finally, the conclusions of these methods are discussed. Additionally, this chapter refers to *Appendix C* where a description of a fuzzy logic controller (FLC) is detailed.

Chapter 6 summarizes the main conclusions of this research, proposes future lines of action and lists the publications supporting this PhD thesis.

To conclude, *Appendix D* includes a summary of this PhD thesis in Spanish.

Chapter 2

Technical background

This chapter introduces a brief description of the required technical background to follow the rest of the chapters.

The structure of this chapter is as follows: Section 2.1 describes the main characteristics of the LTE standard. Section 2.2 introduces *Self-Organizing Networks* (SON). Section 2.3 presents femtocells and the importance of SON for femtocells. Section 2.4 proposes the concept of context information, focusing on indoor positioning and its importance for SON mechanisms. Finally, Section 2.5 includes the conclusions of this chapter.

2.1   Overview of the LTE standard

The LTE standard is defined by the 3GPP (*3rd Generation Partnership Project*) and it is specified in its Release 8 document series, with minor enhancements described in Release 9. An overview of the LTE standard is briefly described in this subsection with the aim of providing the main information regarding the following chapters.

The high-level network architecture of a mobile cellular network is comprised of three main parts:

- **Terminal:** It is any device used for an end-user communication. It connects to the radio access network. In the LTE standard, this element is referred as *User Equipment* (UE).

- **Radio Access Network (RAN):** It implements a radio access technology and provides connection between the terminals and the core network. In the

LTE standard, this element is known as *Evolved UMTS Terrestrial Radio Access Network* (E-UTRAN).

- **Core Network:** It is the central part of the network, providing the main functionalities to the mobile cellular network: access control, mobility management, etc. In the LTE standard, this element is called *Evolved Packet Core* (EPC).

The LTE standard aims to provide high data-rates, low latency, low power consumption, spectral flexibility and reduced operators' expenditures [23]. The network architecture supports only packet switching (IP-based network) for any service and significantly reduces latency compared to the network architecture of 3G (third generation) [24]. The LTE network comprises the infrastructure of E-UTRAN and EPC, also known as *Evolved Packet System* (EPS).
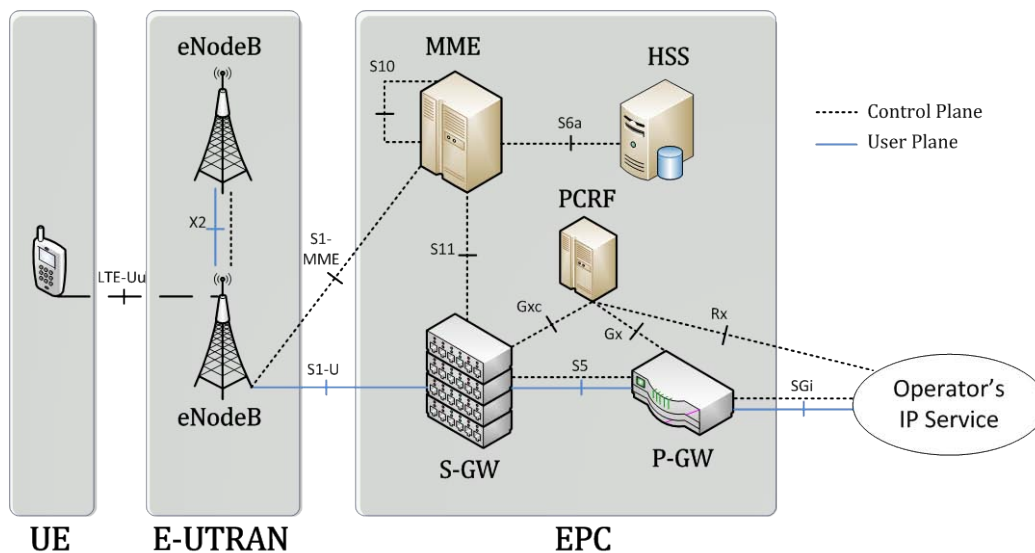
Figure 2.1: 3GPP LTE architecture [25].

Figure 2.1 illustrates the main parts of the LTE network, as well as its elements and interfaces:

- **eNodeB (eNB):** The evolved base station is the only component between UE and EPC. It sends and receives radio transmissions from UE and controls the low-level operations by signaling messages.

- **Mobility Management Entity (MME):** This element is the main entity of the *control plane.* It controls the high-level operations such as the radio access

bearers and the connection between the UE and the network. Each MME manages a group of eNBs and UEs.

- **Serving Gateway (S-GW):** This element is the main entity of the *user plane.* It forwards user data between the E-UTRAN and the *PDN Gateway* (P-GW). It is the reference component of each UE in the EPC when it moves between eNBs (inter-eNB handover and inter-RAT handover).

- **Home Subscriber Server (HSS):** This component provides user authentication information and user profiles to the MME.

- **Policy and Charging Rules Function (PCRF):** It makes policy decision and provides the QoS (Quality of Service) and charging rules to the P-GW.

- **Packet Data Network Gateway (P-GW):** This component provides the communication with external networks.
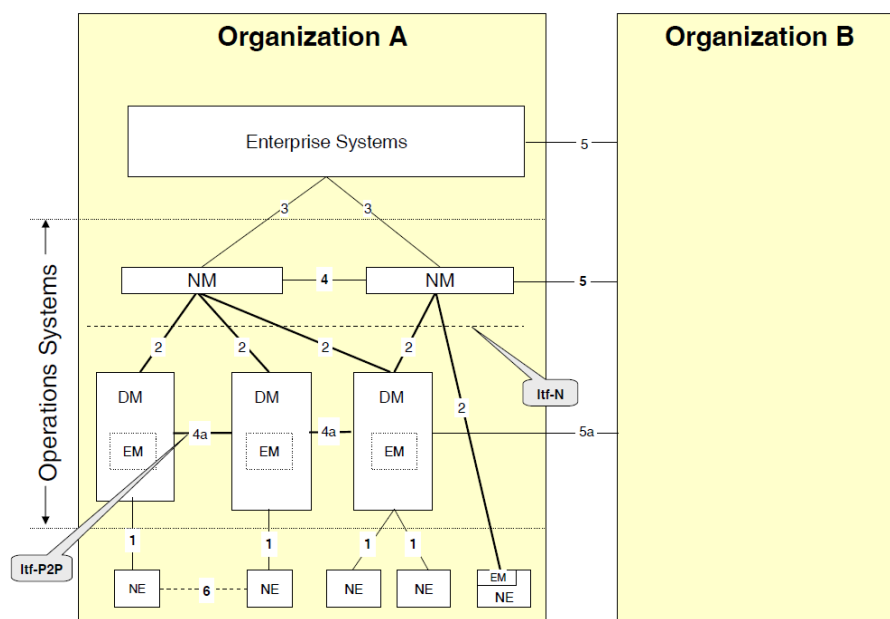
Figure 2.2: 3GPP management reference model [26].

Regarding the management operations, 3GPP defines OAM levels to implement these functionalities [26]. These levels are illustrated in Figure 2.2 and described below:

- **Network Element (NE):** At this level, each element (NE) is defined to manage one or more eNB.

- **Domain Manager (DM):** The elements (DMs) of this layer are concerned with managing NEs.

- ***Network Manager (NM):*** This level connects via open interfaces systems from other vendors.

The LTE air interface supports both *Time-Division Duplex* (TDD) and *Frequency-Division Duplex* (FDD) modes. A particular frame structure is defined for each one. Downlink and uplink transmission are based on *Orthogonal Frequency Division Multiple Access* (OFDMA) and *Single-Carrier Frequency Division Multiple Access* (SC-FDMA), respectively. These schemes use *Orthogonal Frequency Division Multiplexing* (OFDM) to encode multiple carrier frequencies. OFDM splits the available spectrum into several narrowband channels referred to as subcarriers.

Table 2.1: LTE summary.

Parameter	Description
Frequency Range	FDD bands and TDD bands
Duplexing	FDD, TDD, half-duplex FDD
Latency	5 ms round trip
Mobility	350 km/h
Channel Bandwidth	1.4, 3, 5, 10, 15 and 20 MHz
Radio Resources	6, 15, 25, 50, 75, 100 PRBs
Modulation Schemes	UL: QPSK, 16-QAM, 64-QAM (optional) DL: QPSK, 16-QAM, 64-QAM
Access Schemes	UL: SC-FDMA supports 50 Mbps (20 MHz) DL: OFDM supports 100 Mbps (20 MHz)
Multiple Antenna Scheme	2x2 MIMO 4x4 MIMO
Effective Peak Data Rates	UL: 75 Mbps (4x4 MIMO, 20 MHz) DL: 300 Mbps (4x4 MIMO, 20 MHz)

OFDMA and SC-FDMA access schemes support flexible bandwidths. Channel bandwidths are variable, from 1.4 to 20 MHz with subcarrier spacing of 15kHz. The smallest radio resource that the scheduler can assign to a user is called *Physical Resource Block* (PRB). A PRB occupies 0.5ms in the time domain and 180kHz in the frequency domain [27] and comprises 12 subcarriers at 15kHz spacing. Conventional modulation schemes: QPSK (Quadrature Phase Shift Keying), 16-QAM (Quadrature Amplitude Modulation) and 64-QAM modulate each subcarrier at low symbol rate. The combination of these subcarriers creates an OFDM symbol. This technology supports high-peak data rates up to 346Mbps in the downlink and 85.5Mbps in the uplink at 20 MHz and 4x4 MIMO. However, a percentage of these ratios are used for

overhead (e.g., synchronization signals, pilot overhead, etc.). This leads to effective data rate of about 300Mbps and 75Mbps, respectively [28].

A summary of the LTE technology is shown in Table 2.1. Further details and specifications about this technology could be easily read in the literature [29].

2.2 Self-Organizing Networks

The continuous advances in mobile technologies and personal devices (e.g., smartphones and tablets) have led to the deployment of HCNs to support the extreme traffic demand of new services. HCNs comprise different RATs and several cell sizes (e.g., macrocell, microcells, picocell, femtocells, etc.), resulting in a non-easily manageable complex mobile network infrastructure. In this sense, *Self-Organizing Networks* (SON) have been identified by the 3GPP in Release 8 [2] and the *Next Generation Mobile Networks* (NGMN) [3] as a key feature to intelligently automate network operation, administration and management procedures in future mobile networks. The use of SON techniques [8] [9] aims to reduce OPEX and CAPEX by:

1. reducing the level of human intervention in network design, configuration and operations.

2. optimizing the use of available resources in the network.

3. reducing the number of human errors.

For that purpose, several self-x functionalities have been defined by 3GPP and NGMN to self-manage the network resources:

- ***Self-configuration:*** to automate network configuration and planning of newly deployed base stations. The new base stations are able to configure itself the *Physical Cell Identity* (PCI), transmission power, transmission frequency, etc.

- ***Self-optimization:*** to automatically tune the network parameters (e.g., antenna tilt, handover parameters, etc.) of a deployed mobile cellular infrastructure for obtaining the best network configuration and performance over time. This function includes optimization of handover, capacity, coverage and interference.

- ***Self-healing:*** to automatically detect, identify, compensate and recover failures of a deployed mobile cellular infrastructure.

These SON functions could be located at different OAM levels in the 3GPP OAM architecture as Figure 2.3 shows. They could be either centralized or de-centralized.
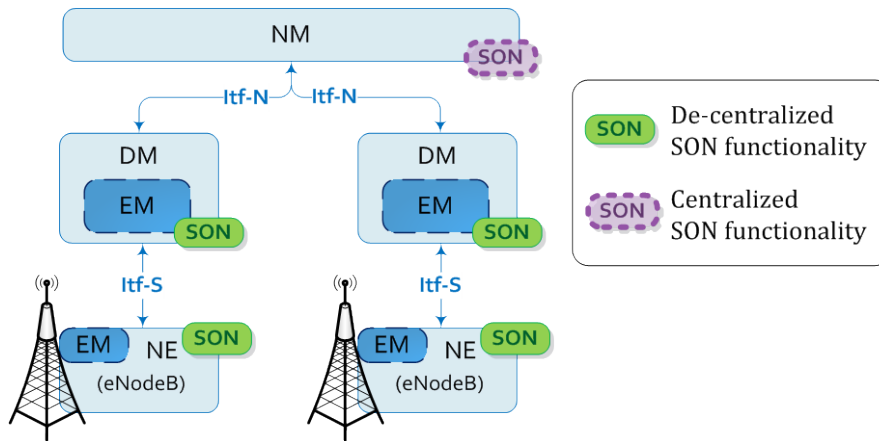
Figure 2.3: Location of SON functions in the 3GPP OAM architecture [8] [26].

Self-optimization is one of the most important functionalities in SON because it ensures the network operates to its best level of efficiency once the base stations have been deployed. Since this PhD thesis is focused on self-optimization, the following section will further describe this function.

2.2.1   Self-optimization

Self-optimization is necessary due to the changes that the environment around the base station might suffer once it is installed and well-configured. Some of these changes are related to:

-   *Changes in deployments:* Modifications in a base station could affect the others. New base stations could be integrated in the network, a base station could be optimized, etc.

-   *Changes in traffic patterns:* The concentrations of users evolve over time. Some examples could be beaches on summer season, sporting events, etc.

-   *Changes in propagation characteristics:* This could arise or have a significant effect when new buildings are erected or demolished, leaves from trees fall in autumn, etc.

The main self-optimization use cases are the following [2] [30]:

- ***Coverage and capacity optimization:*** parameters such as transmitter power levels and antenna tilts are adapted to maximize coverage and minimizing interference levels.

- ***Energy saving:*** operators aim to reduce the power consumption as well as carbon dioxide emissions. Hence, there are a number of option to accomplish this goal such as decreasing active carries for off-peak times, switching cells to sleep mode, etc.

- ***Mobility robustness optimization:*** operators are interested in robust mobility and handovers within the mobile network to avoid the disruption of the service. It would minimize the number of unnecessary handovers, dropped calls, etc.

- ***Mobility load balancing:*** congested cells should transfer calls to other cells with spare resources. Antenna tilts, handover margins and transmitter power levels are the main adapted parameters.

This PhD thesis is focused on the *Mobility Load Balancing* (MLB) use case. A graphical explanation of this functionality is depicted in Figure 2.4. Left image shows an overloaded situation. Here, left cell suffers congestion which decreases network performance and increases the number of unsatisfied users. Conversely, adjacent cells are less loaded in the network. Under this situation, as the right image illustrates, MLB forces users from its serving cell (left cell) to handover to target cells (right top cell) by changing configuration management parameters (e.g., transmitter power level of serving cell or handover margins from serving cell to target cell).
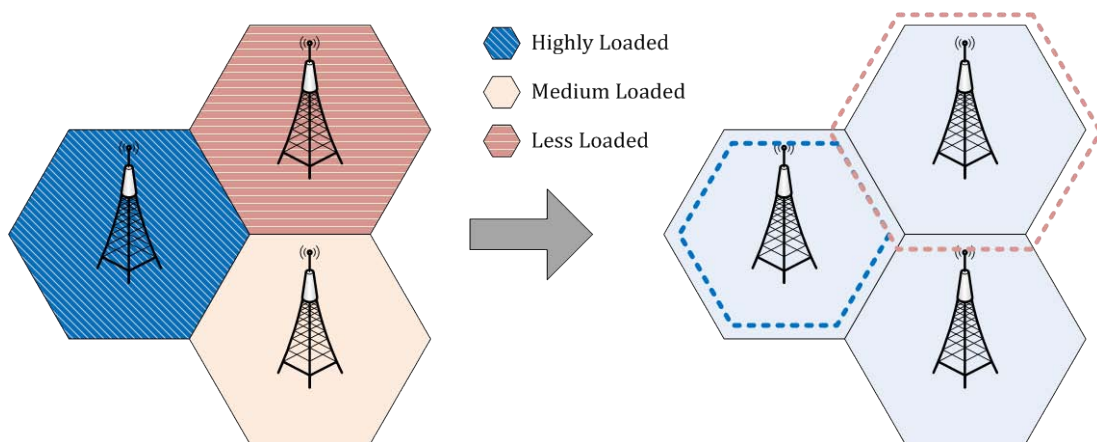
Figure 2.4: *Mobility Load Balancing* use case.

A simple solution to support these congested scenarios could be to plan the network to offer the maximum expected resources all the time but it would largely increase CAPEX. Nevertheless, by applying MLB in the network, this temporal congestion would be overcome without further investments.

2.3   Femtocells

Nowadays, most cellular traffic is generated indoors (e.g., home, work or shopping malls), where there is often a lack of coverage or insufficient QoS [10]. In these cases, network operators are offering small cells to overcome the indoor issues, being femtocells the main deployed base stations.

The deployment of femtocell networks provides significant benefits to network operators and their clients. The most common benefits result in:

- reduction of operational costs.
- potential macrocell offloading gain.
- improvement of the end-user QoE.
- terminals save battery and increase lifetime.

However, the smooth integration and maintenance of femtocells into classical macrocell networks is an important challenge for operators.

2.3.1   Characteristics

Femtocells are simple and small versions of standard macrocells, manufactured to be deployed at indoor environments. These low-cost and low-power devices cover areas of several meters, work in the licensed frequency band and are under operator management. Additionally, femtocells are connected to the operator's network by a broadband connection, i.e., through client's broadband backhaul (e.g., cable or xDSL) as Figure 2.5 shows. Thanks to this singularity, they are plug and play devices and operators offer unplanned deployments, which means, the client is free to locate the femtocell anywhere. For this reason, default femtocell transmission power is the maximum transmission power.

Another important characteristic of femtocells is the control access (see Figure 2.5). The accessibility could be close, i.e., access is restricted to subscribers. The *Closed Subscriber Group* (CSG) is in charge of registering those specific users. Home femtocells are an example of close access, as they are deployed for private usage. In an

open access scenario (e.g., public buildings), any terminal could be connected to the femtocell without any restriction, like a macrocell. Enterprise femtocells are usually open access. Hybrid access is also supported.
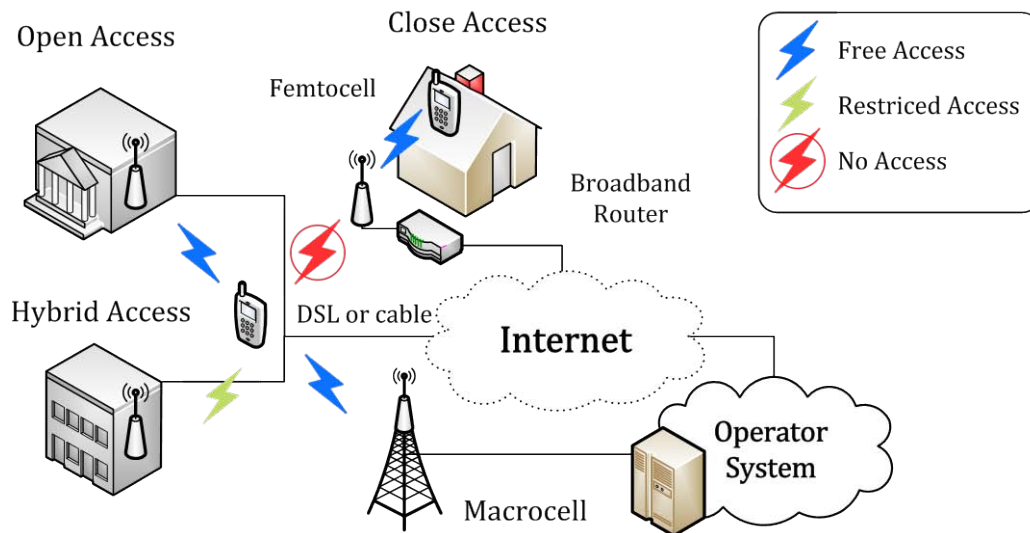
Figure 2.5: Femtocell scenario.

Since femtocells operate in residential or enterprise spaces and users may move between indoor and outdoor scenarios, a handover process is required between macrocells and femtocells to keep the service alive.

Femtocell manufacturers have mainly developed two types of femtocells. Focused on home environments, the datasheet in [31] presents a femtocell with a baseband capacity of maximum 4 simultaneous connected users (voice call or data session). Thinking in crowed indoor scenarios such as offices or shopping centers, the datasheet in [32] provides a solution up to 64 (i.e., 8, 16, 32 or 64 users) active users in the femtocell.

Based on the maximum capacity of the femtocell, the *Admission Control* (AC) algorithm is in charge of managing the access of new users. The AC algorithms are not standardized, i.e., different vendors would run different AC schemes. Then, the AC could reject those attempt connections once the maximum number of connected users is reached or drop specific connected users (e.g., per service, time connected, etc.) even if there are free radio resources. Note that this limitation is independent of the *Scheduler*, the availability of radio resources or the circuit/packet-switched channel. Additionally, it is also beyond the cellular technology (GSM, UMTS or LTE). For example, the 3G femtocell in [31] supports four devices at the same time.
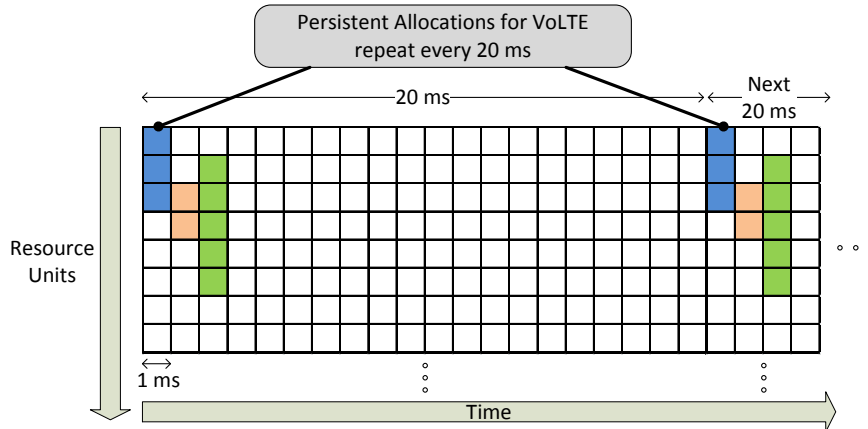
Figure 2.6: Persistent allocation for VoLTE.

Focusing on the LTE technology (IP-based technology), the resources could be scheduled and allocated in the next frame if the current frame is full (depending on their priority). However, VoLTE service is special. *Semipersistent Scheduling* (SPS) [33] would be in charge of managing and allocating VoLTE traffic. In this sense, the mechanism could assign predefined chunk of radio resources for VoLTE users with interval of 20ms (see Figure 2.6). It would decrease control channel overhead, reduce jitter and increase the QoS. Nevertheless, before scheduling a new connection, it must be accepted by the AC scheme and, as previously explained, that new user is blocked if the maximum femtocell capacity is reached (normally from 2 to 64 users). Therefore, even if there are available radio resources in the current frame or in the following one, that new user would be rejected by the AC. Note that other AC schemes could accept this user but an active user is dropped or tried to be handover to another cell. As an example, in [34] the maximum number of active users is restricted to 8 users: either VoLTE users or other data bearer per QCI (Quality Channel Indicator).

2.3.2 LTE architecture

The 3GPP defines a base station as eNB while femtocells are defined as Home eNB (HeNB). HeNB is integrated in the LTE architecture as a new NE. The functions supported by the HeNB shall be the same as those supported by an eNB (with the possible exception of NAS Node Selection Function - NNSF) and the procedures run between a HeNB and the EPC shall be the same as those between an eNB and the EPC.

The E-UTRAN architecture may deploy a Home eNB Gateway (HeNB GW) to allow the S1 interface between the HeNB and the EPC to scale to support a large

number of HeNBs. The HeNB GW serves as a concentrator for the *control plane*, specifically the S1-MME interface. The S1-U interface from the HeNB may be terminated at the HeNB GW, or a direct logical *user plane* connection between HeNB and S-GW may be used. This logical architecture is shown in Figure 2.7.
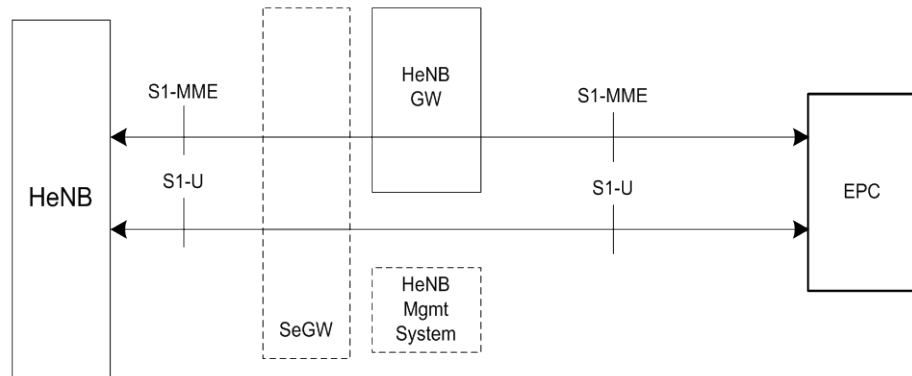
Figure 2.7: E-UTRAN HeNB logical architecture [24].

The E-UTRAN architecture with deployed HeNB and HeNB GW is depicted in Figure 2.8. The HeNB GW appears to the MME as an eNB. The HeNB GW appears to the HeNB as an MME. The S1 interface between the HeNB and the EPC is the same whether the HeNB is connected to the EPC via a HeNB GW or not. Release 9 does not support X2 connectivity of HeNBs. However, X2 connectivity of HeNBs is supported in LTE-Advance (Release 10 [24]).
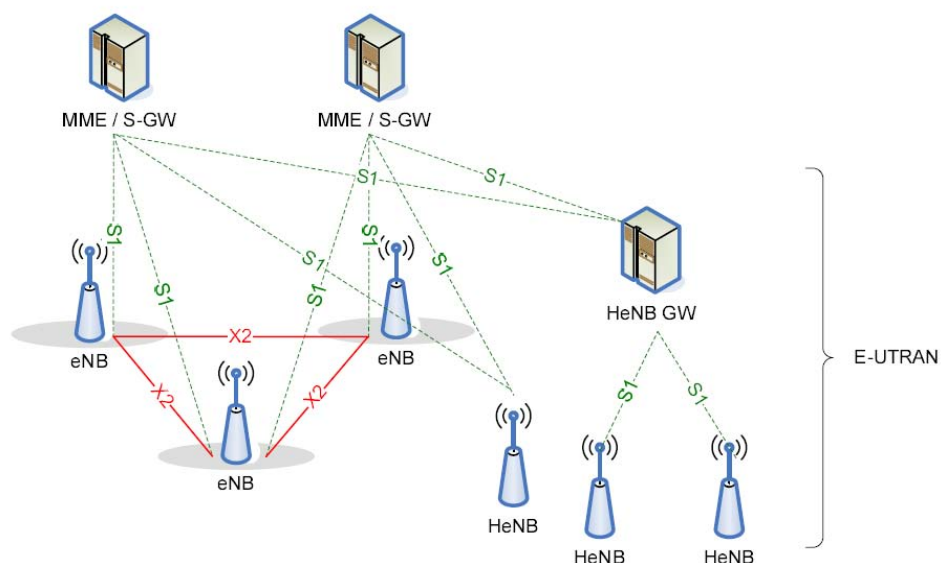
Figure 2.8: Overall E-UTRAN architecture with deployed HeNB GW [24].

2.3.3   SON for femtocells

SON techniques play an important role at commercial and corporate indoor scenarios. Despite some classical SON mechanisms could be implemented indoors, their performance could be degraded compared to their application on macrocell scenarios. The main reasons are the particularities of femtocells, the characteristics of indoor scenarios and the influence of users' mobility pattern:

1) *Particularities of femtocells:*

   a) The number of simultaneous users connected to a femtocell is very restricted in comparison to macrocell stations. In this way, femtocell equipment reduces the number of simultaneous users (from 2 to 64 users). It must be taken into account for the application of SON mechanisms.

   b) The deployment of femtocells is normally unplanned, contrary to the deployment of macrocells. As a consequence, some femtocells can be highly loaded while others are low loaded. In this sense, SON mechanisms would ensure a good cellular network performance.

   c) As low-power base stations, the coverage area of femtocells is short-range. That means, depending on the users' mobility pattern, users could easily handover several times from one femtocell to another. That increases the network signaling overhead and femtocell congestions may occur. Therefore, the time to trigger SON methods should be as fast as possible to detect and solve these situations.

   d) Femtocells are normally placed at fixed positions. However, the customer could freely (i.e., without operator's approval) and easily move a femtocell to another place as a plug and play device. By moving the femtocell, the customer might intend to solve specific issues, such as a lack of coverage or low throughput in an area, but other issues could arise with this change. In these cases, SON mechanisms are required to ensure a good network performance by automatically adjusting femtocells configuration parameters.

2) *Characteristics of indoor environments:*

   a) Indoor radio channel conditions suffer continuous changes due to multi-path reflections, wall obstacles, number of people, etc. Those situations are a challenge for SON mechanisms.

   b) Occasional events or unpredictable occurrences provoke unexpected temporal overload situations in surrounded femtocells, which could negatively affect

network performance. For example, restaurant zones would increase the traffic at launch/dinner time while sales period would create occasional hotspots in shops. In all these situations, the femtocell in charge of serving that area would be overloaded.

c) Due to the geometry of indoor environments, a tridimensional deployment of femtocells on the different stages of a buildings, airports, shopping malls, etc., is often required.

Based on this, classical SON mechanisms at indoor environments should take into account these characteristics before their implementation in femtocell networks. However, the design of new SON mechanisms for indoors would provide optimal solutions for these networks. For example, from the point of view of MLB, the number of active users at each femtocell should be analyzed in addition to the availability of radio resources to allocate new connections.

2.4 Context information

A new concept is emerging thanks to the ubiquity and quality of electronic devices with stable Internet connections: *context-awareness*. Location, activity, time and identity are the primary context types for characterizing a situation of a particular entity.

"*Context is any information that can be used to characterize the situation of an entity. An entity is a person, place or object that is considered relevant to the interaction between a user and an application, including the user and applications themselves* [35]".

Nowadays, smart-devices like smartphones integrate many *radio frequency* (RF) technologies as WiFi, Bluetooth, NFC and even UWB, in addition to the classical cellular technologies: GSM, UMTS or LTE. Furthermore, they are supported by dozens of integrated sensors like compass, barometer, gyroscope, GPS, etc. Besides, other systems like surveillance cameras are able to characterize an element or scenario. Valuable information about the people distribution, their position, the weather, etc. could be obtained through a digital image processing. Finally, the imminent development of apps (applications) in smartphones and other smart-devices achieve specific information of users such as the calendar events, the battery level of the

terminal, the age, etc. or particular information about the environment such as the temperature, etc.

2.4.1   Indoor positioning systems

One of the key challenges for the mobile market is to find killer applications for the new terminals and data plans in order to increase service providers, manufacturers and application developers' revenues. In this field, *Location-based Services* (LBS) will support new applications on several fields: health-care, advertising, emergency-response, etc. Most suitable scenarios for LBS are indoor areas (e.g., airports, hospitals, malls, etc.) given the large concentration of users in these environments. Based on this, the challenging deployment of indoor positioning techniques is a hot topic.

In this sense, smartphones could be well-located (position error below one meter) thanks to the analysis of wireless technologies like Infrared Laser, UWB, etc. The drawback is that these kinds of systems are very expensive due to their low position error and high accuracy. Nevertheless, systems based on the analysis of the *received signal strength indicator* (RSSI) of wireless technologies such as RFID or WiFi [36] or cellular technologies [37] could reduce these expenses although the location accuracy would be degraded (position error of few meters). Additionally, the synergy of those technologies and the wide variety of integrated sensors into the smartphones could enhance the performance of these positioning systems in terms of location accuracy [38].

2.4.2   Context-aware SON

SON mechanisms are based on the analysis of the mobile network alarms, counters and metrics (e.g., handover failure rate). Indoor environments present specific characteristics (e.g., high level of coverage overlapping, rapid performance changes, user distribution variability, etc.) which make these SON methods solely based on the analysis of those network indicators, prone to take a long time to get the best configuration parameters.

Context-awareness provides profitable information about the actual status of the environment such as smartphones position, mobility patterns, etc., which properly managed could help SON mechanism to speed up its convergence time, to get the optimal configuration parameters, to improve the network performance, etc.

2.5   Conclusions

LTE provides reduced latency, increased peak data rates and scalable bandwidth while backwards compatibility with legacy mobile cellular technologies. Additionally, SON paradigm provides these networks with intelligent and autonomous procedures to automatically overcome network degradations and failures. Indoor environments with femtocells deployments are one of the most challenging scenarios to be managed. Here, SON mechanisms play a key role to guarantee coverage and capacity while ensuring the end-user QoE. These SON mechanisms are only based on the analysis of the network performance indicators. However, the expansion of smart-devices, systems and applications could provide valuable additional information from external sources to the network management layers, being important and useful for SON mechanisms.

Chapter 3

Context-aware SON framework

This chapter proposes to apply the context-awareness concept to SON. Context information provides valuable additional data to enhance the performance of SON mechanisms.

The structure of this chapter is as follows: Section 3.1 introduces the context-awareness concept in SON. Section 3.2 details the related work. Section 3.3 presents the problem description. Section 3.4 describes a framework for context-aware SON at indoor environments. It is supported by the design of an OAM architecture and a particular self-optimization use case. Section 3.5 evaluates the benefits of the proposed approach. Finally, Section 3.6 includes the conclusions and perspectives of this chapter.

3.1   Introduction

Current cellular networks are HCNs, comprising several RATs, cell sizes and frequencies. In this context, macrocells and incoming small cells coexist in the same radio environment. Small cells may support the growth in mobile data traffic by offloading macrocells. However, the deployment of this kind of cells also brings a number of challenges to mobile network management. These difficulties must be addressed to maintain a consistent QoE in the cellular infrastructure, making SON concept an important part of the recent mobile network deployments.

In parallel, electronics and software applications evolve rapidly, and devices, systems, and applications are everywhere. Mobile devices offer widespread access to instantaneous information about what is happening in the world and, furthermore, information or estimations about what is going to happen in the next minutes, hours,

or days. Devices like smartphones, systems like surveillance cameras, or applications like social networks can provide these additional valuable data to SON mechanisms. Advanced SON algorithms based on this context information could be the first step for a new approach in automatic and expanded mobile network management, enhancing network performance.

The main contributions of this chapter are:

- The description of a context-aware SON framework to integrate context data from smart-devices, systems or applications into SON systems.

- The design of an OAM architecture to support context-aware SON systems at commercial and corporate small cell networks.

Finally, a SON strategy, in particular the mobility load balancing (MLB) use case, will evaluate the capabilities of the proposed framework in a simulated scenario.

3.2   Related work

SON mechanisms are widespread in cellular network deployments and advanced SON algorithms are proposed in the literature.

From the architectural perspectives, few works addressed the requirements to take into account the integration of context information into the OAM layers. The work in [39] defined a high-level particularization of the possible entities of a context-aware system. The authors in [40] introduced a high level logic framework for intelligent service adaptation to user context-awareness in next generation networks. However, the proposed architectures did not refer on how to apply context information to mobile communications, SON or indoor scenarios. Furthermore, no specific mechanisms were defined.

Regarding the context-aware SON mechanisms, few works addressed the use of context information, in particular for the indoor cases [41]. The authors in [19] proposed a framework for base stations configuration and deployment based on the network topology, state, environment and operator's inputs. The work in [21] developed a context-aware decision algorithm to improve the interworking between LTE and WiFi wireless technologies. It considered multiple context variables like terminal type, battery, velocity, etc. This efficient mechanism was integrated within the ANDSF (Access Network Discovery and Selection Function) server. Additionally, the authors in [39] presented a possible framework to support context information for public safety networks in LTE. Particularly, it sketched the elements for context-aware

radio resource management (RRM) in a very high level. Other works made use of the position of terminals as context information. In this respect, reference [20] proposed self-optimization of inter-RAT handover parameters supported by location information in macrocell scenarios. Conversely, BeFEMTO project proposed a local location manager in femtocells networks [42], but it only presented the conceptual design, without any integration with SON algorithms.

3.3   Problem description

In SON, especially in self-optimization, the periodicity to run the mechanisms is very important to quickly adapt radio network parameters to variations of the radio channel conditions in a short period. For this reason, recent OAM architectures present a distributed model (as proposed in BeFEMTO's project [42] for femtocell deployments), and tend to place SON functions in low layers (e.g., NEs). In that way, a fast analysis of the radio changes can be made and network can be configured to ensure good end-user experience and network performance. Nevertheless, depending on the inputs of these functions, they might not fulfil timing requirements expected by the operator or the network performance might be further optimized and enhanced. In this scenario, context-awareness becomes a solution to overcome these limitations.

The objective of the proposed context-aware SON framework is the integration of context information into OAM layers. For that purpose, the design of a local system with OAM functionalities is required. Focusing on the MLB use case, main topic of this PhD thesis, the proposed approach would, initially, increase the users' satisfaction (e.g., by reducing accessibility issues) at commercial or corporate scenarios when radio and environment conditions change. Secondly, it would reduce the time the SON mechanisms need to converge to the optimal solution.

To measure the first objective, a utility function based on the dissatisfaction of users (UR) has been selected [16]. The UR is interpreted as a combination of *Call Blocking Ratio* (CBR) and *Outage Ratio* (OR),

$$UR = CBR + (1 - CBR) \cdot OR, \qquad\qquad (3.1)$$

where CBR is defined as the ratio of the number of blocked calls ($N_{blocked\_calls}$) to the number of calls that attempt to access the network ($N_{attempted\_calls}$). and $N_{accepted\_calls}$ is the number of accepted calls:

$$CBR = \frac{N_{blocked\_calls}}{N_{attempted\_calls}} = \frac{N_{blocked\_calls}}{N_{blocked\_calls} + N_{accepted\_calls}}. \qquad (3.2)$$

OR is defined as the ratio of unserved connection time due to a bad *Signal to Interference-plus-Noise Ratio* (SINR) of users (OR_q) or a temporary lack of network resources (OR_s), i.e., $OR = OR_q + OR_s$. Low values of UR are desirable.

To analyze the second objective, an indicator, t_{opt}, has been defined to measure the time the SON algorithms need to reach the permanent regime (see Figure 3.9). Low values of t_{opt} are desirable.

3.4   Framework for context-aware SON

This subsection describes the characteristics of the proposed framework for context-aware SON in commercial and corporative indoor environments. It is supported by an OAM architecture and a particular self-optimization use case.

3.4.1   Framework characteristics

Input parameters for SON algorithms are usually coming from the mobile network, such as KPIs (*Key Performance Indicators*), counters, etc. However, the automatic adaptation of applications, systems and devices to users' context changes, provides useful external mobile network information, rarely included in SON mechanisms.

Location, activity, time and identity are the primary context types for characterizing a situation of a particular entity. Context data is proposed as additional inputs for SON algorithms. Thus, the information about the status of a place, people or even things and devices in the mobile network environment can help to increase system capacity while the end-user QoE and network performance is improved.

Other advantages of context information are, for example, the time span to acquire and share this information. The periodicity of monitoring network indicators for centralized OAM architectures is usually fifteen minutes, one hour or even one day, avoiding fast network adaptation. Although the development of distributed OAM architectures partially solve this time problem, external mobile network data might complement the lack of information in short periods and provide additional data.

Another benefit is related to the prediction capabilities. Network configuration could be automatically prepared to an incoming situation such as a social event (e.g.,

book signing event, etc.) that would decrease network performance due to the huge concentration of users connected to the same cell.

This wide variety of information could be obtained from several sources as Figure 3.1 shows, consolidating these data into the *Context-Aware Module* (CAM). The CAM collects and provides that context information to any network item.
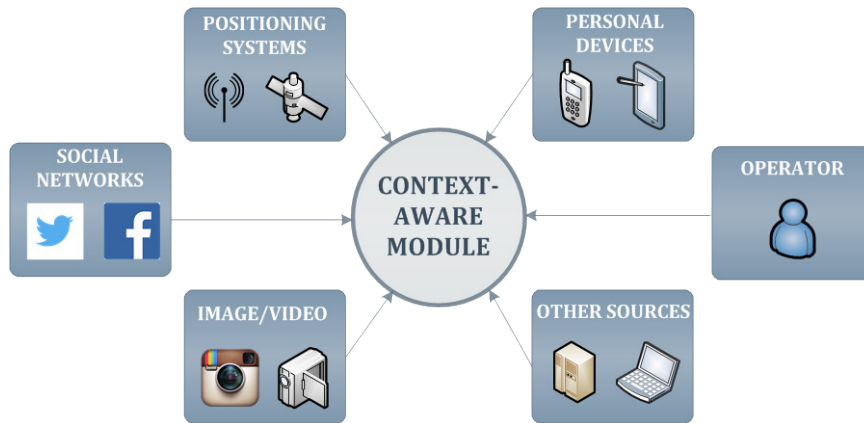
Figure 3.1: Context-aware module (CAM).

All these information sources provide valuable data about current or future environment situations. Some of them send real-time information, whereas some others provide data to the CAM with a lower frequency. Some possible information sources are the following:

- **Personal devices:** They are one of the most powerful sources in this field thanks to the heterogeneous features, such as accelerometers or compass. These sources could offer personal information about the users' habits: activities, mobility patterns, etc. This information can be used in SON algorithms, e.g., to avoid coverage holes by adapting antenna tilt or transmit power level.

- **Positioning systems:** Several novel positioning systems are being developed to locate users in indoor environments. Some SON applications based on this real-time position information could be related to energy saving, e.g., a small cell is turned off to save energy when no users are allocated close to its coverage area.

- **Social networks:** Plenty of information is publicly shared in these networks (Twitter, Facebook, etc.), providing real-time data besides a prediction of what is going to happen in a certain place at a specific moment. For example, a celebrity is seen in a shopping center and a lot of people move there to take a

picture with him/her or ask for an autograph, provoking a huge concentration of users in a small area where most of them use their smartphones to share that moment in social networks.

- *Image/Video:* Photographs or video images are collected from online photo-sharing or video-sharing as Instagram, Youtube, etc., or from surveillance cameras installed on a specific place, providing information about its context. For example, images could provide valuable green context information if SON algorithms turn off a small cell when no one is close to it, saving useless energy. These systems usually take some time to process all these data.

- *Operator:* An operator manually introduces data into the CAM, about what he or she is monitoring.

- *Other sources:* New smart and intelligent devices, such as drones, or even current context information that is not taken into account in current state-of-the-art SON algorithms, like weather, could be also very helpful in the future in this kind of systems.

Notice that several sources can provide the same type of final information, e.g., number of people in an area. This redundancy is very important in case of CAM connection loss or access restrictions to any of these sources.

As mentioned before, some of these sources provide automatic and instantaneous information to the CAM while some others need some time to collect and send it to the CAM. Depending on the time required for data collection and transfer, the context-aware SON algorithms will run at set intervals as follows:

- *1 hour:* Context data is supplied to the CAM every hour, e.g., by an operator.

- *30 minutes:* Image/video processing systems need time to get the pictures.

- *15 minutes:* Sophisticated image/video processing systems are faster.

- *5 minutes:* Personal devices could have delays in the information delivery.

- *1 minute:* More accurate and online updating technologies could reduce this time to less than a minute. For example, positioning systems, social networks, personal devices, etc.

- *Predictions:* The information is proposed to the system once an event is programmed, for example in social networks or into a personal device calendar.

The proposed framework could present some challenges in the communication with external sources:

- ***Signaling overhead:*** It depends on the communication protocols, the transmitted message and the context information. The transmitted message consists of attribute-value pairs (e.g., XML, JSON, etc.) to easily manage the information. The well-known *Transmission Control Protocol* (TCP) is in charge of transporting reliable data at reduced overhead. Also, more advanced (SCTP, DCCP, etc.) or simple (e.g., UDP) protocols could reduce even more the signaling cost.

```
<index>
    <context> user_location
    <id> 3589870105
    <time> 1413124586
    <x> 14.2547
    <y> 85.6214
<end>
```

Figure 3.2: Example of context message.

In order to provide an assessment of the cost, a preliminary message formatting is described to estimate and quantify the volume of data per message (see the example in Figure 3.2). This is a simple context message to provide the user location to the CAM. Each character is computed by 1 byte (there are 84 characters on the message). Consequently, the transmitted message is composed by this context data (84 bytes) plus the communication headers (TCP+IP=40 bytes). Therefore, for this kind of message, 124 bytes are transmitted from the external sources to the CAM. Mention that, any other message or communication protocol is also supported by the system (e.g., JSON).

- ***Delay:*** The lack or delay in the information transmitted from the external sources would degrade the system performance as SON mechanisms will not properly work. However, the high speed of communication infrastructures (e.g., xDSL), the low signaling overhead and the redundancy of context information supplied to the system from multiple sources, could overcome this limitation.

- ***Security:*** Most of the information supported to the CAM is public data, hence, no strategies or techniques of information security are mandatory. Nevertheless, the information from private sources or private data would be encrypted.

Furthermore, it is crucial to confirm the veracity of the information against possible issues (e.g., malicious modification, delayed data, etc.), while the system shall be able to reject false or incomplete samples. In case the CAM is not able to do it, the context-aware SON methods might degrade the network performance. In that case, the

context-aware SON algorithms will be disabled to come back to conventional SON mechanisms (algorithms only use information from the mobile network).

The location of the CAM could be in middle layers of the operator's OAM architecture (e.g., DM) to reduce the signaling overhead. However, other solutions like NEs or *indoor local mobile network management systems* are possible at indoors.

3.4.2   OAM architecture[1]

Following the idea of *indoor local mobile network management system*, the design of a novel OAM architecture that interacts with the classical OAM layers is required. The proposed OAM architecture is defined by several interrelated entities, where different approaches can be adopted in order to establish its functional scheme: *centralized*, (where a unique entity is in charge of managing the rest of the elements); *distributed* (peer-to-peer); and *hybrid*. The proposed solution follows a hybrid scheme, a combination of the characteristics of centralized and distributed schemes. Here, some mechanisms are completely local while others require coordination among distributed entities. It allows easy reuse of classical centralized OAM architecture, while the implementation of distributed mechanisms is also supported.

The 3GPP OAM architecture [26] is maintained, adding new capabilities, functions, entities and interfaces to it. The placement of SON functions in the standard OAM elements (see Figure 3.3 on the left: NM, DM and NE) follows a similar scheme to that presented in [8]. The functions involving a specific subnetwork can be implemented at the DM layer. For functions involving more than one subnetwork, they will reside on higher layers of the OAM hierarchy. Conversely, distributed SON functions would be placed at NEs (e.g., small cells).

These levels at the OAM architecture chain are directly related to the time span for monitoring/configuration and also the level of abstraction over the network layers (see Table 3.1). However, even for the lowest layer standard centralized entity (DM), time spans (in the range of hours) are still large. Also, DM usually operates non-overlapped subnetworks covering wide areas. Hence, a novel additional OAM functional block, the *OAM Context-Aware System* (OCAS), is proposed to support innovative context-based SON mechanisms. This new proposed centralized entity is implemented at the lowest levels of the OAM hierarchy, being in charge of managing the set of small cells of one specific indoor area.

---

[1] This work has been performed in collaboration with Sergio Fortes Rodriguez.

Table 3.1: Characteristics of 3GPP OAM layers [8].

	Task	*Parameter Abstraction*	*Time Span*
NM	Planning	Vendor independent	weeks/month
EM/DM	Network Operation	Vendor independent/specific	hours/days
NE	Element Configuration	All parameters	secs/mins

3.4.2.1   Functional architecture

The proposed OAM architecture is shown in Figure 3.3. The standard 3GPP OAM architecture is represented (left square) containing the standard NM, EM/DM and NE elements. These are connected to the OCAS by newly defined interfaces (see Section 3.4.2.2 "Interface protocols"), which implements the following roles:

- To register available context services (CSs) and obtains context information from them.

- To implement context-aware SON functions.

- To act as coordinator between the OAM elements of the mobile network, context-aware SON algorithms and CSs. It propagates the results of the context-aware SON algorithms to the OAM standard elements for their authorization to apply the decided commands in the network. Then, these commands may be applied through standard OAM elements or directly to the devices by the OCAS itself depending on the operator policies.

Additionally, *monitoring and reporting* functions (M/R) can be incorporated into the UEs, so they can directly report to the OCAS information of the network status or their location. This M/R capability can be part of the context-based applications present in the terminals (e.g., navigation apps) or being implemented by means of directly invoking functionalities in the terminal API (*Application Program Interface*).

The described OCAS roles are distributed in different functional elements, which allow a better insight into the defined functionality:

- **SON Algorithmic Unit (SAU)** implements the local SON algorithms in the system. It can contain multiple interdependent SON functions for self-configuration, self-optimization and self-healing. If multiple SON use cases are implemented, it would be also responsible for the proper coordination and trade-off between the different SON use cases and mechanisms by the *SON Coordination Layer*, being its particularities dependent of the specific use cases implemented. One benefit of the integration of multiple SON mechanism in the

SAU is that it supports the use of the same context sources (as well as network indicators/measures) for the multiple use cases implemented, reducing the possibility of collisions generated by using different information sources, as well as allowing a straightforward coordination between techniques.

- **Context Service Registering (CSR)** is in charge of the incorporation and authentication of different sources of context information into the *Registered Context Services Database*. For a CS to be included, the main parameters for the information exchange with the OCAS have to be defined: IP address and format characteristics for the communication with the CS. These parameters have to be compiled in a set of profiles to be used by the *Context Data Collector Unit* (previously referred as CAM) in order to communicate with the different CSs available.

- **ACtuator Unit (ACU)** configures the network elements with the new parameters calculated by the context-aware SON algorithms, directly or by the standard OAM pile through the *OAM Coordination Unit.*

- **Context Data Collector Unit (CDCU)** gathers the information coming from the CSs or the terminals registered in the system.

- **MEasurement Unit (MEU)** obtains information from the network elements, by direct network element connection or through standard OAM elements using the *OAM Coordination Unit.* It is also in charge of the possible acquisition of direct network measurements from the UEs (e.g., received power levels, etc.).

- **OAM Coordination Unit (OCU)** serves as the interaction element between the OCAS and the OAM standard architecture. It translates the configuration orders coming from the ACU into commands for the operator's OAM tools and it turns the OAM monitoring into a format usable by the MEU. Furthermore, it also supports the configuration of any of the OCAS functionalities by commands coming from the standard OAM architecture elements as well as by *Local Network Manager Agents.*

- **Local Network Manager Agent (LNMA)** represents the specific operator or administrator that may be required to manage the OCAS. The LNMA will have two main capabilities:

  - It may register, via the CSR, new CSs to be used by the OCAS.
  - It may alter the policies and/or functionalities of the OCAS via the OCU. This capability should be restricted through the permissions defined in the *Access Identities and Privileges Database* to avoid erroneous/malicious access.
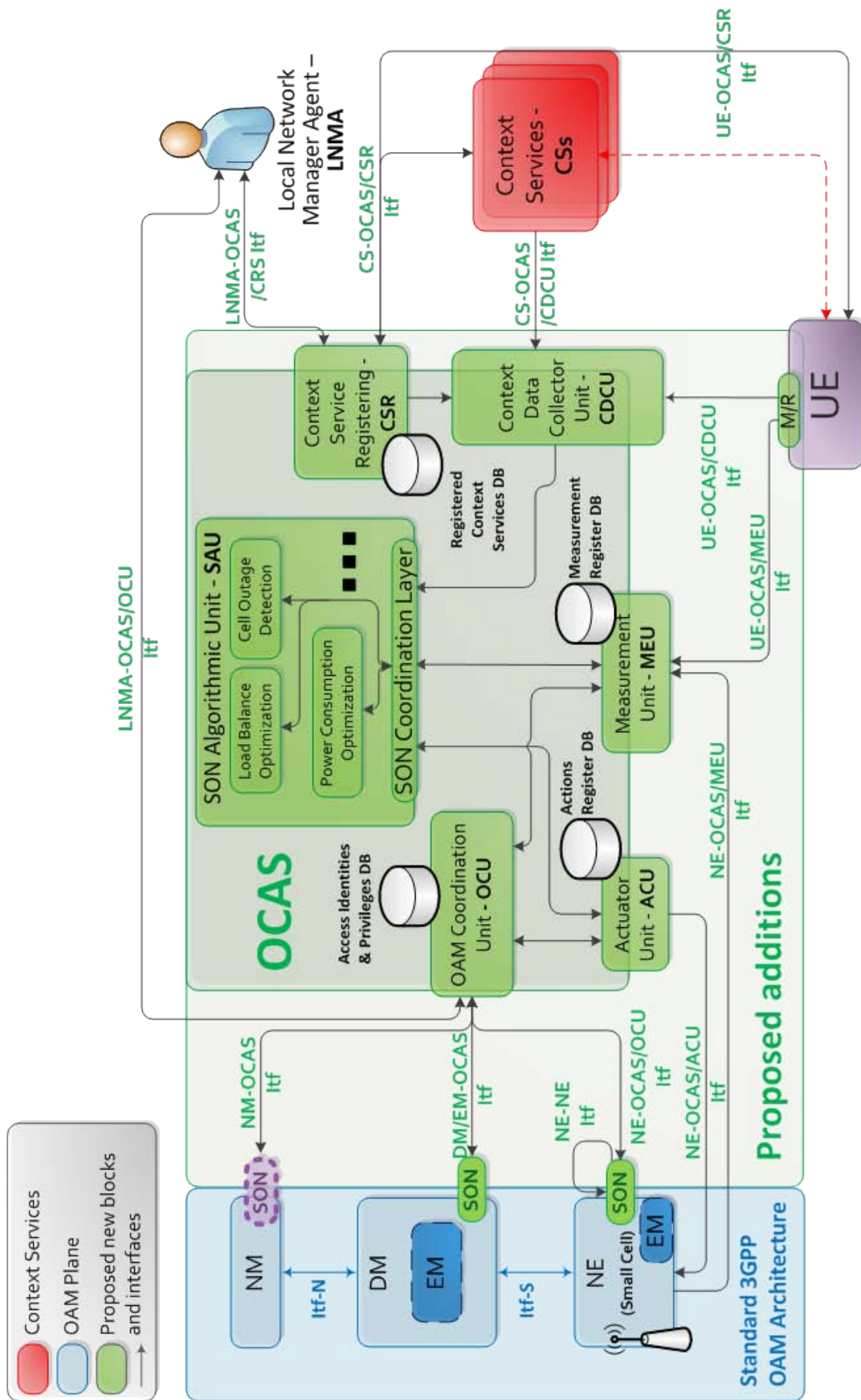
Figure 3.3: Proposed OAM architecture.

3.4.2.2   Interface protocols

According to the proposed architecture, the new main OCAS block introduces self-management at the local mobile network. Consequently, new interfaces, protocols and applications should be implemented in order to coordinate this system with the rest of the OAM architecture as well as to measure and modify network devices:

- **NM-OCAS** and **DM/EM-OCAS** are used for the coordination between OCAS and the elements of the operator's OAM core.

- **NE-OCAS** exchanges monitoring and configuration messages between the small cells and the OCAS through three different interfaces:

    - **NE-OCAS/MEU** focuses on monitoring and providing information about counters, alarms, KPIs, etc. to the MEU.
    - **NE-OCAS/ACU** carries direct configuration commands or files to the NEs.
    - **NE-OCAS/OCU** transports both monitoring and configuration messages when these cannot be directly sent/received to/from the NE by the OCAS blocks.

- **CS-OCAS** interfaces communicate information from the CSs to the OCAS. This could be context-awareness messages in order to support the context-based SON functions (through the CS-OCAS/CDCU Itf) or the procedure to register a new context service in the CSR (through the CS-OCAS/CSR Itf).

- **LNMA-OCAS/OCU** interface allows (subject to operator permission) the configuration of the OCAS system by the LNMA. In turn, LNMA-OCAS/CSR serves for the manual registration of a CS by the LNMA.

- **UE-OCAS** logical connections send direct UE monitoring information to the OCAS (through the UE-OCAS/MEU interface) and UE provided context information (by the UE-OCAS/CDCU) that may be required for the SAU. For non-cellular external context services, this interface would be UE-dependent. Therefore, it may be only available for specific UE models such as smartphones.

All the interfaces connecting the OCAS with the OAM architecture should follow the same standards as defined for 3GPP interfaces, being mainly based on TR-069 and XML [43]. CS-OCAS and UE-OCAS interfaces, however, are defined with elements that are independent of the mobile communications OAM network, as they are encapsulated on the user plane, so any communication protocol (over IP) can be freely defined for these data flows.

3.4.2.3   3GPP LTE/LTE-A femtocell network

The physical implementation of the proposed architecture for LTE/LTE-A systems, is centered on the case where the deployed small cell are open access femtocells (HeNBs). These are chosen because their limited capabilities, high vulnerabilities and wide usage make this case specially challenging and comprehensive from an OAM perspective.

OAM-SON functionalities follow the standardized 3GPP architecture [26], with the novel addition of the OCAS, which implements local context-based SON functionalities. OCAS implementation can be local (if performed by hardware connected to the same LAN – local area network) or remote (by an external hardware connected to the system via the Internet). Remote solutions have high versatility in terms of using existing or leased equipment. However, the need of exchanging a high amount of information through the often limited network backhaul, highly encourages the adoption of local implementations as the one it is adopted here. Challenges for this approach include the need of OCAS additional on-site hardware, its installation and maintenance, although the related cost is expected to be minimal over the total deployment expenses.
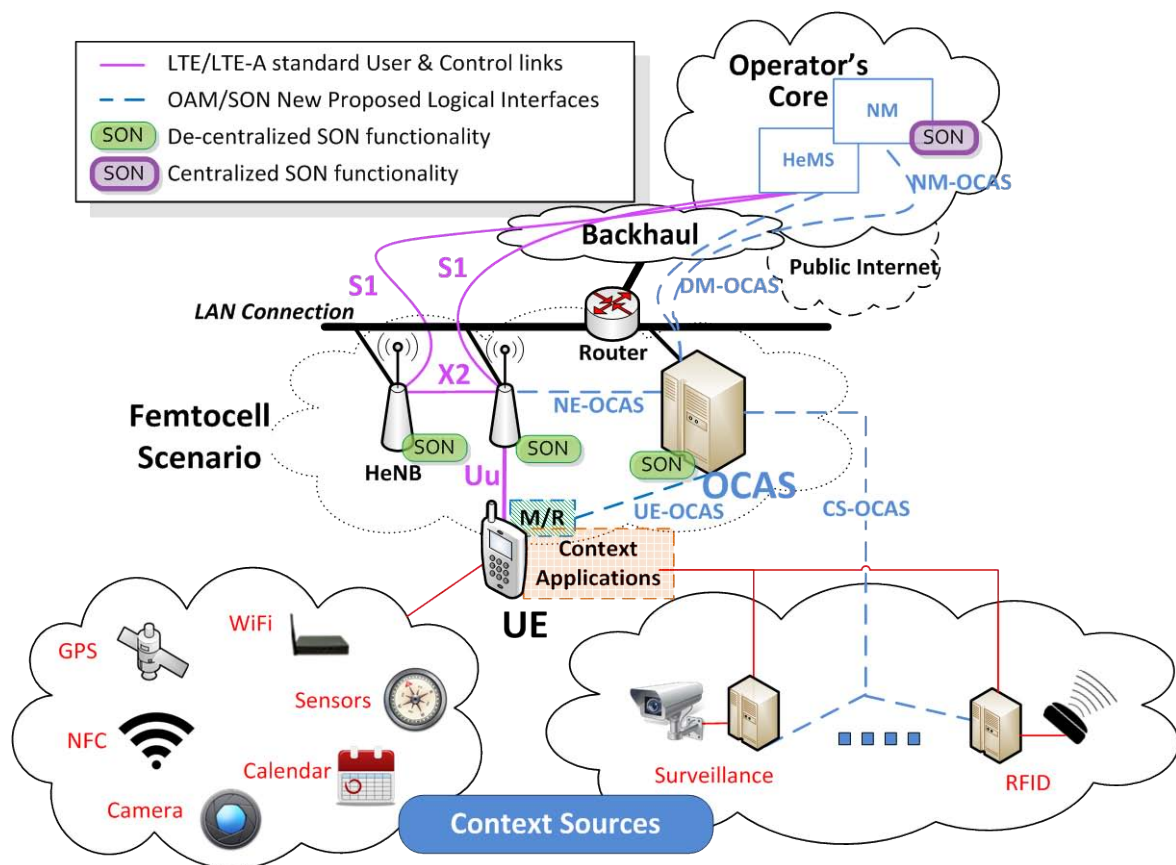
Figure 3.4: Proposed OAM architecture for LTE/LTE-A femtocells.

Figure 3.4 presents the local physical implementation, for LTE/LTE-A commercial or corporate femtocell scenarios. The DM role is implemented by the HeMS. HeNBs user and control planes connect to the operator's core through the S1 interface, while the X2 interconnects the femtocells for distributed cooperation (in LTE-A). The defined logical links are implemented by physical connections as follows:

- **UE-OCAS** and **NE-OCAS**: The information transmitted from the UEs to the OCAS is sent through the Uu interface to the femtocell. This data (as well as the particular commands/information from the stations transmitted by the NE-OCAS interface) is then retransmitted through the LAN to the OCAS.

- **CS-OCAS:** The interface used to transmit the context information (in case it is not directly obtained from the terminals) is implemented by the CSs through the LAN or the Internet connection to the OCAS.

- **NM-OCAS** and **DM-OCAS**: The information between the OCAS and the operator's core (i.e., the highest elements of the standard OAM layers: DM, NM) is sent by the router through the backhaul to the operator's core.

The use of LAN for exchanging data between the OCAS and the UEs greatly minimizes the traffic in the backhaul and the operator's core at reduced delay. This traffic local breakout has been envisaged by standards like *Local IP Access* and *Selected IP Traffic Offload* (LIPA-SIPTO) [44] or projects [42].

3.4.2.4   Domain responsibility and security

This characteristic refers to the commercial/legal entity in charge of managing the proposed OAM architecture. The responsible entities include the *mobile network operator*, the *user/administrator of the local system* or a *third party*.

Even if the considered scenarios are essentially local, the small cells are currently part of the mobile network operator infrastructure and make use of its radio spectrum. Therefore, as SON will alter the cells configuration, OCAS should remain on the operator's domain but they could transfer the responsibilities of the local-centralized system to a local user/administrator.

The connections between the OCAS and the CSs shall avoid the disclosure of network status information that may be sensitive. Thus, the extent, authenticity, accountability and correctness of the information exchanged will be critical. Standardization on the CS-OCAS and LNMS-OCAS and related processes may be necessary to limit this issue.

3.4.3   SON use case

In this subsection, some baseline MLB algorithms are presented to verify the context-aware SON framework. For that purpose, a novel design is proposed to integrate context-awareness into these MLB algorithms. It is shown that context-aware SON compared to baseline algorithms achieves better network performance and reduces the optimization time to reach the permanent regime (steady state).

3.4.3.1   Mobility load balancing use case

MLB is a use case defined by the 3GPP [45]. It has the ability to manage and direct voice and data traffic from loaded cells to the most suitable cell, independently of the end layer (macrocell or small cells) or RAT (LTE, UMTS or GSM).

Normally, most non-context-aware algorithms that follow an adaptive process to optimize the cellular network work properly (i.e., a few iterations and short time to reach the optimal network parameters) when users are homogenously widespread around the coverage area of the loaded cell, due to the fact that neighboring cells equally catch some of those users [16] [17]. However, if the users' distribution is concentrated in certain part of the cell coverage area (top Figure 3.5), most non-context-aware mechanisms follow a similar process: all neighboring cells try to catch those users (e.g., by tuning cells transmission power as illustrated in Figure 3.5(a). The consequence of this act could be either the degradation of the network performance or the algorithm oscillation to reach the steady state. That conclusion will be seen in the evaluation subsection. Figure 3.5b illustrates an optimal solution to face that problematic situation. This scenario could be identified thanks to users and objects context-awareness. In this case, only the closest neighboring cell to the loaded cell should catch users. For example, by increasing its transmission power and, at the same time, the transmission power of the loaded cell is reduced. Those variations of transmission power are restricted to the cell transmission power range (e.g., from 0.016 to 250 mW). Additionally, some cellular methods to avoid high interference could limit that maximum value whereas other methods that analyze the QoS, limit the minimum value of transmission power to avoid coverage holes.

Several MLB algorithms in open access femtocell scenarios have been developed in the literature. The *Power Traffic Sharing* (PTS) algorithm [16] has been chosen as a baseline method. Additionally, a modified version of *Power Load Balance* algorithm [15] is developed: *Power Load Sharing* (PLS). The objective of these procedures is to intelligently optimize an indicator or *Figure of Merit* (FM) while maintaining the network performance.

(a) Classical MLB　　　　　　　　　　　(b) Context-aware MLB
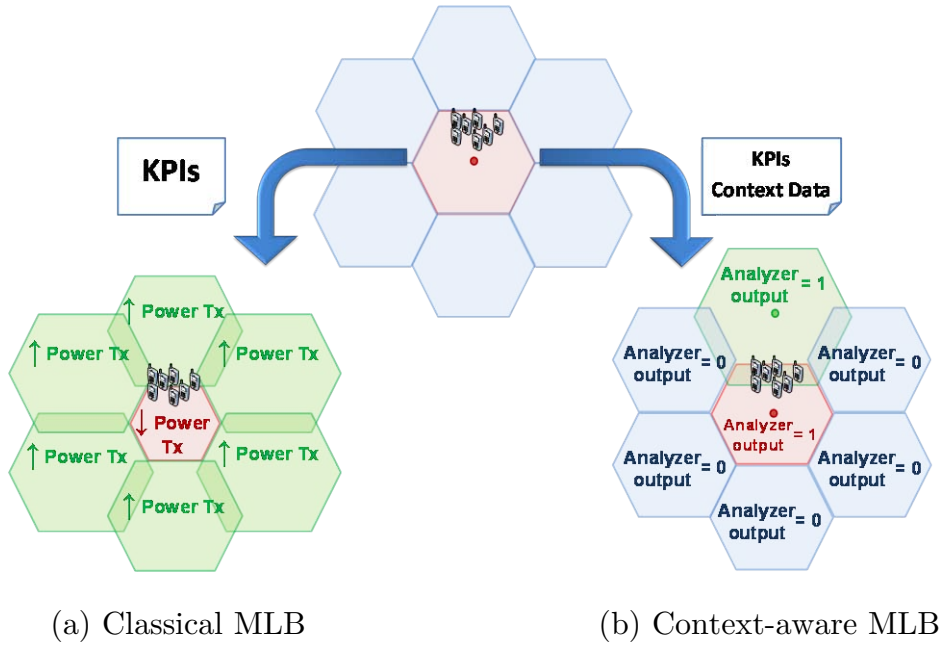
Figure 3.5: Classical MLB vs context-aware MLB.

The main scheme of these PTS and PLS algorithms is presented in Figure 3.6 where the essential block of the MLB is a *Fuzzy Logic Controller* (FLC) [46] (an FLC approach has been detailed in *Appendix C*). These mechanisms have the control and the decision of the next network configuration depending on its inputs, which are network counters or indicators, and on the feedback of the previous FLC response. The optimization is carried out by tuning femtocells transmission power to balance or share traffic between neighboring cells, increasing the system capacity and reducing the global user dissatisfaction. These algorithms are briefly explained:

- **Power Traffic Sharing (PTS)**: Baseline algorithm that tunes cell transmission power to balance users' traffic. The input parameters of the FLC are two: the difference between the serving cell blocked calls and the average neighboring cells blocked calls, as well as the output parameter of the previous FLC response (feedback). This output parameter tunes the cell transmission power by increasing/decreasing or no variation current cell transmission power. This mechanism is periodically launched per cell.

- **Power Load Sharing (PLS)**: In this case, the input parameters are, the difference between the number of slots used per *Physical Resource Block* (PRB) over the total available slots per PRBs in the serving cell and the average of the same indicator per neighboring cell. The second input is, as previously, the feedback of the FLC. It has the same output as PTS method. This mechanism is also periodically launched per cell.
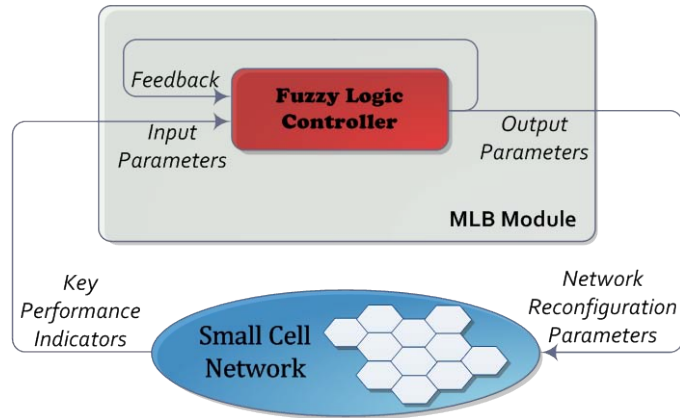
Figure 3.6: PTS and PLS scheme.

A long convergence time or/and a large period to get the input data for the algorithms could provoke the no-convergence in time to the optimal network performance, in case the radio or environment conditions change rapidly. For this reason, context information is very important to quickly achieve the optimum network parameters and reach the permanent regime in the shortest period possible.

3.4.3.2   Context-aware SON algorithms

Based on the described framework for context-aware SON and the aforementioned MLB algorithms, a novel context-aware approach is developed. The proposed technique is supported by the CAM (or CDCU element, see Figure 3.3), which is in charge of classifying context information and removing redundancies, i.e., the same kind of data is grouped, labelled (e.g., *user_position*, *mobile_orientation*, etc.) and dated to ease further processing. After that, this information is forwarded to the context-aware SON mechanisms (or SAU element, see Figure 3.3). For this specific work, a new module, *Integration Module* (IM), is defined to integrate the context information into the MLB algorithms (PTS or PLS).
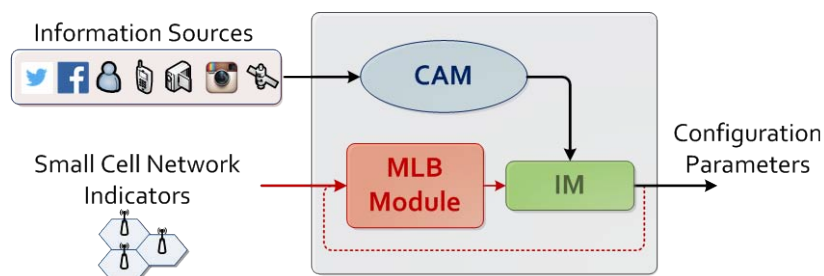
Figure 3.7: Context-aware MLB scheme.

The IM analyzes the context data provided by the CAM and decides whether the MLB algorithm outputs are set in the cellular network or whether they must be modified. That decision would be the new feedback of the MLB module. Although the IM location would depend on the cellular operator's decision, close integration to the MLB algorithm is preferred in order to avoid delays and overhead of information due to the high amount of data exchanged (e.g., implemented in SAU element, see Figure 3.3). The global context-aware MLB scheme is shown in Figure 3.7.
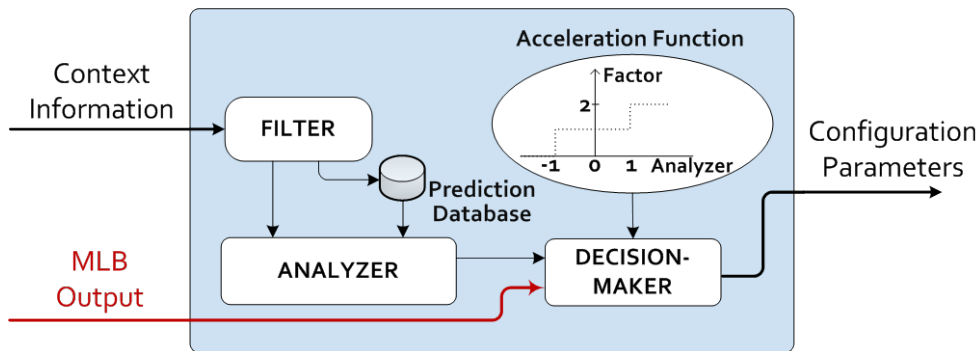
Figure 3.8: Integration module (IM).

Figure 3.8 details the IM. The context information is processed at the *Filter* module to remove the data not used by the particular SON algorithm (e.g., the smartphone orientation and weather are discarded for the presented algorithm) and to select the useful information for this approach: *users' position* and *distribution*. Therefore, those messages labelled as "*user_position*" or "*users_distribution*" are accepted whereas any other message is discarded. After that, real-time data is forwarded to the *Analyzer* while those data which provide information about upcoming events (e.g., a book signing event) are stored into the *Prediction Database* for future use. Any other information out of date is also rejected. Both, online data from the *Filter* and stored data from the *Prediction Database* are interpreted by the *Analyzer*. In this approach, the *Analyzer* is sensitive to cell congestion and users' concentration close to the edge, therefore, some parameters are calculated as follows.

Firstly, it is necessary to determine whether the serving cell situation is considered as congested or not, which is calculated as the serving cell load being higher than the average load of its neighboring cells or not. Secondly, the situation where users' concentration is close to the cell edge, is evaluated based on the context information and the received power per user. The user concentration is considered high when most users are located in the same area. For this approach, that situation happens when most users are inside a quarter of the cell area. The user should be located at the cell

border when receives similar power from its serving cell and another neighboring cell. This module provides three output values (see Figure 3.5(b)):

- If the *studied cell* is a congested cell or it is the nearest neighboring cell of a congested area then output value is 1,
- If not, in case the *studied cell* is a neighboring cell of a congested cell then output value is 0,
- Otherwise, output value is –1.

The *Analyzer* output is sent to the *Decision-Maker*, together with the *Acceleration Function*, to decide the modification applied to the MLB algorithm output. The *Acceleration Function* selected for this approach is a simple step function where depending on the *Analyzer* output, the MLB algorithm output is multiplied by a factor (step function). Other functions might improve the convergence time and network performance. In this case, if the *Analyzer* output is:

- 1, the MLB algorithm output is doubled,
- 0, no variation is applied to the MLB algorithm output,
- –1, the MLB algorithm output is cancelled.

3.5   Evaluation

In this section, the proposed context-aware SON framework is assessed by the analysis of the proposed context-aware approach. These context-aware MLB algorithms are evaluated by the dynamic system-level LTE simulator described in [47].

3.5.1   Simulation set-up

A simple and realistic simulation scenario simulates part of a shopping center comprising four particular areas such as shops, offices, restaurants or social places where there is a small cell deployed inside each one. These base stations are denoted by red markers on the bottom images of Figure 3.9. Outside the building, a single tri-sectorized macrocell is also placed, completing the realistic setup. This deployment presents a frequency reuse factor of 1 and all small cells share the same backhaul connection. The OCAS architecture is selected to implement the SON methods. A random waypoint model has been implemented for users' mobility management, where users move freely between those areas through the corridors. Additionally, an indoor positioning system is emulated to provide the users' position.

(a) Optimized network   (b) Conditions change   (c) New configuration
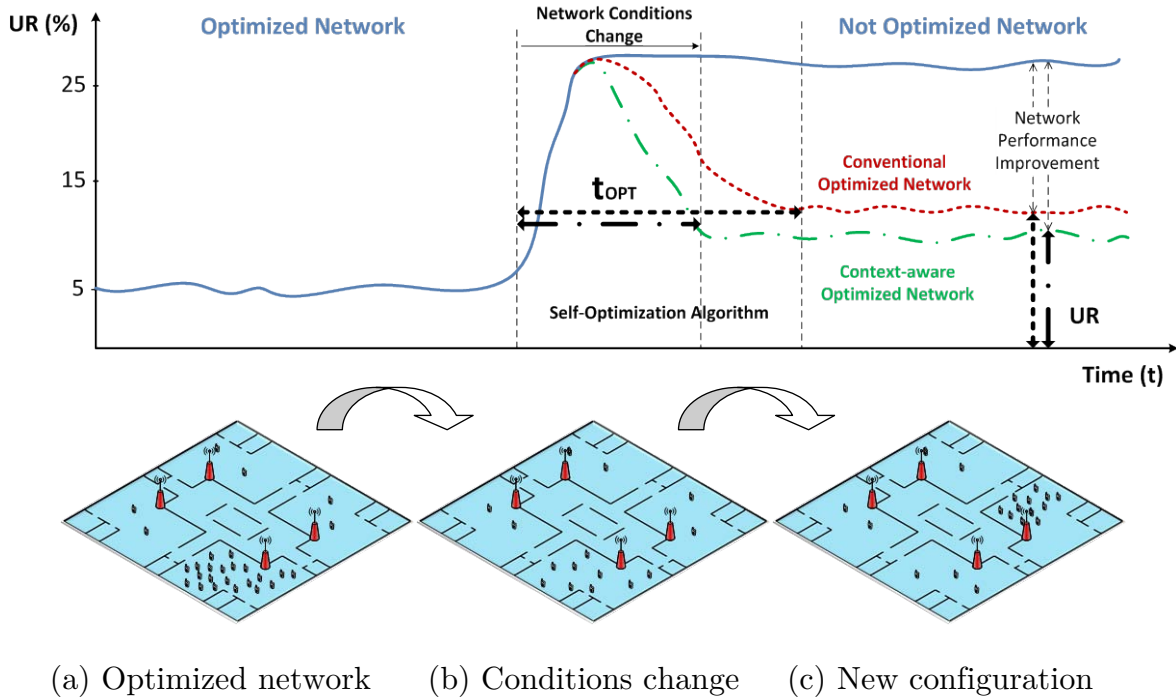
Figure 3.9: Temporal and spatial user distributions in the scenario.

To test the benefits of context-awareness in the reference MLB algorithms, three different spatial user distributions have been simulated along the time as presented in Figure 3.9. Initially, as shown in Figure 3.9(a), the network starts from an optimized situation, as the UR graph shows (5%). Most people are grouped in the same area (e.g., lunch time in a restaurant). Next, in Figure 3.9(b), people begin to move away from that place (e.g., at the end of lunch time) and new users fill a new area within a short period (e.g., a clothing store opens). Therefore, the previous optimized network configuration is out of date and network performance starts to get worse, in other words, bad users' experiences. This consequence can be observed in the UR graph (Figure 3.9 top, blue line). The red dotted line shows the reaction when a *conventional MLB algorithm* catches this situation and the time, t_{opt}, to converge to the optimal UR. The same behavior is shown for a *context-aware MLB algorithm* in green dotted and dashed line. Finally, in Figure 3.9(c), the network parameters are optimized and the new crowded area is well-managed, obtaining high network performance improvement compared to a non-optimized network, as UR graph shows.

3.5.2   Simulation results

The simulation results for each method are described here. Concretely, as mentioned before, two kinds of indicators are studied: the UR and the t_{opt}. For this

purpose, the algorithms have been launched at different periods: *1 hour and 30-15-5-1 minute* (as described in Section 3.4.1 "Framework characteristics"). Each simulation lasts 24 hours in order to ensure the steady state of the UR. In consequence, depending on the period of the algorithm execution, the number of these tests is 24 for the 1 hour algorithm execution or 1.440 for that of 1 minute.

On the one hand, the UR acceptable by the network operator could be a challenge in many situations. In these simulations, as shown in the UR graph in Figure 3.9, the network has been heavily overcrowded getting an UR indicator over 25% (blue line). In Figure 3.10, the average UR at the steady state and the error bars (maximum and minimum values of UR) achieved for these algorithms at different execution periods are presented. Firstly, in the left diagram, the integration of context information into the original PTS algorithm (CA-PTS) is compared to the original PTS algorithm. On average, a relative gain of 15% in satisfied users is achieved thanks to the additional information provided by the external sources. In addition, a reduction in UR is also obtained when the execution period of the algorithms is shortened from 1 hour to 1 min (from 13.1% to 10.5% in the PTS method and 11.8% to 9.1% in the CA-PTS method). In the same context, the right diagram analyzes the PLS algorithm and context-aware PLS method (CA-PLS), and similar results are obtained. The explanation is related with the correlation among input data, CBR and PRBs activity: once all PRBs are getting full, the network refuses new incoming connections. For that reason, these two algorithms converge to similar UR approaches.
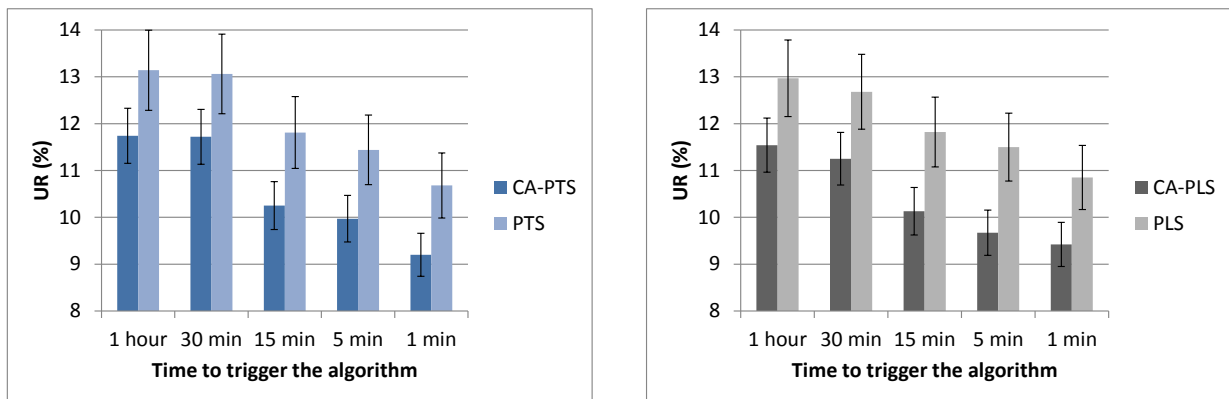
Figure 3.10: Average UR and error bars.

On the other hand, the time required for UR convergence (t_{opt}) has been studied (Figure 3.11). As expected, the shorter algorithm execution period, the faster optimal UR convergence. Furthermore, the enhancement obtained thanks to context awareness in these algorithms is evident. This additional information reduces the normal convergence time by nearly 50% in both algorithms. That means, several users suffer

bad QoE during the convergence time. Therefore, those users could leave their current cellular operators to look for better service (and, consequently, the operators' revenues would be reduced).
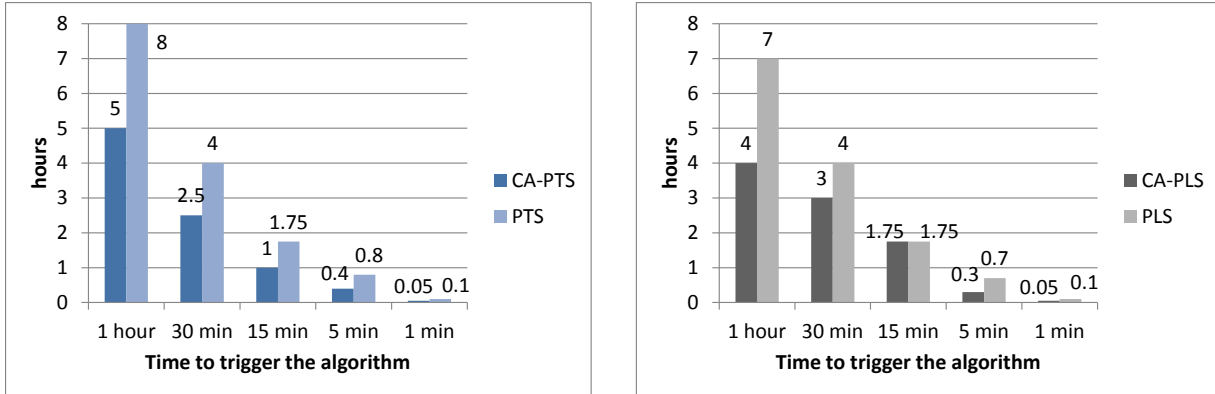
Figure 3.11: Convergence time (t_{opt}).

3.6   Conclusions

A framework for context-aware SON has been presented, proposing different context sources and time intervals to get that information. Additionally, a novel OAM architecture extension for 3GPP-based SON is proposed for commercial and corporate indoor small cell scenarios to support the context-aware SON framework.

An MLB mechanism has been taken as a baseline to be upgraded with extra data provided by external network sources. The results show that the proposed approach leads to a significant improvement in the response time by using position awareness. In consequence, the convergence time has been reduced about 50%. Subsequently, the optimal UR values have been enhanced, decreasing the number of dissatisfied users in the cellular network.

These results and the qualitative analysis of the OAM impact in terms of signaling overhead and delay, demonstrate that placing most of the SON functionalities at the lowest levels of the OAM hierarchy is the right decision.

Chapter 4

Indoor positioning strategies

This chapter presents a multi-antenna RFID-based indoor positioning system using active tags. In addition, it is studied the improvement of the positioning system accuracy by the integration and analysis of RF measurements from cellular technologies. For that purpose, an experimental analysis of simultaneous RF measurements from RFID and macrocellular networks is carried out.

The structure of this chapter is as follows: Section 4.1 introduces current indoor positioning systems. Section 4.2 details the state of the art, focusing on wireless heterogeneous techniques. Section 4.3 presents the problem description. Section 4.4 describes the proposed indoor positioning strategies. Section 4.5 evaluates the accuracy of these indoor positioning systems. Finally, Section 4.6 includes the conclusions and perspectives of this chapter.

4.1   Introduction

Nowadays the requirements of *Location-Based Services* (LBS) in terms of location-accuracy at indoor environments go from few centimeters to several meters or even the detection of a room/office. Cost reduction of wireless devices makes RF (radio frequency) solutions good candidates for low cost indoor positioning systems. Several RF technologies have been proposed for providing indoor positioning such as UWB, which presents position errors of few centimeters, or RFID, which is in the range of few meters. However, accurate indoor positioning systems are still expensive and present high costs in terms of hardware price, deployment expenditures, computational cost and complexity, especially for very accurate solutions, such as UWB.

The identification of being inside a room or office could be easily performed with many RF-based indoor positioning systems. Nevertheless, other indoor scenarios like halls and corridors are commonly a challenge as they would require more accuracy. The use of multi-antenna devices could help to improve location accuracy in such a challenge scenarios and reduce the infrastructure costs.

In parallel, a wide variety of wireless communication networks coexist simultaneously with human beings. These networks are the so-called HCNs where several wireless technologies surround daily life to create massive communication layers at different frequencies. These infrastructures provide a cloud of parallel information that could be, not only used for communication purposes, but also for enhancing accuracy and robustness of several, a priori, unrelated applications, such as indoor positioning. In this way, mechanisms for opportunistic radio positioning based on multiple technologies (e.g., WLAN together with GSM, etc.) have been devised as promising solutions. The integration of those technologies in current indoor positioning systems could lead to the required levels of accuracy for new applications at reduced costs.

Based on these claims, the use of multi-antenna readers for RF-based indoor positioning systems to minimize infrastructure costs and achieving high accuracy is studied. Herein, RFID multi-antenna readers with active tags are selected as a low cost RF technology. In parallel, the combination of the RFID-based indoor positioning system with other low cost RF solutions is analyzed and developed in order to reduce the position error. Macrocellular networks, one of the most widely extended RF technologies, are selected.

The main contributions of this chapter are the study and assessment of:

- Techniques for data fusion when having multiple sets of RFID measurements, each one referred and collected by an antenna, at indoor challenge scenarios like halls and corridors.

- Trade-off between the number of RFID tags and antennas in the reader.

- Integration of cellular technology information into RFID-based indoor positioning systems.

- Measurement campaign for an experimental analysis of both RFID and cellular technologies.

Finally, real field measurements are used to evaluate the capabilities of the proposed indoor positioning systems.

4.2   Related work

In indoor positioning and navigation fields, the large diversity of application environments leads to a large diversity of solutions. A summary of the main positioning technologies, techniques and their performances for typical applications are detailed in [48]. For these applications, several performance criteria can be defined, such as robustness, responsiveness, consumption, size, scalability, compatibility with human beings, accuracy or precision.

Literature presented several RF-based indoor positioning systems. The authors in [49] and [50] evaluated *Channel State Information* (CSI-based) positioning versus RSSI-based positioning in three typical environments such as a research laboratory, a lecture theatre and a corridor. With the RSSI-based system the median position error is less than a meter for the laboratory and 2 m in the lecture theatre, while it is 2.5 m in the corridor. The cumulative distribution function (CDF) of the position error with 90% of probability is 1.5 m and 3 m for the two first environments, while it is almost 3.5 m for the corridor. Conversely, CSI-based method is the most accurate technique but the corridor environment is still harsher than the others; the 90th percentile of position error is more than 1.75 m while it is 1.5 m for the laboratory.

The work in [51] proposed LuPI (Locating using Prior Information). It considered that human motion can be distinguished and recorded by radio information (RSSI deviation between different positions) and a pedometer (based on accelerometer embedded in a smartphone). LuPI utilized the RSSI and the sensor-based pedometer to build a RSSI variation space as prior information. In order to assess this solution, extensive measurements were made on the third floor of a middle-size building with different types of room/areas. In the analyzed corridor, the average error of the proposed system is 5.9 m. In a big room, the average error is 1.4 m, while it is 1.9 m in a small one. Focusing on RFID technology [52] [53] [54] and multi-antenna indoor positioning systems, several works can be found in literature [55] [56]. These works used the antenna diversity to assess the probability of a position when a tag was detected or not, or to provide *Direction-of-Arrival* (DoA) estimation by phase arrays in small covered areas, typically less than 10 m^2. Other works studied the impact of the number of antennas and its configuration on location accuracy [57] or compared position estimation methods [58] [59]. The study described in [57] considered four different multiple antenna configurations: SISO, SIMO-MISO and MIMO. The best results were performed with MIMO and the average position error is 1.5 m with 3 dB shadowing standard deviation. When increasing the number of antennas from 2 to 14, the position error decreased from 2.3 m to 0.9 m. Conversely, [58] proposed three estimation methods for an increasing number of transmit antennas (2 to 4), the position error varies from 2 m to 1.5 m in 7x7 m^2 room. Finally, [59] presented the

accuracy and stability results for RADAR, *Area Based Probability* (ABP), *Simple Point Matching* (SPM) and *Bayesian Networks* (BNs) algorithms. For each one, the CDF of the position error was calculated when averaging and not averaging the antenna data, and when applying a Gaussian distribution to the measured RSSI. The experimentation area was about half of a floor measuring 66.75x51.5 m^2 and the best accuracy was 1.5 m. Experimentations at a *desk level* were small one-foot movements around a main center placement with accuracy of 0.9 m.

In outdoor scenarios, the signal coming from macrocell base station can be processed in order to obtain just a rough estimation of a mobile terminal position (hundreds of meters). In indoor scenarios, some studies characterized GSM/UMTS signals from macrocells to check the reliability of building indoor radio maps for fingerprinting purposes [60]. Other works [37] [61] presented a fingerprinting technique based in the mapping and use of radio signals from femtocells for positioning terminals in indoor environments. The accuracy of those systems was few meters. However, such indoor cellular deployments are still no widely implemented and costly. The proposed option of combining RFID with macrocell technology measurements could successfully provide the level of accuracy required in RFID-based indoor positioning systems for pedestrian navigation in buildings.

In this respect, the first works integrating diverse RF technologies for indoor positioning were presented a few years ago [62] [63] [64] where RFID, WLAN and GSM technologies were analyzed. The main purpose of combining different technologies is to increase the accuracy [65], or the density of the devices to be localized [66], or to overcome the continuity indoor/outdoor challenge [67], where these systems need to handle heterogeneous devices [68] and vertical handovers [63]. European Project WHERE2 [69] presented results of real-life experiments based on ZigBee and *Orthogonal Frequency Division Multiplexing* (OFDM) devices (emulating a multi-standard terminal moving in typical indoor environments), with measurements using RSSI and *Round Trip Delay* (RTD). A comparison between non-cooperative and cooperative positioning was done and several positioning algorithms were tested in both cases. The 90th percentile of position error is 4 m. In reference [63], algorithms with realistic heterogeneous wireless networks, including GSM, DVB, FM and WLAN, were evaluated with measurements of RSSI. That paper proposed two positioning algorithms: *Direct Multi-Radio Fusion* (DMRF) reorganized the information in a transformed space and *Cooperative Eigen-Radio Positioning* (CERP) used the spatial discrimination property. The mean position error of this approach is 1.5 m.

Based on these works, the accuracy of these indoor positioning systems could be further improved to accomplish the requirements of current LBS applications (e.g., position error below 1m for pedestrian indoor navigation).

4.3   Problem description

RF-based techniques are widely used for indoor positioning, but they usually do not provide enough accuracy for indoor navigation. In such techniques, metrics as RSSI, *Angle of Arrival* (AoA) or *Time of Flight* (ToF) may not be directly related to distance or relative position between transmitter and receiver. This is due to multipath and fading phenomena that can be dominating in indoor environments. Therefore, position estimation suffers from this initial uncertainty and sophisticated positioning algorithms and filtering are needed to compensate these drawbacks.

Three main types of environments could be found for indoor positioning in a building: halls, corridors and offices. For offices and rooms, simple detection of presence in the room could be enough for many applications. However, accurate indoor positioning systems are specially required in corridors and halls with multiple doors. Such areas (e.g., hospital corridors surrounded by patient rooms) act as distributors to different locations making essential a precise position estimation, e.g. in order to indicate a specific door. Hence, the proposed indoor positioning system would be focused on a corridor environment which is a more critical scenario than halls in terms of multi-path propagation. *Fingerprinting techniques* are good candidates to overcome multi-path propagation uncertainty. Fingerprinting techniques compare several features of the fingerprinting pattern (large data) with current information. That identifies the original data with the analyzed information [70].

Focusing on RFID systems, they could be active or passive (in terms of tags activity). Passive systems could work in a reliable way for reading distances up to 3 m in indoor environments or 15 m in free space conditions [71]. Furthermore, passive tags embed a shunt resistance in order not to damage circuitry when the tag is near to the reader, avoiding the loading effect. Therefore, when tag-to-reader distance is less than $10\,\lambda$, the system does not ensure the received power is linked to the distance by any propagation model [72] [73]. In consequence, passive systems are not convenient for indoor challenge scenarios like corridors where tags and readers would be very close to each other. Conversely, active technology copes with these limitations regarding the tag-to-reader distance and reading distances are up to 15 m in indoor scenarios. Even so, passive tags cost ten times less than the active ones but the price of the readers is also very important. The use of multi-antenna readers would improve the system performance. It could be done by increasing the number of antennas of a reader or placing two (or more) readers together. The later would require a higher investment with readers for passive tags compared to the readers for active tags. Taking it into account, each device (e.g., smarthphone) would need a reader, thus, the price of the reader would be more important than the price of the tags.

In this respect, RFID systems with active tags: are not expensive compared to passive tags, have an operating range of several tens of meters and are easy to deploy, which comply with the application requirements for pedestrian navigation. However, the accuracy of this RFID-based indoor positioning system should be improved to reduce the position error (few meters). In addition, none of the previous work analyzed the promising approach of combining RFID and macrocell signal processing as a low cost solution. In fact, up to the author knowledge, there has not been any deep study in the field of combining RFID with macrocellular signals. Hence, this is a suitable option for enhancing precision for pedestrian navigation in buildings with a highly reduced implementation costs in comparison with previous solutions.

Further details about RFID and cellular technologies are summarized in *Appendix A*. It describes their general characteristics and theoretical models in indoor scenarios. Additionally, *Appendix B* presents a signal study of these technologies based on their theoretical models and the measurement campaign. It would assess their applicability for indoor positioning systems.

4.4   Methods for indoor positioning

To determine the possible improvement achievable by the use of different techniques and multi-antenna RFID reader or the combination of RFID and cellular technologies, different baseline single-technology solutions are defined.

Firstly, the description of the selected scheme for the implementation of the proposed indoor positioning system is detailed. Then, several techniques and methods for data fusion are analyzed for the RFID-based indoor positioning system. Finally, the integration of the cellular technology into RFID-based positioning system is presented.

4.4.1   Fingerprinting-based scheme

Fingerprinting is selected to provide indoor positioning, being a widely applied scheme for positioning in these environments [74]. It is defined by two main phases as Figure 4.1 depicts; *calibration phase* (offline) and *localization phase* (online). These stages are explained focused on the proposed approach:

- *Calibration phase:* This stage is performed prior to the provision of the positioning service. RSSI $(\mu_{\alpha,\tau}^{Prx}(\gamma_f))$ is collected by the antenna(s) of the reader (where α represents the particular antenna of the set of antennas A of the reader, $\alpha \in A$) from different transmitters (where τ represents the particular

transmitter of the set of transmitters T, $\tau \in T$). That information is gathered from known positions (also called fingerprinting positions) $\gamma_f = \left(x_f, y_f, z_f\right)$ of the scenario and it is referred as fingerprinting measurements or calibration data.

- *Localization phase:* It is in charge of the online positioning service. The set of measured RSSI ($\mu_{\alpha,\tau}^{Prx}(\gamma_{curr})$) collected in real time by the device to be localized, are used to estimate its current position $\gamma_{\text{curr}} = (x, y, z)$ by means of comparing it to the stored fingerprinting data. Different techniques can be implemented.

4.4.2 RFID-based positioning system

An RFID-based system with active tags is proposed. Different positioning techniques and methods for data fusion are analyzed for multi-antenna readers.

This system collects information ($\mu_{\alpha,\tau}^{Prx}$) from each fingerprinting position in the *calibration phase*. Then, the *localization phase* processes the current measurements. This phase is divided in three main steps as Figure 4.2 shows:

- *Step 1 - Candidates ranking:* Each of the fingerprinting positions is assigned with a certain weight $w\left(\gamma_f, \gamma_{curr}\right)$ based on different possible criteria (techniques): the similarity of the $\mu_{\alpha,\tau}^{Prx}$ values received from each transmitter in respect to those stored in the fingerprinting database, the posterior probability of being in the fingerprinting positions given the current $\mu_{\alpha,\tau}^{Prx}$ values, etc.

- *Step 2 - Candidates filtering:* Based on the ranking generated in the previous step (weighted fingerprinting positions), one or several of them, *candidates*, are selected as possible estimated positions. The rest are discarded.

- *Step 3 - Position estimation:* From the set of the selected candidate positions, the current position of the device is estimated.

It could be observed in Figure 4.2 that the *localization phase* could be executed in parallel for each set of collected data from each antenna. This means, several single-antenna RFID-based positioning systems with multiple position solutions (one per system). Conversely, the system information from each antenna could be merged into a single flow at the beginning of each step (any of the 3 steps) or at the end of *step 3*, as the flowchart illustrates through the green dashed blocks (*fusion methods*). Four *fusion methods* are proposed to integrate the diversity of multi-antenna in the general positioning scheme. Note that, only one *fusion methods* could be triggered. An analysis to assess the optimal *step* to data fusion would be performed. Additionally, Figure 4.2 illustrates the different *techniques* developed at each *step*.
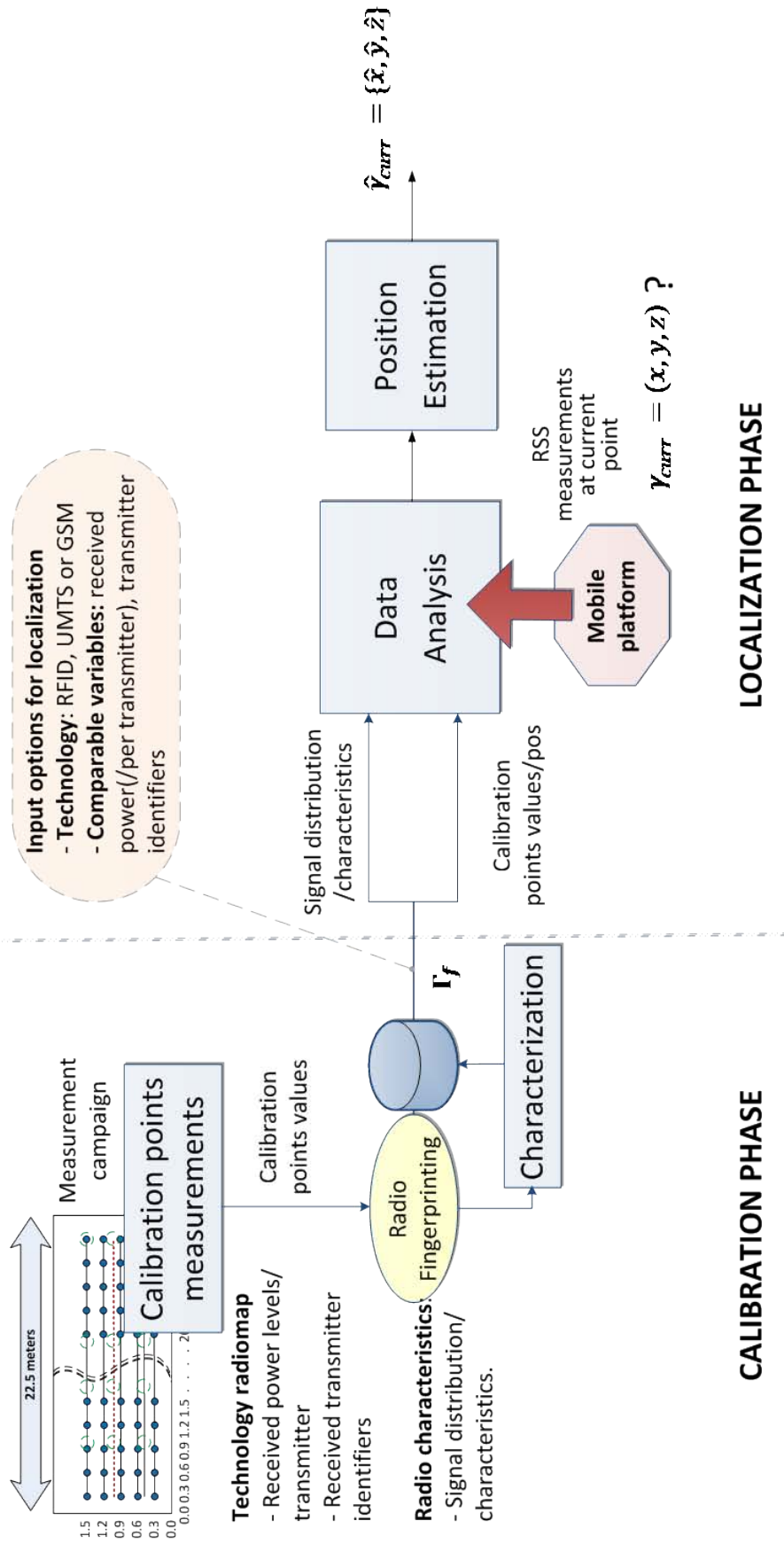
Figure 4.1: Fingerprinting-based scheme.

4.4.2.1   Step 1: Candidates ranking

This step processes the information supplied to the indoor positioning system (current measurements and fingerprinting measurements) to get ranked candidates (ranked fingerprinting positions). Firstly, the input data is gathered. Afterwards, a technique is selected for candidates ranking. The outputs of this step are the ranked fingerprinting positions, $w_{Prx}(\gamma_f, \gamma_{curr})$. The input data and the ranking techniques are detailed below:

1) Inputs

Inputs could be either information from each antenna that would be processed in parallel and individually, or, information from all the antennas that would be processed together in a single positioning system:

- *Individually processed measurements*

Each set of information collected per antenna ($\mu_{\alpha,\tau}^{Prx}$) would be the input data of its indoor positioning system. There will be as many positioning systems as number of antennas in the receiver.

- *Fusion method 1: Measurements fusion*

The aim of this method is to collect all the fingerprinting and current measurements gathered from each antenna to be lately processed in a single indoor positioning system. This is depicted on the vertical flow of *fusion method 1* and top horizontal scheme in Figure 4.2. Now, instead of processing the dataset from each antenna α in an individual indoor positioning system, all the data is processed by one of them (e.g., indoor positioning system - 1).

2) Candidates ranking techniques

Different techniques proposed in the literature can be applied to calculate the weights and perform the ranking of all the samples, particularly *Number of RSSI matches*, *Bayes Classifier* or *Euclidean Distance*. Focusing on the multi-antenna case (all the information collected from each single-antenna receiver is processed by a single indoor positioning system), these techniques are described below.

- **Technique 1:** *Number of RSSI matches*

The indoor positioning system performs the ranked candidates by means of calculating the number of matches between the current measurements and the fingerprinting ones:
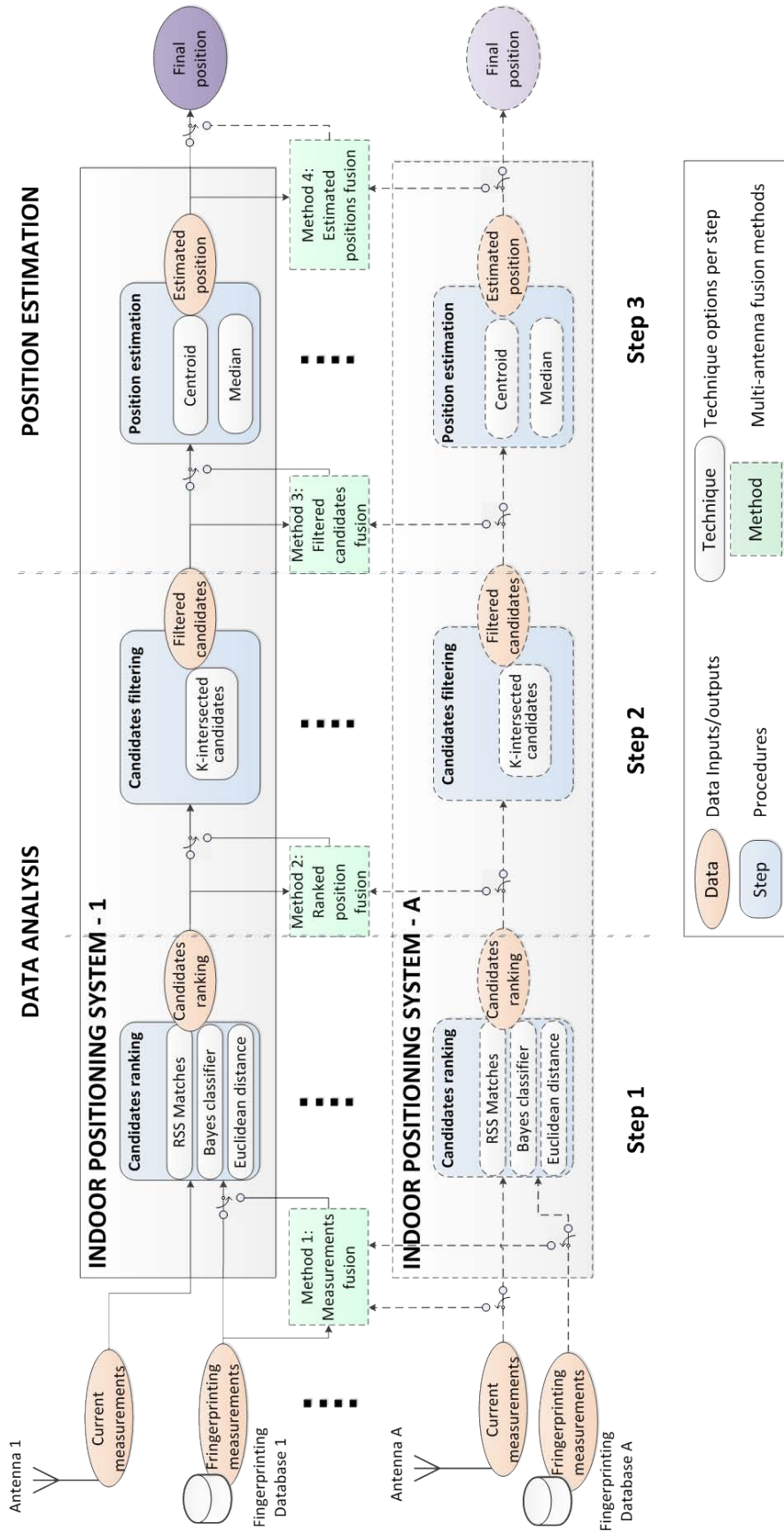
Figure 4.2: Flowchart of the RFID-based positioning systems.

$$match_{Prx_{\alpha,\tau}}(\gamma_f, \gamma_{curr}) =$$

$$= \begin{cases} 1 & if\ \mu_{\alpha,\tau}^{Prx}(\gamma_{curr}) \in \left[\mu_{\alpha,\tau}^{Prx}(\gamma_f) - \Delta Prx,\ \ \mu_{\alpha,\tau}^{Prx}(\gamma_f) + \Delta Prx\right], \\ 0 & otherwise \end{cases} \qquad (4.1)$$

where $\mu_{\alpha,\tau}^{Prx}(\gamma_{curr})$ is the average RSSI from the transmitter τ in antenna α. This data is the mean of the values received during the *acquisition time* in γ_{curr}. The *acquisition time* is the period the reader is collected information before the position is calculated. A tolerance margin ΔPrx is defined to leave some flexibility in the comparison.

Finally, the weight assigned to each fingerprinting position based on the measurements of the current position is calculated as the sum of matches:

$$w_{Prx}(\gamma_f,\ \gamma_{curr}) = \sum_{\substack{\forall \tau \in T \\ \forall \alpha \in A}} match_{Prx_{\alpha,\tau}}(\gamma_f, \gamma_{curr}), \qquad (4.2)$$

where A is the set of antennas of the input data and T is the set of transmitters. Note that, in case *fusion method 1* is not selected, each single-antenna indoor positioning system calculates its own weights, and then $|A| = 1$ for each of them.

- ***Technique 2:*** *Bayes Classifier*

In this technique, $w_{Prx}\left(\gamma_f, \gamma_{curr}\right)$ would depend on the probability of being in γ_{curr} given the values of $\mu_{\alpha,\tau}^{Prx}(\gamma_{curr})$. This probability is calculated by means of the *naive Bayes Classifier*, being the equation that defines the classifier as

$$\hat{p}\left(\gamma_{curr} = \gamma_f \middle| \mu_{A,T}^{Prx}(\gamma_{curr})\right) = \frac{\hat{p}(\gamma_f) \prod_{\substack{\forall \tau \in T \\ \forall \alpha \in A}} \hat{p}(\mu_{\alpha,\tau}^{Prx}(\gamma_{curr})|\gamma_f)}{\hat{p}(\mu_{A,T}^{Prx}(\gamma_{curr}))}, \qquad (4.3)$$

where $\mu_{A,T}^{Prx}(\gamma_{curr})$ is the set of all the average RSSI values from all transmitters and antennas of the reader. Note that $|A| = 1$ for single-antenna indoor positioning systems. $\hat{p}(\mu_{\alpha,\tau}^{Prx}(\gamma_{curr})|\gamma_f)$ represents the conditional probability of receiving $\mu_{\alpha,\tau}^{Prx}(\gamma_{curr})$ assuming that the reader is in a specific candidate spot γ_f of the fingerprinting points.

The values of conditional probability are obtained from the precalculated conditional *probability density function* (PDF) of receiving a certain power in each fingerprinting position of the scenario. This function is defined independently for each transmitter and antenna considering a normal distribution with mean $\mu_{\alpha,\tau}^{Prx}(\gamma_f)$ and a standard deviation of 0.6dB. Laplace smoothing [75] is applied over such initial

conditional probability to avoid given zero likelihood. In this way, given zero weight to suitable candidates just by the incorrect reception of one transmitter is avoided.

The *likelihood of the current evidence* is $\hat{p}(\mu_{\alpha,\tau}^{Prx}(\gamma_{curr}))$, which is equal to all positions. Therefore, it can be discarded from the equation. Equally, the *prior likelihood* of being in each position $\hat{p}(\gamma_f)$, is assumed equal to all positions. Hence, the weight expression can be simplified as:

$$w_{Prx}(\gamma_f, \gamma_{curr}) = \prod_{\substack{\forall \tau \in T \\ \forall \alpha \in A}} \hat{p}(\mu_{\alpha,\tau}^{Prx}(\gamma_{curr}) | \gamma_f). \tag{4.4}$$

- **Technique 3:** *Euclidean Distance*

The *Euclidean Distance* technique is well-known in the literature [76]. The Euclidean Distance between the set of RSSI in γ_{curr} for all transmitters and antennas of the reader and the ones stored for each fingerprinting position, are calculated. The coordinates of a position in the established Euclidean space is defined by the set of values of average RSSI. Integrating the multiple transmitters and antennas of the reader, each dimension of this space corresponds to one transmitter and antenna. This provides a Euclidean space of $|T||A|$ dimensions.

Therefore, in this space the coordinates of any position γ (fingerprinting or current position) are defined as follows. In case of single-antenna indoor positioning systems, $|A| = 1$.

$$\mu_{A,T}^{Prx}(\gamma) = \begin{pmatrix} \mu_{1,1}^{Prx}(\gamma) & \cdots & \mu_{1,|T|}^{Prx}(\gamma) \\ \vdots & \ddots & \vdots \\ \mu_{|A|,1}^{Prx}(\gamma) & \cdots & \mu_{|A|,|T|}^{Prx}(\gamma) \end{pmatrix}. \tag{4.5}$$

Finally, the Euclidean Distance between $\mu_{A,T}^{Prx}(\gamma_{curr})$ and each $\mu_{A,T}^{Prx}(\gamma_f)$ are calculated and assigned as the weight of the candidate γ_f as

$$w_{Prx}(\gamma_f, \gamma_{curr}) = \sqrt{\sum_{\substack{\forall \tau \in T \\ \forall \alpha \in A}} \left(\mu_{\alpha,\tau}^{Prx}(\gamma_{curr}) - \mu_{\alpha,\tau}^{Prx}(\gamma_f) \right)^2}. \tag{4.6}$$

4.4.2.2   Step 2: Candidates filtering

This step processes the ranked candidates proposed by step 1. Firstly, the input data is gathered. After that, a technique is selected to filter and discard useless ranked candidates. The outputs of this step are the most probable candidates.

1) Inputs

Inputs could be either the ranked candidates from *step 1* (each single-antenna positioning system processes its own information) or all the ranked candidates of each indoor positioning system which will be processed together in the same indoor positioning system:

- *Ranked positions per positioning system*

Each set of ranked positions $(w(\gamma_f, \gamma_{curr}))$ of each indoor positioning system would be the input data of its own *step 2*.

- *Fusion method 2: Ranked positions fusion*

The aim of this method is to collect all the ranked positions from each indoor positioning system to be lately processed in a single indoor system. This is depicted on the vertical flow of *fusion method 2* and top horizontal scheme in Figure 4.3.
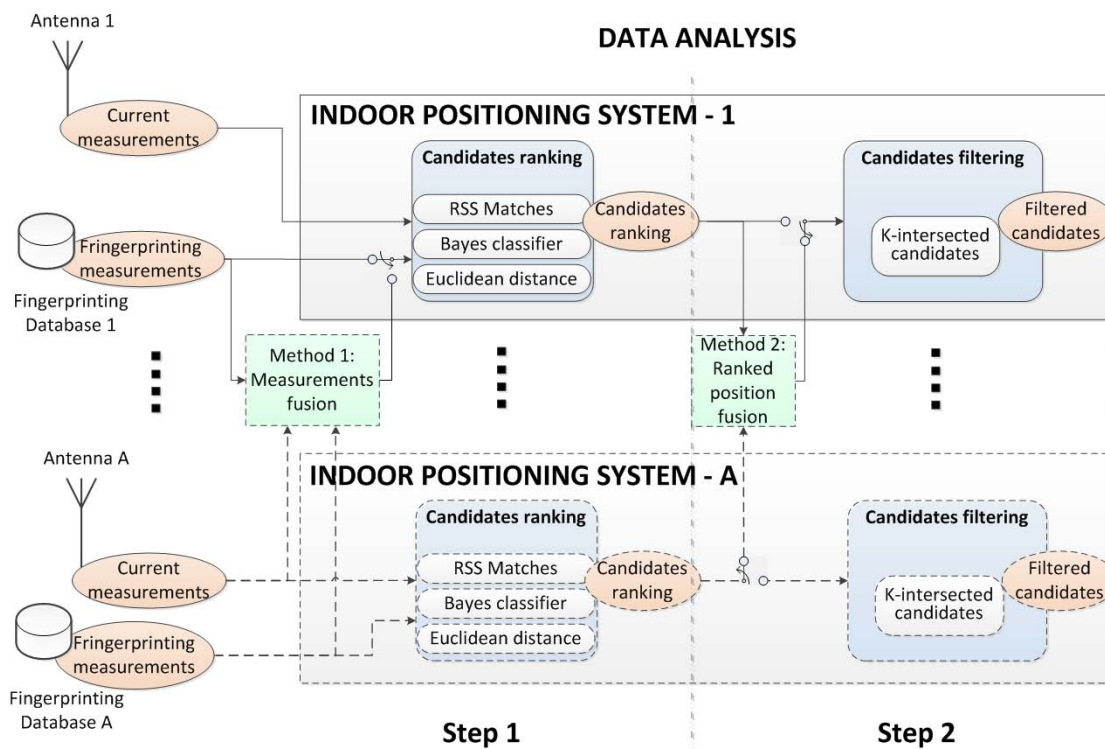
Figure 4.3: Fusion method 2 – Ranked position fusion.

In this way, the inputs of the *fusion method 2* would be the set of ranked candidates $w_\alpha(\Gamma_f, \gamma_{curr})$ from each indoor positioning system (from *step 1*):

$$\{w_1(\Gamma_f, \gamma_{curr}), w_2(\Gamma_f, \gamma_{curr}), \dots, w_{|A|}(\Gamma_f, \gamma_{curr})\}, \tag{4.7}$$

where Γ_f represents the set of all the fingerprinting positions. The output of the *fusion method 2* would be $w_A(\Gamma_f, \gamma_{curr})$, where the weight for each fingerprinting position is assigned as:

$$w_A(\gamma_f, \gamma_{curr}) = \frac{1}{|A|} \sum_{\forall \alpha \in A} w_\alpha(\gamma_f, \gamma_{curr}). \tag{4.8}$$

2) Candidates filtering techniques

Depending on these weights, the list of candidates is filtered. The technique of *k-intersected candidates* is selected. The filtered candidates, $\Gamma_f^{filt}(\gamma_{curr})$, are those with the k highest weights. Those candidates with weights equal to the maximum weight achieved $\max[w(\Gamma_f, \gamma_{curr})]$ and the subsequent *k-1* lower levels are selected. This implies that the number of candidates in the filtered set is equal or higher than k: $\left|\Gamma_f^{filt}(\gamma_{curr})\right| \geq k$.

4.4.2.3   Step 3: Position estimation

The last step calculates the estimated position based on the list of filtered candidates. Firstly, the input data is gathered. After that, a technique is selected to estimate the position from the current measurements. The outputs of this step could be the estimated position or several estimated positions (one per positioning system).

1) Inputs

Inputs could be either the filtered candidates from *step 2* (each indoor positioning system processes its own information) or all the filtered candidates of each indoor positioning system which will be processed together in the same indoor positioning system (*fusion method 3*).

- *Filtered candidates per positioning system*

Each set of candidate positions ($\Gamma_f^{filt}(\gamma_{curr})$) of each indoor positioning system would be the input data of its own *step 3*.

- *Fusion method 3: Filtered candidates fusion*

This method is used considering that the candidates were ranked and filtered individually by each positioning system. The aim of this method is to collect all the candidate positions from each indoor positioning system to be lately processed in a single indoor positioning system. This is depicted on the vertical flow of *fusion method 3* and top horizontal scheme in Figure 4.2.

In that case, the set of candidates is built by the union of the sets of filtered candidates, discarding the repeated elements:

$$\Gamma_{f,A}^{filt}(\gamma_{curr}) = \bigcup_{\forall \alpha \in A} \Gamma_{f,\alpha}^{filt}(\gamma_{curr}) \tag{4.9}$$

2) Position estimation techniques

With the candidates, the estimated current position of the device, $\hat{\gamma}_{curr} = \{\hat{x}, \hat{y}\}$ is calculated. Two techniques are analyzed:

- *Centroid (geometric center)*: The estimated position is calculated as the geometric center of the filtered candidates. Assuming a fixed height, the estimated coordinates of the position are calculated as:

$$\hat{x} = \frac{1}{\left|\Gamma_{f,A}^{filt}(\gamma_{curr})\right|} \sum_{x_f \in X_f^{filt}} x_f \quad ; \quad \hat{y} = \frac{1}{\left|\Gamma_{f,A}^{filt}(\gamma_{curr})\right|} \sum_{y_f \in Y_f^{filt}} y_f \tag{4.10}$$

where $x_f \in X_f^{filt}$ and $y_f \in Y_f^{filt}$ are the x and y coordinates of $\Gamma_{f,A}^{filt}$.

- *Median*: The position is estimated by the median of each coordinate of the filtered candidates.

3) Output

In case the configuration of the indoor positioning system is set to process the information collected by each antenna individually, i.e., none of previous *fusion methods* are triggered, several estimated positions are proposed (one per positioning system). Now, *fusion method 4* would be in charge of estimate the final position.

- *Fusion method 4: Estimated positions fusion*

Fusion method 4 is performed after the *step 3* by calculating the geometric center or median (as *step 3*) of the set of the different estimated positions proposed by each indoor positioning system: $\hat{\gamma}_{curr}^{A} = \{\hat{\gamma}_{curr}^{\alpha 1}, \hat{\gamma}_{curr}^{\alpha 2}, \hat{\gamma}_{curr}^{\alpha 3}, \dots\}$.

4.4.3   Cellular technology into RFID-based positioning system

A new scheme for enhancing the proposed RFID-based indoor positioning system with cellular technologies is proposed in Figure 4.4. The aim of this approach is to analyze and study the advantages of having both cellular and RFID signals at low cost. The proposed cellular-based positioning system follows the same scheme and steps as the one proposed for the RFID-based positioning system (see Figure 4.1 and Figure 4.2).

According to the study carried out in *Appendix B*, the cell identifier (ID) has shown the most promising qualities for the proposed system instead of the PRX from each cellular antenna, so it would be the key input for this system. In this study, a single-antenna indoor positioning system is analyzed.

The *step 1* of the cellular-based indoor positioning system performs the ranked candidates by means of calculating the number of matches between the current measurements and the fingerprinting ones:

$$match_{ID_\alpha}\left(\gamma_f, \gamma_{curr}\right) = \begin{cases} 1 & if\ ID_\alpha(\gamma_{curr}) \cap ID_\alpha(\gamma_f) \neq 0 \\ 0 & otherwise \end{cases}, \tag{4.11}$$

where $ID_\alpha(\gamma_f)$ is the set of received identifiers by antenna α at the fingerprinting position, γ_f, and $ID_\alpha(\gamma_{curr})$ is the set of received identifiers at the current position, γ_{curr}, during the *acquisition time*. The expressions mean that in case both sets shared common identifiers, the match is considered affirmative.

Afterwards, the weight assigned to each fingerprinting position is the same as the matches per fingerprinting position γ_f:

$$w_{ID}(\gamma_f, \gamma_{curr}) = \sum_{\forall \alpha \in A} match_{ID_\alpha}(\gamma_f, \gamma_{curr}). \tag{4.12}$$
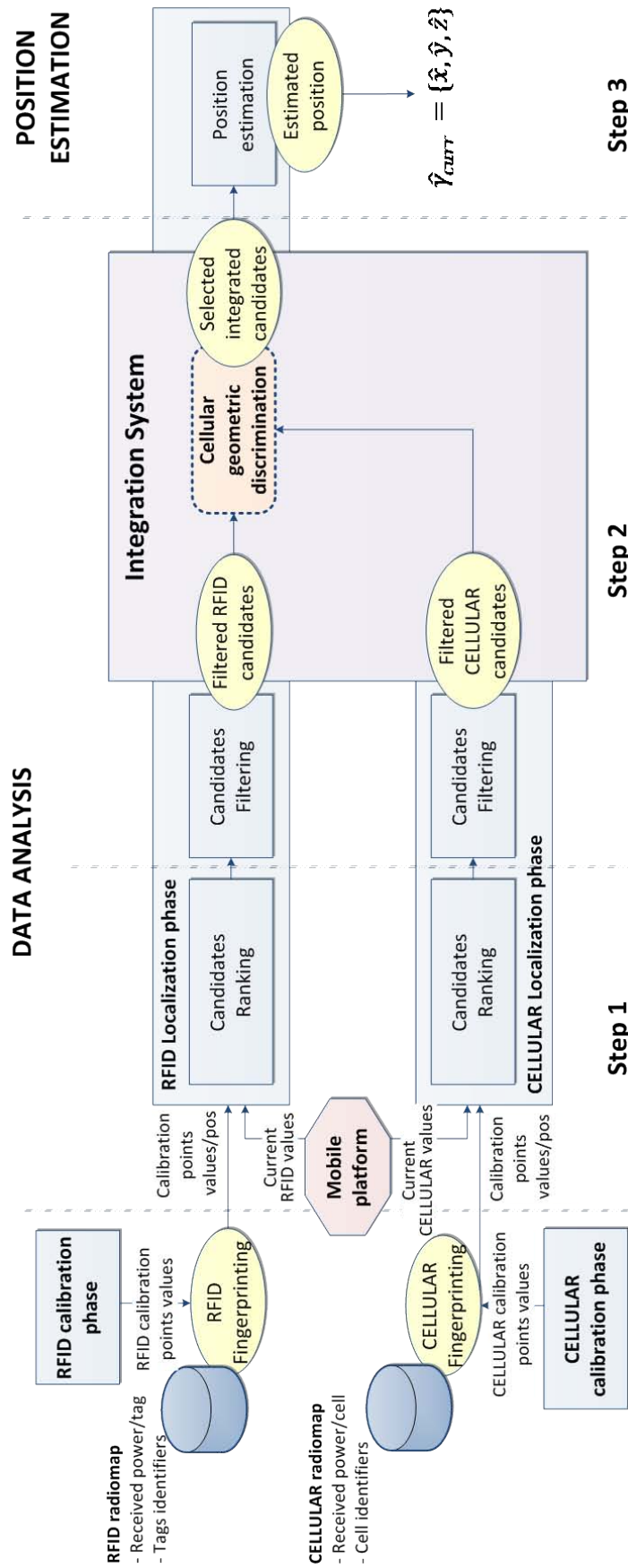
Figure 4.4: Integration of cellular technology into RFID-based positioning system.

The ranked positions are supplied to *step 2* which obtains the most probable candidate positions. Subsequently, these candidate positions from the cellular-based positioning system together with the candidate positions from the RFID-based positioning system are processed by the *Integration system*.

Even if other approaches are possible, this work integrates results from both RFID and cellular systems. These solutions allow a clear comparison of the gain of the integrated system as well as facilitate its integration in already existing services. With this objective, the proposed *Integration system* defines two main steps.

1) Cellular discrimination

The RFID filtered candidates per position $\Gamma_{f,RFID}^{filt}$ are discriminated by the cellular filtered candidates $\Gamma_{f,CELLULAR}^{filt}$ as follows: an area of one squared meter (or maximum distance between two adjacent fingerprinting positions in the cellular calibration phase) is created for each cellular candidate position in order to evaluate if any of the RFID candidates are located inside this area. In this case, that RFID candidate position is selected, whereas any other candidate outside those areas is discarded.

2) Opportunistic localization

Once the new set of candidates has been selected, the estimated position is calculated in the *step 3* by centroid or median metrics.

The cellular-based indoor positioning system is inaccurate itself. Nevertheless, the cellular candidates are used to discriminate aberrant candidates proposed by the RFID-based positioning system rather than adding new possible candidates. In this sense, this discrimination could enhance the solution provided by the RFID system through a reduction of some aberrant of its candidates.

4.5   Evaluation

This section describes the configuration of the scenario, the equipment used and the measurement campaign. Then, the assessment of the proposed indoor positioning systems: RFID-based positioning system, cellular-based positioning system and their integration into a single system, is performed.

4.5.1 Trial set-up

The corridor scenario, the equipment and the measurement campaign are described in the next subsections.

4.5.1.1 Scenario

The selected scenario is a corridor located on the 4th floor of an indoor office building (526 m^2). It is 22.5 m long x 2 m width x 2.5 m height. Standard objects or furniture were not removed from the corridor to assess the proposed systems under real environments conditions and topology. Further visual details about this scenario from both sides of the corridor are depicted in Figure 4.5.
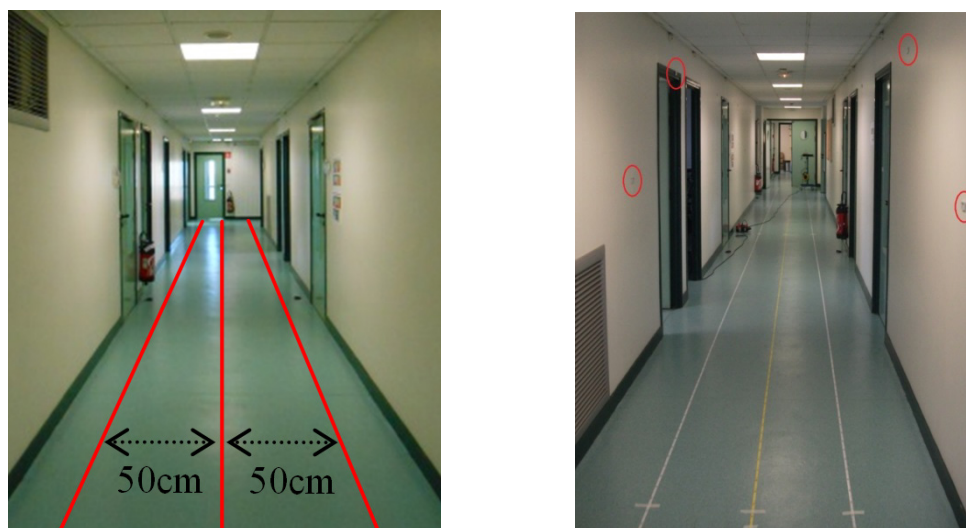
Figure 4.5: Scenario – Corridor.

4.5.1.2 Equipment

The global indoor positioning system scheme is shown in Figure 4.6. Here, a cloud-computing scheme is assumed, where most part of the positioning algorithm computation is performed externally by a remote entity. This is a widely extended approach in positioning systems in order to reduce the computational and storage costs for the device to be located (e.g., smartphone), at the cost of increasing the requirement of maintaining a continuous communication with the external entity. In this scheme, the information transmitted to the external entity can consist just in the RSSI, transmitter/receiver identifiers and timestamp.

4.5.1.2.1   RFID equipment

The UHF RFID technology system works at 433MHz (ISO 18000-7). It is composed by a two-antenna reader and 30 active tags, both from Ela-Innovation [77]. The reader model is "UTPDiff2" with 2 vertical dipole Rx/Tx antennas (see Figure 4.7(b)). Active tags are the "Thinline" model (see Figure 4.7(a)), which could be detected from as far as 20 m in an indoor environment.
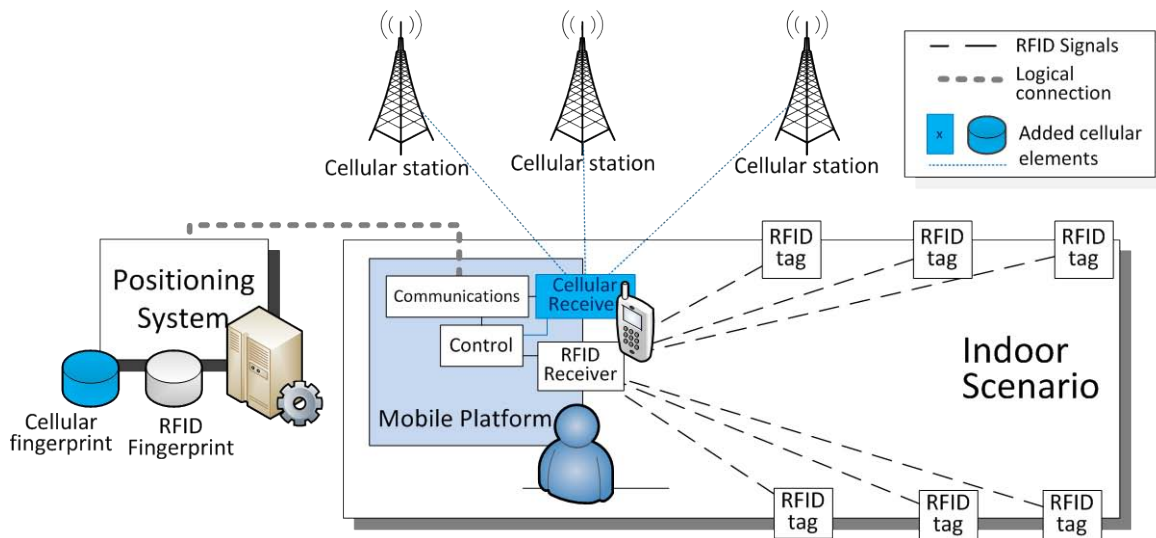
Figure 4.6: RFID-Cellular indoor positioning system scheme.

Measurements collected by the RFID reader are quantified samples. The range goes from level 118 to level 215 in steps of 1 level. This is equivalent to -44 dBm for the lowest level and -106 dBm to the highest level with a resolution of 0.6 dB.
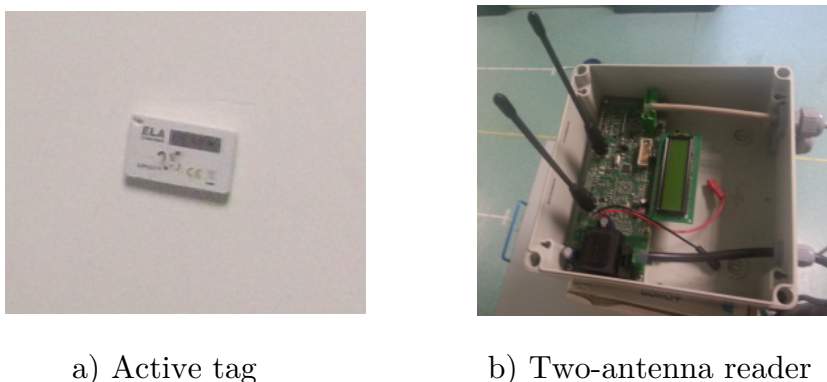
a) Active tag   b) Two-antenna reader

Figure 4.7: RFID equipment.

Active tags were located on the walls of the corridor following a pattern. Some of them are placed at 1.4 m height which corresponds to a doorknob while some others are placed at 2.1 m height, corresponding to a standard door height. The tags are alternatively placed from one height to the other with a distance of 1.5 m between two tags. On both sides of the corridor, a tag is placed at 1.4 m. Figure 4.8 illustrates a scheme of the position of the tags and the layout of the deployment.
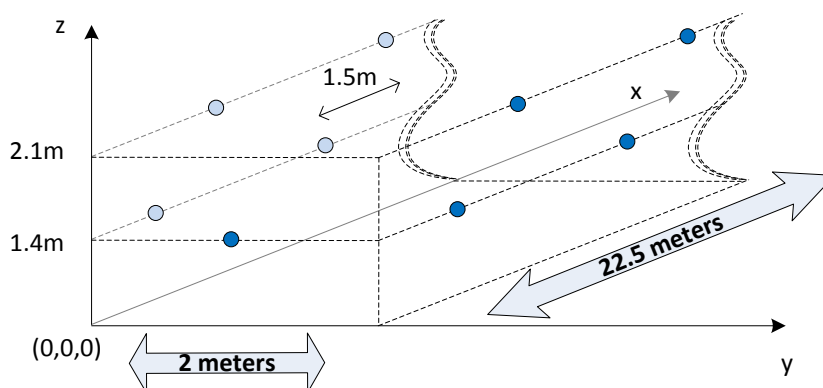
Figure 4.8: RFID active tags position.

Notice that the ceiling is free of tags due to the specific radiation pattern of the two-antennas of the reader. The axis of the dipole has a zero, which means, zero reception on the ceiling-floor line.

4.5.1.2.2   Mobile communications equipment

For cellular network assessment two smartphones were used in the experimental evaluation: *Samsung Galaxy S3* and *Sony Ericsson Xperia X10 Mini E10i* (as it will be later described, the former was used to measure UMTS technology and the later to measure GSM technology). They are widely extended commercial models running *Android 4.2* and *Android 2.1* respectively. Additionally, to measure and record the received power in those devices, a popular free Android application (app) for cellular monitoring, G-MoN [78], was used. This app is a powerful tool for monitoring cellular and other wireless technologies as a drive test tool. It provides cellular network information such as PRX, cell identifier, *Local Area Code* (LAC), etc. Note that, PRX values are averaged at Layer 1 and 3 [79] of the terminal protocol stack minimizing the impact of fast-fading in its values. Therefore, the app reported PRX reflects the path loss and shadowing characteristics of the signal.

4.5.1.3   Mobile platform

The RFID reader and smartphones were placed on top of a trolley as Figure 4.9 depicts. This trolley was the item to be located, referred as the mobile platform. It was moved along the corridor while receivers were reading and collecting information.

Both antennas of the RFID-based system work at 433 MHz and collect samples from each static active tag. Regarding the cellular technology, Samsung smartphone was forced to be camped on UMTS network whose frequency band was 2100 MHz. Likewise, the other smartphone was pushed to be connected to the GSM network at 900 MHz frequency band. LTE networks were only deployed in main cities on the moment of this study. Thus, the analysis of this technology would be a future work.
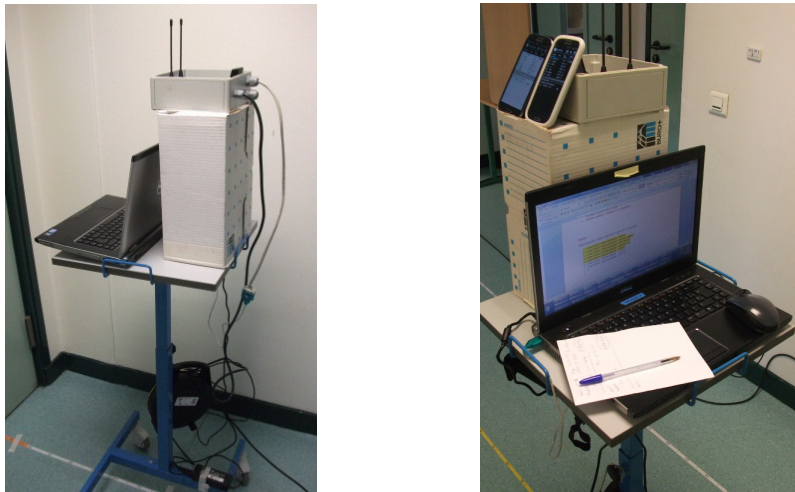
Figure 4.9: Mobile platform.

This technology diversity (433, 900 and 2100 MHz) allows a complete study in indoor conditions in order to enhance positioning systems (see *Appendix B*).

4.5.1.4   Measurement campaign

On the one hand, with the presented RFID equipment, the main parameters that can be measured by the reader in a time slot are:

- *Tag ID:* Numerical identifier of the tags.

- *RSSI:* Quantified received power from a tag. The range is from -44 dBm (level: 118) to -106 dBm (level: 215) with a resolution of 0.6 dB (1 level).

On the other hand, for cellular signals, the main parameters that can be measured by common terminal applications are:

- *Cell ID*: Numerical identifier of the serving cell and neighboring cells.

- *PRX:* Received power from a macrocell. The resolution is 1 dB in the range [-115, -30] dBm.

According to this, a signal assessment of RFID and cellular (GSM and UMTS) systems is performed in *Appendix B* in order to analyze the applicability of these technologies for indoor positioning systems. It is based on the theoretical models of each technology (see *Appendix A*) and a measurement campaign.

Next subsections detail the measurement campaign carried out to collect samples and build the fingerprinting databases, as well as the localization phase of this study.

4.5.1.4.1   RFID-based positioning system

This system is composed by two phases of measurements. The sampling campaign of each phase is explained below.

1) Calibration phase

This phase collects and stores information about RSSI and Tag ID ($\mu_{\alpha,\tau}^{Prx}$) to build the RFID fingerprint model. Firstly, the corridor is divided in a mesh of 75x5 positions (375 positions: 75 positions per line and 5 lines) being the distance of adjacent positions of the same line equal to 30 cms (blue dots in Figure 4.10). Then, the trolley (i.e., two-antenna reader) is placed at each position, sampling and quantifying RSSI measurements. The equipment recorded samples during five minutes per position, which means, the fingerprinting database stores 675000 samples (375 positions, 60 samples per tag/position and 30 tags). These measurements were gathered statically as the period of characterization was large and it is the proper approach for the characterization of each point at calibration phase.

2) Localization phase

Once the fingerprinting database is fully built, the system is able to automatically report the position of the trolley. For this study, the two-antenna reader monitors real time measurements and provides the estimated position of the trolley. Twenty one positions were dynamically estimated along the middle row of the corridor (red dotted line in Figure 4.10), emulating a commercial application. In this context, the

acquisition time at each point is estimated in 5 s while the system takes a mean time less than 0.1 s to calculate the estimated position.
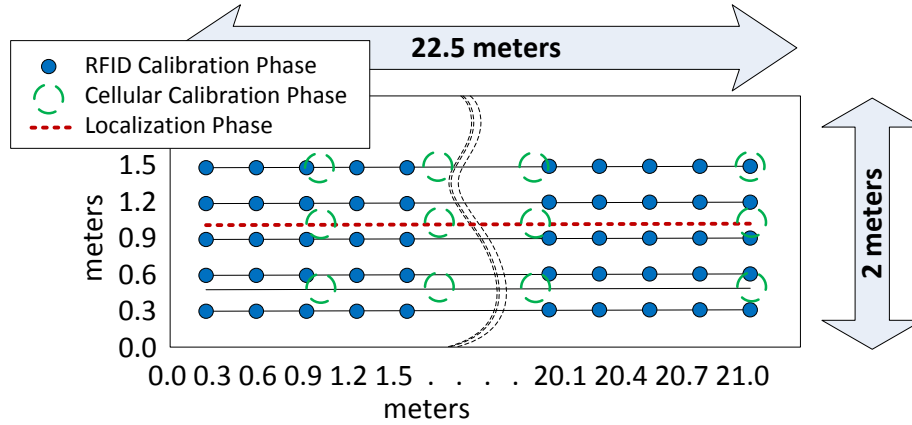
Figure 4.10: Positions.

4.5.1.4.2   Cellular-based positioning system

This system is composed by two phases of measurements as well. The sampling campaign of each phase is explained below.

1) Calibration phase

The measurements are recorded along the corridor every meter following 3 lines on the floor with a distance of 50cm from each other (63 positions) as Figure 4.10 shows (green dotted circles). In this case, the selected parameter is the Cell ID, i.e., the macrocell identifier (ID_α). Therefore, Cell ID information was recorded during five minutes at each point, which implies that around 37800 samples in the whole scenario from the cellular networks (18900 samples per technology GSM or UMTS) were stored.

2) Localization phase

The localization phase was carried out at the same time as RFID localization phase, therefore, it followed the same period as RFID system to collect measurements and similar time to calculate the estimated position (less than 0.1s).

4.5.2   Trial results

The proposed indoor positioning systems (RFID-based and cellular-based), the use of multi-antennas for RFID readers, the influence of the number of active tags and the

achieved synergies due to the integration of cellular technologies in RFID-based positioning systems, are analyzed in the field of heterogeneous localization.

4.5.2.1   RFID-based positioning system

In order to assess the RFID-based indoor positioning system, the *techniques* and *fusion methods* described in subsection 4.4.2 "RFID-based positioning system" are evaluated. Firstly, the study is focused on single-antenna system. Afterwards, the same analysis is performed with two-antenna and different *fusion methods*. Finally, a trade-off between the number of antennas and the number of tags is detailed.

4.5.2.1.1   Single-antenna

The evaluation of this system is carried out in the middle line of the corridor by moving the mobile platform along it (see Figure 4.10). Only one antenna (A1) is used for this study. The error between the real position and the computed positions are calculated for each technique at each step in the *localization phase*: three techniques in *step 1* (with two different tolerance margins for *technique 1* – ±0.3 dB and ±0.9 dB), one technique in *step 2* (with two different *k-intersected candidates* – *k=1* referred as *mic* and *k=5* referred as *kic*) and two techniques in *step 3*. As only information from one antenna is processed, no data fusion (*fusion methods*) is performed.

Figure 4.11 shows the CDF of the position error for the presented *techniques*. Figure 4.11(a) selects the candidates by the "*Number of RSSI matches*" technique (*technique 1*). The tolerance margin is set to ±0.3 dB, i.e., equal values in the quantified RSSI levels of the fingerprinting and the measured positions. The four combinations present similar characteristics, 95th percentile is around 4-5 m.

Figure 4.11(b) also illustrates the results of the "*Number of RSSI matches*" technique. Nevertheless, the tolerance margin is set to ±0.9 dB. In this situation, the 95th percentile of position error is reduced to 3 m when the computed positions are calculated based on *kic* (blue and green lines). In case the *mic* approach is selected, i.e., the maximum intersected candidates are selected (*k=1*), the position error is increased. As observed, there is no significant difference between the *centroid* and the *median* metrics.

Similar behavior is observed in Figure 4.11(c) for the "*Bayes Classifier*" technique (*technique 2*). In case *k=1*, the 95th percentile of position error is around 3 m and

centroid and *median* metrics present the same results because there is only one candidate in the last step. Conversely, when *k=5,* this error is reduced below 2.5 m.

In Figure 4.11(d) the results of the "*Euclidean Distance*" technique (*technique 3*) are depicted. Clearly, this technique shows the best performance compared to the others. It could reduce the 95th percentile of position error to less than 2 m. That error is improved when *k=5* and the *centroid* metric is selected.
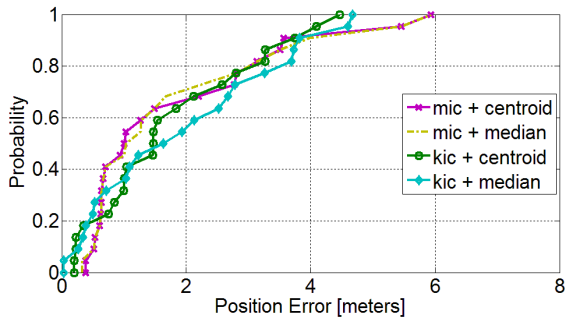
(a) Technique 1 ($\Delta Prx = 0.3$)
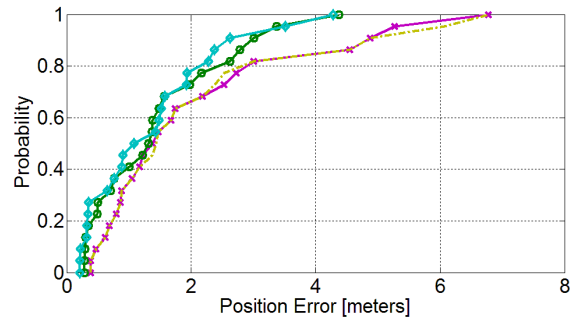
(b) Technique 1 ($\Delta Prx = 0.9$)
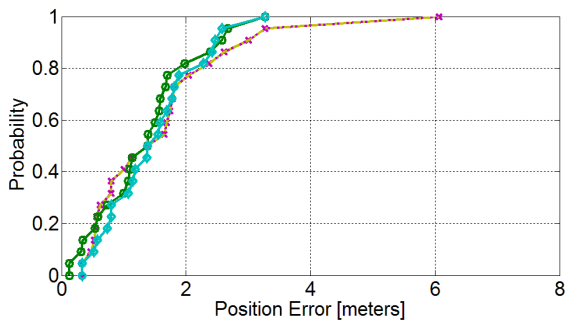
(c) Technique 2 (*Bayes Classifier*)
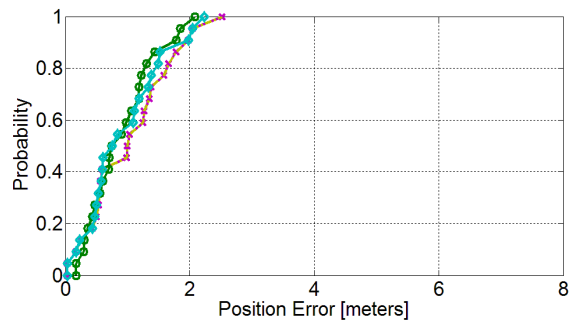
(d) Technique 3 (*Euclidean Distance*)

Figure 4.11: Position error of one antenna (A1).

Focusing on the best techniques of *step 2* and *step 3* (*kic, k=5* and *centroid* metric) with each *technique* of *step 1*, the system performance based on each antenna (A1 and A2) is discussed (see Figure 4.12). "*Bayes Classifier*" and "*Euclidean Distance*" techniques (*techniques 2* and *3*) give the most accurate positions with the 95th percentile of position error bellow 2.5 m and 1.8 m respectively for antenna A1, and 2 m and 1.5 m for antenna A2.

These performances in corridors are as good (or better) than those indoor positioning systems presented in the state-of-the-art. In reference [49], the RSSI-based positioning method showed a 90th percentile of position error around 3.5 m and CSI-based positioning method reduced that error to 1.75 m. Other works RFID-related

presented a higher position error. The 95th percentile of position error is 3 m in [54] where the RFID system is quite similar in terms of hardware to the one proposed here (19 sensors and 19 active RFID reference tags while this work uses 30 active tags). Conversely, the proposed approach presents less than 1.5 m for the 90th percentile.

(a) Antenna 1 (A1)   (b) Antenna 2 (A2)
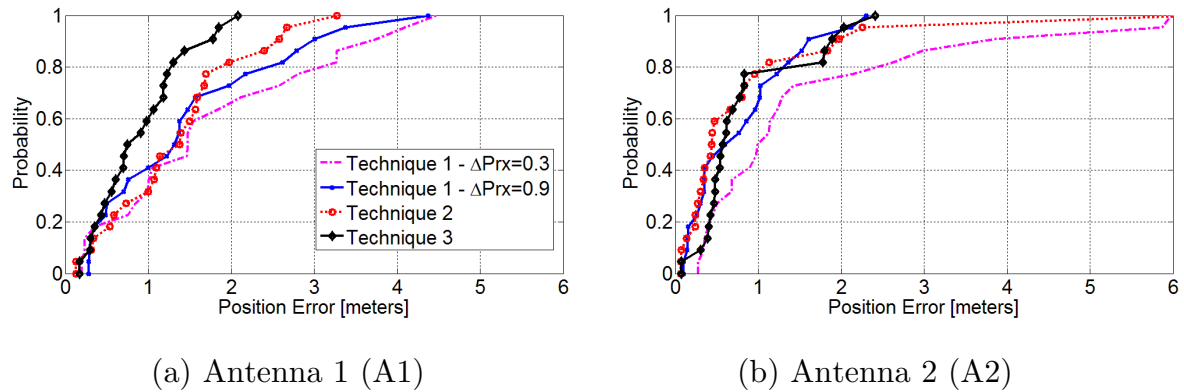
Figure 4.12: Position error of each antenna.

4.5.2.1.2   Two-antenna

The four proposed *methods* for data fusion based on antenna A1 and A2 are assessed. Hereafter, these four methods are tested for each *technique* at *step 1* and the best combination of techniques of *step 2* and *step 3* (*kic*, *k=5,* and *centroid* metric).
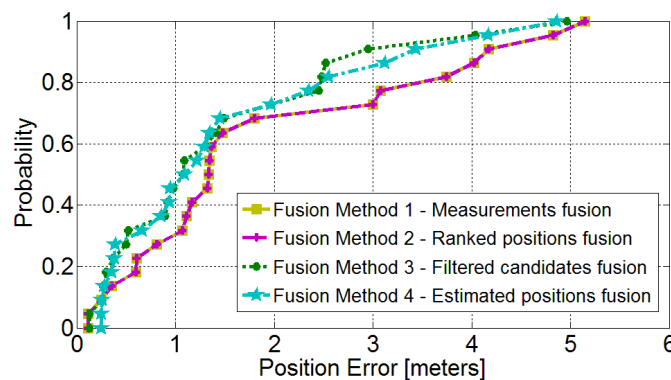
Figure 4.13: Performance of *fusion methods* for *technique 1* - $\Delta Prx = 0.3$.

For the *technique 1* (Figure 4.13), "*Number of RSSI matches*" with $\Delta Prx = 0.3$, *fusion method* 3 and 4 show the lowest position error, an accuracy for the 90th percentile of 2.5 m, while with single antenna the position error was around 4 m for each case (A1 and A2). *Fusion methods* 1 and 2 give the same results because the

input weighted candidates at *step 2* would be same in both cases for this technique (number of matches per fingerprinting position).

For the *technique 1* (Figure 4.14), "*Number of RSSI matches*" with $\Delta Prx = 0.9$, almost all the *fusion methods* have an accuracy for the 90th percentile less than 2 m. This performance is worse than the one obtained with antenna A2 (1.7 m) but better than antenna A1 (3 m). This method suffers from the poor accuracy of antenna A1. Here, *fusion methods* 1 and 2 also give the same results but improve the average position error compared to *fusion methods* 3 and 4.
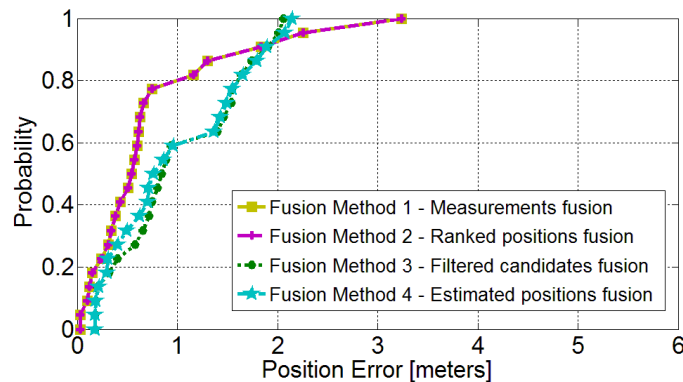
Figure 4.14: Performance of *fusion methods* for *technique 1* - $\Delta Prx = 0.9$.

For the *technique 2* (Figure 4.15) "*Bayes Classifier*", any of the *fusion methods* outperforms the results with a single antenna (accuracy for 90th percentile is 2.6 m for antenna A1 and 2 m for antenna A2). *Fusion method 1* is the best with a 90th percentile of 1.2 m position error. For the other *fusion methods*, the position error is around 1.8 m. Note that, *fusion method* 3 and 4 present the same results: merging the selected candidates and then, calculating the mean position error is equivalent to calculate the position for each antenna and then calculate a mean position error.
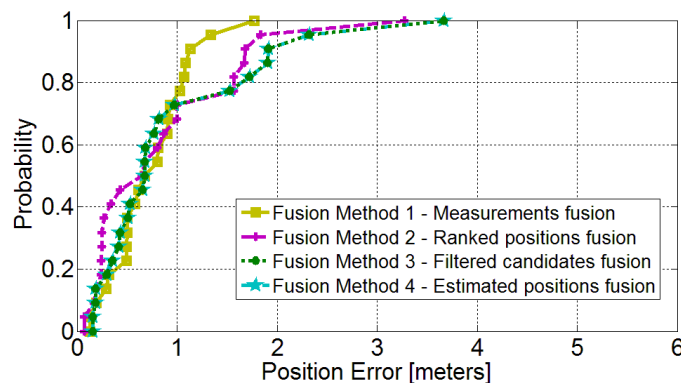
Figure 4.15: Performance of *fusion methods* for *technique 2*.

For the *technique 3* (Figure 4.16), "*Euclidean Distance*", any of the *fusion methods* gives better results than single antenna (around 1.8 m for both antennas). The position error at the 90th percentile is 1.5 m for *fusion method* 1 and 2.
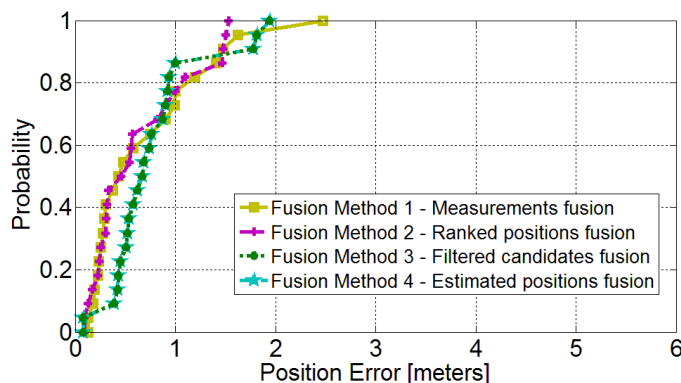
Figure 4.16: Performance of *fusion methods* for *technique 3*.

As a conclusion, *Bayes Classifier* (*technique 2*) and *Measurement fusion* method (*fusion method 1*) presented the lowest position error: the average is 0.75 m and the 90th percentile is around 1.1 m. Comparing these results with multi-antenna systems in the state-of-the-art, the study in [57] showed an average position error of 1.5 m with 3 dB shadowing standard deviation. When increasing the number of antennas from 2 to 14, the position error decreases from 2.3 m to 0.9 m but this performance is still higher than the one of the proposed system with only 2 antennas.

4.5.2.1.3   Number of tags vs number of antennas trade-off

Considering the use case of 30 tags and 15 tags for single and two-antenna system, Figure 4.17 shows the CDF for the best *technique*: *Bayes Classifier* (*technique 2*) and the best *fusion method*: *Measurement fusion* (*fusion method 1*). As aforementioned, the two-antenna configuration for 30 tags has better accuracy (with position error at the 90th percentile bellow 1.5m) than single antenna configuration. In addition, it can be also observed that the same or better accuracy is obtained with two antennas and 15 tags compared to a single antenna and 30 tags. It would reduce the system costs.

In the case of the number of tags is reduced to 6 tags per experiment, the use of the two antennas notably increases the accuracy of the system. The 90th percentile is less than 5m as the red circle-mark line illustrates in Figure 4.18. For one antenna, this value is 8m (black diamond-mark and yellow square-mark lines). Note that the best performance is not as good as the one with 15 tags and one antenna (blue cross-mark

and magenta dashed lines) but 6 tags is less than the half part of 15 tags. The reason to keep 6 tags instead of 7 or 8 is because of the layout of the tags.
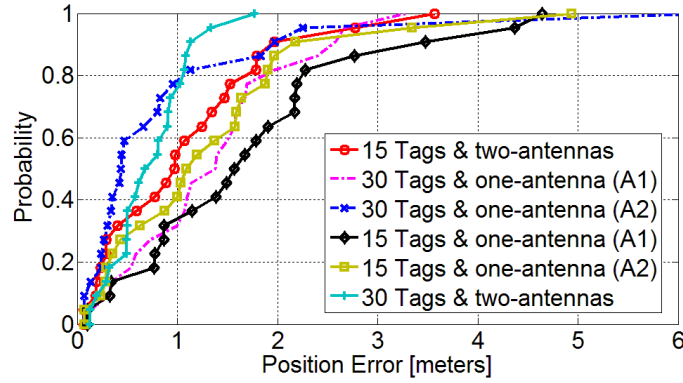
Figure 4.17: 30 tags & 15 tags vs one & two antennas.
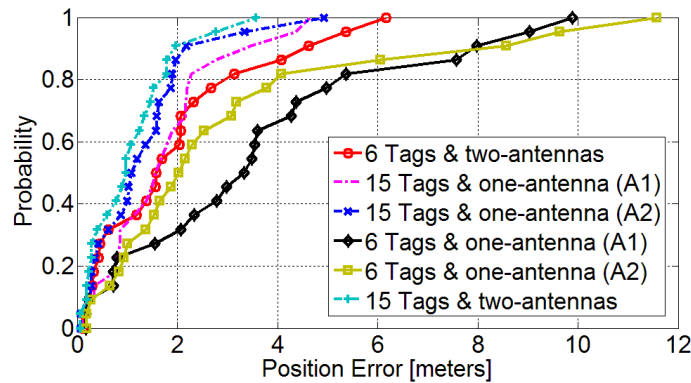
Figure 4.18: 15 tags & 6 tags vs one & two antennas.

Table 4.1 summarizes the mean, the MSE (Mean Square Error) and the 90th percentile of the position error for the different experiments. This table shows that with two antennas, the system accuracy is not the mean of both antennas but the performance indicators (mean, MSE and 90th percentile of the CDF) are much better than the performance indicators for a single-antenna.

Table 4.1: Summary of number of antennas vs number of tags.

	30 tags		30 tags &	15 tags		15 tags &
	A1	**A2**	**two-antennas**	**A1**	**A2**	**two-antennas**
Mean (m)	1.39	0.93	0.75	1.77	1.35	1.1
MSE (m²)	3.90	2.59	1.16	4.56	3.05	1.99
90th percentile (m)	2.58	1.97	1.13	3.47	2.8	1.97

4.5.2.2   Cellular-based positioning system

The evaluation of the cellular-based positioning system is based on the measured Cell IDs (ID_α) of UMTS technology as *Appendix B* concluded. As expected, the accuracy is much lower than RFID-based positioning system. Figure 4.19 shows the CDF of this cellular system where the position error is quite high. The 95th percentile is around 10 m.
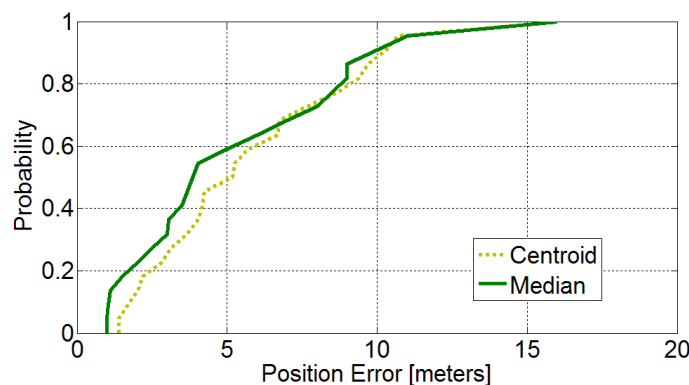
Figure 4.19: Position error of cellular-based positioning system.

As previously mentioned, the cellular candidates are used to discriminate aberrant candidates proposed by the RFID-based positioning system rather than being an indoor positioning system itself.

4.5.2.3   Opportunistic positioning system

The integration of cellular technologies in single-antenna (A1) RFID-based positioning systems is evaluated. The period to calculate the estimated position was established in every 5 s, however, as the algorithms do not involve high computational costs, the position is estimated in 100 ms: 60 ms to get RFID candidates and 35 ms to get cellular candidates (parallel processes could reduce this time). Table 4.2 compares the results obtained with the RFID-based positioning system to the opportunistic positioning technique. Only *centroid* metric has been included in the table.

On the one hand, for the RFID system the mean position error is below 2 m and the 95th percentile is around 4 m for *technique 1* ($\Delta Prx = 0.3$ and $\Delta Prx = 0.9$). On the other hand, the integration of cellular information into the discrimination procedure, discards some candidates that could be far away from the real position. Thanks to it, the proposed system is able to reduce the mean position error 15-25% in comparison to

the RFID-based positioning system. This enhancement provides mean position error values from 1.1 to 1.8 m. In the same context, the 95th percentile is reduced, reaching values from 2.2 m to 3.7 m. The "*Bayes Classifier*" and "*Euclidean Distance*" techniques are slightly improved when more than one candidate is selected (*kic, k=5*). In other case (*k=1, mic*), there is only one candidate and this opportunistic approach is not practical. For the best technique (Euclidean Distance, *kic*), results show 1.4 m for the 80th percentile and 1.8 m for the 95th percentile.

Table 4.2: Summary of indoor positioning systems performance.

	Technique 1 ($\Delta Prx = 0.3$)		Technique 1 ($\Delta Prx = 0.9$)		Technique 2		Technique 3	
	mic	kic	mic	kic	mic	kic	mic	kic
RFID System Mean absolute error (m)	1.9	1.8	2.1	1.3	1.6	1.3	1.1	0.9
RFID System MSE	6.7	5.9	7.4	4.5	5.6	3.9	3.6	3.1
RFID System 95th percentile	5.5	4.1	5.3	3.5	3.4	2.6	2.0	1.9
Oportunistic System Mean absolute error (m)	1.5	1.4	1.8	1.1	1.6	1.2	1.1	0.9
Oportunistic System MSE	5.5	4.0	5.8	3.7	5.6	3.7	3.6	3.0
Oportunistic System 95th percentile	3.2	3	3.7	2.2	3.4	2.5	2.0	1.8

Compared to other positioning systems with more than one technology in the state-of-the-art, the work presented in [69] had a position error of 4 m at 90th percentile. Other works like in [63] had a mean position error of 1.5 m. Showing these results, the proposed system outperforms both of them, having a mean position error of 0.9 m and 1.8 m for the 95th percentile. Focusing on corridors, this approach outperforms the system proposed in [51] where the mean position error was 5.9 m compared to 0.9 m.

4.5.2.3.1   Sensitivity study of number of tags

A sensitivity study has been performed to evaluate this approach in the same scenario with a low-dense number of tags. The number of tags has been reduced according to 1/2, 1/3 and 1/5 from the original amount (30 tags). Table 4.3 and Table 4.4 present the MSE of the RFID system and the proposed system respectively. It could be observed in both tables how the less number of tags are placed, the worse

values are obtained. Furthermore, with high density of tags, cellular technology improves the location accuracy over the RFID system. However, when the number of tags is extremely reduced, the influence of cellular technology does not enhance the location error as much as expected. The reason is related with the low number of candidates the RFID system proposes. Therefore, the discrimination of cellular technology is much more limited to those candidates.

Table 4.3: Sensitivity study of RFID system based on the number of tags (MSE).

RFID System MSE	Technique 1 ($\Delta Prx = 0.3$)		Technique 1 ($\Delta Prx = 0.9$)		Technique 2		Technique 3	
	mic	kic	mic	kic	mic	kic	mic	kic
30 tags (ratio 1)	6.7	5.9	7.4	4.5	5.6	3.9	3.6	3.1
15 tags (ratio 1/2)	15.6	9.9	9.1	6.5	9.2	6.0	5.6	4.8
10 tags (ratio 1/3)	24.4	20.8	14.3	11.0	13.5	10.9	9.8	8.7
6 tags (ratio 1/5)	43.8	38.9	31.7	21.2	26.7	19.6	16.9	14.6

Table 4.4: Sensitivity study based on the number of tags (MSE).

Integrated System MSE	Technique 1 ($\Delta Prx = 0.3$)		Technique 1 ($\Delta Prx = 0.9$)		Technique 2		Technique 3	
	mic	kic	mic	kic	mic	kic	mic	kic
30 tags (ratio 1)	5.5	4.0	5.8	3.7	5.6	3.7	3.6	3.0
15 tags (ratio 1/2)	15.0	9.1	9.1	5.9	9.2	5.8	5.6	5.1
10 tags (ratio 1/3)	23.1	11.8	12.2	8.1	13.5	10.7	9.8	9.6
6 tags (ratio 1/5)	40.0	38.8	27.9	19.5	26.7	18.5	16.9	15.8

4.5.3 Considerations for real deployments

By the time of this work, cost of each active tag is in the range of tens of USDs (United States dollars) while a RFID reader rounds few hundred USDs costs. Therefore, the defined RFID system is based on the distribution of RFID tags in the infrastructure, while the localized platform (e.g., pedestrian equipment) to be positioned is provided with a RFID tag reader, which is the optimal solution if a reasonable amount of mobile devices are to be localized in a wide and complex area. In this way, the infrastructure costs are minimized, while placing the cost in the positioned object. This greatly reduces installation costs and allows the implementation of the system in large areas at minimum expense. Additionally, the commercial penetration of portable RFID readers is growing, being also included in mobile phones as peripherals or embedded systems [80]. In any case, scenarios where

the located system is equipped with RFID active tags instead of a transceiver (being the transceivers part of the fixed infrastructure of the scenario) are also possible [81] [82], keeping the same general scheme and conditions in terms of performance and architectural needs.

In order to cover an entire floor of a public building of some hundreds square meters with passive tags, a few hundreds readers must be deployed, as their read range is 1-3 m. Using active tags allows to cover a whole floor, without increasing the total number of tags. Further studies on the optimal number of tags and their placement are being carried out for the corridor [83] and the entire floor. Therefore, active RFID solution still cost effective when covering large areas even if we locate a hundred of mobile readers.

In the proposed approach, the main elements of classical architectures for RFID-based positioning are maintained: a remote localization server performs the calculation of the position based on the signals received from the RFID tags and the previously stored fingerprinting data. The only additions to this classic structure imply the inclusion of cellular signal fingerprint information as part of the localization server databases and the existence of a cellular receiver as part of the localized platform. The cellular receiver may be already part of the localized platform (e.g., for communications reasons). Otherwise, adding the cellular receiver to the previously existing pure RFID platforms can be done at a very low cost due to the wide popularity of the cellular technology: a low-budget smartphone may be enough. Additionally, the increasing availability of RFID commercial portable readers for active RFID tags could make this approach even more accessible for pedestrian applications in the close future.

The acquisition of cellular technologies fingerprinting data should also not suppose any significant cost in terms of the calibration phase, as the cellular scenario characterization can be performed simultaneously to the RFID one.

A shortcoming of the proposed system is that if the cellular infrastructure changes due to modifications done by operators (e.g., change of configuration parameters) or failure, the accuracy of the cellular based discrimination can be jeopardized and a new calibration phase may be required. This is the same case as for changes in the RFID infrastructure, but the latter are usually more accessible and under the control of local administrators. In order to overcome this challenge, coordination between the mobile operator and the positioning system should be defined, fitting in the initiated process by cellular standardization aiming to integrate localization (including the one coming from third party solutions) as part of the standard architecture interfaces [84].

Another issue arises when the indoor area is covered by only one (or few) base stations, which makes the cellular information useless or not be as helpful as expected. However, the experience has shown that most time a certain level of signal is received from several cells simultaneously (it does not mean the quality of the signal is appropriate to attempt a call) or cellular technologies. Furthermore, the increasing deployments of small cells will help to further avoid this restriction.

To conclude, the use of common application layer apps for the mobile terminal is assumed as the source of signal information. However, one of the main limitations of some terminals (due to their manufacturers) is their inability to report information about neighbor cells (e.g., PRX, Cell ID, etc.). That issue would affect the fingerprinting procedure as it could suffer from lack of information. However, handover/cell-reselection process would be useful in order to overcome this lack of information from several cells. Regarding this issue, this study has taken into account that restriction, focusing on this kind of terminals (e.g., Samsung) as a high percentage of smartphones has this limitation.

4.6   Conclusions

An active UHF RFID-based positioning solution in a corridor has been analyzed. Several techniques and data fusion methods for multi-antenna reader and the fundamentals for innovative and opportunistic use of GSM and UMTS technologies with these systems have been presented.

The approach is evaluated in a real corridor field-trial, comparing the position error of single-antenna and two-antenna readers, for different positioning techniques (*number of RSSI matches*, *Bayesian Classifier* and *Euclidean Distance*) and applying the proposed method for multi-antenna data fusion (measurements, ranked candidates, filtered candidates and estimated positions). The best results with the multi-antenna approach are obtained with a *Bayes Classifier* and measurements fusion. In this case, the achieved mean position error is 0.75 m and the 90th percentile is 1.1 m. The proposed solution achieves better accuracy than previous RFID solutions experimented in corridors, even with other technologies and indoors scenarios.

Additionally, a trade-off between the number of antennas and the number of tags has been presented. This study shows that the two-antenna approach can provide equivalent accuracy as single-antenna approach but half number of tags in the infrastructure.

Finally, the analysis assesses the possibilities of using signals coming from already existent non-positioning oriented cellular networks to provide support to RFID-based indoor positioning mechanisms, which could highly benefit of such pre-existent communications infrastructure. Furthermore, the use of a first-approach, fingerprinting mechanism for positioning shows promising results in terms of accuracy enhancement.

Chapter 5

Indoor mobility load balancing techniques

This chapter is focused on the development of novel MLB mechanisms to mitigate temporary traffic fluctuations and focused network congestion issues in open access LTE femtocell networks in commercial and corporate environments.

The structure of this chapter is as follows: Section 5.1 introduces MLB techniques in indoor scenarios. Section 5.2 details the related work. Section 5.3 formulates the problem description. Section 5.4 describes some MLB mechanisms for corporate femtocell networks. In addition, Section 5.5 presents the design of innovative MLB mechanisms based on context information. Section 5.6 and Section 5.7 evaluates the proposed methods in a simulator and field trials, respectively. Finally, Section 5.8 summarizes the main conclusions of this chapter.

5.1   Introduction

Most cellular communications take place at indoor environments (at work, home, shopping malls, etc.) [1] [10], especially in commercial and corporate scenarios. Hence, operators tend to deploy small cells, such as femtocells, indoors to enhance network capacity, to reduce outage coverage areas, to provide high-speed data traffic, etc.

In this indoor scenarios, voice calls and data traffic, as well as local user densities, vary in temporal and spatial domain. Those situations lead to degraded indoor cellular networks because many people want to use their mobile devices at the same time, close to the same area and/or for a short period. For example, people waiting for a delayed flight at the boarding gate of the airport could collapse a femtocell for a while or, a

celebrity walking through a mall where everybody is interested in taking pictures and sharing them instantaneously in social networks or calling friends to share the experience. A simple solution to support these extreme situations could be to plan the network resources according to the peak traffic. Nevertheless, this solution would increase operators' expenditure.

The self-optimization use case of *Mobility Load Balancing* (MLB) has been proposed by 3GPP [45] to solve these situations. MLB use case aims to shift users from overloaded cells to other cells with spare resources. These MLB techniques tune network configuration parameters to reach a better configuration that alleviates the congestion situation. Focusing on indoor and femtocell environments, the following parameters are mainly modified: 1) femtocells handover margins to resize service areas and/or 2) femtocells transmission powers to resize cell coverage areas.

Compared to traditional macrocells, femtocells are simple and efficient access points which present hardware restriction in the number of simultaneous active users. This means, the number of active users is usually limited from 2 to 64 by power of two (depending on the femtocell model [31]). As usual, the number of users that can be properly served also depends on the availability of radio resources of the cell. However, the limitation in the maximum number of connected users is commonly much more critical than the availability of resources, since the bandwidth normally supports higher number of simultaneous users than the femtocell is able to manage.

SON mechanisms are commonly based on network alarms, counters and *KPIs*, or estimated information from radio propagation models. However, nowadays, smart-devices and its embedded sensors (e.g., accelerometers, gyroscopes, etc.) and applications, measure and provide additional context information such as users' position, WiFi *Service Set IDentifier* (SSID), temperature, etc., that could be used by SON mechanisms to both accelerate their convergence and improve their performance. Focusing on users' position, that information could be easily obtained at indoor environments thanks to the immediate interest on indoor LBS. That means, new key location-aware applications for emergency response, advertising, healthcare, domotics, etc. are showing up. Based on this, indoor positioning mechanisms have to evolve in order to be accurate and robust systems, being a hot topic in both academia and industry (e.g., Google Maps - Indoor).

Additionally, classical MLB methods might not properly work in indoor femtocell networks due to the special characteristics of femtocells (restriction in the number of users per femtocell, unplanned deployments, short-range, etc.), indoor environments characteristics (multi-path reflections, occasional events, etc.) or users' indoor mobility pattern (increase number of handovers, etc.). Hence, the development of new MLB

mechanisms based on context information from external mobile network sources might improve the performance in commercial and corporate environments.

The main contributions of this chapter are:

- The design of innovative MLB mechanisms in commercial and corporate LTE femtocell networks with open access.

- The integration of context-aware information into novel MLB methods.

- The reduction of temporal and focused overloaded situations at commercial and corporate indoor scenarios due to the high concentration of users in temporal and spatial domain.

- The estimation of the impact of indoor positioning system accuracy on the designed location-aware MLB mechanisms.

Finally, the proposed SON methods are discussed and compared in both, simulator and field trial scenarios to evaluate their capabilities.

5.2   Related work

Among SON techniques and focusing on self-optimization mechanisms, several works have been centered on the macrocell case in both, literature and European projects [7] [8] [9]. By contrast, indoor environments present hard and difficult conditions to manage the cellular network due to the cell overlapping, lack of coverage, interference, etc. This implies a challenge for researchers and engineers in the development of SON mechanisms. In this sense, self-x techniques in femtocell networks are currently a hot topic [12] [13] [14] [85] [86] [87] [88] [89] [90].

MLB mechanisms have been also widely studied by both, academia and industry, at outdoor and indoor scenarios [4] [5] [6] [15] [16] [17] [91] [92] [93] [94] [95]. The most suitable solution to reduce or avoid cellular congestion situations is by resizing the cell coverage areas. It could be addressed from two ways: tuning physical parameters in the cell (e.g., antenna tilt [96] or pilot transmission power [94]) or changing parameters in *Radio Resource Management* (RRM) processes (e.g., handover, HO, [92] or cell reselection, CR, [97] parameters). The best configuration parameters could be found by formulating classical optimization problems [18]. However, information to build the analytic models is rarely available, thus, the operators use heuristic methods.

Concerning MLB mechanisms in corporate femtocell environments, simple and low-complexity methods based on FLCs are proposed in [15], which investigated the

problem of re-distributing traffic demand between LTE femtocells. A similar fuzzy logic approach is presented in [16], where cell transmission power and handover margins are tuned to solve congestion problems on traffic distribution in enterprise LTE environments. A more computationally complex method [17] obtained better performance than previous studies through a fuzzy rule-based reinforcement learning system, while reference [95] proposed a distributed method to achieve automatic load balancing based on a flowing water method. However, none of the previous works analyzed the femtocell limitations in the maximum number of simultaneous connected users (macrocells or other type of small cells do not have such a restricted condition), which could degrade the network performance. In addition, those previous works were designed to solve localized and persistent congestion problems since a long time was usually necessary to obtain the optimized parameters, disregarding the challenge related to temporary congestion issues at indoor environments. The femtocell limitation in the maximum number of simultaneous users was taken into account in [88], where a handover algorithm based on the users' speed and QoS was proposed. That work evaluated whether a handover was necessary or not according to the previous metrics (speed and QoS), but the algorithm was not analyzed under overload situations.

Some other mechanisms introduced the use of context information in self-optimization methods. More specifically, in location-awareness, the authors in [18] introduced users' position into the MLB mechanisms to reduce handovers and call blocking rates in overloaded cells by modifying the coverage area. However, it was focused on outdoor UMTS macrocell networks. In [14], a method that adjusted hysteresis margins depending on an estimation of the distance from the cell to the terminal, reduces the number of redundant handovers while keeping the throughput of femtocells as high as possible. But, it did not take into account the number of active users in the femtocells. The work in [94] presented a dynamic power control for balancing data traffic in femtocell networks. It built Voronoi diagrams based on COST231 multi-wall radio propagation model to estimate the data traffic per femtocell based on the users' position. However, the integration of this mechanism into a real environment was limited to the values calculated with the propagation model. Furthermore, it only analyzed the network load in terms of occupied radio resources (traffic volume). Other studies utilized users' position in their SON mechanisms [98] [99] [100]. Nevertheless, those works are out of the scope of MLB use case.

The MLB techniques proposed in this chapter are based on resizing cell areas by modifying cell transmission power. In this context, reference [100] introduced the fingerprinting technique as a method for cellular optimization. It compared the PRX measurements with a propagation model to predict the PRX. However, that work was oriented to outdoor environments. Conversely, the study in [94], as previously

mentioned, was focused on femtocell networks and presented a balancing data traffic method by resizing cell area based on PRX and users' position. The authors in [101] and [102] analyzed the PRX in the handover decision process. Another work [103] applied a sliding window function on the PRX measurements to proceed with the decision. Although some of them analyzed the users' position, none of them took into account the number of active users in the femtocells or the way the users are located in the scenario.

Based on these works, the designed MLB mechanisms will focus on the prevention or reduction of temporary network congestion issues in open access LTE femtocells and commercial or corporate environments. This goal is accomplished by changing cell transmission power, hence, the cell service areas. In addition, the algorithms will be supported by classical mobile network indicators and context information such as users' position to be able to improve the network performance in short period.

5.3   Problem description

Femtocells are proposed as a solution to solve some of the current cellular challenges. Due to the proximity between femtocells and users, the user battery lifetime is increased and the user *Quality of Experience* (QoE) is enhanced. At the same time, operators also reduce CAPEX and OPEX. Nevertheless, femtocell networks present some shortcomings that must be addressed. Some of them are the unpredictable occurrences or occasional events that could provoke unexpected overload conditions in the network. These temporal and spatial variations, combined with the coverage holes and time-variant fading caused by reflections and obstacles, could negatively affect network performance.

5.3.1   Operators' policy

From the point of view of femtocell versus macrocell use, the operators could decide two different policies. On the one hand, the operator could be interested in a macrocell offload solution where macrocell data traffic hands over to femocells (when possible) to increase network capacity. Hence, once the femtocell is full (e.g., the maximum capacity of active users is reached), new incoming voice calls (e.g., VoLTE - Voice over LTE) that attempt to access are redirected to the macrocell, while the incoming data connections are accepted after handing over a voice traffic call to the macrocell. That situation could block many voice calls if the quality of the macrocell signal is poor indoors.

On the other hand, other operators could conversely decide that femtocell deployments are aimed at enhancing the signal quality and extend the coverage at indoor environments where the macrocells present bad conditions (coverage holes, poor signal, etc.). According to this policy, the operator would prefer that indoor voice calls are carried out through femtocells and indoor data services hand over to the macrocell. The reason is related to the user point of view. These operators consider that, once the femtocell is full, the client frustration is higher when a voice call is rejected or dropped than when the client has no access to any other service. Therefore, the priority to accept an incoming voice call is higher than to accept data traffic. Consequently, those data connections should hand over to the macrocell when an incoming voice call attempts to access a crowded femtocell.

Additionally, the impact of mobility failures on *VoLTE* calls is discussed in the recent drive test presented in [104], where the *Handover Failure Ratio* (HFR) for pedestrian users is over 21%, which is an unacceptable user experience for operators.

5.3.2   Network configuration parameters

MLB algorithms set different radio configuration parameters to adjust service areas. Consequently, the traffic is shared along the network by handing over those users served by a congested cell to the most suitable neighboring cell with spare resources. The most typical configuration parameters to resize cell areas are:

- **HandOver Margin (HOM)**: The HOM parameter determines the minimum exceeded PRX from a neighboring cell i compared to a serving cell j in order to trigger a power budget (PBGT) HO from $cell_j$ to $cell_i$. Hence, a PBGT HO is triggered when:

$$\overline{PRX}(cell_i) > \overline{PRX}(cell_j) + HOM(cell_j, cell_i), \qquad (5.1)$$

  where $\overline{PRX}(cell_i)$ and $\overline{PRX}(cell_j)$ are the average PRX from the serving cell j and neighboring cell i in dBm, respectively. $HOM(cell_j, cell_i)$ is the handover margin in dB from cell j to cell i.

  An overloaded cell j could decrease its HOM(j,i) to force users to start the handover process to move to a low-loaded neighboring cell i. For that purpose, the HOM(j,i) should be reduced Δ dB. This MLB technique is illustrated in Figure 5.1.
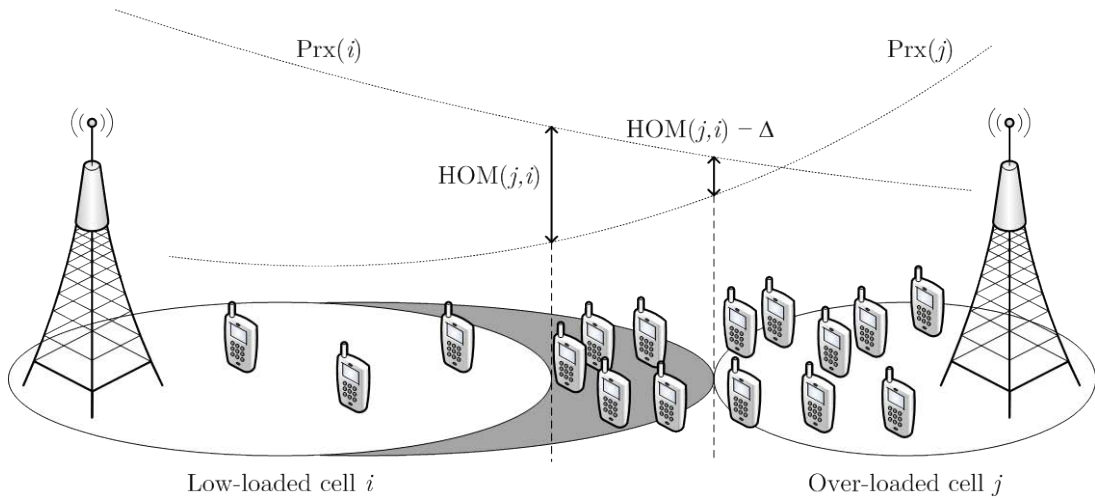
Figure 5.1: MLB based on HOM parameter.

HOM is adjacency-based defined as observed in equation (5.1). Hence, the influence of tuning this parameter in a single adjacency is only referred to that particular adjacency. However, to avoid ping-pong effects and instabilities in the HO process, changes in both directions of the adjacency should be complementary (i.e., if the HOM from cell j to i is reduced by Δ dB, the HOM from i to j is increased by Δ dB). This reasoning presents a shortcoming; those attempt calls in the border of the cell j might handover to its neighboring cell i immediately. To avoid this behavior, the same modifications should be done in the *cell reselection* process.

Cell transmission power ($\mathbf{P_{TX}}$): The coverage area of a cell can also be modified by adjusting its transmission power, $P_{TX}(j)$ as Figure 5.2 shows. A higher/lower transmission power in a base station is directly linked to higher/lower received signal levels in that cell, which has an influence on cell dominance areas. Unlike HOM, transmission power is defined on a cell basis, so that all neighbors are equally affected by changes in the transmission power of a cell. In addition, normally both pilot and data power are jointly tuned to not only impact in connected users (HO process) but also in idle users (CR process).

Resizing cell coverage areas might impact negatively on the QoE of some users. In LTE networks, this shortcoming is partly alleviated by *adaptive modulation and coding* (ACM). Nevertheless, a carefully study of the adaptation of radio configuration parameters should be performed in MLB techniques to keep a satisfactory level of QoE.

As aforementioned, cell transmission power is the radio configuration parameter that would be tuned in the proposed MLB mechanisms.
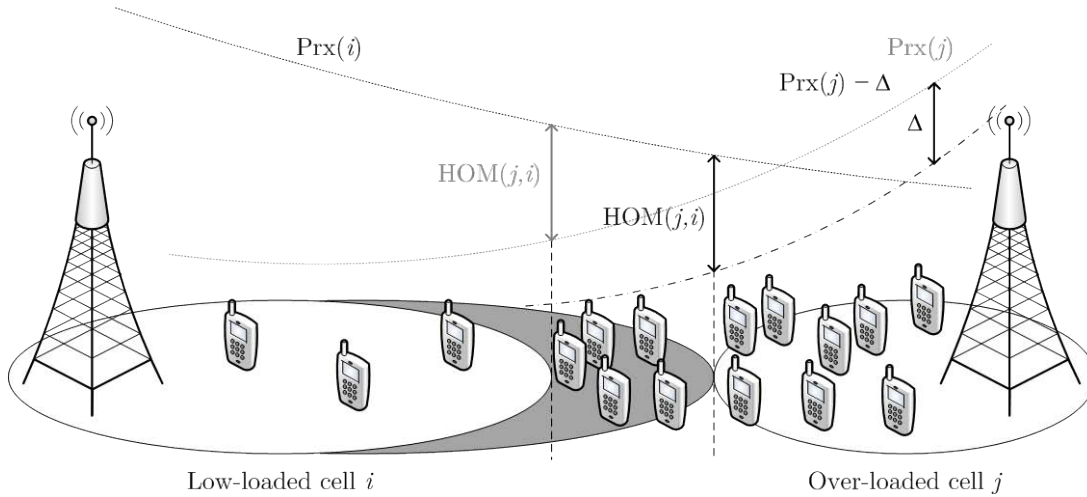
Figure 5.2: MLB based on $P_{TX}(j)$ adaptation.

5.3.3   Key performance indicators

Since for some operators the overall users' satisfaction is more critical in voice calls rather than in any other kind of service, in the proposed algorithms data traffic users are handed over to macrocells when a femtocell is considered overloaded. Additionally, the periodicity to trigger the mechanism should be low to solve temporal network congestions in indoor environments. These cellular networks usually present a frequency reuse of, at least, 2 to reduce interference issues.

Temporal network congestions must be solved from two perspectives:

- **From the user point of view**: the performance is measured according to the user experience, which can be mainly improved by minimizing two network indicators: the *Call Blocking Ratio* (CBR) as the ratio of the number of calls that attempt to access the network but fail ($N_{blocked\_calls}$) to the number of calls that attempt to access the network ($N_{attempted\_calls}$):

$$CBR = \frac{N_{blocked\_calls}}{N_{attempted\_calls}} = \frac{N_{blocked\_calls}}{N_{blocked\_calls} + N_{accepted\_calls}}, \qquad (5.2)$$

  and, the *Connection Dropping Ratio* (CDR) as the ratio of the number of dropped connections in the network ($N_{dropped\_connections}$) to the number of active connections in the network ($N_{accepted\_calls}$). CDR depends on the channel quality and the availability of network resources, i.e., a bad *Signal to Interference-plus-Noise Ratio* (SINR) of users (CDR_q) or the lack of temporary resources (CDR_s):

$$CDR = \frac{N_{dropped\_connections}}{N_{accepted\_calls}}. \tag{5.3}$$

To summarize this information into one indicator that measures the users' dissatisfaction, the *User Dissatisfaction Ratio* (UDR) [105] is used and it is calculated following a similar expression as UR. It is interpreted as a combination of CBR and CDR:

$$UDR = CBR + (1 - CBR) \cdot CDR. \tag{5.4}$$

This indicator is also a valuable parameter from the operator point of view as the experimented users experience is important to keep clients.

Additionally, the quality of the signal received by the users should be also taken into account: the *Channel Quality Indicator* (CQI) in LTE networks. This indicator is reported by the users to the base station. In this sense, the mean CQI (MCQI) is calculated as:

$$MCQI = \overline{CQI} = \frac{1}{N_{accepted\_calls}} \sum_{u=1}^{N_{accepted\_calls}} CQI_u, \tag{5.5}$$

where $N_{accepted\_calls}$ is the number of active users and CQI_u the quality experienced by the user u. CQI is a number from 0 (very bad channel quality) to 15 (very good channel quality). A high value is desirable in this indicator.

- **From the operator point of view**: in addition to the previous indicators, an important criterion is also given by the amount of signaling data necessary to control the network fluctuations. A key indicator to measure that information is the *User Handover Ratio* (UHR) [17], described as the number of handovers over the accepted calls:

$$UHR = \frac{N_{handovers}}{N_{accepted\_calls}}, \tag{5.6}$$

where $N_{handovers}$ represents the number of handovers and $N_{accepted\_calls}$ the number of accepted calls in the same period. Low values of UHR are desirable.

Therefore, the proposed heuristic methods aim to shift traffic from overloaded femtocells to low-loaded femtocells by resizing the services areas, while a good trade-off between the described indicators is pursued. To accomplish this goal, the femtocells

transmission power is adjusted according to the study of some network indicators: *ratio of active users*, *ratio of occupied radio resources*, etc. and some external network information: *users' position*.

5.4   Methods for MLB in femtocell networks

Several MLB methods have been proposed in the literature, as described in Section 5.2 *"Related work"*. MLB mechanisms for femtocell networks could be based on different techniques or controllers. Simple and elementary equations can be applied for this use case [6]. However, the best system configuration is usually hard to find. Other mechanisms based on FLCs [16], where efficient rules are defined by experts, present adaptive solutions to reach the best system configuration. Some others propose complex equations or techniques [95], even based on FLCs [17], which lead to high computational cost not really feasible to be implemented in real deployments.

The MLB mechanisms proposed in the following subsections are based on FLCs. The main reasons for choosing FLCs are related to the easiness for the integration and translation of expert human knowledge into a set of fuzzy rules, its simplicity for implementation and managing rules based on experience and the low computational cost.

5.4.1   Fuzzy-based MLB mechanisms

The basic structure of an MLB mechanism based on FLC in cellular networks is depicted in Figure 5.3. The inputs of the FLC approach can be alarms, counters and/or KPIs acquired from network statistics or call traces, being the collection of this information a standard and usual procedure in cellular networks. Other inputs, such as a feedback of the FLC outputs, are also of interest. The outputs propose the reconfiguration of cellular network parameters. Further information about the functions and parameters of FLCs are detailed in *Appendix C*.

A reference fuzzy-based MLB mechanism [16] and newly proposed fuzzy-based MLB methods are detailed below. The number of input indicators provided to each method is two (as Figure 5.3 shows). Depending on the algorithm, these two input indicators could be classical indicators (such as *CBR* or *ratio of occupied radio resources*), the feedback of the FLC, or the indicator: *ratio of active users*. In consequence, new *membership functions* as well as *fuzzy rules* must be designed according to each input indicator.
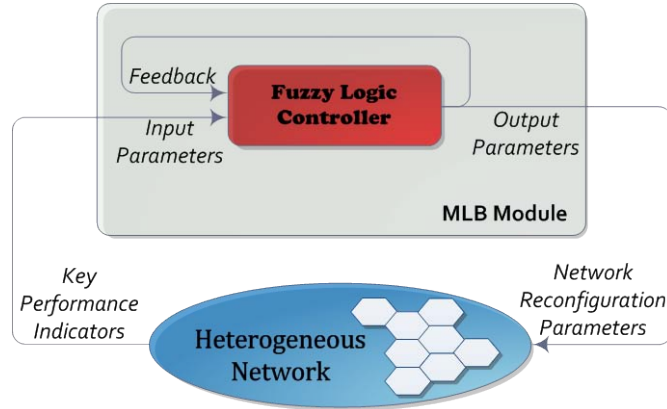
Figure 5.3: Fuzzy Inference System.

5.4.1.1   Power Traffic Sharing (PTS) - Baseline

This method, presented in [16], has been selected as the reference fuzzy-based MLB algorithm. The FLC inputs are the difference between CBR of the analyzed serving cell $cell$ and the average CBR of its neighbors, ($CBR_{diff}(cell)$), as well as the current femtocell transmission power deviation from the default transmission power value, $\Delta PTx(cell)$. The latter, $\Delta PTx(cell)$, is calculated as the default femtocell transmission power value (normally maximum transmission power), $PTx_{max}(cell)$, minus the current femtocell transmission power $PTx(cell)$. The output of the algorithm, $\delta PTx(cell)$, is the transmission power that must be tuned (increase or decrease) in the femtocell in that moment. $\delta PTx(cell)$ affects both pilot and data transmission power.

This optimization procedure improves the performance in heavily loaded enterprise femtocell networks by distributing the users along the unloaded femtocells. Nevertheless, this algorithm is not suitable to solve temporary congestion issues due to the proposed CBR indicator provides valuable information once the network already presents accessibility issues. A prediction of this inconvenient situation would be desirable to avoid or reduce users' dissatisfaction as soon as possible. Therefore, this algorithm cannot achieve the optimal network configuration parameter under temporary traffic fluctuations. For further details about the PTS method, the reader is referred to the original work [16].

5.4.1.2   Power Load Sharing (PLS)

This algorithm, which was originally presented in [15], aims to avoid the previous PTS issues. Following the same scheme, the first step is to change the inputs of the

algorithm to prevent blocked calls. According to this, the new input indicator is related to bandwidth, by measuring the current cell capacity in radio resource terms. This indicator is hereafter described for LTE networks, although equivalent indicators can be defined for other technologies. Therefore, in PLS method, the load balance is performed based on the occupied PRB, whereas the previous PTS optimizer depended on blocked calls. According to this, the key network indicator for this system is represented as the following function, which is calculated for each cell:

$$Load_{diff}(cell) = Load(cell) - \frac{1}{N}\sum_{i=1}^{N} Load(i), \qquad (5.7)$$

where N is the number of neighboring cells and $Load(i)$ is the ratio of occupied PRBs of the cell i, defined in equation (5.8). $Load_{diff}(cell)$ is used as FLC input together with the femtocell transmission power deviation $\Delta PTx(cell)$.

$$Load(i) = \frac{occupied\_resources(i)}{max\_resources(i)}. \qquad (5.8)$$

The method in [15] has been modified for solving temporary overloaded situations. The difference compared to [15] consists of changing the membership functions and fuzzy rules to converge to the optimal configuration in the shortest time. Hence, the range of outputs of the FLC is larger (from ± 2 dB to ± 6 dB). In this context, based on expert knowledge, some membership functions and fuzzy rules configurations have been evaluated. A large enough number of membership functions has been selected to achieve a reasonable level of detail while keeping the number of fuzzy sets small enough to build easy sets of fuzzy rules.

Figure 5.4(a) shows the three membership functions of $\mu_x(\Delta PTx(cell))$. It analyzes if femtocell transmission power deviation is very negative "*Very Negative*", negative "*Negative*" or zero "*Zero*". These functions were proposed by the PTS method and they are the same in PLS method to accomplish consistent and comparable results. The function $\mu_y(Load_{diff}(cell))$, in Figure 5.4(b), depicts five membership functions to characterize the inputs in "*Very Negative*", "*Negative*", "*Zero*", "*Positive*" and "*Very Positive*" according to the difference between the studied cell load ratio and the average load ratio of its neighboring cells, keeping the symmetry around 0 (i.e., the point where the load ratio between the studied cell and its neighbors is the same) to balance the load in the network. Each membership function is defined in an interval based on the expert knowledge, and for simplicity and computational efficiency, the selected membership functions are trapezoidal and triangular.
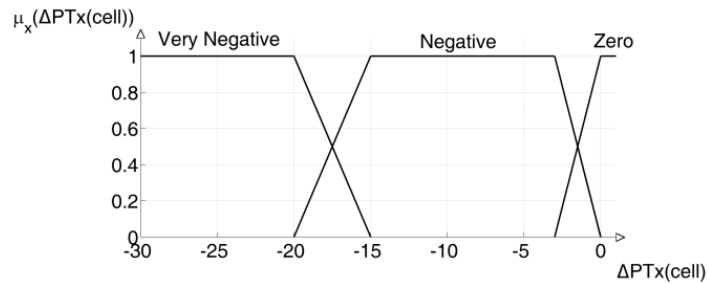
(a) Input 1
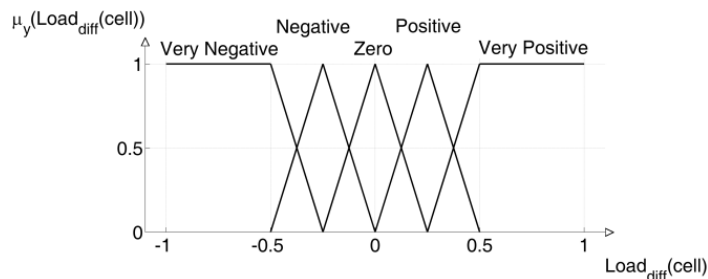
(b) Input 2
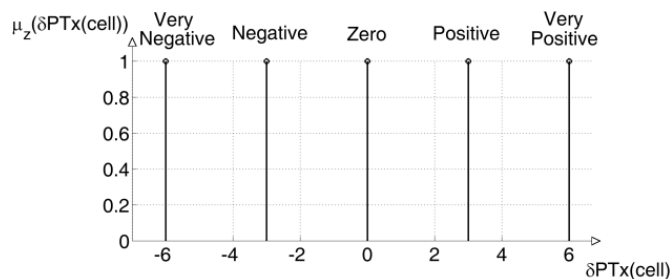
(c) Output

Figure 5.4: Membership functions of PLS method.

Table 5.1 defines the common-sense fuzzy rules in the form of "if-then" statements, following the syntax of equation (C.1) in *Appendix C*. These rules are built to balance the load in the network. In consequence, the more positive the $Load_{diff}(cell)$ is (i.e., the studied cell is overloaded), the more negative the transmission power deviation should be (rules 10 and 11), and vice versa (rules 1 to 6). In case the network is balanced ($Load_{diff} = "Zero"$), the algorithm tends to return to the initial transmission power configuration in order to improve SINR and reduce the number of PRBs per user as the CQI is increased (rules 7 to 9). In consequence, the cell would have more available free resources decreasing the probability of cell congestion.

Based on the output function $\mu_z(\delta PTx(cell))$ shown on Figure 5.4(c), the femtocell transmission power is increased or decreased $\delta PTx(cell)$. The functions can take the

following labels and values: "*Very Negative*" and −6 dB, "*Negative*" and −3 dB, "*Zero*" and 0 dB, "*Positive*" and +3 dB and "*Very Positive*" and +6 dB. Finally, the femtocell transmission power $PTx(cell)$ is tuned according to the output.

Table 5.1: Fuzzy rules of PLS method.

	Load$_{diff}$	Operator	ΔPTx	δPTx
		IF		THEN
1	Very Negative	AND	Very Negative	Very Positive
2	Very Negative	AND	Negative	Very Positive
3	Very Negative	AND	Zero	Positive
4	Negative	AND	Very Negative	Very Positive
5	Negative	AND	Negative	Positive
6	Negative	AND	Zero	Positive
7	Zero	AND	Very Negative	Very Positive
8	Zero	AND	Negative	Positive
9	Zero	AND	Zero	Zero
10	Positive	AND	-	Negative
11	Very Positive	AND	-	Very Negative

This method has been defined focusing on an LTE network, although it could be easily extended to any other cellular technology. The PRB is bandwidth-related, therefore, an equivalent available bandwidth indicator can be used as input for any other cellular technologies.

5.4.1.3 Power User Sharing (PUS)

Femtocells are usually designed to support from 2 to 64 users in connected mode, either voice or data traffic [32]. Rather than a wireless cellular bandwidth limitation, this characteristic is a restriction in the femtocell processing capability. For that reason, PRBs activity (as proposed in the PLS method) may not be always an appropriate indicator for balancing traffic in femtocell environments where most of the time there could be free resources to allocate user data but the femtocell is not able to process them due to the limit in the maximum number of active users. According to this, this PhD thesis proposes the PUS method, which considers the number of users in connected mode as the main indicator to offload temporary congested cells.

In this case, the input indicator of the FLCs is defined as the ratio of active users, i.e., the number of simultaneous users in connected mode *active_users*, to the

femtocell user limitation max_users (see equation (5.10)) of the studied cell $User(cell)$, in relation to the same average ratio in its neighboring cells $User(i)$:

$$User_{diff}(cell) = User(cell) - \frac{1}{N}\sum_{i=1}^{N} User(i), \qquad (5.9)$$

where N is the number of neighboring cells and $User(i)$ is defined for a cell i as:

$$User(i) = \frac{active\_users(i)}{max\_users(i)}. \qquad (5.10)$$

This mechanism presents the same FLC structure as the previous PTS and PLS methods, but the inputs of the FLC are the new indicator, $User_{diff}(cell)$ as presented in equation (5.9), and the femtocell transmission power deviation, $\Delta PTx(cell)$. The output of the FLC would increase/decrease the current femtocell transmission power.

In order to get a moderate level of detail and straightforward fuzzy control rules, an acceptable number of membership functions have been selected for each indicator based on experienced human knowledge. The membership functions of this controller are shown in Figure 5.5. As it can be observed, the membership functions $\mu_x(\Delta PTx(cell))$ are the same as the previous membership functions of the PTS and PLS methods (Figure 5.5(a)), and the membership functions, $\mu_y(User_{diff}(cell))$, of the new input, $User_{diff}(cell)$, are: "*Very Negative*", "*Negative*", "*Zero*", "*Positive*" and "*Very Positive*" (Figure 5.5(b)). Notice that the shape of these membership functions are similar to those of the previous method. However, the interval of definition is adjusted by experts to get the best algorithm's performance. For simplicity and computational efficiency, the implemented membership functions are triangular and trapezoidal.

Fuzzy rules are depicted in Table 5.2 and aim to equalize the ratio of active users in the studied cell and the average ratio of its neighboring cells. According to this, the more positive $User_{diff}(cell)$ is (i.e., the ratio in the studied cell is high), the more negative the transmission power deviation should be (rules 8 and 9), and vice versa (rules 1 to 4). Once the network is equalized ($User_{diff}(cell) = "Zero"$), the PUS method avoids very negative transmission power adaptations (label "*Very Negative*" - rule 5) in order to increase the end-users QoE. However, as this method is restricted by the number of users (instead of the available resources in the cell), returning to the default transmission power could increase the interference but the cell congestion would not be reduced. That is why "*Negative*" or "*Zero*" values of transmission power deviation (rules 6 and 7) do not return to the default value.
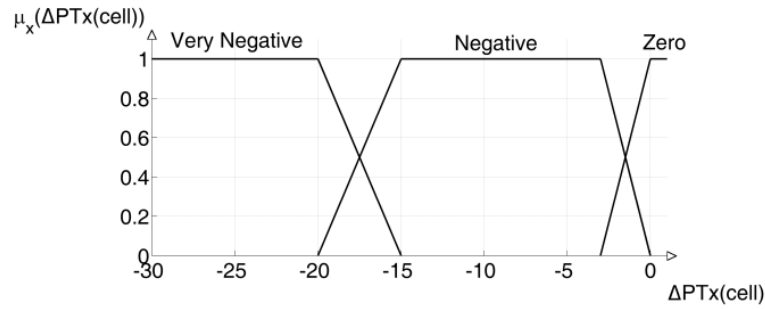
a) Input 1
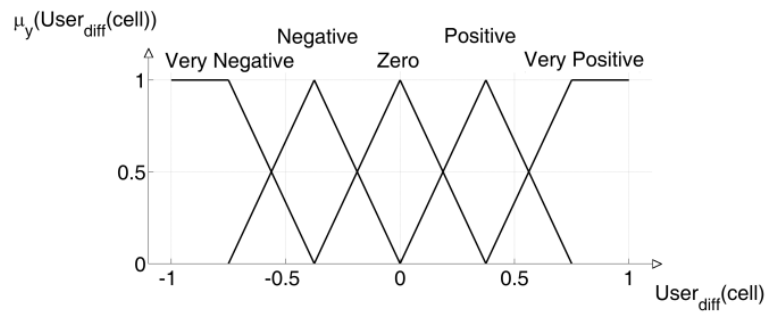
b) Input 2
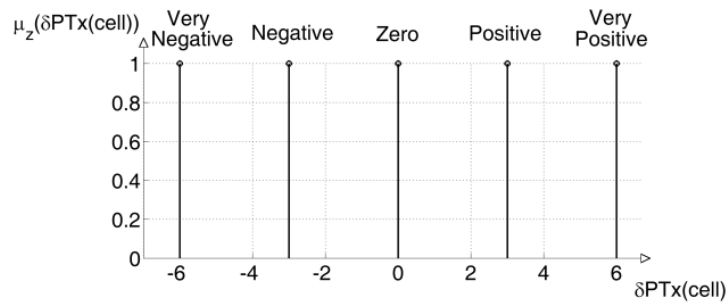
c) Output

Figure 5.5: Membership functions of PUS method.

The same output functions $\mu_z(\delta PTx(cell))$, as in previous algorithms, are defined for this one (illustrated on Figure 5.5(c)).

Most of the time, this mechanism is suitable for achieving good performance in femtocell networks, above all in LTE deployments which support high-peak data rates up to 346 Mbps in the downlink and 85.5 Mbps in the uplink at 20 MHz and 4x4 MIMO. However, it could present some shortcomings when propagation channel is very poor (bad SINR) or users require high transmission rates (e.g., to watch streaming television in high definition).

Table 5.2: Fuzzy rules of PUS method.

	$User_{diff}$	Operator	ΔPTx	δPTx
	IF			THEN
1	Very Negative	AND	Very Negative	Very Positive
2	Very Negative	AND	Negative	Very Positive
3	Very Negative	AND	Zero	Positive
4	Negative	AND	-	Positive
5	Zero	AND	Very Negative	Positive
6	Zero	AND	Negative	Zero
7	Zero	AND	Zero	Zero
8	Positive	AND	-	Negative
9	Very Positive	AND	-	Very Negative

5.4.1.4   Power Load and User Sharing (PLUS)

The previous mechanisms, as explained, might not guarantee their proper operation in some situations. The shortcomings of each algorithm (PLS and PUS methods) could be complemented by the other, leaving outside the PTS method due to the long time needed to evaluate its main indicator (CBR). That means, the analysis of the two indicators (cell load and number of active users) is required to ensure an efficient MLB process in femtocell networks. According to this, the works described in the literature in the context of MLB at femtocell networks that did not analyze at least these two indicators, might not properly work. However, in case the operators' policies and priorities are focused on voice traffic (e.g., VoLTE), the analysis of active users might be enough while for data traffic, the analysis of radio resources would be desirable.

In the proposed PLUS method, both previously defined indicators ($User_{diff}(cell)$ and $Load_{diff}(cell)$) are the inputs of the FLC to properly prevent or reduce occasional indoor congestions. For simplicity, this method does not include the cell transmission power deviation as an input indicator.

The same membership functions proposed for PLS and PUS methods are implemented in this FLC to compare these methods under the same conditions (reader is referred to Figure 5.4(b) and Figure 5.5(b)).

New fuzzy rules are defined based on these two indicators and the expert knowledge. Table 5.3 presents the set of control rules implemented in this system. These rules prioritize the indicator $User_{diff}$ over the $Load_{diff}$ since a new user in a femtocell network usually implies a greater impact on the maximum allowed number of user than on the available resources. That means, the network resources assigned to

each user could be reduced in order to accept new users, even if some of them could be slightly dissatisfied (decrease the QoE, throughput, etc.). For example, under a "*Very Negative*" situation of $Load_{diff}$ and a "*Very Positive*" situation of $User_{diff}$, it is preferred to decrease the transmission power of the studied cell (fuzzy output is "*Negative*").

Table 5.3: Fuzzy rules of PLUS method (Operator: AND; output: δPTx).

$Load_{diff}$ / $User_{diff}$	Very Negative	Negative	Zero	Positive	Very Positive
Very Negative	Very Positive	Very Positive	Positive	Zero	Zero
Negative	Very Positive	Positive	Positive	Zero	Zero
Zero	Very Positive	Positive	Positive	Negative	Very Negative
Positive	Zero	Zero	Negative	Negative	Very Negative
Very Positive	Negative	Negative	Very Negative	Very Negative	Very Negative

The same constant output functions $\mu_z(\delta PTx(cell))$, as in the previous algorithms, are applied here to compare all the algorithms under the same conditions.

Table 5.4: Summary of Fuzzy-based MLB Mechanisms.

	PTS*	PLS	PUS	PLUS
Input 1	ΔPTx	ΔPTx	ΔPTx	$Load_{diff}$
Input 2	CBR_{diff}	$Load_{diff}$	$User_{diff}$	$User_{diff}$
Output	δPTx	δPTx	δPTx	δPTx

* Reference [16]

A summary of the supported inputs and outputs of the MLB mechanisms is depicted in Table 5.4.

5.5   Methods for context-aware MLB in femtocell networks

Context information could enhance the mobile network performance as it could support mechanisms in real-time, add extra information about the scenario, inform about future events, etc. However, current OAM architectures usually manage network

parameters in periods of fifteen minutes, hours or even days, or they are not able to integrate such as context information. It could be inefficient in dynamic scenarios such as indoor environments. In this sense, the local-centralized OAM architecture presented in *Chapter 3* is a solution for implementing real-time self-management mechanisms supported by context information.

The following subsections initially describe the information sources and subsequently, the proposed heuristic context-aware MLB methods are explained. These methods aim to mitigate temporal and focused overloaded situations at commercial and corporate indoor scenarios due to the high concentration of users in temporal and spatial domain, thanks to the knowledge of users' position. Two context-aware MLB methods are proposed. The first method uses the geometrical distances between users, their distributions and their PRX to estimate the new femtocells transmission power. The second method updates femtocells transmission power based on the average PRX stored in a database when users' position is available, in other case, the average PRX values from *measurement reports* are analyzed. Finally, a simple method of the *energy-saving* (ES) use case [45] is proposed in coordination with a MLB mechanism.

5.5.1   System set-up

The main network parameter that will be tuned is the femtocell transmission power. To address this operation, the PRX per terminal is used by the system to calculate the new cell transmission power. That information could be obtained or estimated from different sources (propagation models, measurement reports, etc.). Radio propagation models, as empirical mathematical formulas, characterize radio wave propagations. These models are very sensitive to pedestrians, obstacles, etc., which vary both in time and space, especially at indoor environments. Other sources such as measurement reports provide instantaneous information about PRX, while historical PRX values provide an average estimation of PRX. Thus, these PRX values could be different depending on the source, the influence of fading and shadowing, etc.

5.5.1.1   PRX from measurement reports

Mobile devices provide valuable information about the network conditions through the *Measurement Reports* (MR). These reports are periodically sent to the cell and contain information about the channel quality (current mobile transmitted/received power, block error ratio of the data channel, etc.). This is vital to assist dynamic

network planning and RRM processes in power control decisions and handover. 3GPP specifications define this type of measurements in [79].

The PRX is included in the measurement reports, although named in a different way depending on the radio technology. For 2G deployments, it is called RxLev (*Received Signal Level*) whereas, for 3G, it is named as RSCP (*Received Signal Code Power*) and in LTE as RSRP (*Reference Signal Received Power*). That information is periodically forwarded to the OAM layer from the base stations. In practice, as aforementioned, the mobile network does not support continuous real-time communication to the OAM elements due to the amount of signaling data and the high-level location of the OAM in the hierarchy. However, the OAM architecture described in *Chapter 3* placed some of its functions in lowest levels, making this real-time process viable. This is in line with distributed SON architectures proposed by 3GPP for future networks [2].

The PRX could be also monitored thanks to context sources such as smartphone apps (e.g., G-MoN application [78]). Unfortunately, some reported information could be incomplete due to terminal compatibility issues, i.e., measurement capabilities would depend on the terminal manufacturer. For example, the PRX from the serving cell is always reported but PRX from neighboring cells is missing. Even if the terminal is monitoring the PRX from its neighboring cells, the app is not able to report it. As a solution, the PRX information per terminal could be requested to a database with historical PRX values based on users' positions.

5.5.1.2   Historical Path Loss Maps (HPLM)

The PRX depends on several factors such as the propagation channel, the cell transmission power, the users' positions, etc. However, since the signal *Path Loss* (PL) is independent of the cell transmission power, the PL information will be used instead of the PRX to create a database. PL values are calculated and stored into this database together with the users' positions, to build the so named *Historical Path Loss Maps* (HPLM). The relationship between PRX and PL is given by:

$$PRX_{cell}(x,y) = PTX_{cell} - PL_{cell}(x,y), \tag{5.11}$$

where $PRX_{cell}(x,y)$ is the received power at (x,y) position from $cell$, PTX_{cell} is the *Equivalent Isotropically Radiated Power* (EIRP) of $cell$ and $PL_{cell}(x,y)$ is the radio signal path loss at point (x,y) from $cell$. The database contains the PL per position received from each cell. This information is calculated based on the MRs (i.e., PRX

values) performed by the terminals over time, the network configuration parameters (i.e., cells transmission power) and the users' positions. Thanks to this HPLM database, the system will be able to get an estimation of the PRX per position based on equation (5.11).

Building the HPLM database is a continuous process composed by two sets of information (Figure 5.6). On the one hand, the measurements reported from the active users are used to calculate the current PL from each cell $PL_{cell}(i,j)_u$, where coordinates $(i,j)_u$ are the position of user u. On the other hand, and synchronized with the MR, the active user position $(i,j)_u$ is supplied to the database by an external indoor positioning system (as a possible system, *Chapter 4* presented an RFID-based indoor positioning system) [38]. With this data (measurements and positions) the average PL of a position and cell is updated according to the following equation:

$$\widehat{PL}_{cell}(i,j) = \frac{1}{M(i,j)} \sum_{m=1}^{M(i,j)} PL_{cell}(i,j)_m, \tag{5.12}$$

where $PL_{cell}(i,j)_m$ are the different path loss measurements over time at position (i,j) and $M(i,j)$ is the total number of measurements at position (i,j) (coming from different users). That $\widehat{PL}_{cell}(i,j)$ would be used to estimate the $\widehat{PRX}_{cell}(i,j)$, according to equation (5.11).

a) Acquisition of information   b) Estimation of PL
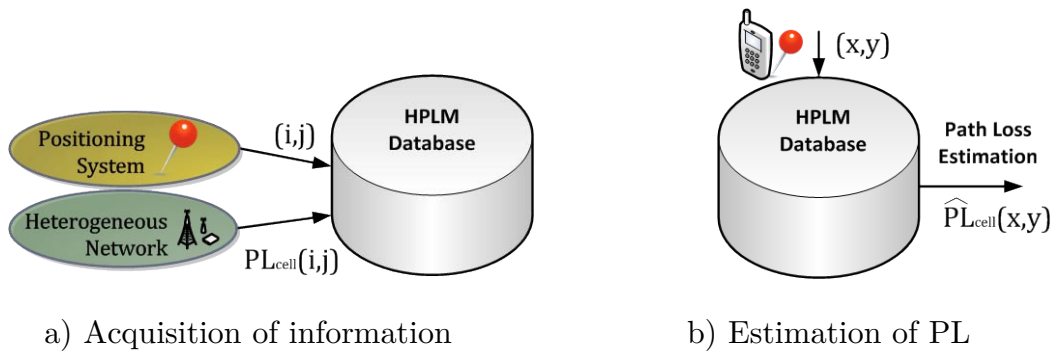
Figure 5.6: HPLM scheme.

The radio channel conditions, especially at indoor environments, suffer continuous changes due to the number of people, obstacles, etc. Therefore, the number of samples, $M(x,y)$, to build the estimated PL value per position should be a configurable parameter and could be quite different depending on the scenario. For this work, the number of samples is limited in time to keep the propagation channel conditions updated:

$$M(x, y) = N_{samples}^{P}(x, y), \tag{5.13}$$

where $N_{samples}^{P}(x, y)$ is the number of samples at (x, y) within last period P.

Note that, at the beginning of the process, no historical information is stored in the database. Additionally, even when a wide range of data is stored, there could be positions with no PL information as (x_p, y_p) in Figure 5.7. In this case, the mechanism needs to guess a possible PL value of that position. To address this problem, PL is calculated through an interpolation. A threshold distance of Int_D_{th} (meters) around the user' position is selected as the interpolation area, as shown in Figure 5.7.
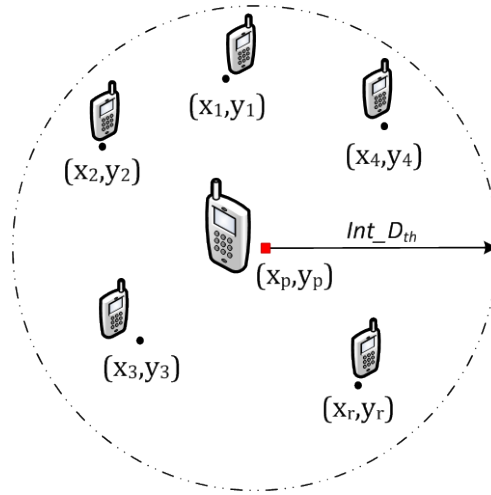
Figure 5.7: Interpolation at coordinates (x_p, y_p).

The path loss value per cell $\widehat{PL}_{cell}(x_p, y_p)$ is estimated as:

$$\widehat{PL}_{cell}(x_p, y_p) \approx \sum_{r=1}^{R} w_r \cdot \widehat{PL}_{cell}(x_r, y_r), \tag{5.14}$$

where R is the number of positions with stored PL information inside the interpolated area, $\widehat{PL}_{cell}(x_r, y_r)$ is the estimated PL value at position r that is already stored in the database and w_r is the weight assigned to each r position depending on its distance to the studied terminal. These weights must be inversely proportional to the distance between the known positions and the user's position in order to give more importance to those PL values close to the user's position. The weights are computed as follows:

$$w_r = \frac{1}{d_{r-p}} \cdot \frac{1}{\sum_{i=1}^{R} \frac{1}{d_{i-p}}}, \qquad\qquad (5.15)$$

where d_{a-b} is the distance from position a to position b and R is the number of the stored path loss values. The range of r would be from 1 to R and the sum of w_r is 1.

HPLM can also be obtained from *Radio Environmental Maps* (REM) [106], which is a cognitive tool for environmental awareness. It consists in a dynamic procedure to store radio environmental information on wireless systems. This idea was defined by the *Virginia Tech team* as a database that contains different kinds of information such as environment radio signal, location of base stations, geographical features, etc. Furthermore, this tool is not just a simple database storing environmental data, but it is also able to process that information to implement spatial interpolation and temporal interpolation/processing mechanisms. These procedures could be either static or dynamic. For example, some positions of a scenario could be without PRX information. Hence, this lack of information is interpolated based on the collected PRX samples and the intelligent entity in charge of spatial interpolation. This information could be periodically updated through static well-located devices. The results are maps based on the processed geo-located data from the mobile networks [107] [108].

REM could be either centralized (or global) which provides extensive processing capabilities and reduces signaling overhead, or distributed (or local) which increases the responsiveness and the computational costs of each cell. Focusing on femtocell networks, the most convenient solution would be to centralize all the information in a global entity as these indoor environments would be small size networks. Additionally, REM could be integrated in the operator's architecture or be part of a third party service provider, which would depend on the operator's policies and decision. The proposed SON system would integrate REM into the middle layers (e.g., domain manager) of the operator's OAM architecture.

5.5.2   Users-distribution-based method

This method is referred hereafter as *UD method*. It aims to avoid localized congestion issues in indoor femtocell networks. The goal is accomplished by analyzing the distribution of the terminals and by tuning the femtocell transmission power.

UD method analyzes two parameters to consider the femtocell congested. The ratio of active users (see equation (5.9), hereafter referred as l_{cell}) over a threshold S_{th} and the ratio of occupied radio resources (see equation (5.8), hereafter referred as r_{cell}) over

a threshold Q_{th}. The definition of these thresholds is based on the experience of the operator or on the sensitivity analysis performed in the studied scenario. Conversely, if the femtocell is well-balanced, the transmission power of that femtocell is changed ± 0.5 dB ($\delta Ptx = \pm 0.5$) till it returns to the initial transmission power configuration.

The procedure of load balancing can be divided in two separate steps: *prediction of PRX per user* and *adaptation of femtocells transmission power*.

5.5.2.1   Prediction of PRX per user

This process estimates the PRX that each user from the overloaded femtocell would receive next time span ΔT (seconds) from each cell. Initially, the system verifies if the current PRX is received from all cells (serving cell and neighboring cells) in real-time (t). In case any piece of this information is missing, last stored PRX value is requested to the HPLM database as a function of the users' position. At the same time, the system demands previous values of PRX in the interval of T times ΔT received from each cell in order to build the PRX vector per cell and user, i.e., $\{PRX(t), PRX(t - \Delta T), \ldots, PRX(t - T \cdot \Delta T)\}$. In the same way as before, if those PRX values are not reported by the terminal or they are available in the system, they are requested to the HPLM database. Finally, the system estimates the values of $PRX(t + \Delta T)$ per femtocell based on the PRX vectors. It is calculated following a simple and low computational cost approach: *a first order polynomial trend line*. This procedure is repeated for each user of overloaded femtocells in the cellular network. Figure 5.8 shows the flowchart of this process for user i from femtocell j in the interval $[t, t - T \cdot \Delta T]$ by steps of ΔT.
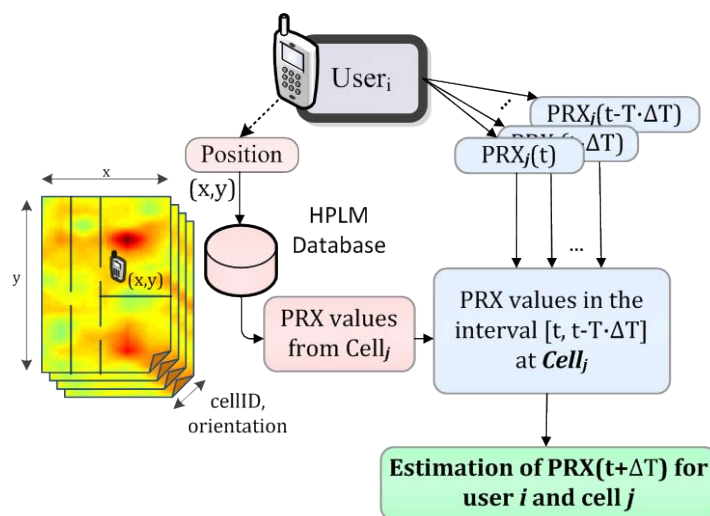
Figure 5.8: Estimation of $PRX(t + \Delta T)$ for user i and femtocell j.

5.5.2.2 Adaptation of femtocells transmission power

The femtocell transmission power adaptation (δPtx) is calculated individually per overloaded femtocell to offload that cell by decreasing the femtocell transmission power (minimum femtocell transmission power is τ_{min}) based on $PRX(t + \Delta T)$ values. δPtx would depend on the users' distributions. Hence, it should be analyzed whether a concentration (or group of users) exists or not, and what type it is.

Several terminals are considered as a group when the distance between all of them is under the average distance of all the users in the service area. In this sense, three kinds of groups are defined as shown in Figure 5.9.The type of group depends on three factors: the distance between users, the group location inside the coverage area and the size (in terms of number of users) of the group. In case the group is composed of all users in the serving cell (Figure 5.9(a)) it is named as *no group*. If the group encloses the femtocell (Figure 5.9(b)), it is called *central group*. Otherwise, the group does not enclose the femtocell, it is named *border group* (Figure 5.9(c)). In case there is more than one group, the one with the highest number of users is selected as *target group*, prioritizing *border groups* over *central groups*.

(a) No group   (b) Central group   (c) Border group
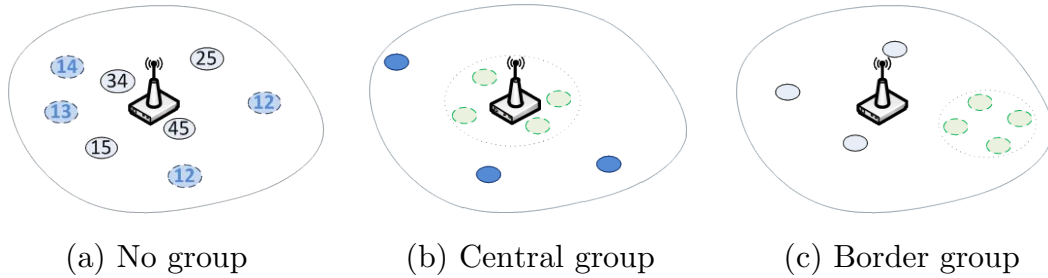
Figure 5.9: Type of users' distribution.

Depending on the target group, a different method is proposed:

- ***No group:*** For each user i of the *studied cell* (overloaded femtocell), the difference between the estimated value of PRX of that cell and the estimated PRX value of the strongest neighboring cell is defined as the *neighboring cell interval, NCI* (dB).

$$NCI_i = PRX_{cell(1)}(t + \Delta T) - max\{PRX_{cell(j)}(t + \Delta T)\}\Big|_{j \neq 1}, \qquad (5.16)$$

where $cell(1)$ refers to the *studied femtocell*. Note that neighboring cells include any kind of cell (macrocell, picocell, etc.).

After that, the median of all the calculated NCI is computed as M_{cell}. As an example, Figure 5.9(a) illustrates the NCI of each terminal where $M_{cell} =$ 14.5 dB. Those users with lower NCI than M_{cell} (blue with dotted lines in the example of Figure 5.9(a)) are supposed to handover to neighboring cells.

- **Central group:** This situation follows the same procedure as before. However, in this case, the analyzed terminals are only those which are not labelled as users of the target group (dark blue circles in Figure 5.9(b)).

- **Border group:** The situation is different because of the lower number of possible target cells. In addition, the probability of overloading a neighboring cell is high. Therefore, the femtocell adaptation should be slower. In consequence, the estimation of the NCI is calculated only for the users of this group (green dotted icon in Figure 5.9(c)). In the same way, the median M_{cell} of these values is calculated following the previous procedure.

The M_{cell} is added to the defined offset of the serving cell to accomplish the handover and avoid ping-pong issues. Then, the transmission power adaptation of the *studied cell* is $\delta Ptx = M_{cell} + offset$. This power reduction can be done without creating coverage holes due to the common overlapping conditions of femtocell environments. In turn, as previously mentioned, those cells without congestion issues change their transmission ± 0.5 dB, to return to the initial power configuration.

Once the studied cell reduces its transmission power, those candidate users that should offload the cell, hand over to the neighboring cells. Those users in the border of a femtocell-macrocell could easily hand over to the macrocell in case the femtocell is overloaded. Conversely, no macrocell-parameters adaptation is desirable because it would affect large areas and huge number of users outside the indoor scenario.

5.5.3   Virtual-maps-based method

The previous context-aware method (UD method) made use of the distribution of the terminals and their geometrical distances to estimate the new transmission power of the femtocells. This analysis could not be always the best way to focus the MLB optimization efforts in indoor scenarios due to the influence of the wall, obstacles, etc. For example, two close users of the same *group* could receive quite different PRX if there is a wall in the middle. Hence, UD method would properly work in open spaces like halls. In this subsection, new context-aware mechanisms are proposed for any kind of indoor scenario. In addition, it would prioritize voice traffic over data traffic users.

A new MLB mechanism is designed but two configurations are supported. The first location-aware approach (hereafter named Virtual-Maps, VM, method) analyzes the average estimation of the PRX and requires the users' positions to create historical PRX databases (see subsection 5.5.1.2 *"Historical Path Loss Maps (HPLM)"*) and afterwards to process it. Conversely, the second approach is named *MR method* and PRX values from MRs are required (see subsection 5.5.1.1 *"PRX from measurement reports"*). MR method is not a location-aware approach but it is described in parallel to the location-aware VM method because they share the same procedures but different information sources.

5.5.3.1   Internal procedures

Internal procedures would be in charge of creating virtual maps (VMs) based on the information provided by the HPLM. These maps support the VM method.

5.5.3.1.1   Serving cell maps

A method is proposed to estimate coverage maps where some cellular irregularities such as overshooting cell issues are eliminated and the most suitable serving cell for each position is represented. Figure 5.10(a) shows the classical coverage for femtocells (omnidirectional antennas) where an indoor network issue is illustrated: *overshooting.* It might happen due to the geometry of these environments, multi-path reflections, wall obstacles, number of people, etc. Therefore, a femtocell (red femtocell "r" in top left of Figure 5.10(a)) could serve users out of its expected coverage area due to propagation channel conditions. These occasional small coverage areas could be a shortcoming for many SON algorithms. That situation also presents problems to operators in terms of signaling cost because the number of handovers around the overshooting area will be increased.

(a) Classical coverage areas (overshooting)   (b) Proposed cell areas (SCM)
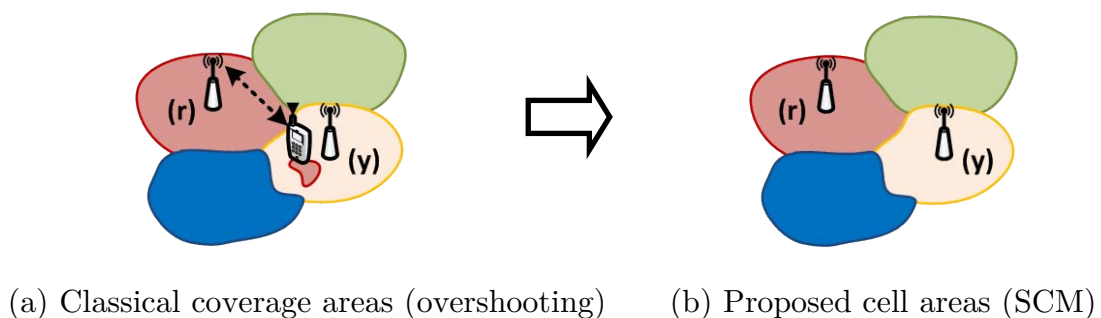
Figure 5.10: Calculation of SCM.

Those situations would be managed thanks to the so-called *Serving Cell Maps* (SCM). Calculating SCM is a process composed of two steps. In the first step, the new coverage areas are defined based on geo-located PRX matrices supported by the HPLM database. This procedure is based on *Thiessen Polygons* [109] where, for each cell, an irregular polygon $A_{cell(k)}$ that delimitates its serving cell area is generated:

$$A_{cell(k)} = \{(x, y) \in (X, Y) | \; PRX(x, y)_{cell(k)} > PRX(x, y)_{cell(j)} \; \forall \, j \neq k, \quad (5.17)$$

where (X, Y) are the coordinates of the scenario. This process builds a network map as that presented in Figure 5.10(a), where for a certain femtocell (r) two disconnected coverage areas are presented. Therefore, the next step is to determine which the main area is. For that purpose, those areas $A_{cell(k)}$ that are split into S subareas, $A^i_{cell(k)}$, must be analyzed. Those subareas are compared to find the biggest one in order to remove overshooting and keep the most suitable area:

$$A'_{cell(k)} = max\{A^i_{cell(k)} | \; A_{cell(k)} = \sum_{j=1}^{S} A^i_{cell(k)}\}. \quad (5.18)$$

In this sense, those removed areas must be joined to other/s area/s. Therefore, each area $A_{cell(p)} | p \neq k$ must be updated by including those discarded areas $A^i_{cell(k)} | A^i_{cell(k)} \neq A'_{cell(k)}$ according to:

$$A'_{cell(p)} = A_{cell(p)} + \sum_{h=1}^{H} A^h_{cell(p)}, \quad (5.19)$$

where H is the number of new coverage subareas belong to $cell(p)$ and $A^h_{cell(p)}$ is calculated as equation (5.20) but focusing on those discarded areas and avoiding the PRX information of $cell(k)$:

$$A^h_{cell(p)} = \{(x, y) \in \left(X^i_{cell(k)}, Y^i_{cell(k)}\right)|$$
$$PRX(x, y)_{cell(p)} > PRX(x, y)_{cell(q)} \; \forall \, q \neq p, k\}. \quad (5.20)$$

This process is repeated till all subareas are joined to a main cell. Finally, the proposed serving cells coverage areas are illustrated on Figure 5.10(b), where the small subarea of the red cell (r) is embedded into the yellow cell (y) area.

5.5.3.1.2   Neighbor cell maps

A new virtual map, named *Neighbor Cell Maps* (NCM), is designed to estimate the neighboring cells of each serving cell. The aim of these maps is to create the *proposed neighbor cell lists.*

(a) Proposed SCM   (b) Proposed NCM
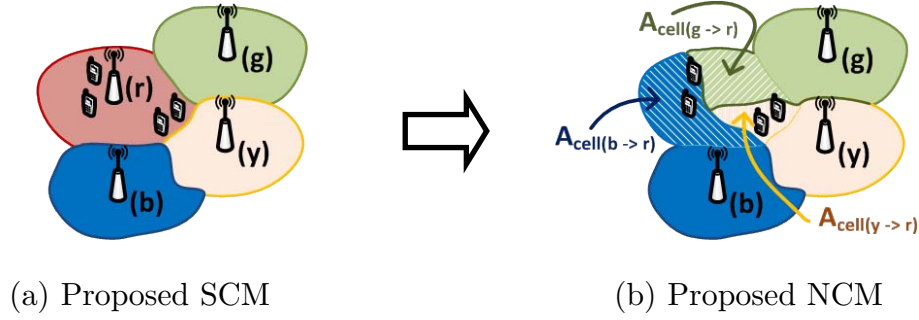
Figure 5.11: Calculation of proposed neighbor cell list.

For that purpose, the same procedure to build SCM is followed now but, removing the PRX values of the serving cell $cell(k)$. Then, equations (5.17) to (5.20) generate the new NCM (see Figure 5.11(b)). Those new areas which cover the original area $A'_{cell(k)}$ (from SCM) are denoted as $A_{cell(j\rightarrow k)}$, where $cell(j\rightarrow k)$ means that the cell $cell(j)$ covers the area of the serving cell $cell(k)$. Figure 5.11(b) depicts an example where three cells ($j = \{b, y, g\}$) are adjacent to the serving cell ($k = \{r\}$). Finally, the proposed neighbor cell list is created as follows:

$$C_{cell(k)} = \{cell(j) \mid A_{cell(j\rightarrow k)} \in A'_{cell(k)} \forall\, j \neq k\}. \tag{5.21}$$

5.5.3.2   System implementation

The proposed context-aware MLB system (based on VM or MR methods) ensures a consistent solution to those operators aiming at prioritizing voice traffic users over data traffic users in indoor femtocell environments, as the impact to the end user is more frustrating in voice calls than in data traffic. For that purpose, the system provides free resources for voice traffic when the indoor network is temporary congested, whereas data traffic is handed over to macrocells or suffers outage for a while (that would be managed by the AC or the Schedulers). Additionally, the ratio of occupied radio resources is considered negligible in comparison with the ratio of active users in LTE networks due to the high-peak data rates supported and the very low

number of active users. For this reason, cell load is only analyzed based on the ratio of active user (see equation (5.10)).

The global scheme of the proposed heuristic rule-based mechanism is depicted in Figure 5.12. It shows an iterative mechanism to estimate the new transmission power variations of the femtocells, δPTx_{cell}. The system iterates while it evaluates that any femtocell could be overloaded with the calculated new transmission power variation. That new network configuration would be estimated based on the *VMs*. Once the system achieves a balance situation, those new transmission power variations are set in femtocells. The system inputs are the cellular network KPIs, the PRX and the position of the terminals. The system output is a vector, $\overrightarrow{\delta PTx}$, with the transmission power variation that should be applied to each femtocell. Additionally, another vector, $\vec{F}$, indicates the activity of the femtocells (whether a femtocell has active users or not).
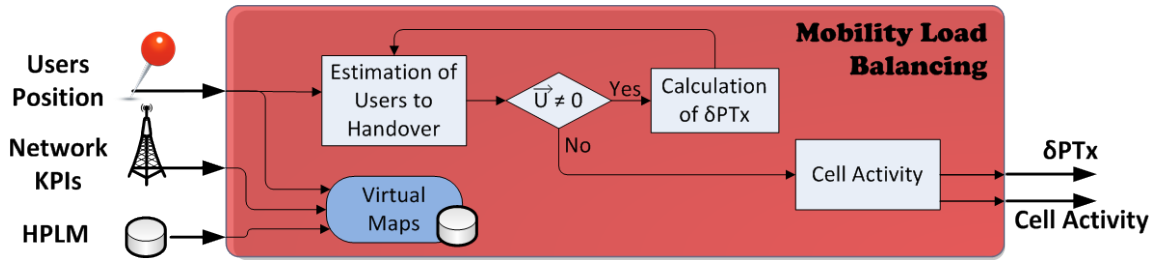
Figure 5.12: Context-aware MLB scheme.

Note that, when users' positions are not available or the indoor positioning system statistical parameters are unsuitable for improving the performance of the system due to high position error, PRX and cell data are directly read from the MRs and KPIs.

Additionally, two thresholds are defined to consider a serving cell is overloaded and its neighboring cells are low-loaded:

- S_{th} is the minimum ratio of users (see equation (5.10)) to consider a serving cell as highly loaded. Its range goes from 0 (cell is considered highly loaded) to 1 (cell is considered highly loaded).

- T_{th} is the maximum average ratio of users in the neighboring cells of the studied cell to consider the neighboring cells as low loaded and, consequently, available to catch users to offload the studied cell. Its range goes from 0 to 1.

These thresholds are configured based on a sensitivity study or on the operators' experience, policies or priorities. The initial condition $S_{th} > T_{th}$ should be mandatory to avoid possible ping-pong effects and oscillations in the MLB process.

The main modules of the MLB method are described in the next subsections according to Figure 5.12. As an iterative system, once the new femtocells transmission powers are estimated, this procedure analyzes the network again based on these estimations to detect possible overloaded femtocells with the new configuration.

5.5.3.2.1   Estimation of users to HO

The aim of this module is to provide an estimation of the number of users that should leave the selected overloaded cell, u_{cell}, to hand over towards a target cell. The scheme of this module is depicted in Figure 5.13. Firstly, the system examines the ratio of users per femtocell k (see equation (5.10), hereafter referred as $l_{cell(k)}$), where $active\_users_{cell}$ could be either 1) the number of active users in the femtocell (for the MR method) or 2) the number of users in the coverage area of the femtocell based on the SCM when users' positions are available (for the VM method).
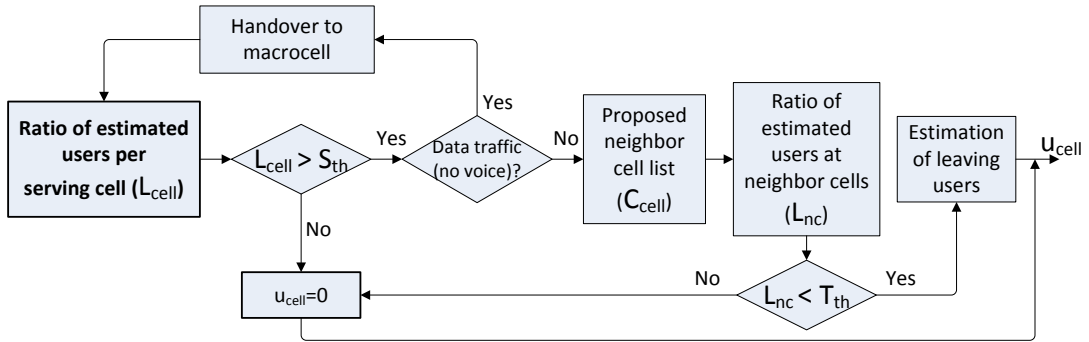
Figure 5.13: Scheme of estimation of users to HO.

All $l_{cell(k)}$ are ranked to get the maximum ratio, L_{cell}, and the highest overloaded cell. Hereafter that cell will be called *studied cell.* The procedure could return to this point to select the next ranked cell when the *studied cell* could not be offloaded in this iteration (see next subsection).

The condition $L_{cell} > S_{th}$ makes the algorithm continue, in other case, this module finishes with $u_{cell} = 0$ (no users should leave the *studied cell* in this iteration). In case the condition is accomplished, users are classified per service.

Due to the interest of satisfying voice call users, a basic classification of traffic into two main services is taken into account: *voice connections* and *other services*. In case there are users with other services (data traffic), these users are forced to handover to macrocells one by one after evaluating the initial condition again, $L_{cell} > S_{th}$. Note

that, in most cases, there is no macrocell coverage indoors. Hence, most of these data traffic users could be in outage for a while till a femtocell is available.

Since normally there is a high overlapping between femtocells because of their unplanned deployments, the studied cell would usually include a lot of cells in the *neighbor cell lists*. However, when users' positions are available, these lists would be changed by the *proposed neighbor cell lists* of the studied cell, C_{cell}, based on NCM, described in *"5.5.3.1.2 Neighbor cell maps"*. It would reduce overshooting issues.

Now, it is time to determine whether the neighboring cells have space to allocate new users or not. In this sense, the average of the ratio of users in the neighboring cells is calculated (same as the summation term of equation (5.9)):

$$L_{nc} = \frac{1}{NC_{cell}} \cdot \sum_{i=1}^{NC_{cell}} l_{cell(i)}, \qquad (5.22)$$

where $l_{cell(i)}$ is calculated according to equation (5.10), i refers to the identification of the neighboring cells and NC_{cell} is the length of that list.

After that, the situation could be:

- $L_{nc} \geq L_{cell}$, which means that the *studied cell* has less camped users than the average camped users of its neighboring cells. Therefore, no users should leave that cell because the situation out of this cell is the same or worst.

- $L_{nc} < L_{cell}$, which means that the situation of the *studied cell* could be critical but it could be solved as, in average, its neighboring cells present lower number of camped users. In consequence, some users of the *studied cell* will hand over to the most suitable neighboring cells.

To ensure good QoE, avoid ping-pong effects and continue with the offloading of the *studied cell*, the condition $T_{th} > L_{nc}$ should be accomplished. Otherwise, there are no close offloaded cells to share and move users towards. This situation could be solved by offloading those neighboring cells in the following iterations. Hence, the system would return to the first module and select the next ranked **cell** in terms of the ratio of active users (l_{cell}). That new **cell** would be the new *studied cell*. Note that, if the system is not able to solve this unlikely situation, an event would be trigger to warn the network engineers about this problematic situation. Engineers will study this case and evaluate the planning of the deployment of additional femtocells (if this case is repeated several times in the same place) or doing nothing because it is an isolate case or because S_{th} and T_{th} should be reconfigured (bad configuration or very restricted thresholds).

Finally, the number of users, u_{cell}, that should leave the *studied cell* are calculated:

$$u_{cell} = active\_users_{cell} - ceil\{\max\_users_{cell} \cdot \left(\frac{L_{cell} + \sum_{i=1}^{NC} l_{cell(i)}}{NC_{cell} + 1}\right)\}, \qquad (5.23)$$

where $ceil$ function gets the nearest integer towards infinity, $active\_users_{cell}$ could be either 1) the number of active users in the femtocell (for the MR method) or 2) the number of users in the coverage area of the femtocell based on the SCM when users' positions are available (for the VM method), max_users_{cell} is the total number of users that the femtocell could allocate, L_{cell} is the ratio of users per cell and NC_{cell} is the number of neighboring cells.

5.5.3.2.2   Calculation of $\overrightarrow{\delta PTx}$

This module decides the transmission power variation that must be applied to each femtocell to move users and to avoid overloaded cells in the network. The scheme is illustrated in Figure 5.14.
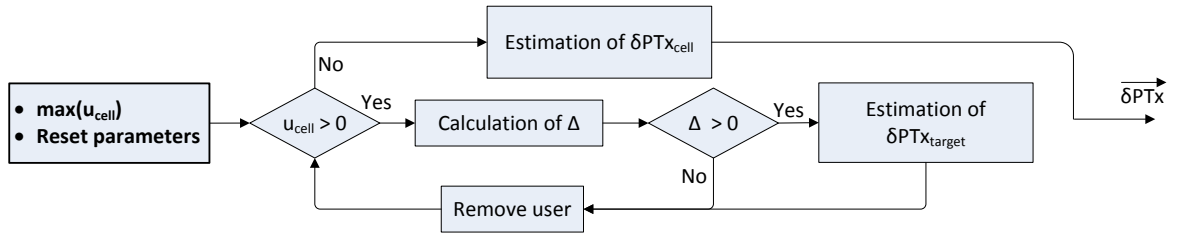
Figure 5.14: Scheme of calculation of $\overrightarrow{\delta PTx}$ block.

Once the candidate cell to be offloaded has been selected and the number of users that should leave the cell calculated, it is necessary to determine the PRX of users in that cell. The system proposes two ways to obtain the PRX depending on whether the users are located or not:

- *PRX from HPLM:* users' positons are required to estimate the value of its PRX. In this case, equation (5.11) estimates those values of PRX for each user' position and femtocell, based on the stored information of HPLM and equations (5.12) and (5.14).

- • **_PRX from MR:_** the PRX is directly acquired from the mobile reports. It provides actual data about the propagation channel.

When there is no information about the PRX from a given neighboring cell, the PRX for such cell is set to -130 dBm.

This process starts with the initialization of $\overrightarrow{\delta PTx}$ to zero or, in case the system had already iterated, with its previous value. Then, the calculation of Δ is performed. These parameters are calculated by elementary equations: additions, and operators: maximum and minimum. It would reduce the computational complexity and costs.

For each user $g(m)$ (where $m = \{1,2,\dots active\_users_{cell}\}$) of the *studied cell*, the PRX value from its serving cell, $PRX_{cell}^{g(m)}$, and the maximum PRX value from its neighboring cells, $RSSI_{nc(m)}^{g(m)}$, are defined. Being $nc(m)$ the neighboring cells with the highest value of PRX for the studied user m. Remind that this process could be done, either with information from MRs or, based on the VMs (SCM and NCM).

The following two vectors composed of those values are created:

$$\overrightarrow{PRX_{cell}} = \left\{ PRX_{cell}^{g(1)}, PRX_{cell}^{g(2)} \dots PRX_{cell}^{g\left(active\_users_{cell}\right)} \right\}, \qquad (5.24)$$

$$\overrightarrow{PRX_{nc}} = \left\{ PRX_{nc(1)}^{g(1)}, PRX_{nc(2)}^{g(2)} \dots PRX_{nc(active\_users)}^{g\left(active\_users_{cell}\right)} \right\}. \qquad (5.25)$$

After that, the minimum value of the difference between these two vectors is saved:

$$\Delta_{target} = \min\left\{ \overrightarrow{PRX_{cell}} - \overrightarrow{PRX_{nc}} \right\}, \qquad (5.26)$$

where **_target_** refers to the neighboring cell that minimizes previous equation. That neighboring cell $nc(m)$ which makes Δ_{target} minimum, is selected ($target = nc(m)$, possible target cell for that user). In case that Δ_{target} is positive, the transmission power variation δPTx_{target} applied to that target cell is calculated as follows in equation (5.27), where δPTx_{target} is equal to $\frac{\Delta_{target}}{2}$ the first iteration because initial values of δPTx_{target} are set to zero. Otherwise, Δ_{target} is negative, this step is skipped and the transmission power variation δPTx_{target} is not estimated.

$$\Delta PTx_{target} = max\left\{ \Delta PTx_{target}, \frac{\Delta_{target}}{2} \right\}. \qquad (5.27)$$

That user is removed from vectors $\overrightarrow{PRX_{cell}}$ and $\overrightarrow{PRX_{nc}}$ and u_{cell} decreases one unit. The loop is repeated till u_{cell} reaches the zero value, then, the *studied cell* transmission power variation δPTx_{cell} is calculated:

$$\delta PTx_{cell} = -\left(offset + max\{\overrightarrow{\delta PTx_{target}}\}\right), \tag{5.28}$$

where ***offset*** is the parameter involved in the handover process (e.g., event A3 in LTE [79]) defined to reduce ping-pong handovers, etc. and $\overrightarrow{\delta PTx_{target}}$ is the vector composed of all the target neighboring cells transmission power variations. Note that the decrease in the *studied cell* transmission power is truncated by τ_{min}, as well as the neighboring cells transmission power has an upper limit of τ_{max}. This condition is required to guarantee the QoS and to accomplish the maximum transmission power of the cells, respectively. Finally, the output of this module is the vector:

$$\overrightarrow{\delta PTx} = \{\delta PTx_{cell}, \overrightarrow{\delta PTx_{target}}\}. \tag{5.29}$$

The system emulates how the new network configuration, $\overrightarrow{\delta PTx}$, impacts on the deployed cells and determine whether it would be well-balanced or another cell needs to be analyzed because there are still overload issues ($L_{cell} > S_{th}$).

In order to do that, new values of PRX must be estimated per user (PRX'). To determine those values of PRX', the variable PTX_{cell} of equation (5.11) is replaced by $PTX_{cell} + \delta PTx_{cell}$, i.e., the new EIRP that should be configured in that cell. According to PRX' values and going back to the first block *"5.5.3.2.1 Estimation of users to HO"*, the new number of active users per $cell_i$ is estimated based on the number of users that accomplish: $\{PRX'_{cell_i} > PRX'_{cell_j} \forall i \neq j\}$. With the availability of users' positions, new SCM and NCM are built to estimates the serving areas and the *proposed neighboring cell list*.

5.5.3.2.3   Cell activity

Once the system has determined the network would be well-balanced ($L_{cell} < S_{th}$), the last block provides the configuration as an output file. It contains information about cells transmission power variation, $\overrightarrow{\delta PTx}$, and the activity of the cells, $\vec{F} = \{f_{cell(1)}, f_{cell(2)}, ... f_{cell(k)}\}$. The latter indicates when a cell has camped users:

$$f_{cell} = \begin{cases} 1 & cell\ has\ camped\ users \\ 0 & otherwise \end{cases}. \tag{5.30}$$

5.5.3.3   Load balancing and energy savings coordination

As MLB mechanisms are femtocell transmission power related, the modification of this parameter might be highly susceptible to logical or parametric dependencies with other SON algorithms. As a consequence, many conflicts could arise (e.g., tuning the same network parameter) during mobile network operation due to these dependencies, undermining the stability of the network performance. The coordination of SON algorithms is an important challenge that must be addressed to ensure the highest network performance [110].

Those cells with no close users could turn off its radio propagation activity and standby their internal procedures by keeping the cell in dormant mode or switched off. As a consequence, a substantial reduction of mobile network energy consumption could be reached. This use case is referred as *Energy-Savings* (ES) [45]. Since it is power related, the coordination between this mechanism and other power related SON methods is mandatory to avoid potential conflicts in the network parameters adaptation, ensuring the system robustness and reliability [110].

Based on this, a location-based ES algorithm and its coordination with proposed MLB mechanisms are developed to ensure users' accessibility and retainability, at the same time reducing the overall power consumption. These mechanisms analyze the network indicators and the information about the positions of the terminals (see the scheme in Figure 5.15).
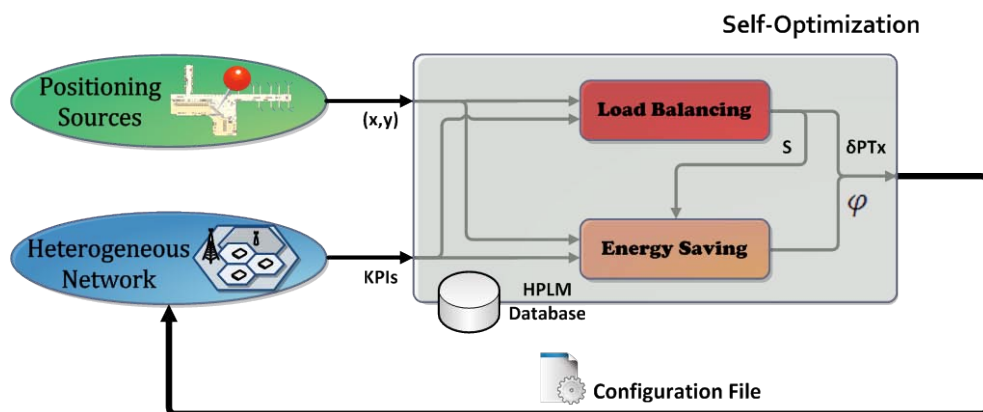

Figure 5.15: Coordinated location-based self-optimization scheme.

This mechanism switches on/off or turns into dormant mode the femtocells depending on the users' position, the network KPIs and the information provided by the MLB mechanism. In dormant mode, the femtocell is recovered in few seconds,

whereas it takes tens of seconds when it is switched off. This algorithm will be triggered once the MLB algorithm had finished.

5.5.3.3.1   System implementation

The ES system is illustrated in Figure 5.16, which is mainly composed of two modules. The first module computes the *reference distance* based on the SCM. The second module introduces a FLC to evaluate the status of each femtocell:

- **Reference distance:** This module calculates an indicator named *reference distance* for each user and cell, which is proportional to the distance from the users' position to the *studied cell*.
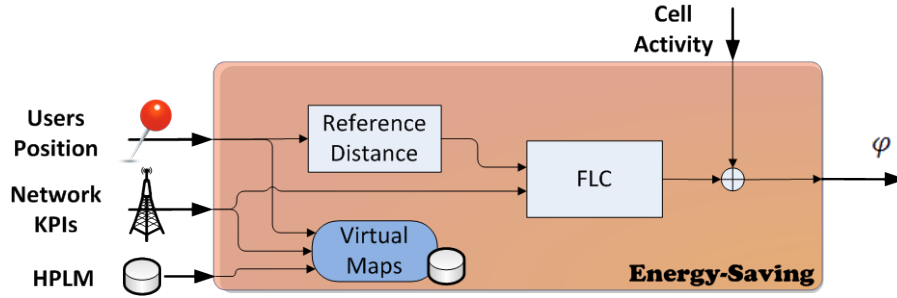
Figure 5.16: Energy-savings scheme.

For that purpose, a process similar to that defined for *NCM* (see Figure 5.11) is applied in this method for each *studied cell*. In this case, instead of removing the studied cell, the femtocells of its *proposed neighbor cell list* (see equation (5.21)) are removed from the network. In consequence, a new layer is created with three different areas: 1) the original studied cell coverage area is defined as "blue area", 2) the new extended coverage area of that cell is the "green area" and 3) the rest of the scenario is denoted as "red area" (see Figure 5.17).
After that, a vector $\overrightarrow{E_{cell}}$ is obtained with the *reference distances* of all users in the scenario for each *studied cell*. It is built as:

$$\overrightarrow{E_{cell}} = \big(e_{cell}(g_1), e_{cell}(g_2) \dots e_{cell}(g_n)\big), \tag{5.31}$$

where g_x identifies the user, n is the total number of active users in the scenario and $e_{cell}(g_x)$ is described as follows:

$$e_{cell}(g) =$$

$$= \begin{cases} 0.5 \cdot \dfrac{d_{cell-user}}{d_{cell-blue\_edge}} & if\ g \in original\ cell \\ 0.5 \cdot (1 + \dfrac{d_{cell-user} - d_{cell-blue\_edge}}{d_{cell-green\_edge} - d_{cell-blue\_edge}}) & if\ g \in extended\ area \\ 1 & if\ g \in rest\ of\ scenario \end{cases} , \qquad (5.32)$$

where d_{a-b} is the distance from position a to position b. In consequence, the subindex **cell** identifies the position of the *studied cell* and **user** refers to the position of each terminal. The subindexes **blue_edge** and **green_edge** are calculated as the intersection between the line $(cell - user)$ and the area edge. Finally, the minimum *reference distance*, $\varepsilon_{cell} = \min\{\overrightarrow{E_{cell}}\}$, is selected.
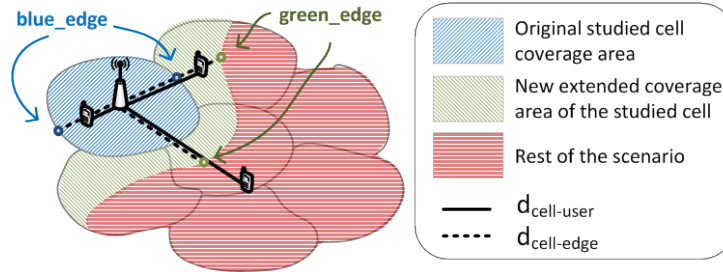
Figure 5.17: Reference distance scheme.

- ***Fuzzy logic controller (FLC):*** This module decides whether the femtocell should be switched on/off or kept in dormant mode. For that purpose, a FLC has been selected to evaluate the *reference distance* information, ε_{cell}. The main reason to select a FLC is its simplicity in implementing and managing rules based on the recommendations of expert as well as its low computational cost to be implemented in a real network. *Appendix C* details the FLC approach based on the Takagi-Sugeno-Kang (TSK) [111] approach. The FLC is defined according to the requirements of the energy efficiency mechanism. The input parameters to the FLC are: the *Reference Distance* (RD), which comprises the ε_{cell} value for each studied cell; and the *Cell Status* (CST), which presents the current status of the studied cell (on, off or dormant mode). The *Proposed Cell Status* (PCS) is the output of the system, whose possible values are: *'ON'* (value = 1), *'Dormant Mode'* (value = 0) and *'OFF'* (value = -1) (see Figure 5.18c). A membership function is defined for each input. RD possible values are: *'Very Close'* (VC), *'Close'* (C), *'Far'* (F) and *'Very Far'* (VF). Likewise, CST possible values are: *'ON'* (ON), *'Dormant Mode'* (DM) and *'OFF'* (OFF). These membership functions are shown on Figure 5.18(a) and Figure 5.18(b).
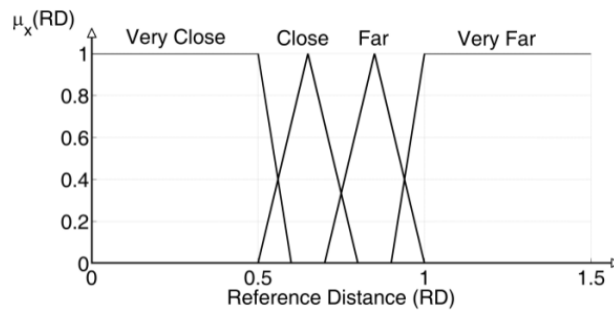
(a) Input 1
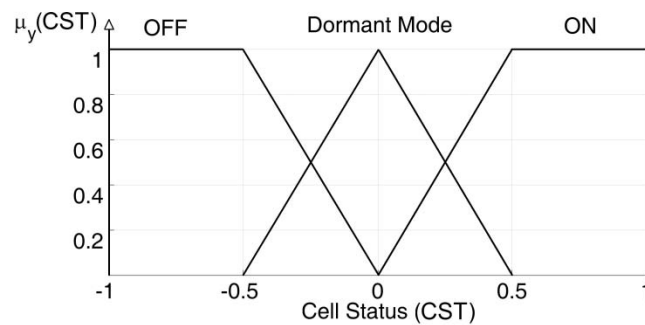
(b) Input 2
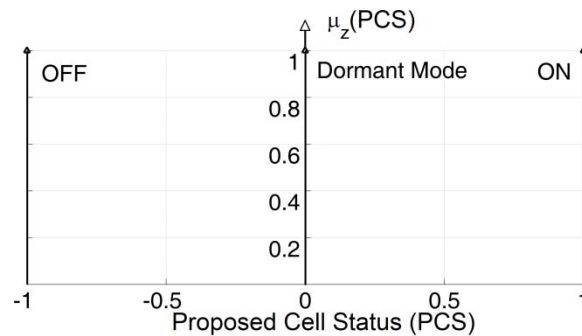
(c) Output

Figure 5.18: Membership functions.

The fuzzy rules are described in Table 5.5, which are based on the AND operator. This means, all the conditions of the expression must be true. For a better understanding, an example rule is described: 'IF RD is *'close'* AND CST is *'dormant mode'* THEN PCS is *'ON'*.

The two membership functions are computed to get the degree of truth of each rule i:

$$\alpha_i = \mu_x(RD) * \mu_y(CST), \tag{5.33}$$

where $*$ is the AND operation included in the antecedent of the rules. Finally, the FLC presents the output value, o_{cell}, based on the center-of-gravity method:

$$o_{cell} = \frac{\sum_{i=1}^{B} \alpha_i \times \omega_i}{\sum_{i=1}^{R} \alpha_i}, \tag{5.34}$$

where α_i is the degree of truth for rule i (equation (5.33)), ω_i is the value of the constant output (1, 0 or –1) of rule i and B is the number of defined rules.

The last step of the ES algorithm is to integrate the output value of the FLC (o_{cell}) with the Cell Activity (S_{cell}) provided by the MLB mechanism, as the latter is more critical.

$$\varphi_{cell} = \begin{cases} -1 & if \ S_{cell} = 0 \ and \ o_{cell} \in (-1, -0.5) \\ 0 & if \ S_{cell} = 0 \ and \ o_{cell} \in [-0.5, 0.5], \\ 1 & otherwise \end{cases} \tag{5.35}$$

where φ_{cell} could take the same three values as PCS: –1, this mean the femtocell must be OFF, 0, the femtocell must be in dormant mode and 1, the femtocell must be ON.

Table 5.5: Fuzzy rules.

Reference Distance (RD)	Cell Status (CST)	Proposed Cell Status (PCS)
VC	-	ON
VF	-	OFF
C	OFF	DM
C	DM	ON
C	ON	ON
F	OFF	OFF
F	DM	OFF
F	ON	DM

5.6   Simulation evaluation

The evaluation of the proposed mechanisms is presented in this section. Firstly, an introduction to the simulation tool and the selected scenario is provided. Then, the proposed SON methods are assessed.

5.6.1   Simulation set-up

5.6.1.1   Simulator overview

The dynamic LTE system-level simulator described in [47] is selected to prove and evaluate the proposed SON mechanisms. Winner II [112] is the implemented propagation model at the simulator, as several propagation configurations and conditions are considered: indoor, outdoor, outdoor-to-indoor and indoor-to-outdoor scenarios. Likewise, shadowing is modeled following a spatially-correlated log-normal distribution with different standard deviations for outdoor and indoor users, whereas fast-fading is modeled following the *Extended Indoor A* (EIA) approach for indoor users [113]. Users can demand both VoIP or data services. Round-robin best channel scheduling is selected for VoIP traffic and proportional fair scheduling for data service. Common RRM features are also integrated into the simulator, such as *Cell Reselection*, *Directed Retry* (DR), HO based on 'A3' and 'A5' events [79], etc. The most important simulation parameters and features are shown in Table 5.6. A full simulator description can be found in reference [47].

Table 5.6: Simulation parameters.

Propagation Model	Indoor-indoor	Winner II A1
	Indoor-outdoor	Winner II A2
	Outdoor-outdoor	Winner II C2
	Outdoor-indoor	Winner II C4
Base Station Model	EIRP	3 (HeNB) / 43 (macro) dBm
	Directivity	Omni (HeNB) / tri-sector (macro)
	Access	Open (HeNB) / open (macro)
Mobile Station Model	Noise Figure	9 dB
	Noise Density	-174 dBm/Hz
Traffic Model	Calls	Poisson (avg. 0.43 calls/user $\cdot$ h)
	Duration	Exponential (avg. 100 sec)
Mobility Model	Outdoor	3km/h, random direction & wrap-around
	Indoor	Random waypoint
Service Model	Voice over IP	16 kbps
	Full Buffer	
RRM Model	Bandwidth	1.4, 3 and 5 MHz (6, 15 and 25 PRBs)
	Access Control	Directed Retry (Threshold=-44dBm)
	Cell Reselection	Criteria S, R
	Handover	Events A3, A5
	Scheduler	Voice: Round-Robin Best Channel
Time Resolution		100ms
SON Algorithm	Epoch Time	60 seconds

5.6.1.2   Scenario

A realistic scenario has been designed and introduced into the simulator to verify the proposed algorithms. A tri-sectorized LTE macrocell is deployed in a 3 km long and 2.6 km wide area where the wrap-around technique avoids edge effects (left image in Figure 5.19). A building is placed inside this environment 500 m far from the site. This building models the Departure Lounge of Malaga Airport, which is a 265 m long and 180 m wide building (right image in Figure 5.19). In order to guarantee the cellular network coverage and to increase the indoor capacity, twelve open access LTE femtocells (HeNB) have been placed in the building. They are distributed to ensure coverage area by at least two femtocells in the whole building. This scenario presents a frequency reuse factor of 1. In this context, outdoor macrocells might introduce indoor interference due to the building proximity to the sites. Handovers between macrocells and femtocells are supported. At the beginning of the tests, macrocells and femtocells have been set up to transmit 43 dBm and 3 dBm, respectively.
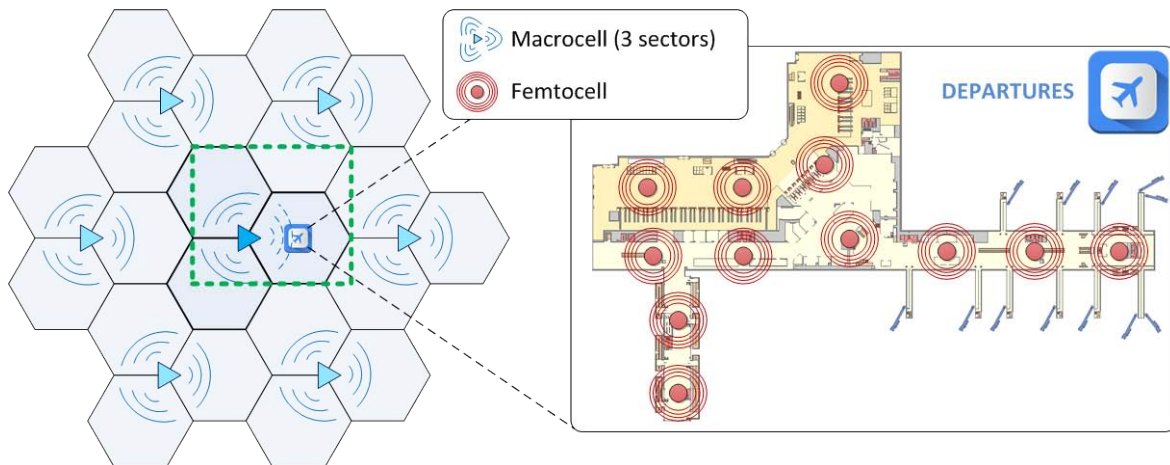
Figure 5.19: Simulated scenario.

Femtocells need a period to set the configuration file to update femtocell parameters (i.e., to change the transmission power for the proposed SON methods) which normally takes tens of seconds. For these reasons, the algorithms are triggered every minute while different hotspots are created every hour and the simulation lasts 24 hours. Conversely, macrocell parameters are not modified.

At the airport, the user mobility is based on a random waypoint model [114], which reproduces normal passenger behavior and movement at the airport. These movements are defined to create non-homogeneous user distributions and hotspots where network congestions may occur. A specific femtocell could be overloaded during certain

minutes, emulating a delayed boarding (passengers use their smartphones waiting for boarding). Hence, the simulated scenarios are initially well-balanced and there are no congestion issues. After several minutes, new passengers arrive to the boarding gate, thus overloading the femtocell in charge of covering that area. That situation lasts several minutes until the passengers of the delayed flight can start boarding and network congestion issues disappear.

5.6.1.3   Analysis of internal procedures

Figure 5.20 shows examples of HPLM for some of the deployed cells. Initially, beacons were placed each 2 m to emulate the transient response and to gather PRX samples at those positions. In addition, the resolution of the HPLM is set to 50 cm. Thus, those positions with no PL information are estimated based on equation (5.14).

(a) Macrocell I (Sector 1)

(b) Femtocell II

(c) Femtocell IV

(d) Femtocell XI
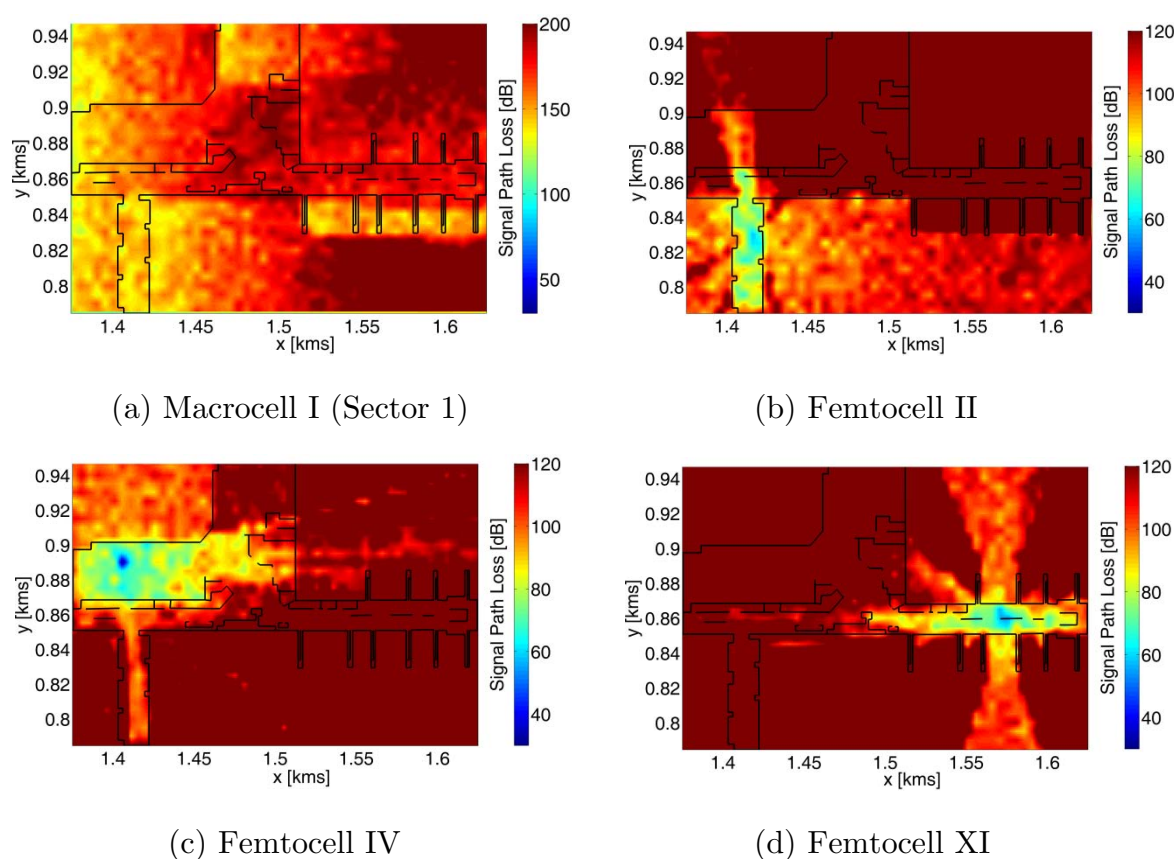
Figure 5.20: Example of HPLM.

Figure 5.21(a) presents an example of the classical coverage area in the studied scenario. In turn, the proposed SCM is depicted in Figure 5.21(b).
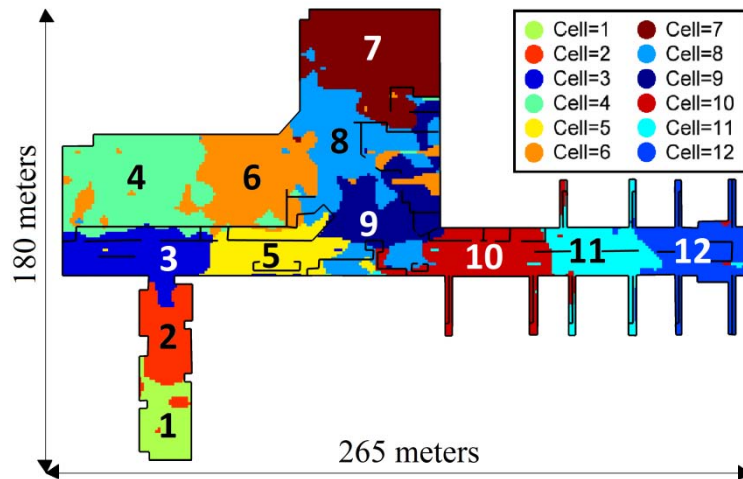
(a) Classical coverage areas
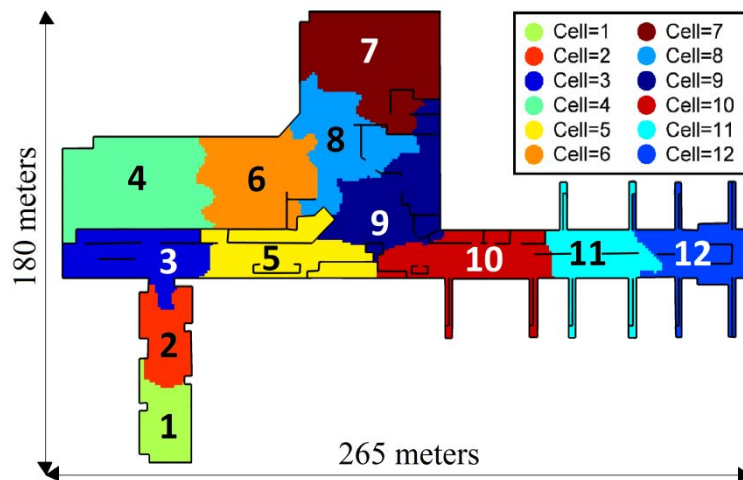
(b) Proposed cell areas (SCM)

Figure 5.21: Estimated SCM.

To ensure that all positions are always simultaneously covered by at least two femtocells (it would be a requirement of the cellular-indoor positioning system detailed in the field trial), the minimum value of transmission power variation is limited to -30 dB. The maximum increment is set to 10 dB as the femtocells maximum transmission power is restricted to 13 dBm (initially 3 dBm).

5.6.2   Simulation results

Initially, the fuzzy-based MLB mechanisms are assessed. Then, the proposed context-aware SON methods are discussed.

5.6.2.1 Fuzzy-based MLB mechanisms

Firstly, a sensitivity study is performed to analyze the performance of the algorithms with regard to the changes in the membership functions. Secondly, the global network and hotspot (most congested cell) simulation results are presented and described in a specific scenario: femtocells are limited to maximum 8 connected users and 1.4 MHz bandwidth. Thirdly, the study is extended to different femtocells' capacity deployments (max. 4, 8, 16 and 32 users) and bandwidth (1.4, 3 and 5 MHz).

5.6.2.1.1 Sensitivity study

Initially, five sets of membership functions with different interval of definition are adjusted by experts for each input indicator ($Load_{diff}$ and $User_{diff}$). These intervals change in steps of 0.025 in the range of ±0.05 (keeping the shape of the membership function and the symmetry) according to the ones illustrated in Figure 5.4(b) and Figure 5.5(b). Additionally, another five sets of membership functions with different intervals, out of these recommendations, were evaluated. A sensitivity study is performed in the previous scenario where the maximum number of active connections is restricted to 4 users and the femtocell bandwidth is 1.4 MHz. Table 5.7 shows the performed sensitivity study where the UDR indicator has been evaluated. On the one hand, the analysis shows that the algorithm's performance was not very sensitive to the set of membership functions proposed by experts (see the evaluation of Set 1 to Set 5). On the other hand, membership functions different to the recommendations of experts (Set 6 to Set 10) show (as expected) lower system performance. Therefore, it is assumed that membership functions that significantly differ from experts' recommendations would probably decrease the algorithm's performance.

Table 5.7: Sensitivity analysis (UDR [%]).

	Max. 4 users/femtocell (1.4MHz)									
	Set 1	Set 2	Set 3	Set 4	Set 5	Set 6	Set 7	Set 8	Set 9	Set 10
PLS	3.6458	3.6594	3.6487	3.6624	3.6548	5.157	5.2368	5.4861	5.1958	5.3682
PUS	1.2351	1.241	1.2115	1.2254	1.2388	4.1253	4.3672	4.6985	4.1687	4.8372

Finally, the set of membership functions with the lowest UDR (Set 3) is implemented (functions presented in Figure 5.4 and Figure 5.5). Note that, these membership functions are also implemented in other deployments where femtocells present different capacities (8, 16 and 32 users) and frequencies (3 MHz and 5 MHz).

5.6.2.1.2   Assessment of the results: 8 users at 1.4 MHz

The first analysis corresponds to the situation in which all femtocells limit is set to
8 active users and the network bandwidth is 1.4 MHz, i.e., it supports 6 PRBs. Both,
the global network and the hotspot performance are assessed in these tests.

Figure 5.22(a) illustrates the UDR indicator during one hour simulation. This
indicator is collected every minute as vertical lines depict. This figure represents the
network analysis when there is no optimization method implemented at this scenario
(No OPT - blue stem) and the performance of the four MLB algorithms. The average
value during the simulation is also shown for each method (horizontal lines).

The non-optimized situation (blue stem with circles), which represents the absence
of MLB methods, shows no congestion issues at the beginning and at the end of the
evaluation, i.e., no users are dissatisfied. However, the network displays a high
percentage of dissatisfied users during the overloaded period (from minute 30 to 50).
Sometimes, the ratio of dissatisfied users reaches UDR=50%, i.e., half of the users that
attempt to access the network in that minute are rejected or connected users are
dropped. On average, this network indicator is 10% (horizontal blue line), which is
higher than the values typically accepted by mobile operators.
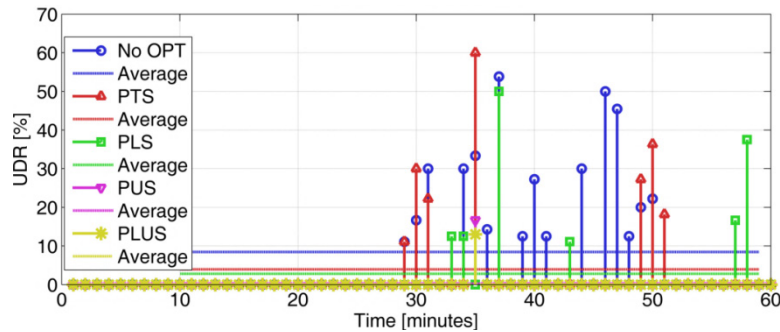
(a) Network performance (max. 8 users/femto and 1.4 MHz)
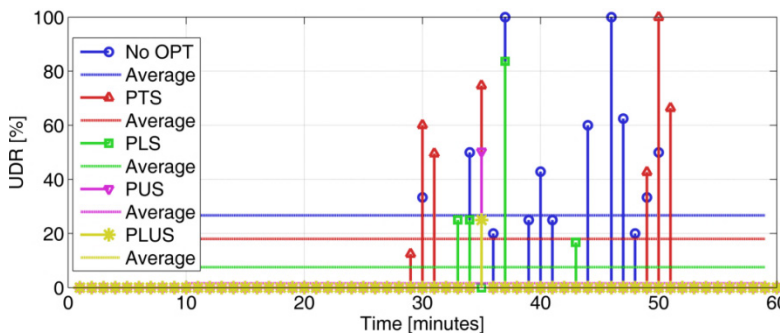
(b) Hotspot performance (max. 8 users/femto and 1.4 MHz)

Figure 5.22: UDR performance (1.4 MHz).

The PTS method (red stem with triangles) starts to reduce the blocked calls after detecting them, therefore, the UDR decreases as well. Nevertheless, due to the traffic fluctuations, peaks of UDR are obtained. Thanks to this mechanism, the average UDR is reduced to about 4%. However, as previously explained, this mechanism needs a large period of time to converge.

The PLS mechanism (green stem with squares) shows improved results because it makes use of the occupied radio resources as input, decreasing the number and the value of dissatisfied users' situations. The horizontal green line in Figure 5.22(a) shows an improvement over 7% from the non-optimized situation and 1% from the PTS method, getting an average value of UDR below 3%. Nevertheless, its $Load_{diff}(cell)$ input does not reflect the most restricted factor for femtocells because it usually offers enough bandwidth to serve more users than the femtocell is able to support in connected mode. Thus, there are free radio resources and the algorithm is not triggered but the femtocell is totally congested (no more users are accepted).

The PUS method (magenta stem with inverse triangles) reduces the users' dissatisfaction. However, the performance of the algorithm decreases when the required user's QoE is very high (huge amount of radio resources are demanded by the users). With this method there are only problems for an instant (minute 35) where few users are connected to the network but a lot of radio resources are required. Average UDR is lower than 1% (horizontal magenta line).

The PLUS method (yellow stem with stars), as expected, provides the best results. In this case, the algorithm is aware of the amount of free space to access the femtocell both, in terms of active users and radio resources. The figure shows the same problem as with the PUS method for an instant (minute 35), where few users are connected to the network but a lot of radio resources are required. However, the UDR is lower because it also optimized the parameters according to the occupied radio resources. In average during one hour (horizontal yellow line), the value of UDR is around 0.2%, which complies with the usual operators' requirements.

UDR indicator at the most overloaded cell (hotspot) is shown in Figure 5.22(b). UDR evolves in the same way as in Figure 5.22(a), although it is higher in all cases. In average, around 30% of users are dissatisfied, while the optimization PTS, PLS, PUS and PLUS methods get around 18, 7, 2 and 1% of UDR respectively.

5.6.2.1.3   Assessment of the results: Other configurations

The previous study has been extended to other femtocell deployments (different number of maximum connected users) and different bandwidth. The performance in

terms of the average value of UDR is depicted in Figure 5.23 for the different use cases.
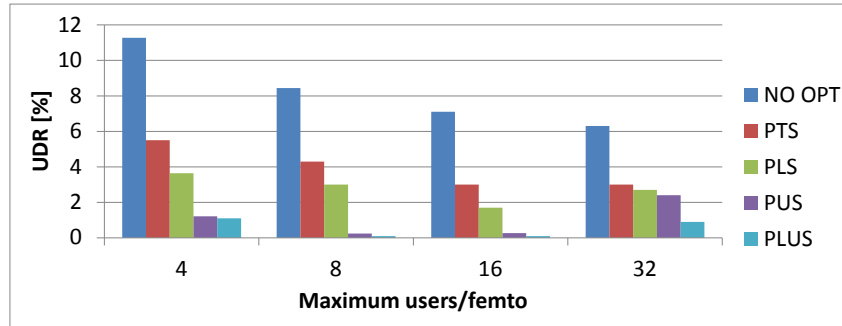
(a) 1.4 MHz (6 PRBs)
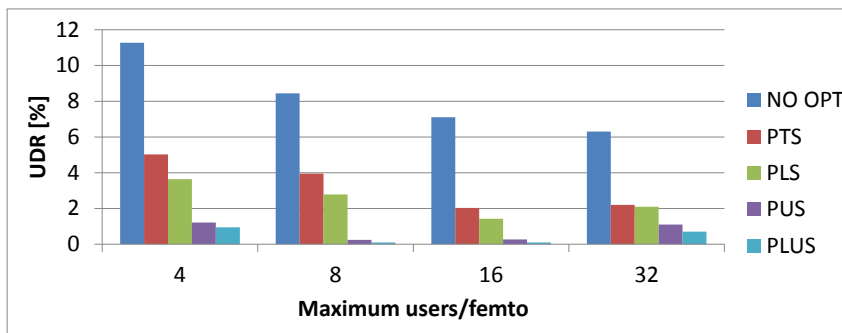
(b) 3 MHz (15 PRBs)
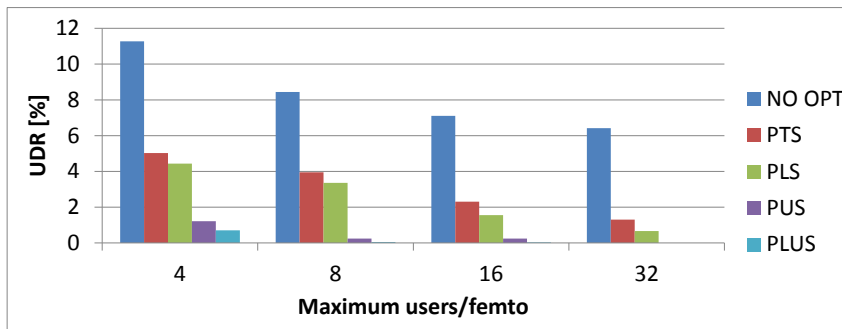
(c) 5 MHz (25 PRBs)

Figure 5.23: Average UDR performance

The minimum LTE bandwidth (1.4 MHz) is depicted in Figure 5.23(a). The UDR is reduced when the femtocell limitations in the maximum number of active users is increased. For the scenarios of maximum 4 and 16 active users per femtocell, the same explanation of previous subsection (8 active users at 1.4 MHz) is valid. Conversely, for the scenario of maximum 32 active users per femtocell, depending on the experienced

users' quality and demand, sometimes the femtocell allows less than 32 simultaneously connected users because there are no available resources. Likewise, at another time, the femtocell allows 32 users because there are free radio resources. The reason is related to the RRM configuration. According to this, all the algorithms have comparable average UDR value except the PLUS method. Those situations overload femtocells adjacent to the hotspot and, many handover attempts fail (dropped connections appear) because those adjacent cells are already fully occupied (active users or radio resources). It means that the PUS method will not properly work all the time, the same for the PLS method. However, this issue is successfully fixed thanks to the PLUS method. Additionally, commercial femtocells could avoid this problem because most of them work with wider bandwidth (normally > 3 MHz).

Similar simulations have been carried out with higher bandwidth (3 MHz), as Figure 5.23(b) depicts. This time, the maximum 32 users per femtocell deployment has enhanced UDR and, in particular, the PUS method presents much better performance compared to the 1.4 MHz case because the network available radio resources are higher. For the other use cases, the network performance is similar to the previous bandwidth (1.4 MHz) deployments.

Finally, the network bandwidth was increased to 5 MHz. Figure 5.23(c) shows the overall network improvement achieved thanks to the PLUS method. It should be noticed that the higher the network bandwidth, the worse the PLS method works. This is due to the fact that the network bandwidth is increased but the occupied radio resources are the same (for most network services).

An indicator which concerns operators is the HO signaling load (measured by the UHR). The higher the number of handovers the network manages, the more expenses the operator should afford. At Figure 5.24, results have shown that, in average, there is around one handover per user for all the methods. This is related to both pilot and data transmission powers are jointly tuned. Hence, changing and resizing femtocell areas do not increase signaling load, in consequence operator's expenses are the same.

To summarize, all methods have reduced users' dissatisfaction while the network signaling load is held. At indoor networks where different bandwidth and types of femtocells are analyzed, both femtocell radio resources and maximum number of active users supported by the femtocell must be considered in MLB methods. Proposed PLS and PUS methods provide good results, but their performance depends on the predominant kind of traffic in the femtocells. The proposed PLUS method, however, led to the best network and hotspot performance for all situations with fast traffic fluctuations.
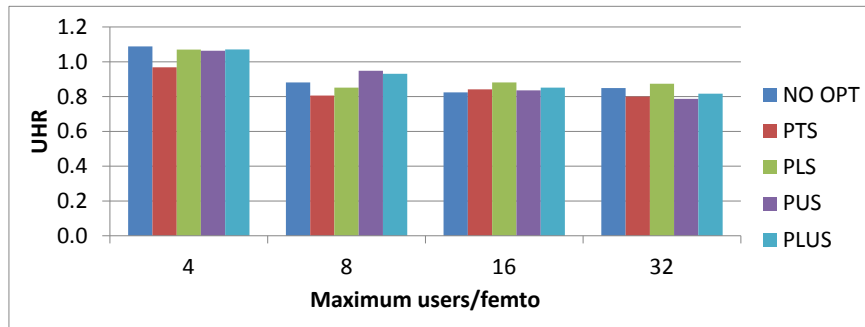
(a) 1.4 MHz (6 PRBs)
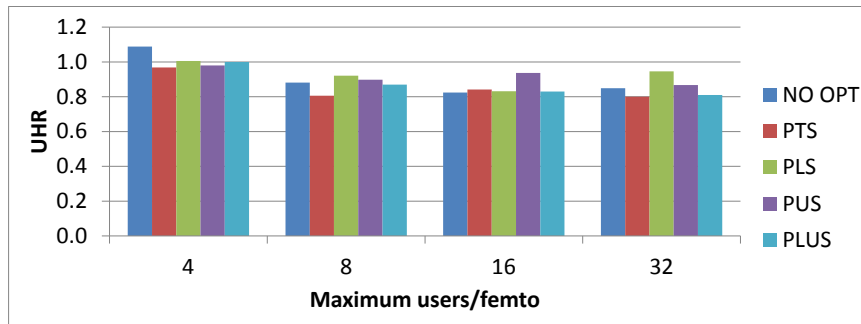
(b) 3 MHz (15 PRBs)
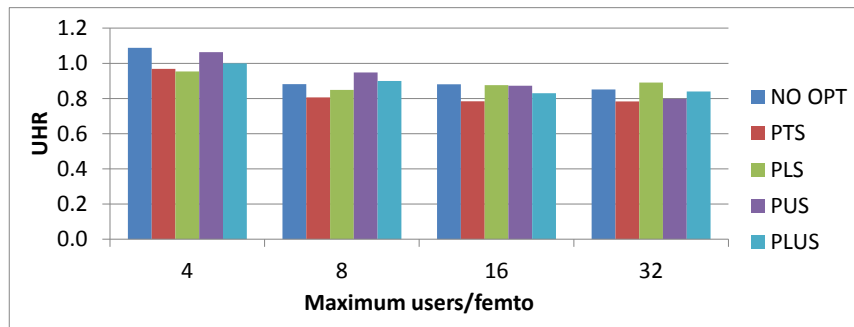
(c) 5 MHz (25 PRBs)

Figure 5.24: Average UHR performance.

5.6.2.2   Context-aware load balancing mechanisms

Firstly, a sensitivity study is performed to analyze the performance of the algorithms with regard to the changes in the defined thresholds. Secondly, the assessment of UD, VM and MR methods is detailed in four scenarios (maximum femtocell capacity: 4, 8, 16 and 32 active users at 5 MHz bandwidth). Thirdly, the study is extended to analyze the impact of users' position error in the proposed context-aware mechanisms. Finally, the results of the coordination of the VM and MR methods and the ES method are discussed.

5.6.2.2.1   Sensitivity study

The performance of the proposed methods would depend on the configuration of their thresholds. These thresholds could be defined based on:

- *The operators' experience, policies or priorities in this field:* expert engineers propose different configuration parameters based on their knowledge in this kind of networks. Then, these thresholds could be slightly modified to reach the optimal configuration.

- *A sensitivity study of the UDR indicator*: the femtocell deployment is simulated with different thresholds to estimate the lowest values of UDR. This procedure is the one followed to get the thresholds of the proposed mechanisms.

UD method

Figure 5.25 shows the average values of UDR depending on S_{th} and Q_{th} in steps of 10 and a deployment of femtocells with maximum 32 active users simultaneously at 5 MHz. The minimum value of UDR is obtained when the ratio of connected users, S_{th}, and the average ratio of occupied radio resources, Q_{th}, is over 50 and 60, respectively. Under this configuration, the algorithm reduces the UDR to 1.6%. Note that the performance of the system is not very sensitive to the parameter selection (it would be around 2.5% of UDR) when the value of the selected parameters is below 100 (100 means the location-aware method is not triggered). In consequence, this system would not require a complex study to select the optimal parameters.
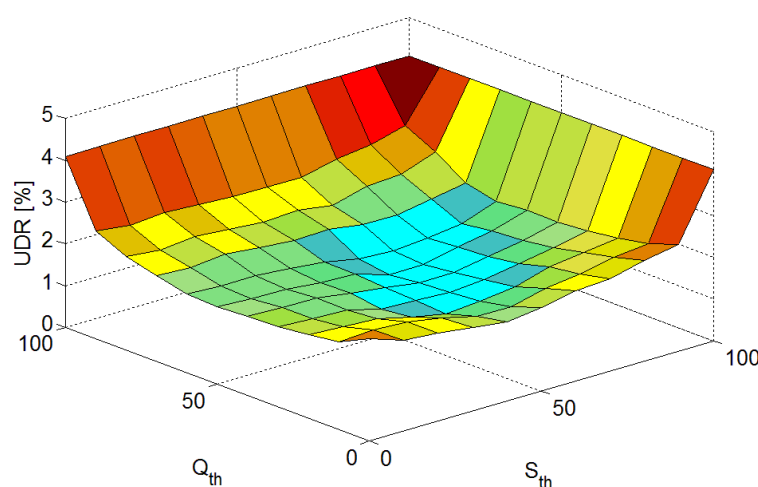
Figure 5.25: UD method - Sensitivity study.

VM method

Figure 5.26 shows the average values of UDR depending on S_{th} and T_{th} in steps of 10 and a deployment of femtocells with maximum 32 active users simultaneously at 5 MHz. The minimum value of UDR is obtained when the ratio of femtocell connected users, S_{th}, is over 70 and the average ratio of neighbors femtocell connected users, T_{th}, is below 60. Under this configuration, the algorithm reduces the UDR to 1.1%. Similar to UD sensitivity study, this system would not require a complex study to select the optimal parameters as the performance of the system is not very sensitive to the parameter selection (it would be around 2% of UDR) when the value of the selected parameters is below 100 (100 means the location-aware method is not triggered).
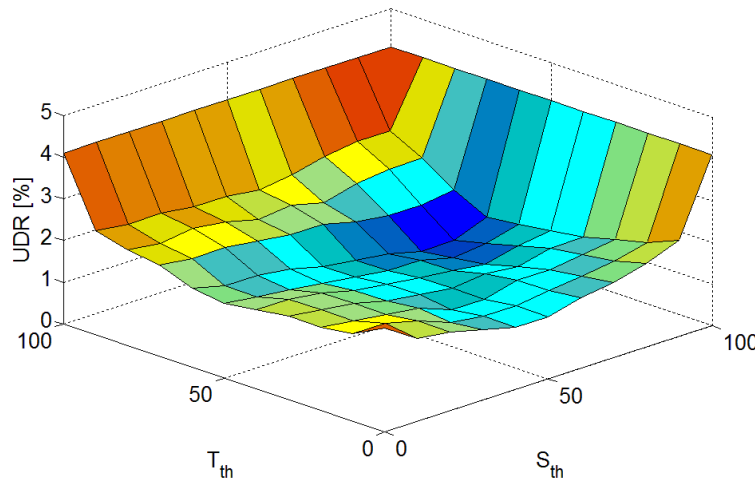
Figure 5.26: VM method - Sensitivity study.

MR method

Figure 5.27 shows the average values of UDR depending on S_{th} and T_{th} in steps of 10 and a deployment of femtocells with maximum 32 active users simultaneously at 5 MHz. The minimum value of UDR is obtained when the ratio of femtocell connected users, S_{th}, is over 50 and the average ratio of neighbors femtocell connected users, T_{th}, is below 40. Under this configuration, the algorithm reduces the UDR to 1.8%. Similar to previous methods, this system would not require a complex study to select the optimal parameters as the performance of the system is not very sensitive to the parameter selection (it would be around 2.5% of UDR) when the value of the selected parameters is below 100 (100 means the method is not triggered).
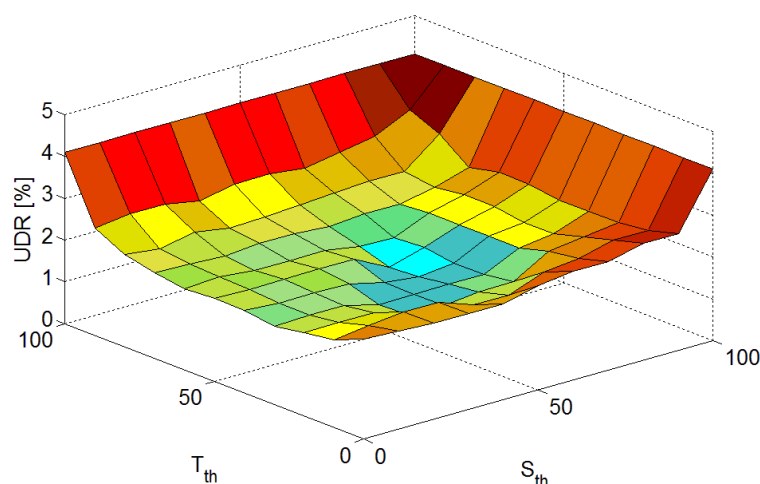
Figure 5.27: MR method - Sensitivity study.

5.6.2.2.2   Assessment of the results

The proposed algorithms are compared to the non-optimized network (baseline) and the PLUS algorithm described in subsection "5.4.1.4". The challenge faced is threefold. Firstly, the UDR must be as low as possible. Secondly, a good QoE is expected to support the communication. Finally, the number of HOs should not be highly increased to keep the signaling data.

According to the sensitivity study of the UDR indicator carried out for each method in the airport scenario, the optimal values for theses thresholds are: $S_{th} = 50$ and $Q_{th} = 60$ for UD method, $S_{th} = 70$ and $T_{th} = 60$ for VM method and $S_{th} = 50$ and $T_{th} = 40$ for MR method.

In order to accomplish an extensive and complete study, the evaluation of the algorithms was performed in four different indoor deployments depending on the femtocell capacity (maximum 4, 8, 16 and 32 active users). The number of users in the scenario has been established according to the analyzed cell capacity, e.g., for a femtocell capacity limit of 4 active users, 500 users per hour are simulated, whereas for a femtocell capacity limit of 8, a population of 1000 users per hour is defined.

As aforementioned, femtocells need a period to set the configuration file (i.e., to change the transmission power) which normally takes tens of seconds. For this reason, the algorithms are triggered every minute while hotspots are created every hour at different places (see Figure 5.29).

Maximum femtocell capacity: 32 active users

Initially, the network is well-managed and there are no accessibility or retainability issues (i.e., all the attempted connections are accepted and none of them are dropped). However, after 10 minutes, the number of active users in the network starts to increase and a specific area of the scenario becomes overloaded (e.g., a boarding gate). At this moment, femtocells close to that area would reach their maximum capacity and would have to reject/drop connections as Figure 5.28(a) shows ('NO OPT' – yellow line with triangles). That situation persists during more than 30 minutes, being UDR around 7%. After that period, the number of active users is reduced and the network can then accept new requests. In average, the UDR is around 4% along one hour, which is over the maximum value accepted by most mobile operators' policies.

Now, the same scenario is optimized by the PLUS method. Figure 5.28(a) shows that this method ('PLUS method' – magenta line with dots) outperforms the non-optimized case when the network is congested (3.5% vs 7% UDR), while the average value of UDR along one hour is reduced below 2%. The performance of the proposed VM method is also shown in Figure 5.28(a) ('VM method' – cyan line with circles), which enhances UDR over 50% in comparison with PLUS method. In the case of the UD method ('UD method' – dark blue line with reverse triangles), UDR is also better than the PLUS method. However, due to the use of the geometrical distances between the users to estimate the new transmission power of femtocells, the performance of this indicator is slightly lower compared to the VM method. This is related to the walls and obstacles in the scenario which makes two close users could receive quite different PRX. Open areas would help to make similar the proposed transmission power adaptation of these two methods. In case the PRX values are directly reported by the users, the MR method ('MR method' – green line with crosses) outperforms the PLUS method but the UDR performance is increased compared to the location-aware methods. The main reason of the increment and the fluctuations of the indicator on the time, is related to the channel instability: shadowing, multi-path reflections, wall obstructions, etc., although the terminal protocol stack (Layer 1 and Layer 3 [79]) minimizes the impact of fast-fading ($\Delta f \approx [\pm 5dB]$).

The channel quality is directly related to the previous UDR indicator. For the non-optimized case, the level of MCQI is the highest even if there are accessibility or retainability issues, as Figure 5.28(b) shows. This is due to the fact that these users present the best CQI levels. Nevertheless, when they have to handover and the target femtocell is full, these users are dropped (mainly due to handover failures). Conversely, the self-optimization mechanisms have to sacrifice network resources per call (i.e., CQI is reduced) in order to avoid accessibility or retainability issues (i.e., enhance UDR). Besides, the level of MCQI is still good enough to ensure high quality connections for

all of them. Note that, blocked/dropped calls are not necessary due to bad CQI, other issues could finish the calls keeping a good CQI (calls could abnormally finish because of a problem of missing neighbor cells, cell capacity, lack of radio resources, etc.). Analyzing this issue from the other side, bad CQI means the calls might be blocked/dropped and the mean performance of MCQI would be decreased.
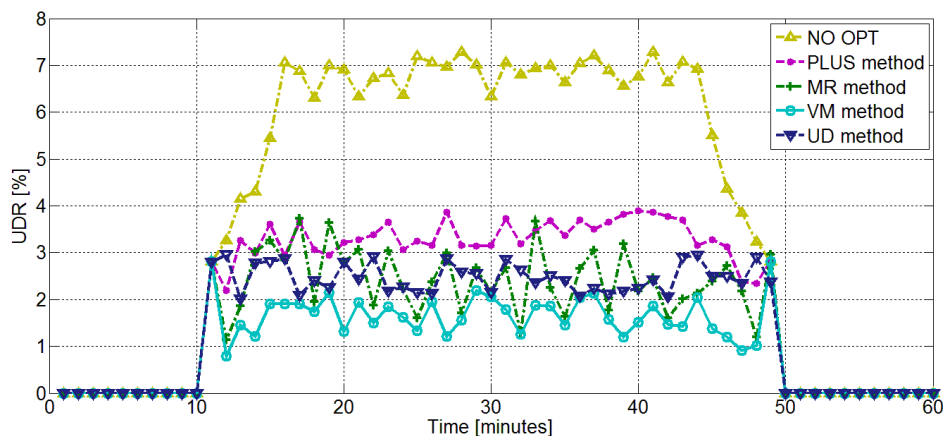
(a) UDR
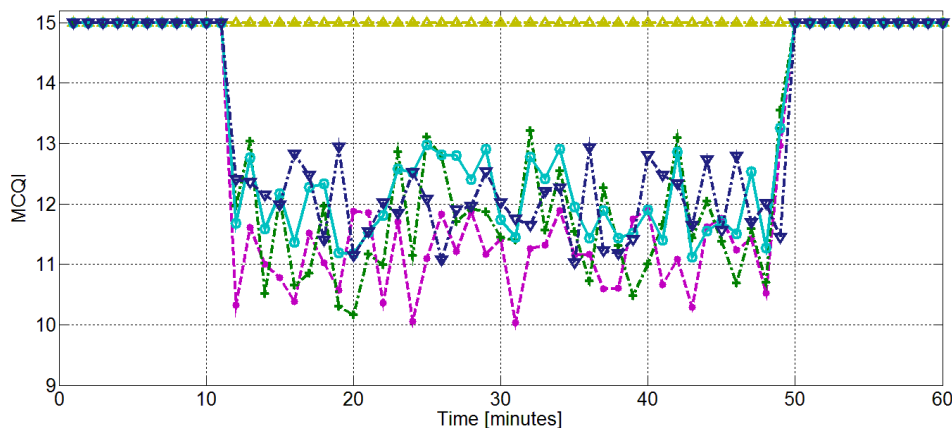
(b) MCQI

Figure 5.28: Network performance – 32 users.

Regarding the impact of the power changes on handovers, the average of UHR is around 0.85 for the non-optimized network. The PLUS method presents a UHR of 0.8, while the MR method increases the UHR to 0.9. The proposed location-based methods (VM and UD methods) have a UHR of 0.83. As expected, re-sizing the coverage area of femtocells involves an increase rate in the number of handovers per user when the self-optimization algorithm is triggered. But, as both pilot and data transmission powers are jointly tuned, once the network is optimized the number of handovers is

decreased compared to the non-optimized network. That is happening because less handovers are required when the traffic in the network is balanced.
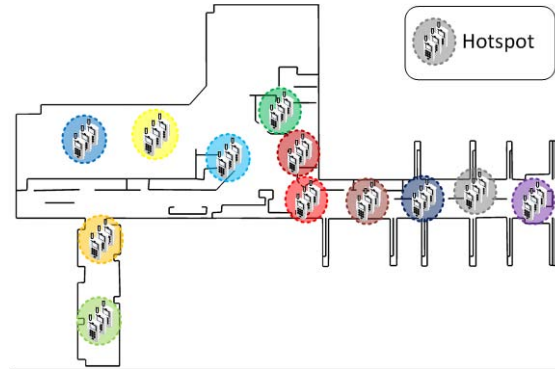
Figure 5.29: Overloaded areas (hotspots).

Additionally, the algorithms were also evaluated during one day simulation where a hotspot was created twice in a different place of the airport each hour as Figure 5.29 shows. Table 5.8 presents the average values of each indicator in that period. It could be observed that the results are comparable to the results of one hour simulation.

Table 5.8: Network performance (maximum 32 active users per femtocell).

	NO OPT	PLUS Method	MR Method	VM Method	UD Method
UDR [%]	4.1	2.2	1.8	1.1	1.6
MCQI	15	12.7	13.0	13.2	13.1
UHR	0.86	0.82	0.91	0.84	0.83

Maximum femtocell capacity: 16 active users

In this scenario, the femtocell capacity has been diminished (up to 16 active users per femtocell) as well as the number of pedestrian sitting/walking through the airport. Table 5.9 illustrates the network performance for one day simulation. Similar behavior to the previous scenario is observed. In this case, the non-optimized network presents an average UDR around 4.4% while the PLUS method is able to reduce that indicator till 2.4%. The MR method is able to improve previous network performances (2.1%). Focusing on the location-aware methods, VM and UD methods reduce this value to 1.3% and 1.8% respectively. Note that the UDR relative-gain of the location-aware methods compared to the MR method has increased. As the number of active users to estimate the transmission power would be fewer, the average error of those estimations

compared to the expected transmission powers would be higher. It impacts on the performance of the MR algorithm. For example, in the MR method, a number of users should hand over but due to fading, the new transmission power adaptations might be not enough to trigger the handover processes for some users. When the femtocell capacity is high, many users would be successfully handed over. However, when the femtocell capacity is low, few users would successfully handover. Then, the ratio of active users in the overloaded femtocell is lower in the first situation than in the second. Regarding the location-aware methods, once the database has a wide variety of PRX samples, that issue is insignificant but the performance of the system would not be improved as much as in the case of the MR method when the femtocell capacity is increased (e.g., from femtocells with 16 active users to femtocells with 32 active users).

From the point of view of the CQI and the UHR, all methods present proportional results to previous scenario. Note that, due to the cited problem of fading in MR method, the increment of UHR value is higher at this method compared to the others.

Table 5.9: Network performance (maximum 16 active users per femtocell).

	NO OPT	PLUS Method	MR Method	VM Method	UD Method
UDR [%]	4.4	2.4	2.1	1.3	1.8
MCQI	15	12.9	13.2	13.3	13.2
UHR	0.89	0.84	0.99	0.86	0.85

Maximum femtocell capacity: 8 active users

Now, the maximum femtocell capacity is 8 active users and the number of users in the airport is reduced to half. For this scenario, as the number of active users is lower, the relative-gain of average UDR value for MR method and context-aware methods (VM and UD) is higher. The location-aware methods outperform the others, being the VM method the one with the lowest UDR. The same behavior is observed from the CQI and the UHR level (see Table 5.10).

Table 5.10: Network performance (maximum 8 active users per femtocell).

	NO OPT	PLUS Method	MR Method	VM Method	UD Method
UDR [%]	4.6	2.7	2.5	1.5	1.9
MCQI	15	13.2	13.3	13.5	13.3
UHR	0.97	0.89	1.22	0.94	0.91

Maximum femtocell capacity: 4 active users

This use case evaluates the network where maximum femtocell capacity is 4 active users and the number of users on the scenario is proportional to previous scenarios. Here, all the methods present similar results to previous scenario as Table 5.11 illustrates.

Table 5.11: Network performance (maximum 4 active users per femtocell).

	NO OPT	PLUS Method	MR Method	VM Method	UD Method
UDR [%]	5.2	3.2	3.0	1.7	2.0
MCQI	15	13.4	13.4	13.5	13.4
UHR	1.12	0.96	1.35	1.05	1.03

To summarize, it has been shown how problematic temporary network congestion could be managed to enhance UDR. The proposed algorithms enhance the operator network over the non-optimized situation and outperform the PLUS algorithm. The VM and UD methods are stable in the four scenarios, whereas the MR method improves when the femtocell capacity and the number of users is high. This means, the higher the number of users is, the more similar the average PRX from MR is, compared to PRX from context-aware methods. Conversely, UD method is recommended for open areas as walls and obstacles between users could reduce its performance. In any case, the VM method outperforms the other methods.

In the previous analysis the influence of the location accuracy has not been addressed. Next subsection assesses the performance of the VM and UD methods when the positioning system provides the users' position with some degree of inaccuracy.

5.6.2.2.3   Impact of users' position error

The indoor positioning system could present some inaccuracy in the users' positions. Consequently, the PRX information obtained from the HPLM might not be the expected PRX value. This situation is evaluated in this study to assess the robustness and reliability of the proposed context-aware MLB methods (UD and VM methods) in indoor femtocell environments.

To emulate this situation, the users' position error is modeled as a normal distribution $N(\mu, \sigma^2)$ where $\mu = \{1, 2, 4, 8, 16, 32\}$ m and $\sigma = {}^{\mu}\!/_3$ m, being the mean and the standard deviation respectively. According to this, Figure 5.30 depicts the four

previous use cases where the users' location accuracy is modified in relation to the precision error supplied by different positioning systems. The average values of the UDR over one day simulation for each MLB algorithm are presented in the graphs.

For all the deployments and location-aware methods, as expected, the users' satisfaction decreases when the average position error increases. Figure 5.30(a) (32 users/femtocell) shows the good performance of the location-aware methods compared to the others when the average position error is around 4 m for VM method and less than 3 m for the UD method. The SON system should trigger the MR method (i.e., get the PRX from the users) or the PLUS method when the accuracy of the indoor positioning system is higher than the cited values. In other case, the network performance would be degraded, being unacceptable for the operators. Figure 5.30(b) (16 users/femtocell) presents similar behavior. Now, the SON system should reject VM method when the average position error is over 4 m while the UD method is limited to average position errors below 3 m. Figure 5.30(c) (8 users/femtocell) continues with similar pattern. In this case, the accuracy of the indoor positioning system is a little less restricted. The average position error could be up to 5 m for the VM method and 3 m for the UD method. The same trend can be observed in Figure 5.30(d) (4 users/femtocell), where the non-location-aware methods should be selected when the average position error is over 6 m for the VM method and 4 m for the UD method.

(a) 32 users/femtocell

(b) 16 users/femtocell

(c) 8 users/femtocell

(d) 4 users/femtocell
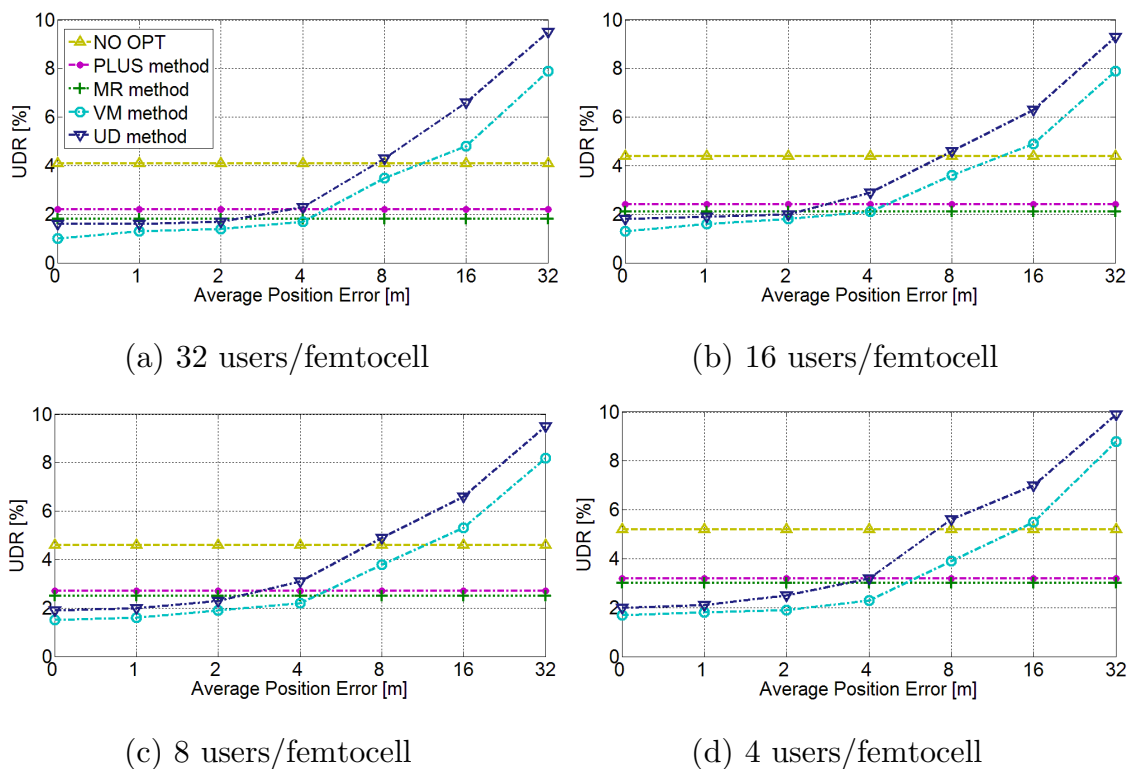
Figure 5.30: UDR based on different average position errors.

The results are performed with information from 100 simulations for each average position error, use case and method. The 95% confidence interval is around ±0.25% of UDR for any use case and method with 1 m of average position error. It is extended when the average position error is increased: from around ±2% of UDR for maximum 4 active users per femtocell to ±0.75% for 32 active users.

These accuracies are not very demanding and could be achieved with the proposed RFID-based indoor positioning system in *Chapter 4*. Other indoor-positioning systems could be also good candidates, like the one described in [115] where the 90th percentile error of the proposed method is lower than 3 m and the average position error is 1.5 m. In addition, smartphone-based indoor-positioning systems, like those cited in [38], improved the average position error to 1 m thanks to the integration of the sensors information into their localization engine [116].

Besides, the mobility pattern of users (i.e., the users' positions change in short periods) and large-scale deployments (i.e., estimation of thousands of users) could be a challenge for current indoor-positioning systems. However, the proposed location-aware systems do not require a continuous estimation of the users' positions (i.e., the periodicity of triggering the indoor positioning system could be the same of the SON methods). In large-scale deployments, distributed indoor-positioning systems could be implemented to address the calculation of the users' positions. Additionally, in case of an indoor-positioning system based on PRX from cellular mobile infrastructure (e.g., femtocells), both positioning system and SON entities must be coordinated. Each time a SON algorithm tunes femtocells transmission power, it must be notified to the positioning system algorithm in order to update the fingerprint databases.

5.6.2.2.4   Load balancing and energy savings coordination

The proposed coordinated SON system is analyzed in the same scenario where the maximum femtocell capacity is 32 active users.

An indicator based on the percentage of active cells over the number of deployed cells in the scenario is computed as:

$$ACR \ [\%] = 100 \cdot \frac{N_{active\_cells}}{N_{cells}}. \tag{5.36}$$

ACR (Active Cells Rate) provides an estimation of the energy consumption, although it does not measure or take into account the cell transmission power.

Therefore, a significant indicator to measure the overall power saving is the power transmission ratio (PTR), calculated as:

$$PTR \, [\%] = 100 \cdot \frac{\sum_{i=1}^{N_{cells}} PTx_i}{\sum_{k=1}^{N_{cells}} PTx_{max}^k}, \qquad (5.37)$$

where N_{cells} is the number of deployed cells, PTx_i is the current transmission power of cell i and PTx_{max}^k is the maximum value of transmission power that cell k can be set. Hence, to reduce the energy consumption, low values of these indicators are desirable.

The defined ES method has been adapted to gather PRX directly measured by the users. This means, no users' position is required. Therefore, the assessed algorithms are referenced as: the MR method and the non-location-aware ES method as the non-location-aware coordination system (COOR), and the VM and the location-based ES methods as the location-based coordination system (COOR+LOC).

(a) UDR

(b) MCQI

(c) ACR

(d) PTR
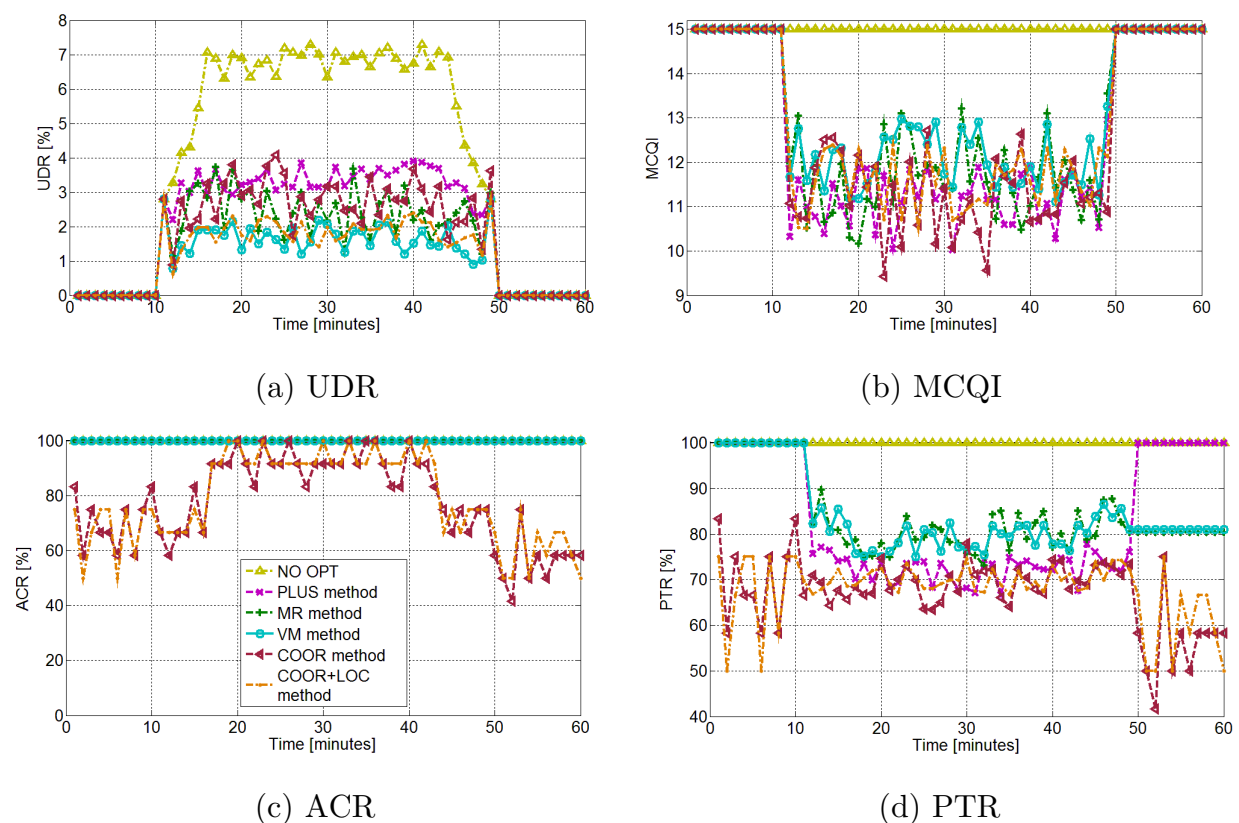
Figure 5.31: Network performance.

The performance of the proposed VM method is shown in Figure 5.31(a) ('VM method' – cyan line), which enhances UDR around 50% in comparison with the PLUS

method. In the case of the COOR+LOC ('COOR+LOC method' – orange line), UDR is also better than the PLUS method. However, due to the time femtocells need to be switched on or awake, the performance of this indicator is slightly lower compared to the VM method. A shorter execution period for changing the status of the femtocell would help to fix this shortcoming. The MR ('MR method' – green line) and COOR ('COOR method' – red line) methods outperform the PLUS method but decrease the UDR performance compared to the location-aware SON methods. As previously detailed, it is due to the radio channel instability.

From the point of view of the system energy consumption, Figure 5.31(c) and Figure 5.31(d) illustrate the network energy performance. On the one hand, the ACR indicator shows how the COOR and COOR+LOC mechanisms either switches off or turns into dormant mode many femtocells of the scenario, while the other methods keep all femtocells awake. On the other hand, the PTR is lower for the PLUS, MR and VM methods. This is due to the fact that the femtocell transmission power is decreased to balance traffic (in comparison to the maximum transmission power level set by default). The PLUS algorithm tends to return to the maximum power level once the network is balanced while the MR and VM algorithms keep the last power configuration. The COOR and COOR+LOC methods provide even higher energy-savings in the network because femtocells could be switched off.

Regarding the impact of the power changes on handovers, the average of UHR is around 0.85 for the non-optimized network. The PLUS method presents a UHR of 0.8, while the non-location-aware methods, MR and COOR methods, increase the UHR to 0.9 and 0.91 respectively. The proposed location-based methods (VM and COOR+LOC) have a UHR of 0.83.

Finally, the algorithms were also evaluated during one day simulation where a hotspot was created in a different place of the airport each hour (see Figure 5.29). Table 5.12 presents the average values of each indicator in that period. It could be observed that the results are comparable to the results of one hour simulation.

Table 5.12: Network performance (maximum 32 active users per femtocell).

	NO OPT	PLUS Method	MR Method	VM Method	COOR Method	COOR+LOC Method
UDR [%]	4.1	2.2	1.8	1.1	1.9	1.2
MCQI	15	12.7	13.0	13.2	12.6	12.9
ACR [%]	100	100	100	100	80.2	78.4
PTR [%]	100	81.8	88.1	86.7	71.3	68.4
UHR	0.86	0.82	0.91	0.84	0.93	0.85

5.7   Field trial evaluation

Some of the previous algorithms have been also evaluated in a field trial. Next subsections will detail the global infrastructure and the trial results.

5.7.1   Trial set-up

The global indoor-positioning system devised to supply real-time information about users' position to SON mechanisms is based on the management architecture for context-aware self-organizing small cell networks defined in *Chapter 3*. In such architecture a local centralized element is in charge of running the SON system functionalities, serving also as aggregator of the information coming from the femtocells and context-aware data. With this local centralized element, non-additional direct communication between the femtocells is introduced by the system.

5.7.1.1   System overview

The global system overview is presented in Figure 5.32. It shows the two main system blocks (Positioning system and SON system), the interfaces between them and the femtocells network and the designed messages for the exchange of information. Context information (PRX, users' position and orientation) is obtained through users' applications following the architecture in *Chapter 3*. These data are the main information sources for the Positioning and the SON systems. Note that the availability of some of these data would depend on the terminal manufacturer.

5.7.1.2   System interfaces

To connect the Positioning and the SON systems, two interfaces labeled as SS-LS interface and LS-SS interface have been defined (see Figure 5.32). The interface LS-SS is conceived to send the real-time users' position to the SON system. The interface SS-LS is in charge of providing to the positioning system notifications about the cellular network such as a cell outage or cell transmission power variations, which can be used in the position assessment procedure. In order to ensure no information is missing in the global system, the well-known TCP is selected as the communication protocol.

5.7.1.3   Smartphone APP[2]

In classical OAM systems, PRX information is normally acquired from users' measurement reports. However, that information is rarely provided in real-time to the OAM layer. In order to obtain real-time reports, different solutions are envisaged: control plane approaches (making use of the RRM-related terminal reports available at the femtocells), user plane (via applications installed on the terminal) or making use of specific OAM features such as *Minimization of Drive Test* (MDT).

MDT solutions are often limited to specific users in a non-real-time way so they are not ideal to support online SON mechanisms. While control plane messages could support the required information, such solution would require either the operators to give access to their networks or the adoption by femtocell manufacturers, leading to possible compatibility issues. Therefore, as the provision of indoor navigation would be performed through user applications, the integration at application level of the PRX reporting to the OAM system is assumed, without discarding other solutions. Additionally, PRX values are averaged at Layer 1 and 3 [79] of the terminal protocol stack minimizing the impact of fast-fading in its values.

A smartphone app reports this type of data as well as it might provide to the SON mechanisms any other relevant context information required.
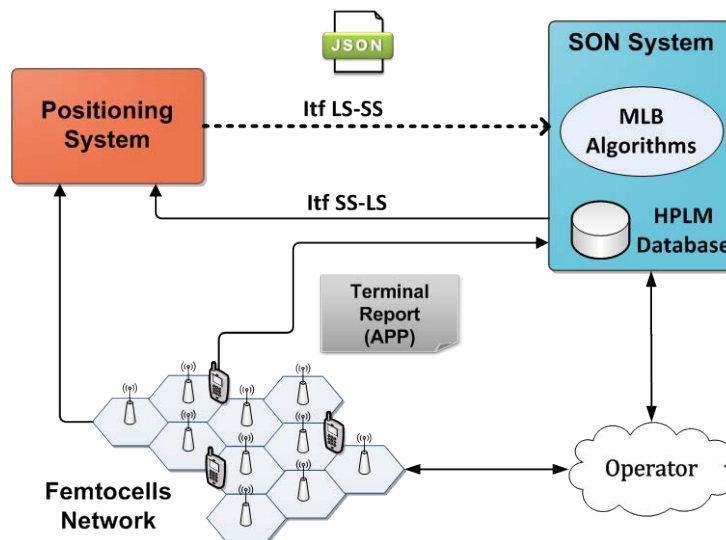
Figure 5.32: Global location-aware SON architecture.

---

[2] The smartphone app and the communication between each element have been developed by the *Universidad Carlos III de Madrid* (UC3M), partner of MONOLOC project.

5.7.1.4   Cellular-based indoor positioning system[3]

A fingerprint-based positioning engine, known as MILES (Mobile Indoor Localization Engine for SON), estimated the users' positions. This positioning engine takes advantage of the interaction with SON mechanisms. It is conceived both to support SON mechanisms and use network information supplied by the SON system to update the positioning system according to power-related changes (cell outage, transmission power variations, etc.).

Fingerprint-based techniques include both a training offline phase and a real-time phase. In the training offline phase, also known as calibration phase, a location fingerprint database is generated. To create this database, geo-referenced PRX readings in the four orientations (north, east, south and west) from different femtocells are measured by a terminal at known positions, which are referred as training points. In the real-time phase, a comparison between the real-time PRX measurements and the PRX stored in the offline phase is performed. The PRX information was easily gathered thanks to the use of smartphone terminals. The aforementioned application was installed in the terminals in order to report the captured information about the terminal, radio conditions and cellular network.

This real-time positioning engine provided the users' positions, having a CDF position error of 3 m for the 50% and of 5.9 m for the 90% in the field-trial (see scenario in subsection 5.7.1.6). This system made use of PRX and orientation information of the terminal to calculate its position.

5.7.1.5   JSON messages

The messages to communicate the different entities of the system are defined using the open standard format known as JSON. An example is illustrated on Figure 5.33. The ASCII text-encoding standard is used to code the characters of the messages.

The Positioning system receives the PRX from the cellular network terminals involved in the positioning process, evaluates these measurements and estimates their position inside the indoor scenario. After that, the positioning system generates a notification which contains, among other information, the position of the user. This notification is sent to different entities of the system. A specific and well-defined JSON

---

[3] The cellular-based indoor positioning system has been implemented by the *Universidad Politécnica de Madrid* (UPM), partner of MONOLOC project.

message as the one presented on the right of Figure 5.33 is transmitted through the LS-SS interface to the SON system.

HPLM → SON	POSITIONING SYSTEM → SON

{
  "type":3,
  "id":"355136052451195",
  "timestamp":1372672468913,
  "cellsGSM":[
    {
      "mCellIdentityGsm":{
        "mCid":4551,
        "mLac":16070,
        "mMcc":214,
        "mMnc":1,
        "mPsc":50
      },
      "mCellSignalStrengthGsm":{
        "mAsu":7,
        "mBitErrorRate":0,
        "mDbm":-99
      },
      "mTimeStamp":1372672468835,
      "mRegistered":true,
      "mNetworkType":10,
      "mTimeStampType":0,
      "type":0
    }
  ]
}
	{
	  "type":4,
	  "id":"356708049297193",
	  "timestamp":1371804697246,
	  "timestampMeasure":1371804694362,
	  "position":{
	    "latitude":40.512499903448,
	    "longitude":-3.674777418556,
	    "altitude":7.5,
	    "accuracy":1
	  },
	  "localPosition":{
	    "x":47.0975629391100700,
	    "y":28.1624215751835540,
	    "z":1.0000
	  },
	  "referencePoint":{
	    "latitude":40.512400000,
	    "longitude":-3.67510000,
	    "altitude":7.5000,
	    "x":9.86,
	    "y":-23.73,
	    "z":7.50,
	    "orientation":-24.00
	  },
	  "lastReliableMeasure":1371804695308
	}

Figure 5.33: JSON messages.

5.7.1.6   Scenario

A small-sized unplanned network composed by four 3G femtocells (Alcatel Lucent 9361 Home Cell v2 [31]) has been deployed in a real office environment (see Figure 5.34) in order to evaluate the proposed SON algorithms. Several macrocells are located outside the office. The femtocells are limited to 4 simultaneous connected users. This network provided data and voice services, being connected to the operator core network through a traditional ADSL (Asymmetrical Digital Subscriber Line) router. Three of them were directly plugged to the router through an Ethernet cable with the fourth femtocell being wireless connected (WiFi).

The network has been initially configured to offer location based services, thus a specific configuration has been done taking into account different aspects:

- The identifiers unequivocally label each femtocell into the environment. These identifiers are the PSC (Primary Synchronization Code) or the PCI depending on the underlying access technology, 3G or LTE respectively. To avoid

PSC/PCI collision or confusion, and to guarantee the required simultaneous coverage to offer indoor location services, four different PSCs have been configured in the network, one PSC code for each deployed femtocell (PSC_x1, PSC_x2, etc.). Areas with simultaneous coverage of two femtocells with the same PSC/PCI are avoided. Figure 5.34 shows the Cell ID (CID) and PSC assignment.

Name: Femto_x4
•**CID:** CID_x4
•**PSC:** PSC_x4

Name: Femto_x3
•**CID:** CID_x3
•**PSC:** PSC_x3

Name: Femto_x2
•**CID:** CID_x2
•**PSC:** PSC_x2

Name: Femto_x1
•**CID:** CID_x1
•**PSC:** PSC_x1
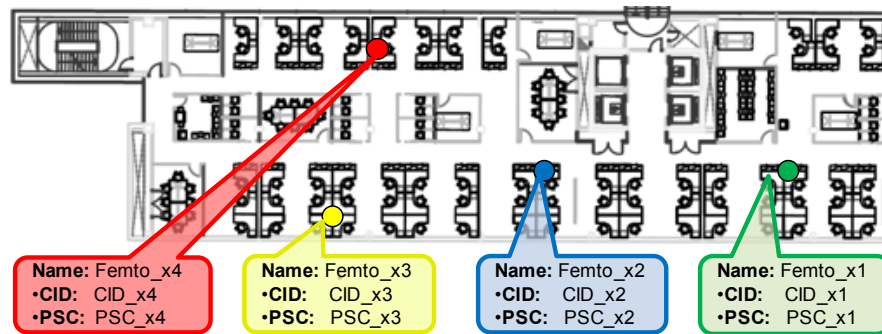
Figure 5.34: Field-test.

- The femtocell network has been configured in close access to have the environment under control and to prevent unexpected troubles caused by external agents. Thereby, only three subscribed terminals are able to connect to the femtocell network.

(a) Femto_x1 (green circle)

(b) Femto_x2 (blue square)

(c) Femto_x3 (yellow reverse triangle)

(d) Femto_x4 (red triangle)
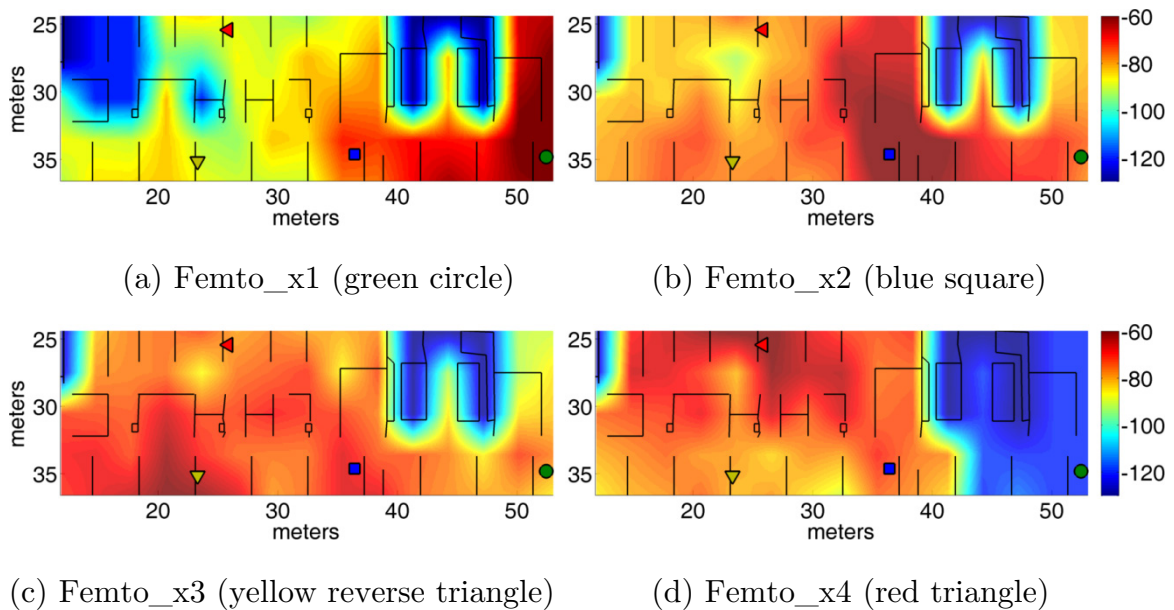
Figure 5.35: Initial RSCP.

- Although the SON mechanisms will vary the transmission power of the femtocells into a range of values, both the CPICH power ([-50... 20] (dBm) step 0.1) and the maximum transmitted power ([-50... 24] (dBm) step 0.1) have been set as initial configuration with the maximum power values.

- Different cell reselection thresholds and handover margins have been configured depending on the access technology and the frequency used. These thresholds are based on the received signal quality of the serving cell.

The average estimated PRX from each femtocell is stored in the HPLM database. These maps are shown in Figure 5.35.
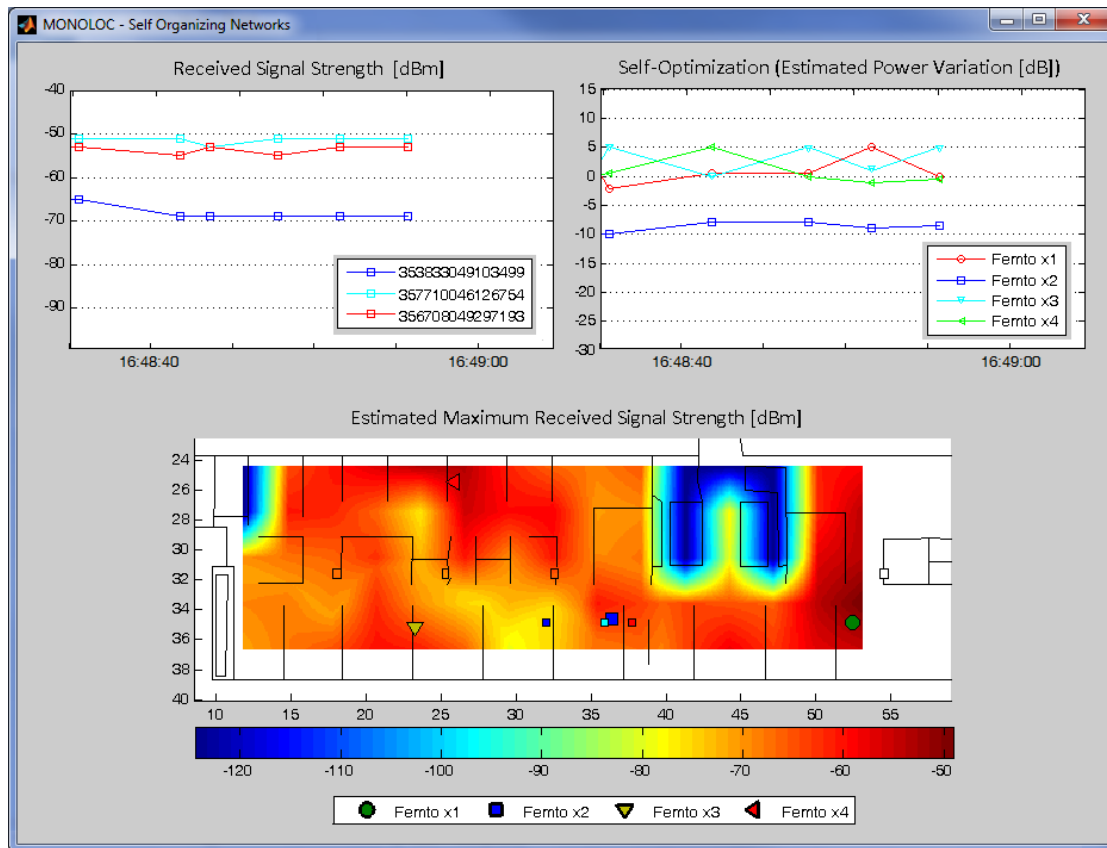
Figure 5.36: Graphical User Interface (GUI).

5.7.1.7   SON application

For monitoring what is happening in the femtocell network, a GUI (Graphical User Interface) has been developed as Figure 5.36 illustrates. It is composed of three parts:

- ***Received Signal Strength [dBm]:*** This window (top left) illustrates the PRX value from the serving cell (the icon identifies the femtocell) for each terminal (the color identifies the user) in real-time.

- ***Self-Optimization (Estimated Power Variation [dB]):*** It depicts the self-optimizing algorithm response (top right). In this case, it is the transmit power variation that should be set up per femtocell to balance the network. Each femtocell is identified by an icon and a color (see bottom bar of Figure 5.36).

- ***Estimated Maximum PRX [dBm]:*** The scenario is showed in this window (bottom) where femtocells and users' position are also integrated. The highest estimated values of PRX per position are represented on the scenario.

5.7.2   Trial results

Due to the complexity and the constraints to set the network configuration parameters on the mobile operator infrastructure, only two experiments were analyzed.

5.7.2.1   Experiment 1

The assessment of the proposed UD method is carried out in the described scenario. The system performance is compared to the non-optimized case and to the PLUS method described in subsection 5.4.1.4. Remember that, the PLUS method does not use the users' position.

These mechanisms are tested under several situations to evaluate both static/dynamic users' distributions and the accuracy of the positioning system. The system parameters S_{th} and Q_{th} are set to 50%. In the same way, ΔT is configured with the periodicity of triggering the algorithm, i.e., every five seconds to ensure stable information into the system.

Static users' distribution

Here, four static (not moving) users are located around Femto_x2 coverage area (Figure 5.37). The UD method is evaluated in two ways. Firstly, users' position is manually introduced into the optimization algorithm (*Manual mode*) in order to avoid errors in users' position. Secondly, the process is repeated having the users' position automatically provided by the indoor-positioning system (*Automatic mode*).
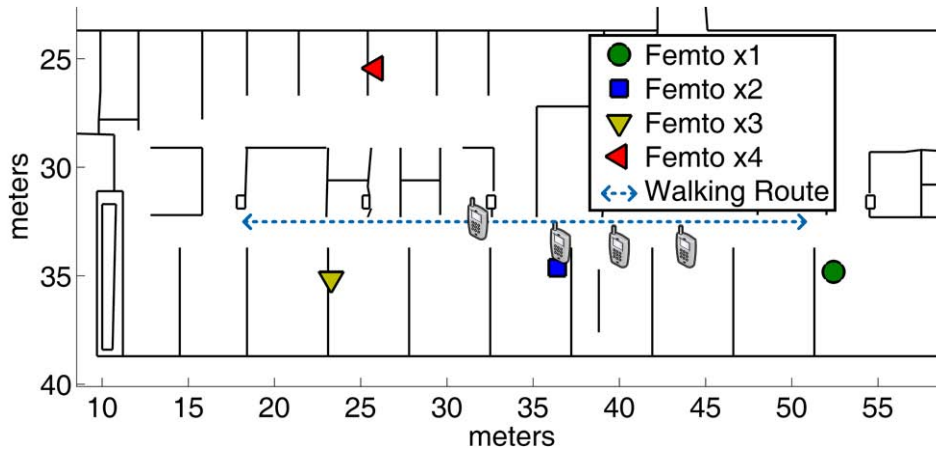
Figure 5.37: Users' distribution.

Initially, at $t = 0$, the situation is a congested femtocell (Femto_x2) with four connected users. Hence, there is no capacity to allocate new users in this femtocell. However, from the point of view of radio resources, this overload is not detected due to the low traffic transferred per user. That situation is analyzed during five minutes.

Subsequently, the UD method and the PLUS method perform a continuous analysis of the network (every 5 s). The algorithms propose the transmission power variation that must be applied to solve that congestion. That means, Femto_x2 power should be decreased. The UD method proposes an average of transmission power variation of Femto_x2 of –9 dB, meanwhile, the PLUS method proposes –6 dB. The latter is an adaptive method and it would require to change the transmission power of femtocells a few times before reaching the optimal values. The average of the transmission power variation (Avg. δPtx) per femtocell of each method is depicted in Table 5.13. Note that, all femtocells were initially set to the maximum power.

Table 5.13: Static users: Network configuration and performance.

	Baseline				Proposed UD method			
	No Optimization		PLUS Method		Manual Mode		Automatic mode	
	Avg. δPtx	Avg. Users	Avg. δPtx	Avg. Users	Avg. δPtx	Avg. Users	Avg. δPtx	Avg. Users
Femto_x1	0	0	0	1	0	1	0	1
Femto_x2	0	4	-6.0	3	-9.0	2	-9.1	2
Femto_x3	0	0	0	0	0	1	0	1
Femto_x4	0	0	0	0	0	0	0	0

After that, the network is reconfigured with the suggested transmission power values. In the case of the UD method, the users are efficiently balanced in the network

(see Manual Mode and Avg. Users in Table 5.13), where a user is handed over to Femto_x1 and another to Femto_x3, leaving free space for new users in Femto_x2. However, the proposed values of the PLUS method are not the optimal ones to fully offload the congestion. Only a user is handed over to Femto_x3. Therefore, this method would need to analyze the new network situation to suggest new transmission power values.

From the point of view of the accuracy of the positioning system, note that the results of the UD method are similar to the case of manually providing the users' positions. That is because the indoor-positioning system introduces a low position error and, in average, the trend of the polynomial function to estimate the PRX is similar in both cases. The performance of that indoor-positioning system is taken as an upper bound for the position error, which means, systems with higher position error would decrease the SON performance. In addition, that position error is consistent to the study in subsection 5.6.2.2.3. The literature [38] proposes many indoor-positioning systems with similar or better accuracy than the one implemented for this testbed.

Dynamic users' distribution

In this case, three static users are located in Femto_x2 coverage area, whereas the fourth user is freely moving across the scenario as dotted blue line of Figure 5.37 shows. Their positions are supplied in real-time by the indoor-positioning system (Automatic mode).

Table 5.14: Dynamic users: Network configuration and performance.

	No Optimization		PLUS Method		Proposed MLB system (Automatic mode)	
	Avg. δPtx	Avg. Users	Avg. δPtx	Avg. Users	Avg. δPtx	Avg. Users
Femto_x1	0	0.2	0	1.3	-2.3	1.4
Femto_x2	0	3.5	-6.0	2.3	-10.2	2.1
Femto_x3	0	0.3	0	0.4	0	0.5
Femto_x4	0	0	0	0	0	0

That situation is analyzed during five minutes. After that, the average of the transmission power variation for each femtocell is set in the network at the end of the evaluation process. These values (Avg. δPtx) are illustrated in Table 5.14. Once the network is reconfigured, the average number of users per femtocell changes. These values are also shown in Table 5.14. In case the network is optimized by the PLUS

method, the average power is –6 dB because only Femto_x2 is overloaded for that mechanism. The adaptive process of this method will improve the network performance. The solution proposed by the UD method tries to, in average, balance the network by keeping Femto_x2 with the 50% of its capacity, i.e., two users, while, the other users are handed over to adjacent femtocells.

5.7.2.2   Experiment 2

The three mobile phones were located on a fixed position, as the GUI shows at the bottom image of the Figure 5.36 (three small squares as they are connected to Femto_x2). As previously explained, the color identifies the mobile phone and the shape of the icon indicates its serving cell, in this case, Femto_x2 (square) for all of them. The user position is manually introduced in the system to avoid position errors. The MLB algorithms (VM and MR methods) analyze the network situation every five seconds. Their configuration parameters are set to $S_{th} = 70\%$, $T_{th} = 60\%$ and $P = 60\,min$. All femtocells were initially set 10 dB below the maximum power.

VM method

On the one hand, the algorithm supported by the VM method is analyzed in Figure 5.38. For this situation, the algorithm is triggered because a femtocell (Femto_x2) is overloaded due to the fact that three active users are attached to it, occupying the 75% of the femtocell capacity $l_{femto\,x2} > S_{th}$ while the neighboring cells are empty, $L_{nc\_femto\_x2} < T_{th}$. The suggested value of the power adaptation of each femtocell is showed in the top right figure of the GUI. Notice that, as the left window illustrates, the PRX values (per user) provided by this method are quite similar in time because they are static users and PRX is calculated based on HPLM database.
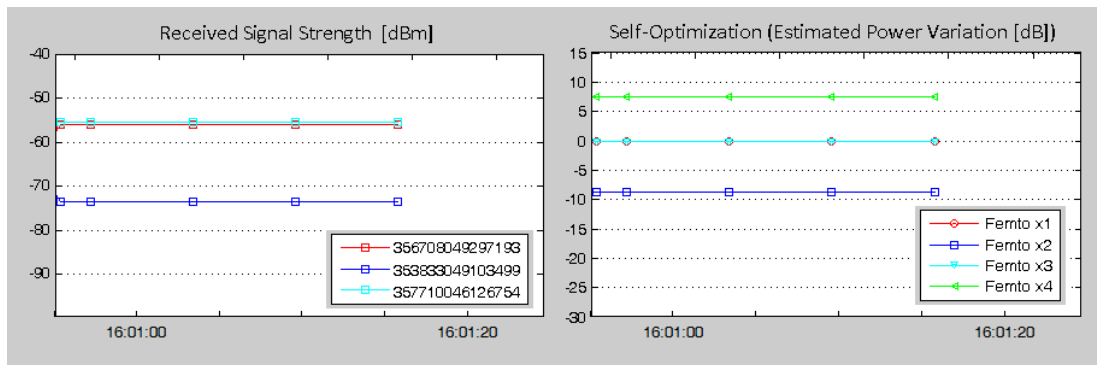

Figure 5.38: VM method.

The new configuration is set on the femtocells through a configuration file to update femtocells transmission power. After that, the femtocells network is monitored again to validate the modifications.

As expected, the blue (left icon in Figure 5.36) phone hands over to Femto_x4, whereas the other two stay on the same serving cell (Femto_x2). After this, the *Self-Optimization window* does not depict any data because the network is balanced and the algorithm is not triggered (until an overloaded situation appears again).

After that, the described real-time indoor-positioning system in subsection 5.7.1.4 supplied online users' positions to the SON algorithms. The VM method (automatic mode) under the inaccuracy of the positioning system proposes similar femtocell transmission power (estimated power variation) to the use case of accurate positions (see Table 5.15). Once these new transmission powers are tuned in femtocells, users hand over and network is balanced. This follows the expected behavior discussed in subsection 5.6.2.2.3 as the accuracy of the indoor positioning system is below 5 m (use case: maximum 4 active users per femtocell).

Table 5.15: VM method performance.

	VM method (Manual mode)		VM method (Automatic mode)	
	δPtx	Users	δPtx	Users
Femto_x1	0	0	0	0
Femto_x2	-9.0	2	-9.0	2
Femto_x3	0	0	0	0
Femto_x4	7.5	1	7.5	1

MR method

On the other hand, the MR method is evaluated in Figure 5.39 where the same problematic situation is deployed. In this case, as previously described, the PRX values fluctuate over time due to the propagation channel conditions as the left figure illustrates (neighboring cells present a similar behavior). In consequence, the algorithm proposes a different solution in time, making three femtocells (Femto_x1, Femto_x3 and Femto_x4) to fight to get the blue (left icon in Figure 5.36) or red (right icon in Figure 5.36) phone. The instability of the PRX values from the neighboring cells generates this situation: either the strongest PRX value from neighboring cells is received by the blue phone (from Femto_x3/x4) or from the red phone (Femto_x1). That means, there is not a unique solution for that situation in time, therefore the number of handovers could be increased (as simulations depict in subsection 5.6.2.2.2).
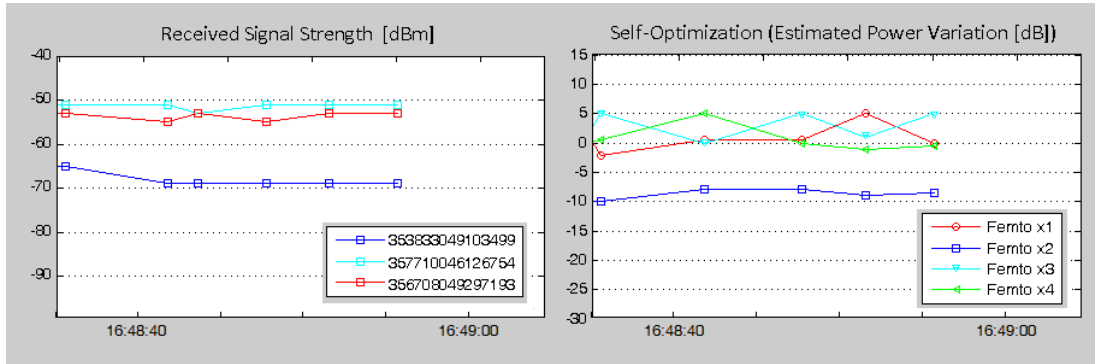
Figure 5.39: MR method.

5.7.3   Additional performance metrics

Additional performance metrics were measured to ensure the information exchange is successfully transmitted from the network and Positioning System to the SON system and no information is missing. The Positioning System must estimate the users' position in milliseconds and the SON system must process the received information in short periods to be able to solve temporal congestion issues.

- **_Successful transmission rate:_** Thanks to TCP, the successful transmission rate in the global system is 100%. However, this protocol increases the communication headers. An analysis to estimate the signaling overhead is performed below.

- **_Signaling overhead:_** The SON System designed in this prototype receives messages from the Positioning System and from each user in the cellular network. Messages from both sources are JSON messages and text is ASCII encoded. It means, the text sizes are around 440 bytes (an example JSON message was depicted in Figure 5.33) plus the communication headers (TCP+IP=40 bytes) for information about a user's position, while the text sizes are around 350 bytes plus the communication headers for information from a user and femtocell (additional femtocell information increases the text 240 bytes) in the cellular network. Therefore, in the last scenario where four users are camped, they receive information from four femtocells and it is forwarded to the SON System every five seconds, the transmission rate supported by this system must be around 10 kbps (3 kbps from the LS and 7 kbps from users).

  Besides, the signaling overhead could be significantly reduced as SON mechanisms do not have to be triggering all the time or in very short periods

(e.g., every 5 s). They could be triggered once an indicator reaches a threshold which means something is getting wrong (e.g., access failure rate is over 0.5%).

- **Delay:** Although the TCP protocol would ensure a hundred per cent of successful transmission rate and communication infrastructures (optical-fiber, DSL, etc.) would support enough transmission speed, the information could be received with a delay. The time to estimate the users' position is around 300 ms per user plus a few milliseconds to transmit the information. Meanwhile, the time to gather cellular information and send it to the SON System is also around a few milliseconds. Therefore, the most critical step would be the calculation of the users' position, being the delay 1.2 s in the described study. Based on this, information is supplied to the SON System with a minimum delay of two seconds. This prototype is set to trigger SON algorithms every five seconds in order to ensure the required inputs have been received in time (three seconds margin). In case information from any of the users is missing, the SON System is not triggered in that period.

- **Processing time of the SON system:** The time to process all that information would depend on the number of users and femtocells in the scenario. The "*Big O notation*" would describe the limiting behavior of these algorithms. The number of users is limited by the femtocell but the number of femtocells would depend on the deployment. The complexity of the PLUS and UD methods would be related to $O(n)$, where n is the number of femtocells deployed. Conversely, the complexity of the VM and MR methods would be related to $O(k \cdot n)$, where k is the number of iterations the algorithm need to converge. Normally, $k < n$ because the algorithm quickly converges to the optimal value of the femtocells transmission power to balance the network load and very few femtocells would be overloaded each iteration.

- **Automatic values of S_{th} and T_{th} (Q_{th}):** Each hour or day the algorithm would change one of these thresholds in steps of X units and the new network performance would be analyzed. According to this, the reference thresholds would be periodically changed to find if any of the new proposed thresholds around the reference thresholds would minimize the UDR. That process could take several iterations to reach the optimal solution.

In case the context-aware SON system might degrade the network performance (due to delays of context data, missing information, etc.), it will be immediately detected and the context-aware SON algorithms will be temporarily disabled and the network would be managed by classical SON mechanisms (e.g., PLUS method).

5.8 Conclusions

Novel and low computational cost MLB methods have been proposed and analyzed for temporary congested indoor femtocell scenarios.

Initially, the importance of analyzing classical input indicators (e.g., the available radio resources) was studied, as well as the specific characteristics of femtocells (e.g., the maximum capability of users' connections) for MLB use case in temporal overloaded situations. Some algorithms were designed but, the PLUS method that integrates radio resources and femtocells capacity information, has been proved as the best combination to build a consistent and reliable MLB mechanisms for femtocell networks.

Nevertheless, those algorithms did not consider the context information which could improve the algorithm performance. As a consequence, two new context-aware MLB systems were designed. Firstly, the UD method introduced the users' position and the PRX information measured from the network to support the MLB mechanisms. It made use of the geometrical distances between the users to estimate the new transmission power of femtocells. This method outperformed other MLB mechanisms. However, those geometrical distances could not be always the optimal solution to focus the optimization efforts for calculating that new transmission power due to the influence of the wall, obstacles, etc. For example, two close users could receive quite different PRX if there is a wall in the middle but they are included in the same *group*. A novel MLB system was designed to outperform the shortcomings of the previous UD method. The proposed method prioritized users making phone calls over any other service following that operators' policy. The VM method proposed the HPLM database to estimate the PRX values and to calculate the estimated transmission power.

The accuracy of these location-aware algorithms depends on the indoor-positioning system where the online user position could be provided with errors (up to several meters). In consequence, the system performance would decrease depending on the position error. Conversely, the MR method outperforms the previous methods when the user position error starts to be over some meters. The position error threshold to choose the VM/UD methods or the MR method depends on the femtocells capacities.

Finally, an ES system was coordinated to homogenously balance users in the network to increase its capacity and coverage, at the same time maintaining a high global quality in voice connections and reducing the power consumption of the network. The coordination of these methods is mandatory to avoid conflicts in self-optimization mechanisms.

Chapter 6

Conclusions

This chapter summarizes the main contributions of this PhD thesis, the future work and the list of publications.

The structure of this chapter is as follows: Section 6.1 details the main contributions of this thesis. Section 6.2 proposes some future work. Finally, Section 6.3 lists the publications which support this thesis and other publications of the author.

6.1   Contributions

This work is focused on the MLB use case defined by the 3GPP, in commercial and corporate femtocell networks. However, to accomplish the input data for the proposed context-aware SON mechanisms, some previous work had to be carried out. In this sense, the main contributions of this PhD thesis are detailed below:

- The description of a context-aware SON framework and the design of an OAM architecture to integrate context data from intelligent devices into SON systems. This framework presented the main context sources, external to the mobile operator infrastructure, to collect valuable information about what is happening in a certain place at a specific moment or even about what the situation will be in the following days. Moreover, the periodicity of collecting that context data was considered, as each context source provides the information at specific time intervals. Based on this, that context data was integrated into the proposed OAM architecture together with cellular network performance parameters (alarms, counters, etc.). This OAM architecture could be either part of the operators' OAM architecture or part of a third party service provider which proposes the new configuration parameters to the

operators' OAM architecture based on its own SON algorithms. Thanks to this
proposal, SON mechanisms will analyze useful external cellular network
information. Hence, new context-aware SON algorithms could be developed to
improve the cellular network performance.

- The development of RFID-based indoor positioning techniques for the location
  of multi-antenna RFID devices and the enhancement of these systems with the
  integration of cellular technology information. Although the literature described
  many indoor positioning systems and most of them are studied under specific
  characteristics and scenarios, this new approach has been focused on more
  critical environments for RF signals such as halls and corridors. Several
  techniques and methods were analyzed based on two-antenna readers to finally
  select the one with the highest accuracy. Besides, a trade-off between the
  number of antennas and the number of active tags was carried out, showing
  that two-antenna readers can provide equivalent or even better accuracy with
  half number of active tags deployed in the infrastructure compared to a single-
  antenna reader. That would reduce the expenditures of indoor positioning
  system almost by half. Moreover, the radio signal from the cellular technologies
  was collected and processed to improve the accuracy of the RFID-based indoor
  positioning system. The accuracy of the global indoor positioning system is
  enhanced with low investment as the cellular infrastructure is already deployed
  and it is managed by the cellular operators.

- The design of novel MLB algorithms based on incoming context information to
  solve temporary congestion problems at commercial and corporate femtocell
  networks. The special characteristics of femtocells (restriction in the number of
  users per femtocell, unplanned deployments, short-range, etc.), indoor
  environments characteristics (multi-path reflections, occasional events, etc.) or
  users' indoor mobility pattern (increase number of handovers, etc.) make
  classical MLB mechanisms prone to failures or to propose non-optimal network
  configurations. Hence, the proposed SON algorithms overcome those classical
  methods for these incoming femtocell networks. Additionally, classical SON
  systems analyzed cellular network performance parameters (alarms, counters,
  etc.) to propose the optimal configuration parameters and improve or solve
  network issues. However, the expansion of smart-devices, systems and
  applications provide valuable and real-time additional information from external
  sources to the mobile operator infrastructure. The proposed context-aware SON
  framework and OAM architecture make possible the integration of that context
  data into SON systems. Focusing on indoor positioning systems as context
  sources, some MLB mechanisms based on users' position were designed and
  evaluated in both, real simulated and field trial environments, where users'

satisfaction was improved compared to classical MLB methods while the operators' expenses are the same.

- The coordination of context-aware self-optimization mechanisms. As MLB mechanisms are femtocell transmission power related, the modification of the parameters is highly susceptible to parametric dependencies with other SON algorithms. A novel energy-saving method based on fuzzy logic controllers and users' position was designed to analyze that situation. Their coordination is mandatory to ensure the ES mechanism does not switch off a femtocell which is the target femtocell of the MLB method to offload an overloaded femtocell.

6.2   Future work

This PhD thesis is focused on the integration of context-awareness in femtocell self-optimization mechanisms to solve temporary congestion issues in commercial and corporate femtocell networks. The author proposes some future lines of research under this field:

- This PhD thesis made use of users' position to design and develop novel self-optimization mechanisms for indoor femtocell deployments. Conversely, the massive expansion of smart-devices makes possible the use of additional kind of context information into SON systems such as mobility pattern, moving speed, location and date of social events, rush hours, etc. The integration and the analysis of these data in novel SON algorithm would further optimize network parameters to reach the optimal status under each network situation. It would also help the operator to prevent future network failures.

- This PhD thesis presented a simple coordination of two self-optimization use cases. The coordination of SON mechanisms is currently a challenge for network engineers. Several SON mechanisms are currently working on parallel and triggered to optimize or heal the cellular network. However, these SON mechanisms are categorized and listed by priority based on the engineers' experience. Once the SON methods are triggered, the one on the top of the list per category which proposes to tune a network configuration parameter is selected, the proposal of any other SON method is discarded. As a consequence, a framework is required to coordinate the SON mechanisms to find the best network configuration parameters according to the operator's policies.

- The indoor positioning strategies are a hot topic in current researches. The accuracy of low cost systems is still high, few meters. That position error could

be good enough for some applications but it would be useless for some other applications. This PhD thesis proposes to increase the number of antennas of the RFID reader as it would be much cheaper than deploying further number of active tags. Additionally, other RF technologies from already deployed infrastructures such as LTE, could be integrated in these systems as a low cost solution to improve the accuracy.

- Finally, the field trial evaluation of the proposed context-aware MLB mechanisms was carried out under very restricted conditions of the number of terminals and femtocells. Hence, the studied coverage area was small. Moreover, there were some constraints by the network operator to set the network configuration parameters which restricted the accessibility to tune these parameters to occasional days. As a consequence, the coordinated SON methods could not be assessed in a real deployment. Hence, further field trials in environments such as malls or even airports, could be deployed to evaluate the proposed context-aware SON methods and their coordination. In the same context, the proposed multi-antenna RFID-based indoor positioning system could be implemented in other scenarios to measure the accuracy of that system under other conditions.

6.3   List of publications

This PhD thesis is supported by the following publications in high impact journals (JCR – Journal Citation Reports) and conferences. Additionally, the author has also participated in other related publications.

6.3.1   Journals

[I]   A. Aguilar-Garcia, R. Barco, S. Fortes, P. Muñoz, "Load balancing mechanisms for indoor temporarily overloaded heterogeneous femtocell networks," *EURASIP Journal on Wireless Communications*, 2015:29. 2015.

[II]   A. Aguilar-Garcia, S. Fortes, E. Colin, R. Barco, "Enhancing RFID Indoor Localization with Cellular Technologies," *EURASIP Journal on Wireless Communications and Networking*, 2015:219. 2015.

[III]   A. Aguilar-Garcia, S. Fortes, M. Molina-Garcia, J. Calle-Sanchez, J.I. Alonso, A. Garrido, A. Fernandez-Duran, R. Barco, "Location-aware Self-

Organizing Methods in Femtocell Networks," *Computer Networks*, vol. 93, part 1, pp. 125-140, 24 December 2015.

[IV]   A. Aguilar-Garcia, S. Fortes, R. Barco, A. Fernández-Duran, "Context-Aware Self-Optimization: Evolution Based on the Use Case of Load Balancing in Small-Cell Networks," in *IEEE Vehicular Technology Magazine*, vol. 11, no. 1, pp. 86-95, March 2016.

[V]   A. Aguilar-Garcia, R. Barco, S. Fortes, "Coordinated Location-based Self-Optimization for Indoor Femtocell Networks," *Computer Networks*, In press, June 2016.

[VI]   A. Aguilar-Garcia, S. Fortes, A. Garrido, A. Fernandez-Duran, R. Barco, "Improving Load Balancing Techniques by Location-awareness at Indoor Femtocell Networks," *EURASIP Journal on Wireless Communications*, Under review (major changes), 2016.

6.3.2   International conferences

[VII]   A. Aguilar-Garcia, R. Barco, S. Fortes, P. Muñoz, "Analysis of overload indicators for traffic balance in indoor femtocell networks," 13th *COST IC1004 MC and Scientific Meeting*, 5-7 May 2015 – Valencia, Spain.

[VIII] A. Aguilar-Garcia, S. Fortes, E. Colin, R. Barco, "Enhancing Localization Accuracy with Multi-Antenna UHF RFID Fingerprinting," *IPIN 2015, Sixth International Conference on Indoor Positioning and Indoor Navigation*. 13-16 October 2015 – Banff, Alberta, Canada.

6.3.3   National conferences

[IX]   A. Aguilar-Garcia, S. Fortes, R. Barco, "Información de contexto en la auto-gestión de redes small cells," *XXIX Simposium Nacional de la Unión Científica Internacional de Radio URSI 2014*, 3-5 September 2014 – Valencia, Spain.

[X]   A. Aguilar-Garcia, S. Fortes, R. Barco, "Location-based self-organizing mechanisms for femtocell networks," *Workshop in indoor localization with small cells. MONOLOC project conclusions*, 28 November 2014 – Madrid, Spain.

[XI]   A. Aguilar-Garcia, S. Fortes, R. Barco, "Análisis de indicadores para el balance de carga en redes de femtoceldas," *XXX Simposium Nacional de la Unión Científica Internacional de Radio URSI 2015*, 2-4 September 2015 – Pamplona, Spain.

6.3.4   Other publications

[XII]   P. Muñoz, R. Barco, J. M. Ruiz-Avilés, I. de la Bandera, A. Aguilar-Garcia, "Fuzzy Rule-Based Reinforcement Learning for Load Balancing Techniques in Enterprise LTE Femtocells," *IEEE Transactions on Vehicular Technology,* vol. 62, no. 5, pp. 1962-1973, June 2013.

[XIII]   S. Fortes, A. Aguilar-Garcia, R. Barco, F. Barba, J. Fernández-Luque, A. Fernández-Durán, "Management architecture for location-aware self-organizing LTE/LTE-A small cell networks," *IEEE Communications Magazine*, vol.53, no.1, pp.294-302, January 2015.

[XIV]   S. Fortes, R. Barco, A. Aguilar-Garcia, P. Muñoz, "Contextualized indicators for online failure diagnosis in cellular networks," *Computer Networks,* vol. 82, pp. 96-113, May 2015.

[XV]   S. Fortes, A. Aguilar-Garcia, R. Barco, A. Garrido-Martín, J.A. Fernández-Luque, "Context-Aware Self-Healing: User Equipment as the Main Source of Information for Small-Cell Indoor Networks," *IEEE Vehicular Technology Magazine*, vol. 11, no. 1, pp. 76-85, March 2016.

[XVI]   S. Fortes, R. Barco, A. Aguilar-Garcia, "Location-based Distributed Sleeping Cell Detection and Root Cause Analysis for 5G Ultradense Networks," *EURASIP Journal on Wireless Communications*, In press, 2016.

[XVII]   S. Fortes, R. Barco, A. Aguilar-Garcia, "Integration of Indoor Positioning into Self-Organizing Small Cell Systems," *12th COST IC1004 MC and Scientific Meeting*, 28-30 January 2015 – Dublin, Ireland.

[XVIII] S. Fortes, R. Barco, A. Aguilar-Garcia, "Location-Based Distributed Failure Management for 5G Ultra-Dense Small Cell Networks," *Workshop on Evolution of Radio Access Network Technologies towards 5G*. 5 May 2015 – Valencia, Spain.

[XIX]   S. Fortes, R. Barco, A. Aguilar-Garcia, P. Muñoz, "Integration of Mobile Context in the Diagnosis of Small Cell Networks," *Joint NEWCOM/COST*

Workshop on Wireless Communications JNCW 2015, 13-15 October 2015 – Barcelona, Spain.

[XX]   S. Fortes, A. Aguilar-Garcia, R. Barco, F. Barba, J.A. Fernández-Luque, A. Fernández Durán, "Diseño Integrado de Redes Auto-Organizadas LTE/LTE-A y Posicionamiento en Interiores," *XXVIII Simposium Nacional de la Unión Científica Internacional de Radio URSI 2013*, 11-13 September 2013 – Santiago de Compostela, Spain.

[XXI]   S. Fortes, A. Aguilar-Garcia, R. Barco, "Detección de Celda Durmiente en Entornos Localizados de Femtoceldas," *XXIX Simposium Nacional de la Unión Científica Internacional de Radio URSI 2014*, 3-5 September 2014 – Valencia, Spain.

[XXII]   S. Fortes, A. Aguilar-Garcia, R. Barco, "Identificación de Fallos Radio en Entornos Celulares Localizados de Interior," *XXX Simposium Nacional de la Unión Científica Internacional de Radio URSI 2015*, 2-4 September 2015 – Pamplona, Spain.

Chapter 3 described the work published in [IV][IX][XIII][XVII][XX] about a context-aware framework and a management architecture for indoor SON. Chapter 4 proposed an indoor positioning system based on RFID and cellular technologies, described in [II][VIII]. Finally, Chapter 5 detailed the proposed self-optimization mechanisms in femtocell networks, published in [I][III][V][VI][VII][X][XI].

6.3.5   Projects

Appendix A

Technology characteristics

The general characteristics and theoretical models of RFID and cellular (GSM and UMTS) technologies are summarily described in indoor scenarios.

A.1   RFID technology

There are two different types of RFID technology systems: *inductive* and *radiative*, operating in a large range of frequencies, from 125 kHz to 5.8 GHz (Figure A.1), but most applications use LF, HF and UHF bands.

Focusing on UHF band, communication of UHF systems are up to several dozens of meters in free space conditions. In order to achieve longer ranges, transponders need a battery to provide power supply to the chip.
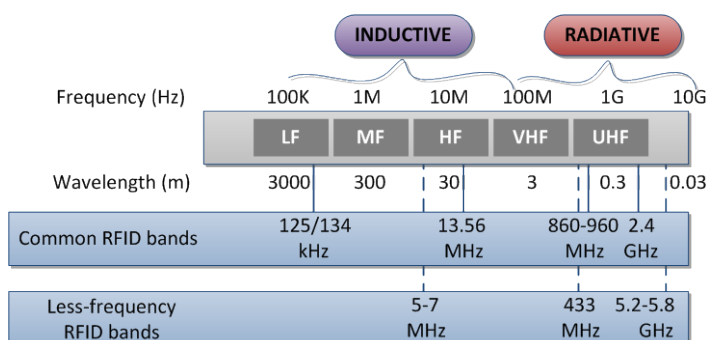

Figure A.1: RFID frequency bands.

The power received for a line-of-sight (LoS) and multiple single reflections environment can be modeled as [117]:

$$RSSI(d) = \left(\frac{\lambda}{4\pi d}\right)^2 \left|1 + \sum_{n=1}^{N} \Gamma_n \frac{d}{d_n} e^{-j(d_n - d)}\right|^2, \qquad (A.1)$$

where λ is the wavelength, d is the length of the direct ray path, Γ_n is the reflection coefficient of the n-th reflecting object, d_n is the length of the n-th reflected ray path and N is the total number of reflections.

The estimation of the multiple reflections in a scenario is computing consuming and needs an accurate description of the environment. In practice, the most commonly channel model used for indoor scenarios is the log-normal shadowing model [118]. It allows to predict the path loss by a statistical analysis of measurements in a given physical surrounding:

$$PL(d) = PL(d_0) + 10\eta \, log_{10} \frac{d}{d_0} + X_\sigma, \qquad (A.2)$$

where $PL(d_0)$ is the path loss for a reference distance d_0, η is the path loss exponent and X_σ is a Gaussian random variable with zero mean and a standard deviation σ.

A.2   Cellular technology

GSM is a standard that describes protocols for 2G mobile networks. GSM systems usually work in the 900/1800 MHz band, whereas in the 3G, UMTS is located at the 900/2100 MHz band (in Europe). Furthermore, there is also an important difference in terms of radio propagation: the carrier spacing is 200 kHz in GSM, whereas it is increased to 5 MHz in UMTS. For this reason, UMTS system is more vulnerable to frequency selective fading than GSM systems. Particularly, the wireless wave will be diffracted, scattered, and absorbed by the terrain, trees, building, vehicles, people, etc., that encompasses the propagation environment as it traverses the path from a transmitter to a receiver. The presence of obstacles along the path causes higher signal attenuation than it would suffer under free space conditions.

Both GSM and UMTS technologies are widely implemented all over the world. Even if GSM is a legacy technology in terms of telecommunications, it is by far the most extended technology in terms of coverage and redundancy of macrocell stations, where also the lower transmission frequencies allow a better reception indoors.

In order to obtain a glance of the cellular signal channel characteristics indoors, COST231-Hata model [119] which is valid from 150 MHz to 2 GHz and WINNER II

model [112] which is valid from 2 GHz to 6 GHz can be adopted as two of the most widely propagation models for cellular communication studies.

COST231-Hata model defines the path loss in different urban and suburban areas as well as in in-building penetration. This model uses a LoS path loss with an indoor component:

$$PL(d) = 32.4 + 20logf_{GHz} + 20log(d_{out} + d_{in}) + PL_{in}, \qquad (A.3)$$

where f_{GHz} is the frequency in GHz, d_{out} is the outdoor path, d_{in} is the indoor path and PL_{in} is defined as:

$$PL_{in} = PL_e + PL_{ge}(1 - sin\theta)^2 + max(\Gamma_1, \Gamma_2), \qquad (A.4)$$

where PL_e is the normal incidence first wall penetration, $PL_{ge}(1 - sin\theta)^2$ is the added loss due to angle of incidence θ which is usually measured over an average of empirical values of incidence and $max(\Gamma_1, \Gamma_2)$ estimates loss within the building.

WINNER II model defines different scenarios and their applicable path loss characteristics. For the case of macrocellular signal reaching in indoor environments the correspondent model is outdoor-indoor C4. The expression for this model path loss is:

$$PL(d) = PL_{C2}(d_{out} + d_{in}) + 17.4 + 0.5d_{in} - 0.8h_{MS}, \qquad (A.5)$$

where d_{out} is the distance between the macrocellular station and the external wall of the indoor scenario, d_{in} is the distance between the wall and the receiver indoors, PL_{C2} represents the path loss for the model for urban macrocell outdoors C2, and h_{MS} is the height of the terminal. For this model, the impact of d_{in} in the factor $PL_{C2}(d_{out} + d_{in})$ becomes usually negligible for the normal distance of dozens/hundreds of meters between the indoor building and the macrocell base station. This makes the evolution of the path loss in the indoor scenario mainly influenced by the term $0.5d_{in}$.

Additionally the impact of the shadow fading can be also modeled for an indoor scenario as a log normal distribution with standard deviation of 8 dB. Finally, fast fading can be modeled as Rayleigh (in Non-Line of sight) and Ricean (in Line of sight situations) distributions. However, fast fading effects are mostly eliminated in the measurements provided by common monitored tools due to received power is averaged at Layer 1 and 3 [79] of the terminal protocol stack. This makes the shadowing the

main component for the difference of received power between positions of the scenario. Still, in order to categorize the characteristics of each position, shadowing effects cannot be calculated without very complex computations and an extremely detailed knowledge of the scenario is required. In addition, the path followed by the signal from the macrocellular base station to the terminal shall be known.

Appendix B

Signal assessment

The signal assessment of RFID and cellular (GSM and UMTS) technologies based on their theoretical models (see *Appendix A*) and the measurement campaign are detailed in this appendix.

B.1   Introduction

The selected indoor scenario consists on a corridor 22.5 m long x 2 m width x 2.5 m height. For the assessment of the RFID and cellular signals, several samples were collected for each technology along the corridor. Three lines of measurements (called hereafter 'left', 'middle', 'right') were performed along it with a distance of 50 cm from each other where multiple samples have been gathered every meter for each position. This provides 63 positions (21 per line) in the whole corridor. Further details about the scenario, the equipment and the mobile platform are described in subsection 4.5.1 "*Trial set-up*".

Both systems (RFID and cellular) acquire samples during five minutes per position. Regarding the RFID system, all tags are sampled every five seconds while the cellular signal (GSM and UMTS) were measured every second. These experiments were carried out in the morning of three days. In order to simplify the assessment, all measurements were taken with the same orientation. Notice that, assuming that the cellular terminals properly report the terminal orientation, the analysis of the signal and/or the calibration phase can be performed and stored for multiple orientations. Then, during the localization phase, data from training sets with different orientations would be selected and combined following common approaches for positioning.

In order to analyze the characteristics of radio signals received from each technology and to assess their applicability for indoor location, the following statistics have been studied:

- *Analysis of the measurements:* referring to the range and distribution of signal values in terms of the received Cell ID ($IDSrx$) and PRX (Prx). From the point of view of the Prx, this distribution is characterized by the mean $\mu_{Prx}^{complete}$ and the standard deviation $\sigma_{Prx}^{complete}$ of all samples gathered in the assessment. From the point of the $IDSrx$, the number of identifiers $N_{IDSrx}^{complete}$ is measured.

- *Analysis per position:* about the variability of the gathered signals received in each fixed position. It gives an idea of the stability of the signal and therefore the achievable accuracy of the positioning system. For this perspective, different statistics have been defined:

    - *Static standard deviation,* $\sigma_{Prx}^{static}(x,y)$, *and mean,* $\mu_{Prx}^{static}(x,y)$, *of Prx (in dB)*: static standard deviation measures the level and stability of the power measurements in a specific position (x,y) as:

    $$\sigma_{Prx}^{static}(x,y) = \sqrt{\frac{1}{|M_{x,y}|} \sum_{\forall m_i \in M_{x,y}} \left(m_i - \mu_{Prx}^{static}(x,y) \right)^2}, \qquad (B.1)$$

    where $M_{x,y}$ is the set of Prx samples m_i measured in the (x,y) position and $\mu_{Prx}^{static}(x,y)$ is the average of the $M_{x,y}$ samples.

    - *Adjacent standard deviation,* $\sigma_{Prx}^{adjacent}(x,y)$, *of Prx (in dB)*: it is calculated as the deviation of the set of the received power values in one position and its adjacent points in the assessment set as:

    $$\sigma_{Prx}^{adjacent}(x,y) = \sqrt{\frac{1}{|M_{x,y}^{adj}|} \sum_{\forall m_i \in M_{x,y}^{adj}} \left(m_i - \mu_{Prx}^{adjacent}(x,y) \right)^2}, \qquad (B.2)$$

    where $M_{x,y}^{adj} = \{M_{x,y} \cup M_{x+x0,y} \cup M_{x-x0,y} \cup M_{x-x0,y-y0} \dots\}$ is the set of Prx measurements used in the assessment, being $\{(x + x0, y), \dots\}$ the adjacent positions (variations in the z axis are not considered due to the fixed height of the target platform). $\mu_{Prx}^{adjacent}(x,y)$ is the mean of the $M_{x,y}^{adj}$ samples. This provides an assessment on the discernibility of a position in respect to its neighbors in terms of Prx.

- *Static number of IDSrx, $N_{IDSrx}^{static}(x,y)$:* it refers to the number of serving cells or tags measured per point.

- *Adjacent ratio of common IDSrx, $\sigma_{IDSrx}^{adjacent}(x,y)$:* it indicates the number of different **IDSrx** between one position and its adjacent ones. Such parameter measures the possibility of using the Cell ID to distinguish between positions.

As support for characterization of the signal in real-world, their behavior is emulated by means of simulations for each technology (see equations in *Appendix A*):

- *RFID:* An active tag is emulated on the left wall of the corridor in the position (0,1). For simplicity, the radio propagation model predicts the signal received in line of sight and multi path component formed predominately by a single reflected wave. The transmission power of the tag was set to -30 dBm.

- *UMTS and GSM:* Three tri-sectorized macrocells have been deployed into a large scenario to cover the designed corridor for both technologies. They are placed 1 km far from the corridor.

In the following subsections, the features of the different signals of the simulated scenario and the real prototype are analyzed and compared.

B.2   RFID signal

B.2.1   Analysis of the measurements

For the simulated signals, the probability distribution function (PDF) of *Prx* for a tag placed on coordinates (0,1) and per line of measurement, are illustrated in Figure B.1. For the middle line, it presents a value of $\sigma_{Prx}^{complete} = 6$ dB.

| (a) Left Line | (b) Middle Line | (c) Right Line |
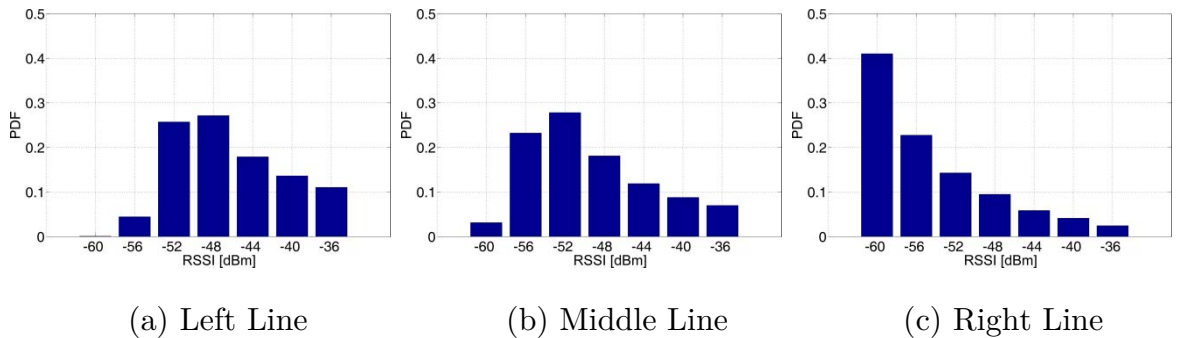
Figure B.1: RFID simulations – Histograms.

Regarding the real campaign, the probability distribution function at each line along the corridor for a random RFID tag is represented in Figure B.2, which has been constructed aggregating 1260 measurements per line (21 positions x 60 samples/position). In this case, the average power $\mu_{Prx}^{complete}$ for this particular tag is around -60 dBm for all lines, but distribution is more symmetrical for the middle line. Here, the received power is between [-73, -43] dBm and a value of $\sigma_{Prx}^{complete} = 7.3$ dB, which is consistent with the simulated results. In addition, all of the installed tags are received at some point of the scenario, making $N_{IDSrx}^{complete}$ equal to 30.

Finally, comparing both figures, quite similar distributions are observed between the simulation results and the measurement campaign.

(a) Left line   (b) Middle line   (c) Right line
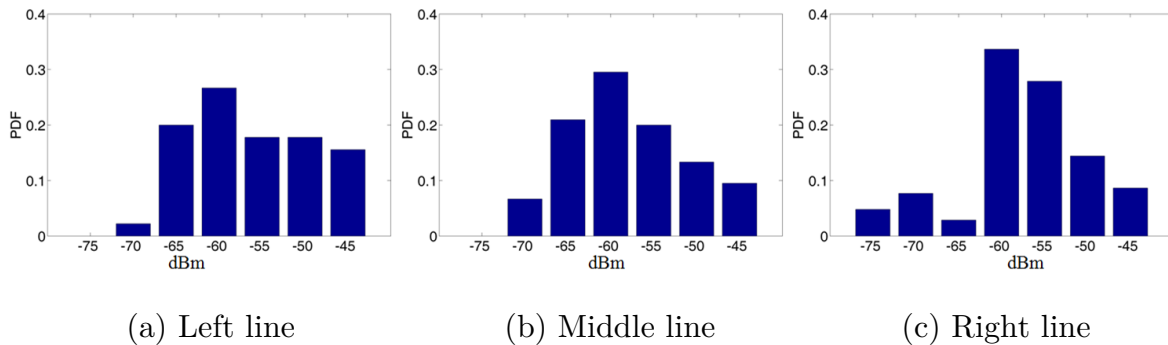
Figure B.2: RFID – Histograms.

B.2.2   Analysis per position

Figure B.3 shows the measurements gathered in the middle line of the corridor coming from two representative tags located at the beginning (a) and in the middle (b) of the corridor.
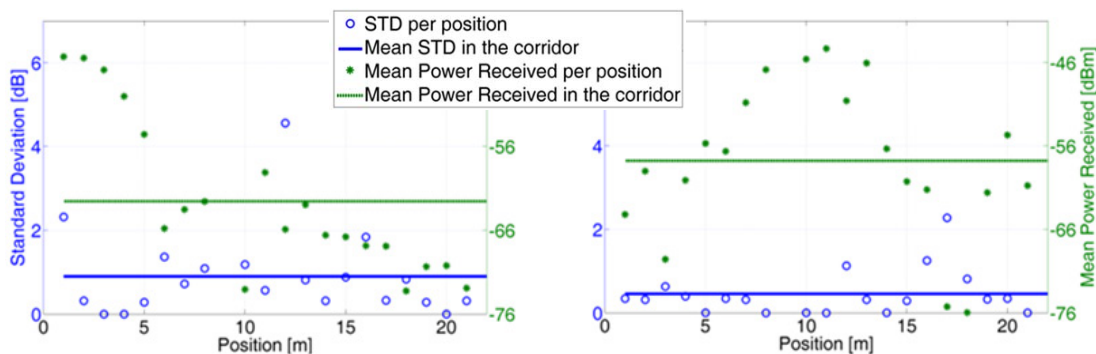
(a) Tag 1: Beginning of the corridor   (b) Tag 7: Middle of the corridor

Figure B.3: RFID – RSSI.

Mean Prx per position along the corridor $\mu_{Prx}^{static}(x, y)$ is ranged from -75 to -45 dBm (green dots) for most positions, which complies with the path loss slope using the log-normal model in this corridor. Prx deviation per position, $\sigma_{Prx}^{static}(x, y)$ is quite low. In average, along the corridor, the mean of the deviation values is less than 1 dB (blue line). Similar results are obtained for the rest of the 30 tags.

B.3   GSM and UMTS signals

B.3.1   Analysis of the measurements

On the one hand, regarding the simulation results, the PDF of Prx for each cellular technology is illustrated in Figure B.4 and Figure B.5 respectively. Prx is considered independently of the serving cell (serving cell received power is used without examining its Cell ID).

UMTS technology presents a value of $\sigma_{Prx}^{complete} = 7.6$ dB, showing a wide variability of the received power, thus, suggesting the presence of important shadowing effects in the corridor.

(a) Left line   (b) Middle line   (c) Right line
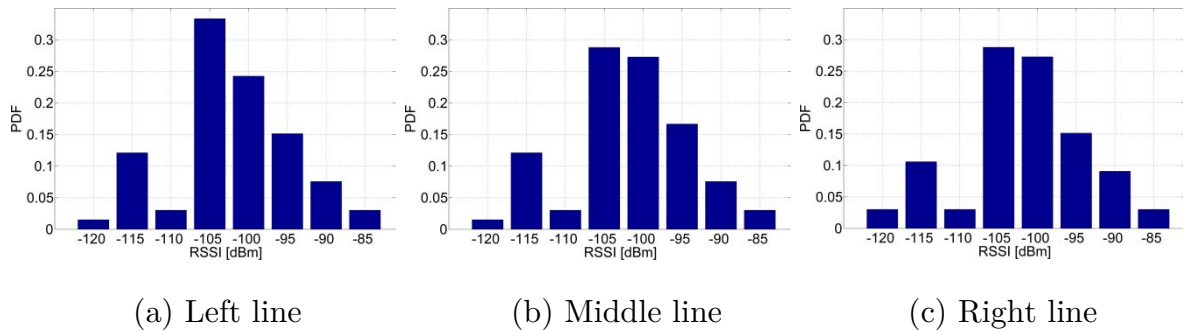
Figure B.4: UMTS simulations – Histograms.

(a) Left line   (b) Middle line   (c) Right line
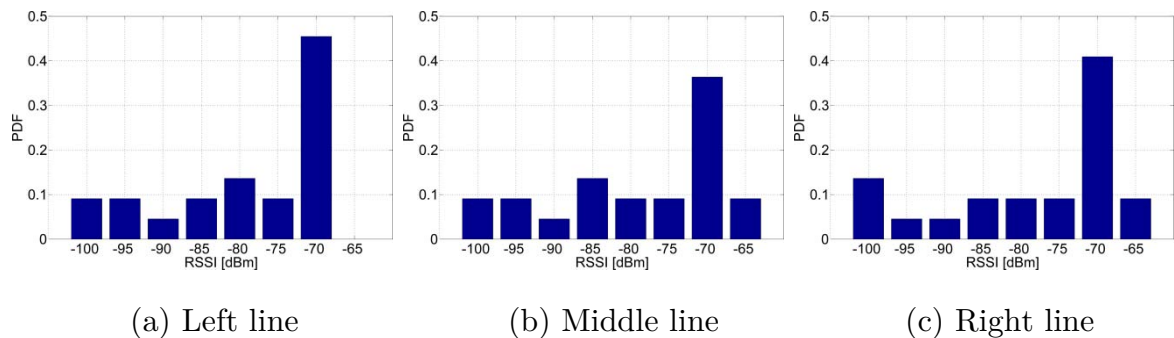
Figure B.5: GSM simulations – Histograms.

Regarding GSM information from the simulation point of view, this has a value of $\sigma_{Prx}^{complete} = 11.2$ dB, having a dominant power component in the three histograms which suggest the presence of a dominant direct line of sight between the macrocell and the corridor. In terms of variable range, both technologies cover around 40 dB from the minimum to the maximum measured values.

On the other hand, the results of the real campaign are described. For that purpose, G-MoN [78] app automatically sniffs cellular signals and provides cellular information each second.

Firstly, for the UMTS technology, the global statistical distribution of all measurements in the corridor is represented in Figure B.6, which has been calculated aggregating 6300 measurements per line (21 positions x 300 samples/position). Here, it can be observed how the measurements are mainly in the range of [-104, -88] dBm in every line, showing the wide variability in the values of the received power along the corridor, with a value of $\sigma_{Prx}^{complete} = 4.13$ dB for the middle line. This could mean two different situations: either the received power suffers quick changes due to the fading or the signal is more or less stable around the same position but it changes a lot with the position. However, the dominant power component around -98 dBm suggests a stable signal in the corridor.

(a) Left line (b) Middle line (c) Right line
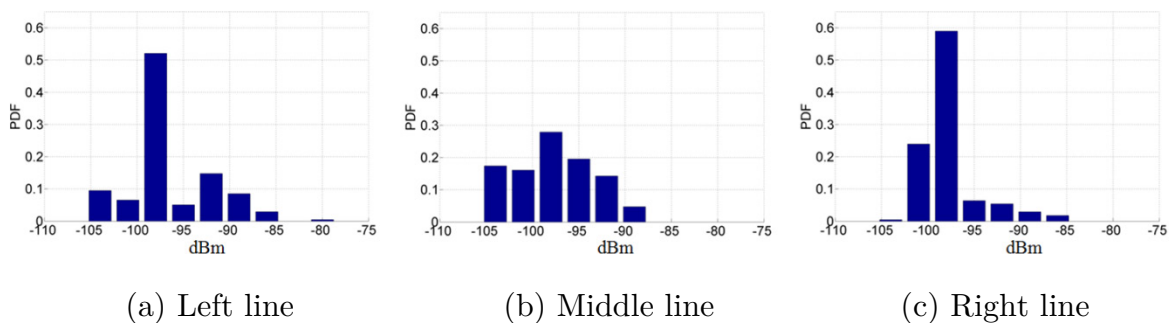
Figure B.6: UMTS – Histograms.

(a) Left line (b) Middle line (c) Right line
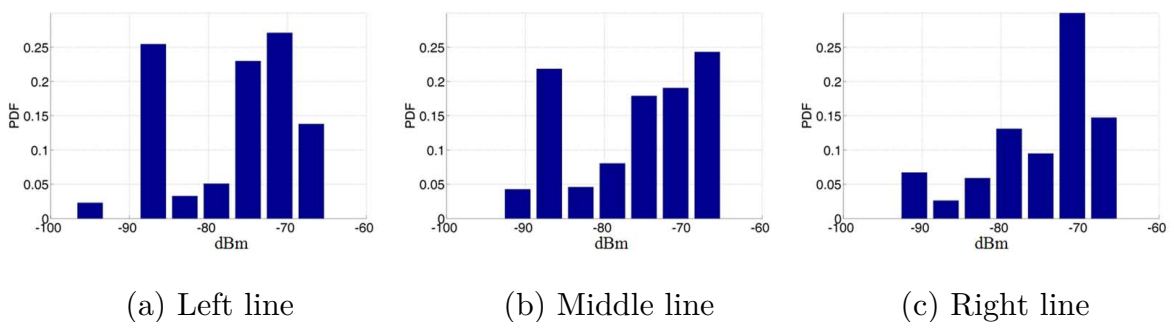
Figure B.7: GSM – Histograms.

Secondly, for the GSM technology, Figure B.7 illustrates the same information. In this case, the average received power is higher than for UMTS. The range width, mainly between [-90, -75] dBm, provides similar values to UMTS but the deviation is higher $\sigma_{Prx}^{complete}$ = 7.5 dB. This is consistent with the GSM band being located in lower frequencies (900 MHz) than UMTS (2100 MHz), which makes it less affected by attenuation and common obstacles in indoor environments. This would depend also on the location of the cellular base station, but in this case, and following common cellular telecommunications operators practices, both technologies share the same site, therefore, the same distance to the studied scenario. In these histograms, two main ranges of dominant power components are detected, which could mean that two serving cells are received in the corridor.

The measurements show a narrower distribution than the simulated results due to the different shadowing conditions. However, the general relation between the characteristics of both technologies, with a higher deviation for GSM, is consistent with the simulated results.

B.3.2   Analysis per position

On the one hand, to analyze the signal stability per position from the point of view of the received power, its standard deviation and mean are calculated for all the measurements gathered in each different position.

(a) Left line   (b) Middle line   (c) Right line
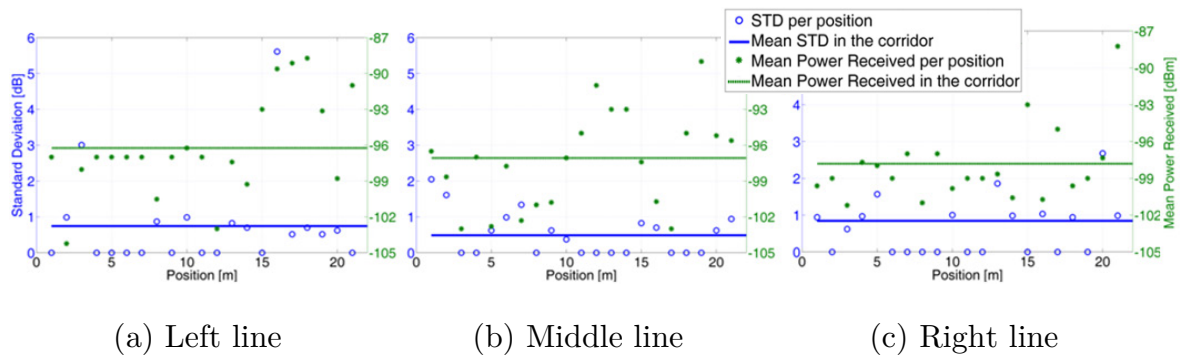
Figure B.8: UMTS – Received Signal Code Power (RSCP).

Firstly, the UMTS study is shown in Figure B.8 for the statistics calculated with the samples gathered at each position of the three corridor lines followed in the campaign. The static standard deviation $\sigma_{Prx}^{static}(x, y)$ (blue circles) of the measurements for most points are lower than 2 dB and its average is lower than 1 dB along the corridor (blue line). That indicates a very strong stability of most received

power measurements for each position as a consequence of the average process performed by the app, which mitigates the fast-fading component of the propagation. Measurements in those positions with high standard deviation might suffer from the effect of handover or cell-reselection due to shadowing. At the same time, the variation of the mean received power (green dots) at each position is also shown in Figure B.8, providing an assessment of the possibilities for discrimination of the different positions along the corridor.

Secondly, for GSM technology, Figure B.9 also shows high stability in each position of the corridor of the three lines, being $\sigma_{Prx}^{static}(x,y) = 0$ dB except for some few positions in each line where its value is increased, sometimes up to 10 dB. Once the serving cell was analyzed in each position, it was observed that these big variations in the received power were caused by the handover/cell-reselection process. However, such behavior could easily be filtered based on the serving Cell ID information, providing still valuable information for those positions.

(a) Left line   (b) Middle line   (c) Right line
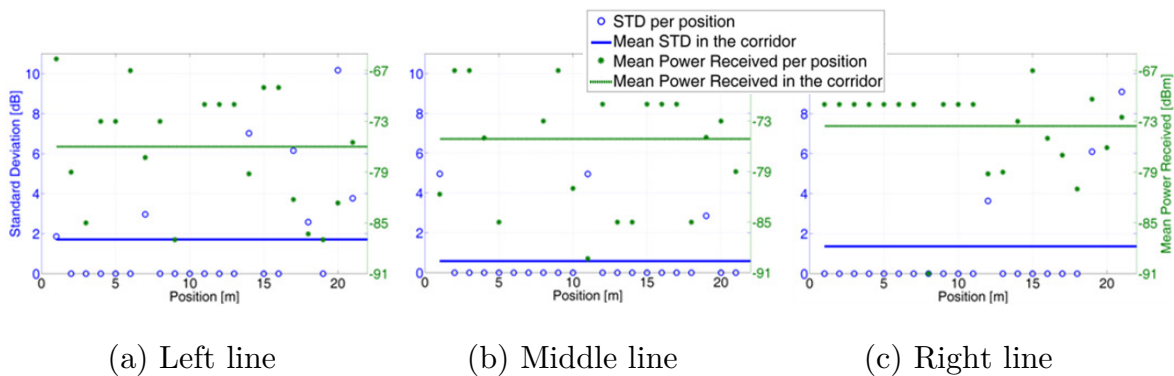
Figure B.9: GSM – Received Signal Level (RxLev).

On the other hand, from the point of view of the serving Cell ID, these are depicted in Figure B.10 where different icons identify each serving cell per position and line along the corridor. Figure B.10(a) shows how UMTS terminals are connected to a wide variety of cells in this scenario, which explains the variations in the signal received in one spot. Conversely, as Figure B.10(b) depicts, the GSM signal presents homogeneous serving Cell IDs in the corridor, except in the right side where the influence of several cells are presented. Such behaviors become convenient for localization purposes as it discriminates positions on the corridor.

In conclusion, both cellular technologies have shown a very strong stability in terms of the received power at the same position, especially if the consistency in the serving Cell ID is taken into account, while it changes considerably along the corridor.
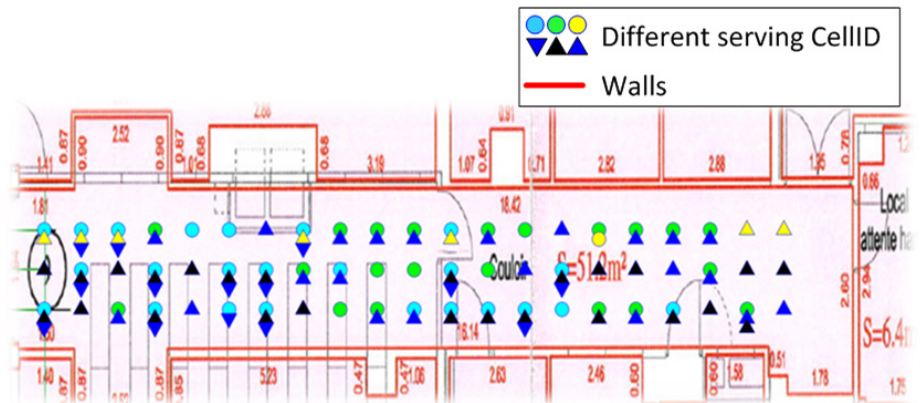
(a) UMTS technology

(b) GSM technology

Figure B.10: Serving cell identifier for UMTS and GSM technologies.

B.4   Applicability of the results

The characteristics of the analyzed technologies are now summarized. Table B.1 shows the statistics for the signal complete distribution along the middle line of the corridor while Table B.2 shows the mean and median of the characteristics of variability obtained per position of the middle line.

For the case of RFID technology, the results on Prx corresponds to a tag placed on coordinates (0,1). In terms of Prx variability per adjacent position it is observed how $\sigma_{Prx}^{adjacent}$ values are consistently high (median $\sigma_{Prx}^{adjacent} = 3.2$ dB), which makes it a good variable as input for the localization phase. However, the signal presents a certain degree of instability per position (median $\sigma_{Prx}^{static} = 0.5$ dB), which may introduce inaccuracies during the real time localization phase. From the point of view of $IDSrx$, it is also observed that almost all tags are read in any position in the corridor. Therefore, the tag ID is not good enough to discriminate the real localization. As a consequence, each position is defined by the set of 30 RSSI fingerprints (each tag provides one).

Table B.1: Summary of signal variability.

Technology	$\mu_{Prx}^{complete}$ (dBm)	$\sigma_{Prx}^{complete}$ (dB)	$N_{IDSrx}^{complete}$ (number)
RFID	-58.2	7.3	30
UMTS	-97.1	4.1	7
GSM	-75.1	7.5	4

In terms of cellular technology, the low values in $\sigma_{Prx}^{static}(x, y)$ (median ≤ 0.2 dB for both cellular technologies) indicate a very strong stability in the measured signal for each point, which is a positive feature for localization purposes allowing a stable support for the positioning calculations. In constrast, the high values in $\sigma_{Prx}^{adjacent}(x, y)$, provide an idea of the capability of distinguishing between different spots based on the cellular received power. Here, GSM signals present the highest values.

Table B.2: Summary of signal variability per position.

Technology	Statistic	σ_{Prx}^{static} (dB)	$\sigma_{Prx}^{adjacent}$ (dB)	N_{IDSrx}^{static} (number)	$\sigma_{IDSrx}^{adjacent}$ (ratio)
RFID	Mean	0.7	3.2	28.7	1.4
	Median	0.5	3.2	29	1.0
UMTS	Mean	0.5	2.6	1.7	0.7
	Median	0.2	2.5	1.0	0.7
GSM	Mean	0.6	6.0	1.1	0.3
	Median	0.0	6.6	1.0	0.0

In terms of $IDSrx$, this means the variability of the received Cell IDs, $N_{IDSrx}^{static}(x, y)$ indicates that in general more cells are received per position in UMTS, while $\sigma_{IDSrx}^{adjacent}(x, y)$ ratio represents the capability of distinguishing between adjacent positions based on the cell identifiers. Here, the latest indicates poor capabilities of GSM for the distinction based on Cell ID as most adjacent positions share the same Cell ID (median $\sigma_{IDSrx}^{adjacent} = 0$). Conversely, in the case of UMTS each position has commonly a distinct pattern of receiving cells (median $\sigma_{IDSrx}^{adjacent} = 0.7$ meaning that it is near one change of identifiers between positions).

It has to be indicated that these general conditions, as in any opportunistic system, may vary for other places, as the distribution and composition of the macrocell environment may be different. Thus, for the use of the macrocell information an analysis of the particularities of each scenario has to be performed to assess the applicability of the scheme.

Appendix C

Fuzzy logic controllers

A *fuzzy logic controller* (FLC) [120] is a non-parametric approach which provides an efficient and systematic solution for incorporating linguistic information from human experts. The use of rules and interactions make this system relatively easy to understand.

A general fuzzy logic system consists of three stages as Figure C.1 illustrates. Firstly, a set of fuzzy membership functions transform crisp inputs into fuzzy input datasets. Secondly, the fuzzy outputs are calculated based on fuzzy input datasets and fuzzy rules (instead of Boolean logic). Finally, those outputs are converted back to crisp values.
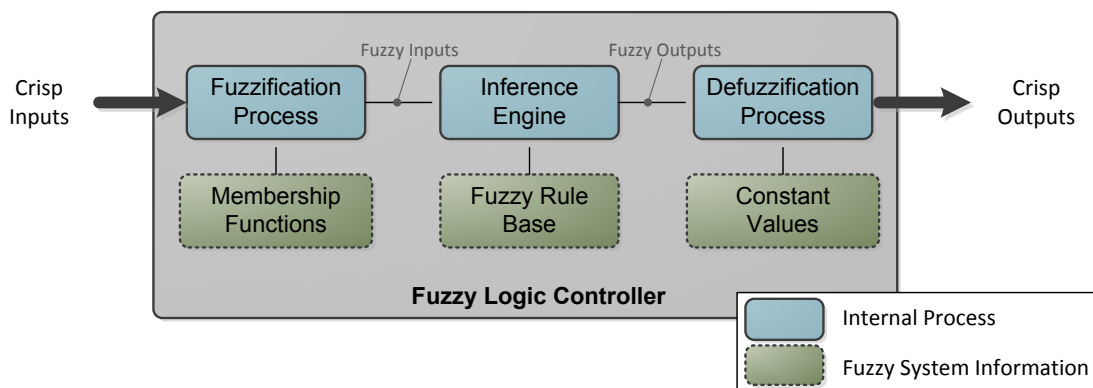
Figure C.1: Fuzzy inference system (Takagi-Sugeno).

The literature offers different implementations of FLCs. This work is focused on the *Takagi-Sugeno* [111] approach due to its simplicity and computational efficiency. Next subsections describe further details about this approach.

C.1   System parameters and functions

The system parameters and functions could be basically divided in four groups:

- **_Linguistic variables:_** Instead of numerical values (continuous values), the system identifies each input and output variable as one or more linguistic variables (discrete variables), e.g., _the base station transmission power adaptation_, whose numerical values are ranged between [-10, 10] dB, is transformed into a dataset of linguistic terms (sentences or words) such as _very negative_, _negative_, _zero_, _positive_ and _very positive_. An example is depicted in Figure C.2 where the available linguistic terms for two different inputs and an output can be found on the top of each function.
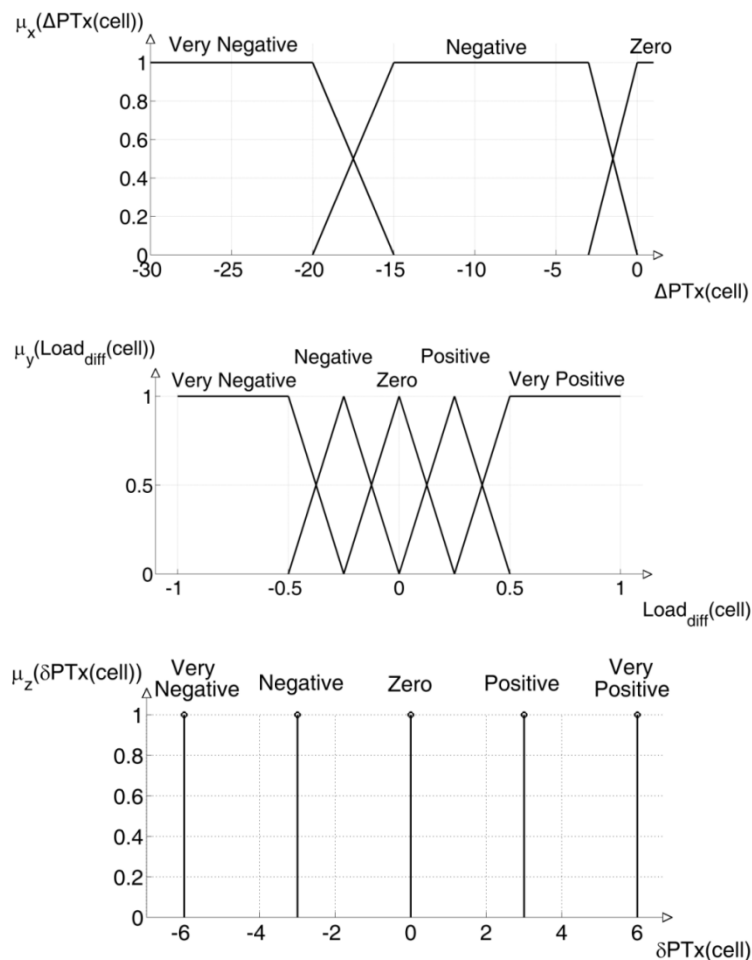
Figure C.2: Example of membership functions.

- **_Membership functions:_** A membership function is a curve that defines the degree of membership of a crisp input (between 0 and 1). Each membership

function $\mu_A(x)$ is labeled with a linguistic variable. These functions map and quantify crisp inputs *(x)* from the fuzzy set A into fuzzy input datasets (labeled with linguistic terms). Figure C.2 illustrates an example of real membership functions. The membership functions to transform fuzzy output datasets into crisp outputs are constant values (for Takagi-Sugeno approach).

- ***Fuzzy rules:*** They are simple IF-THEN structures to control the fuzzy output datasets (e.g., transmission power adaptation as *very negative*, *negative*, etc.) based on the fuzzy input datasets (e.g., call blocking ratio as *very high*, *high*, etc.). A typical fuzzy rule statement, where two crisp inputs are introduced in the system, is similar to the following form:

$$\textit{IF } x \textit{ is } \textbf{R} \textit{ AND } y \textit{ is } \textbf{S} \textit{ THEN } \textbf{Z}, \qquad\qquad (C.1)$$

where x and y are the crisp inputs, while R and S are the fuzzy input datasets defined in x and y, respectively according to their membership functions. Z is the fuzzy output dataset. Table C.1 shows an example of fuzzy rules.

Table C.1: Example of fuzzy rules.

	Load$_{diff}$	Operator	ΔPTx	δPTx
	IF			THEN
1	Very Negative	AND	Very Negative	Very Positive
2	Very Negative	AND	Negative	Very Positive
3	Very Negative	AND	Zero	Positive
4	Negative	AND	Very Negative	Very Positive
5	Negative	AND	Negative	Positive
6	Negative	AND	Zero	Positive
7	Zero	AND	Very Negative	Very Positive
8	Zero	AND	Negative	Positive
9	Zero	AND	Zero	Zero
10	Positive	AND	-	Negative
11	Very Positive	AND	-	Very Negative

- ***Fuzzy set operations:*** A set of crisp inputs could provide several fuzzy outputs (Z) based on fuzzy rule statements (e.g., equation (C.1)). The combination of each rule is carried out using fuzzy set operations, like AND/OR operators, to get the degree of truth of each rule and finally the crisp output.

C.2   System processes

The fuzzy logic system is divided into three internal processes as Figure C.1 shows. The aim of each module, as well as the flow of information between them, is detailed:

1) **Fuzzification process:** The fuzzification process is the first step. This process converts crisp inputs into fuzzy input datasets based on the membership functions. These functions quantify the degree of membership of a crisp input x into a fuzzy dataset.

   For example, the $Load_{diff}$ crisp input value ($x = -0.45$) of function $\mu_y(Load_{diff})$ in Figure C.2, could be labeled as *'Very Negative'* (0.75) and *'Negative'* (0.25). These fuzzy input datasets are forwarded to the next step, the *inference engine.*

2) **Inference engine:** The fuzzy datasets are evaluated at each rule r to calculate the so-called *degree of truth* of that rule ω_r. Fuzzy set operations accomplish this process. This work follows equation (C.1) to generate fuzzy rules and the product operator (PROD) is selected as the fuzzy set operation for AND intersection operator.

   Following this approach, the degree of truth of each rule r for two fuzzy input datasets is defined as:

   $$\omega_r = \mu_A(x) * \mu_B(y), \qquad\qquad\qquad (C.2)$$

   where $*$ is the product operator (PROD) and $\mu_A(x)$ and $\mu_B(y)$ are the values of the membership functions for fuzzy sets A and B and crisp inputs x and y, respectively.

3) **Defuzzification process:** After the inference engine, the fuzzy outputs are computed to get the crisp output. For that purpose, there are different defuzzification methods [121]. This work is based on the center of gravity for singleton method, that is:

   $$output = \frac{\sum_{r=1}^{R} \omega_r \, o_r}{\sum_{r=1}^{R} \omega_r}, \qquad\qquad\qquad (C.3)$$

   where ω_r is the degree of truth of rule r, o_r is the constant value of the output variable for the rule r, and R is the number of rules.

Appendix D

Summary (Spanish)

En este anexo se presenta un breve resumen en español sobre el trabajo realizado en esta tesis. En primer lugar, se hace una breve introducción a la situación actual de las redes móviles y los objetivos que se pretenden abordar. Posteriormente, se presenta el estado del arte, donde se describen los trabajos desarrollados dentro del ámbito de esta tesis. A continuación, se describen las tres líneas de investigación en las que se fundamenta este trabajo: *integración de información de contexto en las redes móviles*, *técnicas de posicionamiento en interiores* y *técnicas de balance de carga en interiores con soporte de información de contexto*. Finalmente, se detallan las contribuciones y líneas futuras de investigación, así como las publicaciones que avalan esta tesis.

D.1   Introducción

Las redes de telefonía móvil desplegadas en la actualidad precisan de la configuración manual de muchos de sus elementos de red. Los parámetros asociados a los diferentes procesos de la red tales como su planificación, configuración, integración o gestión son esenciales para un funcionamiento tanto eficiente como fiable en las operaciones de la red. Sin embargo, los costes asociados a la configuración de estos procesos son un punto a tener en cuenta por las operadoras de telefonía móvil. Los procesos semi-automáticos han sido el modo natural de actuar sobre este tipo de redes, requiriendo para ello, la intervención de ingenieros especializados en los diferentes campos asociados. Estos expertos, con la ayuda de herramientas de visualización y su gran conocimiento y experiencia en afrontar problemas similares, son capaces de actuar sobre la red permitiendo su mantenimiento y estabilidad. El inconveniente de este mecanismo reside en el consumo de tiempo requerido para hacer frente a estos cambios y la alta vulnerabilidad a cometer errores. Además, la variación manual de estos

parámetros introduce normalmente largos retrasos en la actualización de los mismos en respuesta a las constantes y rápidas variaciones que puedan presentarse en este tipo de redes, lo que genera que los parámetros de configuración aplicados no sean los óptimos. De este modo, por un lado conviene automatizar al máximo todos los procesos existentes en la red para ofrecer un mayor rendimiento a un menor coste y por otro lado, ser capaz de ofrecer la capacidad demandada por los usuarios evitando la caída de llamadas, desconexiones en el servicio, etc. Para hacer frente al primer caso, surge el concepto de redes auto-gestionadas, que permiten sacar el máximo partido a las redes de telefonía móviles desplegadas, disminuyendo al mismo tiempo los costes operacionales (OPEX) así como los costes de capital (CAPEX) y mejorando las prestaciones de la red ofreciendo al usuario final mejor calidad de experiencia (QoE). Para el segundo caso, nuevas tecnologías móviles (Long Term Evolution - LTE) están emergiendo para hacer frente a tal demanda de datos, nuevos tipos de estaciones base se están desplegando (small cells), etc. creando escenarios de redes de comunicaciones móviles heterogéneas y difíciles de gestionar.

El concepto de redes auto-gestionadas proviene del término inglés *Self-Organizing Networks* (SON) y forma parte del nuevo paradigma definido por el 3GPP (3rd Generation Partnership Project) [2]. Su objetivo es automatizar las operaciones, la administración y el mantenimiento (OAM) de las infraestructuras de comunicaciones móviles a través de unos mecanismos avanzados que gestionen los procesos de manera inteligente y automática obteniendo los parámetros de configuración óptimos ante variaciones en las condiciones de la red. De este modo, se consigue mejorar su rendimiento así como reducir gastos OPEX y CAPEX [8] [9]. Este nuevo concepto se puede dividir principalmente en tres funcionalidades:

- *Auto-configuración:* Se refiere a la capacidad que presenta la red para realizar una configuración de manera dinámica frente a la incorporación de nuevas estaciones base. Entre los parámetros que se pueden configurar se encuentran el identificador de celda, la frecuencia, la potencia de transmisión, etc.
- *Auto-optimización:* Permite modificar automáticamente parámetros de la red móvil para ofrecer un mejor rendimiento de ésta y ofrecer a los usuarios finales un servicio de calidad. Entre estos parámetros a optimizar se incluyen el área de cobertura, capacidad de la red, traspasos, interferencias, etc.
- *Auto-curación:* Detecta y diagnostica de forma automática los fallos y degradaciones del servicio de la red móvil e intenta resolver los problemas, mediante la identificación de la causa y procede a su recuperación.

Centrándose en el campo de la auto-optimización [45], el 3GPP define y actualiza periódicamente en sus documentos (*Releases*) lo que se conoce como *Casos de uso*, una descripción de las actividades o de los pasos que deben realizarse para llevar a cabo

procesos de auto-optimización. De forma paralela, la alianza NGMN (Next Generation Mobile Networks) [3], una asociación de telecomunicaciones de operadores de telefonía móvil, proveedores, fabricantes y centros de investigación, han trabajado en la definición de unos casos de uso análogos: *Coverage and Capacity Optimisation*, *Energy Savings*, *Mobility Load Balancing*, *Mobility Robustness Optimization*, etc.

Por otro lado, el amplio despliegue de nuevas redes de comunicaciones móviles (LTE.) sobre las ya existentes como son GSM, UMTS, HSPA, WiFi, WiMax, etc. para hacer frente al gran incremento de demanda de datos en las redes actuales, están generando un entorno de redes celulares heterogéneas (HCNs) compuestas por varias tecnologías de acceso radio (RAT) y diferentes frecuencias. Los terminales deben ser capaces de saltar de tecnología automáticamente y de forma transparente al usuario para poder hacer un uso más eficiente de los recursos disponibles en la red y así evitar la saturación de las tecnologías. En este contexto, hay que añadir la reciente inclusión en las redes de telefonía móvil de estaciones base de menor potencia de transmisión, también conocidas como *small cells*. Las small cells son nodos de acceso al medio cuyo rango de cobertura varía en función del dispositivo: microceldas, entorno a uno o dos kilómetros, picoceldas, alrededor de centenas de metros y femtoceldas, con un alcance de decenas de metros. Estos dispositivos coexisten con las actuales redes inalámbricas generando entornos de redes heterogéneas.

Además, el 80% del tráfico móvil se consume en interiores [10]. Por tanto, gracias a estos nuevos nodos, especialmente las *femtoceldas* [122], el tráfico gestionado por las macroceldas se puede derivar en estos dispositivos y así liberar recursos al mismo tiempo que se ofrece una mejora en la calidad del servicio al usuario final y capacidad de la red en entornos de interior. Sin embargo, el despliegue de este tipo de estaciones base pueden generar degradaciones en el rendimiento de la red o incluso en la calidad ofrecida al usuario final si la red no se gestiona correctamente, por ello, el concepto SON vuelve a jugar un papel importante para este tipo de escenarios.

Los mecanismos SON hacen uso de parámetros, indicadores, etc. de la red del operador para, en función de dichos valores, aplicar una nueva configuración de parámetros en la red que mejore el servicio final. Sin embargo, existe información muy valiosa externa a la red del operador y que pueden permitir la mejora de estos mecanismos. La información de contexto o *context-awareness*, es un concepto emergente que cada vez tiene más influencia en las diferentes disciplinas debido a la gran expansión de dispositivos electrónicos en todo el mundo y su permanente conectividad a Internet. Los datos obtenidos por las diversas fuentes proporcionan información de contexto, es decir, parámetros sobre el estado actual de personas, lugares, objetos o dispositivos en un determinado entorno que procesados de la manera adecuada pueden ofrecer grandes ventajas a los mecanismos SON.

Finalmente, para la integración de todos estos conceptos, se precisa del diseño de una arquitectura que sea capaz de gestionar y obtener toda la información necesaria desde las distintas fuentes de contexto y proporcionársela a los mecanismos SON para poder actuar con la mayor brevedad sobre los elementos de red en entornos de interior. De este modo, se obtiene una red robusta y dinámica frente a cambios bruscos, manteniendo unos valores aceptables por las políticas del operador y ofreciendo al usuario final una buena calidad de servicio.

D.1.1   Objetivos

El principal objetivo de esta tesis es el desarrollo de nuevos algoritmos de *balance de carga* en entornos de *small cells*, más concretamente en entornos de *femtoceldas*. Estos mecanismos de balance de carga permitirán rápidas y eficientes adaptaciones de los parámetros de configuración de la red de femtoceldas en entornos comerciales y corporativos ante cambios temporales y espaciales que conlleven a la congestión o sobrecarga de la femtocelda, y por tanto, la degradación de su rendimiento o la calidad del servicio al usuario final. Para ello, los métodos se apoyarán en la disponibilidad de información de contexto, adicional a la proporcionada por el operador de la red móvil.

Como posible información de contexto, cabe destacar la localización de los usuarios en interior. Por tanto, se desarrollarán técnicas de posicionamiento en interiores basadas en la tecnología RFID y soportadas por la infraestructura de la red del operador, permitiendo desplegar un sistema de bajo coste.

Para llevar a cabo la integración entre ambos tipos de sistemas, es necesaria una modificación de la actual arquitectura de gestión con el fin de poder disponer de la información de contexto en los diferentes elementos de red, además de la propia información de la red del operador. Por ello, se aborda el diseño de una arquitectura de gestión para afrontar la integración de ambos sistemas.

D.2   Estado del arte

El concepto de SON se ha aplicado a lo largo de muchos años en diversas disciplinas y ciencias. Sin embargo, su integración en las redes de telefonía móvil es un hecho reciente [2] [8] [9] e impuesto por la tecnología LTE. El beneficio de la auto-gestión de redes en tecnologías previas se ha demostrado en gran cantidad de trabajos. Algunos de estos trabajos han sido la base para la adaptación y el desarrollo de nuevos mecanismos en la tecnología LTE [12] [13] [14] [85] [86] [87] [88] [89] [90].

Una de las funcionalidades de SON es *self-optimization*, un campo donde se han llevado a cabo numerosos estudios. Más concretamente, muchos de estos estudios se centran en un caso de uso determinado: *Mobility Load Balancing* (MLB) en entornos macrocelulares o de *small cells* (nodos de baja potencia con cobertura de pocos kilómetros) e incluso femtoceldas. El objetivo de estas técnicas consiste en mover tráfico de una celda saturada a otra celda vecina con suficientes recursos. En la literatura se pueden encontrar diversos estudios y proyectos sobre técnicas de auto-optimización de balance de carga, tanto en redes de interior como de exterior y entre diferentes tecnologías [4] [5] [6] [15] [16] [17] [91] [92] [93] [94] [95].

Por otro lado, la expansión de dispositivos electrónicos ha dado lugar a un creciente interés en el concepto de *context-awareness*. Esta información de contexto, junto con los actuales indicadores de red (alarmas, contadores, KPIs, etc.), permite mejorar el rendimiento de las funciones SON. La posición del usuario es un tipo de información de contexto y una de las más utilizadas por las técnicas SON. Concretamente en entornos de interior, se numeran diversos trabajos [98] [99] [100]. En cuanto al caso de MLB, alguno de los trabajos presentados en la literatura son los siguientes [14] [18] [94].

Referente a los sistemas de posicionamiento en interiores, existen numerosos sistemas, tecnologías y precisiones. Existe una relación directa en cuanto a la precisión del sistema y los costes. Entre los sistemas de bajo coste más utilizados, se encuentran los sistemas basados en la tecnología RFID, ofreciendo errores de posicionamiento de pocos metros [52] [53] [54]. Sin embargo, el uso de varias antenas en el receptor permite mejorar la precisión de localización, al mismo tiempo que reducir el coste del sistema [55] [56]. Por otro lado, el uso adicional de otras tecnologías mejora la precisión de estos sistemas [63] [64] [69]. Dentro de este concepto, las tecnologías celulares ya desplegadas y cuya gestión es independiente del sistema de posicionamiento, permiten reducir costes a la vez que reduce el error de localización del sistema [63].

Por último, es necesario disponer de una arquitectura para poder integrar la información de contexto dentro de las redes SON. Trabajos como [39] [40] proponen la integración de este tipo de información en las capas de gestión de algunos sistemas pero no hace referencia a redes móviles.

D.3   Información de contexto y métodos SON

En entornos de interior, las condiciones de la red pueden cambiar de forma continua dependiendo de la distribución de los usuarios, los elementos del entorno, la propagación de la señal, etc., degradando las condiciones o el servicio del usuario final.

Por ello, es necesaria la aplicación de unos mecanismos que permitan de forma eficiente y rápida la adaptación de la red móvil frente a estos acontecimientos impredecibles.

Los mecanismos SON implementados en las redes de los operadores de telefonía móvil suelen utilizar parámetros de entrada provenientes de su propia red tales como contadores, alarmas, KPIs, etc. Sin embargo, la adaptación automática de aplicaciones, sistemas y dispositivos, permite acceder a información de contexto proporcionando datos muy valiosos no incluidos hasta ahora (en su totalidad) en los mecanismos SON. Por este motivo, se propone utilizar esta información adicional sobre el estado de un lugar, una persona o incluso dispositivos, como parámetros de entrada en el desarrollo de los algoritmos SON. De este modo, ayudan a incrementar el rendimiento y la capacidad de la red y mejorar la calidad de servicio.

Una de las ventajas añadida a este tipo de información frente a la información monitorizada por la propia red de telefonía móvil es, por ejemplo, el tiempo de adquisición de la información y posteriormente su entrega a los sistemas correspondientes. En este aspecto, la información de contexto suele estar disponible con un retraso muy inferior a la generada por la red del operador, permitiendo que los mecanismos SON puedan adaptar los parámetros de configuración de la red prácticamente de inmediato. En el operador, la periodicidad en la monitorización de los indicadores de red en una arquitectura OAM centralizada suele ser de horas o incluso días, dificultando una rápida adaptación de la red. Por el contrario, con la llegada de la tecnología LTE, las arquitecturas OAM son distribuidas permitiendo reducir y solventar el problema del tiempo. Sin embargo, estos datos monitorizados por la red pueden ser valiosos pero insuficientes para un funcionamiento óptimo. Otro de los beneficios, está relacionado con la capacidad de predicción. La red puede estar preparada para afrontar una situación problemática, por ejemplo, un evento social el cual degradaría el rendimiento de la red debido a la gran concentración de usuarios en la misma celda.

Esta diversidad de información puede ser adquirida desde diferentes tipos de fuentes y en diferentes intervalos de tiempo. Para ello, se ha definido un entorno con las siguientes fuentes de contexto: dispositivos personales, sistemas de localización, redes sociales, imágenes/videos, operario y otras fuentes. Dentro de la periodicidad para disponer de la información de estas fuentes, se han definido varios intervalos: una hora, treinta minutos, quince minutos, cinco minutos y menos de un minuto.

Para poder integrar dicha información en la red del operador, se ha diseñado una nueva arquitectura de gestión de la red móvil, compatible con la arquitectura OAM definida por el 3GPP. Gracias a esta arquitectura, los mecanismos SON podrán actuar

con mayor frecuencia y analizando más datos del entorno donde está desplegada la red que hasta ahora eran inaccesibles.

Para validar el entorno propuesto y la nueva arquitectura de red, se ha implementado un mecanismo de balance de carga, el cual ha analizado diferentes indicadores de la red móvil, así como la posición de los usuarios. Los resultados obtenidos han demostrado que utilizar información complementaria a la proporcionada por la red del operador es muy importante para ajustar los parámetros de configuración frente a situaciones dinámicas. Además, la ejecución de estos mecanismos en periodos de tiempo más cortos, permite a la red actualizar parámetros, para evitar congestiones de tráfico en una determinada celda.

Como conclusión, este capítulo ha presentado un marco que integra la información de contexto dentro de los mecanismos SON en las redes de telefonía móvil. La ejecución de mecanismos SON en tiempo real permite ofrecer grandes mejoras a la red del operador, tanto desde el punto de vista de su rendimiento como de la satisfacción del usuario final.

D.4   Técnicas de posicionamiento en interiores

Existe gran diversidad de sistemas de posicionamiento en interiores. Entre los más habituales, son aquellos que analizan el nivel de señal recibida, sobre todo para entornos con múltiples reflexiones como los pasillos. Centrándose en este tipo de escenarios, se ha propuesto un sistema RFID con etiquetas activas (transmisores) para el diseño de un sistema de posicionamiento en interiores.

Inicialmente, se ha estudiado un sistema donde se proponen diferentes técnicas para estimar la posición del usuario. Posteriormente, se ha analizado el uso de dos antenas en el receptor para ver los beneficios de adquirir el doble de información a un coste mínimo. Para ello, se han propuesto diferentes métodos y fases para la integración de esta información en el sistema anteriormente descrito. Finalmente, se ha utilizado la información de las redes de telefonía móvil como una fuente de bajo coste para mejorar el rendimiento del sistema. Este tipo de infraestructuras están ya implementadas y su mantenimiento es parte del operador móvil.

La evaluación de los sistemas propuestos se ha llevado a cabo en un pasillo y los resultados muestran mejoras frente al estado del arte. Por un lado, se ha seleccionado la técnica que ofrece un menor error de posicionamiento. Por otro lado, se han analizado los diferentes métodos de integración de datos provenientes de dos antenas, mostrando una reducción del error de posicionamiento del 20%. Además, se ha

comprobado el rendimiento del sistema cuando sólo se utiliza una antena y cuando se usan dos antenas y la mitad de etiquetas, observándose resultados prometedores. No se ha conseguido el mismo error de posicionamiento pero de media, se consiguen resultados similares, permitiendo reducir el número de etiquetas del sistema y por tanto, los costes del sistema. Por último, se ha diseñado el mismo sistema con información proveniente de dos redes celulares, GSM y UMTS. El rendimiento del sistema en cuanto a los errores de localización son muy grandes, como es de esperar. Sin embargo, la integración de esta información en el sistema RFID anteriormente propuesto, permite una discriminación significativa de los candidatos propuestos por ese sistema. Se han analizado dos tecnologías, GSM y UMTS, siendo la segunda la que proporciona información más relevante.

Como conclusión, se ha propuesto un sistema de posicionamiento en interiores que permite obtener un error medio de posicionamiento menor a un metro. Diversas técnicas se han analizado, observándose un rendimiento similar cuando la relación número de antenas y etiquetas es proporcional. Además, el uso de infraestructuras ya desplegadas como las redes de telefonía móvil o redes de área local inalámbrica, introducen una mejora en el sistema a un bajo coste. Este tipo de fuente de información, podría ser utilizada por los mecanismos SON para mejorar el rendimiento de las redes de telefonía móvil.

D.5   Técnicas de balance de carga en interiores

En este capítulo se presenta el diseño de diversos mecanismos de balance de carga para resolver problemas de congestión temporal y espacial en redes de femtoceldas para entornos comerciales y corporativos.

Inicialmente, se describen algunos algoritmos de balance de carga que analizan información de la red del operador, como las llamadas bloqueadas, la carga de la red o la tasa de usuarios. A continuación, se han desarrollado nuevos mecanismos, que además de analizar los indicadores de la red del operador, disponen de información externa a dicha red. Concretamente, se ha analizado la posición de los usuarios. Todos estos sistemas, modifican la potencia de transmisión de las femtoceldas, para balancear usuarios de celdas sobrecargadas a celdas menos cargadas. Por un lado, se ha diseñado un mecanismo que estudia la distribución de los usuarios en las celdas congestionadas para, en base a los niveles de PRX de cada usuario, adapten la potencia de transmisión de las femtoceldas. Por otro lado, se ha desarrollado otro método que evalúa el PRX de cada usuario y, en base a valores históricos en la posición de los usuarios, se proponen adaptaciones en la potencia de transmisión de las femtoceldas para

descongestionar la femtocelda sobrecargada. Por último, se han analizado las consecuencias cuando la información de la posición de los usuarios suministrada no es exacta, siendo algo habitual para la mayoría de los sistemas de posicionamiento comerciales en interiores.

Adicionalmente, la modificación de parámetros de configuración de la red puede ocasionar conflictos con otros mecanismos SON que adapten los mismos parámetros para fines diferentes. En este sentido, se ha estudiado un caso particular de coordinación entre algoritmos MLB y el caso de uso de *energy-savings*, ahorro de energía.

La evaluación de todos estos mecanismos de balance de carga se ha llevado a cabo en un escenario realista y mediante un simulador LTE a nivel de sistema. Por un lado se ha observado la ventaja de utilizar la tasa de usuarios en redes de femtoceldas, donde existe un gran ancho de banda para un número de usuarios muy reducido (actualmente hasta 64 usuarios). Por otro lado, el uso de la posición de los usuarios en los métodos SON permite ofrecer un ajuste de parámetros más preciso para afrontar problemas temporales y espaciales de congestión de las femtoceldas. Además, según muestran los resultados, el uso de valores medios de la potencia recibida en cada punto permite una estabilidad mayor del sistema frente al análisis de valores de PRX instantáneos.

También se ha observado que, el impacto de los errores de posicionamiento afecta negativamente a los mecanismos de MLB. Sin embargo, hasta un determinado error de posicionamiento, estos mecanismos incrementan la satisfacción del usuario frente a otros mecanismos del estado del arte. Por último, se han realizado dos experimentos en un entorno de oficinas real, donde se han desplegado cuatro femtoceldas y varios terminales. Corroborando a pequeña escala los resultados obtenidos en las pruebas con el simulador.

Como conclusión, se han diseñado diversos mecanismos de balance de carga para resolver problemas de femtoceldas congestionadas en entornos comerciales y corporativos. Resaltando que, es importante el análisis de la tasa de usuarios conectados a las femtoceldas y de los indicadores externos a la red del operador, para ofrecer un mejor rendimiento de los sistemas SON.

D.6   Conclusiones

Las principales aportaciones de esta tesis son las siguientes:

- La descripción de un marco para la integración de información de contexto en los algoritmos de auto-gestión de red (SON). Para ello, se ha diseñado una nueva arquitectura de gestión de red compatible con la arquitectura OAM definida por el 3GPP. Gracias a esta aportación, los mecanismos SON pueden analizar información externa a la red del operador a cerca del estado del entorno, patrones de los usuarios, etc. Además, se consigue reducir la periodicidad de ejecución de estos mecanismos, permitiendo una adaptación de los parámetros de la red con mayor frecuencia para evitar problemas temporales y espaciales que degraden el servicio del operador.

- El desarrollo de un sistema de posicionamiento en interiores basado en la tecnología RFID y múltiples antenas. Concretamente para entornos de interior como pasillos, donde las técnicas de *fingerprinting* son las más adecuadas. Diversos métodos y técnicas se han analizado para mejorar los resultados propuestos en el estado del arte en este tipo de escenarios. Además, se ha analizado la integración de la tecnología celular como fuente de bajo coste al ser una infraestructura ya desplegada, para el sistema de posicionamiento anteriormente propuesto, permitiendo mejorar su precisión y disminuir el error de posicionamiento.

- El diseño de algoritmos de balance de carga en entornos comerciales y corporativos con despliegues de redes de femtoceldas. Estos mecanismos se basan en las características especiales de las femtoceldas, mejorando el rendimiento de los mecanismos de balance de carga clásicos. Además, se ha incluido la información de contexto como información adicional a la proporcionada por la red del operador, proporcionando un mayor conocimiento a los algoritmos SON sobre el estado del escenario, la movilidad de los usuarios, etc. Gracias a estos nuevos mecanismos, se ha mejorado el rendimiento de las redes de femtoceldas, así como diferentes indicadores de rendimiento a nivel de usuario.

Las líneas futuras de investigación que se proponen son las siguientes:

- En esta tesis se ha analizado la posición de los usuarios como información de contexto para los algoritmos de SON. Sin embargo, gracias a la gran expansión de dispositivos inteligentes como los smartphones, la disponibilidad de otro tipo de información de contexto como información sobre eventos sociales, patrones de movilidad, información sobre el parte meteorológico, etc., es un hecho inminente. El desarrollo de nuevas técnicas basadas en esta información permitirán mejorar el rendimiento de las redes de telefonía móvil.

- En esta tesis se ha propuesto un sistema de posicionamiento en interiores basado en la tecnología RFID. Sin embargo, la precisión de éste, y otros sistemas del estado del arte tienen mucho margen de mejora. Diversos servicios basados en localización (LBS) requieren de una precisión mayor y un error de localización del orden de centímetros, manteniendo unos costes de implementación bajos. Además, el uso de otras tecnologías celulares como LTE, pueden mejorar las prestaciones de dichos sistemas sin incrementar su coste.

- En esta tesis se han evaluado los sistemas desarrollados tanto en entornos simulados como en escenarios reales. Sin embargo, los resultados obtenidos en los entornos reales estaban restringidos a un escenario particular y a un equipamiento específico. Por un lado, el método de posicionamiento en interiores se ha validado en un pasillo. Sería interesante implementar el mismo sistema en otro tipo de pasillos y espacios para generalizar sus prestaciones. Por otro lado, los métodos de balance de carga se han validado en un entorno de oficinas con una tasa de usuarios muy baja. Su implementación en escenarios más amplios y con mayor tasa de usuarios permitirá analizar mejor sus prestaciones.

D.7 Lista de publicaciones

A lo largo de esta tesis se han generado los siguientes resultados de investigación.

Artículos de revista:

[I] A. Aguilar-Garcia, R. Barco, S. Fortes, P. Muñoz, "Load balancing mechanisms for indoor temporarily overloaded heterogeneous femtocell networks," *EURASIP Journal on Wireless Communications*, 2015:29. 2015.

[II] A. Aguilar-Garcia, S. Fortes, E. Colin, R. Barco, "Enhancing RFID Indoor Localization with Cellular Technologies," *EURASIP Journal on Wireless Communications and Networking*, 2015:219. 2015.

[III] A. Aguilar-Garcia, S. Fortes, M. Molina-Garcia, J. Calle-Sanchez, J.I. Alonso, A. Garrido, A. Fernandez-Duran, R. Barco, "Location-aware Self-Organizing Methods in Femtocell Networks," *Computer Networks*, vol. 93, part 1, pp. 125-140, 24 December 2015.

[IV] A. Aguilar-Garcia, S. Fortes, R. Barco, A. Fernández-Duran, "Context-Aware Self-Optimization: Evolution Based on the Use Case of Load Balancing in Small-Cell Networks," in *IEEE Vehicular Technology Magazine*, vol. 11, no. 1, pp. 86-95, March 2016.

[V]   A. Aguilar-Garcia, R. Barco, S. Fortes, "Coordinated Location-based Self-Optimization for Indoor Femtocell Networks," *Computer Networks*, In press, June 2016.

[VI]   A. Aguilar-Garcia, S. Fortes, A. Garrido, A. Fernandez-Duran, R. Barco, "Improving Load Balancing Techniques by Location-awareness at Indoor Femtocell Networks," *EURASIP Journal on Wireless Communications*, Under review (major changes), 2016.

Conferencias internacionales:

[VII]   A. Aguilar-Garcia, R. Barco, S. Fortes, P. Muñoz, "Analysis of overload indicators for traffic balance in indoor femtocell networks," *13th COST IC1004 MC and Scientific Meeting,* 5-7 May 2015 – Valencia, Spain.

[VIII] A. Aguilar-Garcia, S. Fortes, E. Colin, R. Barco, "Enhancing Localization Accuracy with Multi-Antenna UHF RFID Fingerprinting," *IPIN 2015, Sixth International Conference on Indoor Positioning and Indoor Navigation.* 13-16 October 2015 – Banff, Alberta, Canada.

Conferencias nacionales:

[IX]   A. Aguilar-Garcia, S. Fortes, R. Barco, "Información de contexto en la auto-gestión de redes small cells," *XXIX Simposium Nacional de la Unión Científica Internacional de Radio URSI 2014*, 3-5 September 2014 – Valencia, Spain.

[X]   A. Aguilar-Garcia, S. Fortes, R. Barco, "Location-based self-organizing mechanisms for femtocell networks," *Workshop in indoor localization with small cells. MONOLOC project conclusions*, 28 November 2014 – Madrid, Spain.

[XI]   A. Aguilar-Garcia, S. Fortes, R. Barco, "Análisis de indicadores para el balance de carga en redes de femtoceldas*," XXX Simposium Nacional de la Unión Científica Internacional de Radio URSI 2015*, 2-4 September 2015 – Pamplona, Spain.

Otras publicaciones relacionadas con la tesis:

[XII]   P. Muñoz, R. Barco, J. M. Ruiz-Avilés, I. de la Bandera, A. Aguilar-Garcia, "Fuzzy Rule-Based Reinforcement Learning for Load Balancing Techniques in Enterprise LTE Femtocells," *IEEE Transactions on Vehicular Technology,* vol. 62, no. 5, pp. 1962-1973, June 2013.

[XIII]   S. Fortes, A. Aguilar-Garcia, R. Barco, F. Barba, J. Fernández-Luque, A. Fernández-Durán, "Management architecture for location-aware self-organizing LTE/LTE-A small cell networks," *IEEE Communications Magazine*, vol.53, no.1, pp.294-302, January 2015.

[XIV]   S. Fortes, R. Barco, A. Aguilar-Garcia, P. Muñoz, "Contextualized indicators for online failure diagnosis in cellular networks," *Computer Networks*, vol. 82, pp. 96-113, May 2015.

[XV]   S. Fortes, A. Aguilar-Garcia, R. Barco, A. Garrido-Martín, J.A. Fernández-Luque, "Context-Aware Self-Healing: User Equipment as the Main Source of Information for Small-Cell Indoor Networks," *IEEE Vehicular Technology Magazine*, vol. 11, no. 1, pp. 76-85, March 2016.

[XVI]   S. Fortes, R. Barco, A. Aguilar-Garcia, "Location-based Distributed Sleeping Cell Detection and Root Cause Analysis for 5G Ultradense Networks," *EURASIP Journal on Wireless Communications*, In press, 2016.

[XVII]   S. Fortes, R. Barco, A. Aguilar-Garcia, "Integration of Indoor Positioning into Self-Organizing Small Cell Systems," *12th COST IC1004 MC and Scientific Meeting*, 28-30 January 2015 – Dublin, Ireland.

[XVIII]   S. Fortes, R. Barco, A. Aguilar-Garcia, "Location-Based Distributed Failure Management for 5G Ultra-Dense Small Cell Networks," *Workshop on Evolution of Radio Access Network Technologies towards 5G*. 5 May 2015 – Valencia, Spain.

[XIX]   S. Fortes, R. Barco, A. Aguilar-Garcia, P. Muñoz, "Integration of Mobile Context in the Diagnosis of Small Cell Networks," *Joint NEWCOM/COST Workshop on Wireless Communications JNCW 2015*, 13-15 October 2015 – Barcelona, Spain.

[XX]   S. Fortes, A. Aguilar-Garcia, R. Barco, F. Barba, J.A. Fernández-Luque, A. Fernández Durán, "Diseño Integrado de Redes Auto-Organizadas LTE/LTE-A y Posicionamiento en Interiores," *XXVIII Simposium Nacional de la Unión Científica Internacional de Radio URSI 2013*, 11-13 September 2013 – Santiago de Compostela, Spain.

[XXI]   S. Fortes, A. Aguilar-Garcia, R. Barco, "Detección de Celda Durmiente en Entornos Localizados de Femtoceldas," *XXIX Simposium Nacional de la Unión Científica Internacional de Radio URSI 2014*, 3-5 September 2014 – Valencia, Spain.

[XXII] S. Fortes, A. Aguilar-Garcia, R. Barco, "Identificación de Fallos Radio en Entornos Celulares Localizados de Interior," *XXX Simposium Nacional de la Unión Científica Internacional de Radio URSI 2015*, 2-4 September 2015 – Pamplona, Spain.

El Capítulo 3 describe el trabajo publicado en [IV][IX][XIII][XVII][XX] sobre una arquitectura de gestión basada en la información de contexto para redes SON en interiores. El Capítulo 4 propone un sistema de posicionamiento para interiores basado en la tecnología RFID y las redes móviles, descrito en [II][VIII]. Finalmente, el Capítulo 5 detalla los algoritmos de balance de carga en redes de femtoceldas, publicados en [I][III][V][VI][VII][X][XI].

Todas estas contribuciones han surgido en el marco de diversos proyectos de investigación. En particular, las anteriores publicaciones fueron desarrolladas en el marco de estos proyectos:

- El proyecto MONOLOC, financiado por el Ministerio de Economía y Competitividad, dentro del Plan Nacional de Investigación Científica, Desarrollo e Innovación Tecnológica 2008-2011 expediente IPT-2011-1272-430000 y por el Fondo Europeo de Desarrollo Regional (FEDER).

- Consejería de Innovación, Ciencia y Empresa de la Junta de Andalucía (Proyecto de Investigación de Excelencia P08-TIC-4052).

- Consejería de Innovación, Ciencia y Empresa de la Junta de Andalucía (Proyecto de Investigación de Excelencia P12-TIC-2905).

Bibliography

[1] Cisco Visual Networking Index, "Global Mobile Data Traffic Forecast Update, 2015–2020 White Paper," 2016.

[2] 3GPP TS 32.500, "Telecommunication Management; Self-Organizing Networks (SON); Concepts and requirements".

[3] NGMN, "Next Generation Mobile Networks Recommendation on SON and O&M requirements," December 2008.

[4] A. Lobinger, S. Stefanski, T. Jansen, I. Balan, "Load balancing in downlink LTE self-optimizing networks," *Vehicular Technology Conference (VTC 2010-Spring), 2010 IEEE 71st ,* pp. 1-5, 16-19 May 2010.

[5] P. Szilagyi, Z. Vincze, C. Vulkan, "Integrated Mobility Load Balancing and Traffic Steering mechanism in LTE," *International Symposium on Personal Indoor and Mobile Radio Communications (PIMRC), 2013 IEEE 24th ,* pp. 2148-2153, 8-11 September 2013.

[6] R. Kwan, R. Arnott, R. Paterson, R. Trivisonno, M. Kubota, "On mobility load balancing for LTE systems," *Vehicular Technology Conference Fall (VTC 2010-Fall), 2010 IEEE 72nd ,* pp. 1-5, 6–9 September 2010.

[7] SOCRATES-Self-Optimisation and self-ConfiguRATion in wirelEss networkS, *Available: http://www.fp7-socrates.org/.*

[8] S. Hämäläinen, H. Sanneck, C. Sartori, "LTE Self-Organising Networks (SON): Network Management Automation for Operational Efficiency," *John Wiley & Sons,* 2011.

[9] J. Ramiro, K. Hamied, "Self-Organizing Networks (SON): Self-Planning, Self-Optimization and Self-Healing for GSM, UMTS and LTE," *Wiley,* 2011.

[10] Nokia, "Indoor Deployment Strategies, White Paper," 2014.

[11] J.G. Andrews, H. Claussen, M. Dohler, S. Rangan, M.C. Reed, "Femtocells: Past, Present, and Future," *IEEE Journal on Selected Areas in Communications,* vol. 30, pp. 497-508, April 2012.

[12] H. Claussen, L.T. Ho, L.G. Samuel, "Self-optimization of coverage for femtocell deployments," *IEEE Wireless Telecommunications Symposium, 2008,* pp. 278-285, 2008.

[13] D. Lopez-Perez, A. Valcarce, G. de la Roche, J. Zhang, "OFDMA femtocells: a roadmap on interference avoidance," *IEEE Communications Magazine,* vol. 47, no. 9, pp. 41-48, 2009.

[14] Z. Becvar, P. Mach, "Adaptive hysteresis margin for handover in femtocell networks," *6th International Conference on Wireless and Mobile Communications (ICWMC),* pp. 256-261, 2010.

[15] J. M. Ruiz-Avilés, S. Luna-Ramírez, M. Toril, F. Ruiz, I. de la Bandera-Cascales, P. Munoz-Luengo, "Analysis of load sharing techniques in enterprise LTE femtocells," *Wireless Advanced (WiAd),* pp. 195-200, June 2011.

[16] J. M. Ruiz-Avilés, S. Luna-Ramírez, M. Toril, F. Ruiz, "Traffic steering by self-tuning controllers in enterprise LTE femtocells," *EURASIP Journal on Wireless Communications and Networking,* vol. 2012, no. 337, November 2012.

[17] P. Munoz, R. Barco, J. Ruiz-Aviles, I. de la Bandera Cascales, A. Aguilar Garcia, "Fuzzy Rule-based Reinforcement Learning for Load Balancing Techniques in Enterprise LTE Femtocells," *IEEE Transactions on Vehicular Technology,* vol. 62, no. 5, pp. 1962-1973, June 2013.

[18] J. Steuer, K. Jobmann, "The use of mobile positioning supported traffic density measurements to assist load balancing methods based on adaptive cell sizing," *In Proceedings of IEEE International Symposium on Personal, Indoor and Mobile Radio Communications (PIMRC),* pp. 339-343, 15-18 September 2002.

[19] H. Sanneck, Y. Bouwen, E. Troch, "Context based configuration management of plug & play LTE base stations," *2010 IEEE Network Operations and Management Symposium,* pp. 946-949, 19-23 April 2010.

[20] A. Awada, B. Wegmann, I. Viering, A. Klein, "A Location-based Self-Optimizing Algorithm for the Inter-RAT Handover Parameters," *IEEE International Conference on Communications (ICC), Budapest, Hungary,* June 2013.

[21] M. Nahas, M. Mjalled, Z. Zohbi, Z. Merhi, M. Ghantous, "Enhancing LTE - WiFi interoperability using context aware criteria for handover decision," *2013 25th International Conference on Microelectronics (ICM) ,* pp. 1-4, 15-18 December 2013.

[22] MONOLOC - Indoor Positioning and Mobile Network Management, *Available: http://monoloc.grupoinnovati.com/eng/index.html.*

[23] F. Khan, "LTE for 4G Mobile Broadband: Air Interface Technologies and Performance," *Cambridge University Press,* March 2009.

[24] 3GPP TS 36.300, "Evolved Universal Terrestrial Radio Access (E-UTRA) and Evolved Universal Terrestrial Radio Access Network (E-UTRAN); Overall description; Stage 2".

[25] 3GPP TS 23.401, "Technical Specification Group Services and System Aspects; General Packet Radio Service (GPRS) enhancements for Evolved Universal; Terrestrial Radio Access Network (E-UTRAN)".

[26] 3GPP TS 32.101, "Telecommunication management; Universal Mobile Telecommunications System (UMTS); LTE; Telecommunication management; Principles and high level requirements".

[27] 3GPP TS 36.211, "Evolved Universal Terrestrial Radio Access (E-UTRA); Physical Channels and Modulation".

[28] 3GPP TS 36.101, "Evolved Universal Terrestrial Radio Access (E-UTRA); User Equipment (UE) radio transmission and reception".

[29] S. Sesia, I. Toufik, M. Baker , "LTE - The UMTS Long Term Evolution: From Theory to Practice," *Wiley,* February 2009.

[30] 4G Americas, "The benefits of SON in LTE: Self-optimizing and self-organizing networks," December 2009.

[31] Alcatel Lucent, "9361 Home Cell v2 Datasheet," *Available: http://www3.alcatel-lucent.com/wps/DocumentStreamerServlet?LMSG_CABINET=Docs_and_Resource_Ctr&LMSG_CONTENT_FILE=Data_Sheets/Home_Cell_V2_2100_MHz_EN_DataSheet.pdf.*

[32] Alcatel Lucent, "9362 Enterprise Cell v2.2 Datasheet," *Available: http://www3.alcatel-lucent.com/wps/DocumentStreamerServlet?LMSG_CABINET=Docs_and_Resource_Ctr&LMSG_CONTENT_FILE=Data_Sheets/9362_Enterprise_Cell_EN_Datasheet.pdf.*

[33] 3GPP TS 36.321, "Evolved Universal Terrestrial Radio Access (E-UTRA); Medium Access Control (MAC) protocol specification".

[34] Fujitsu, "LS100 Series Residential Femtocell Datasheet," *Available: http://www.fujitsu.com/ca/en/Images/FemtoCellLS100.pdf.*

[35] A. K. Dey, G.D. Abowd, "Towards a better understanding of context and context-awareness.," *Proceedings of the 1st International Symposium on Handheld and Ubiquitous Computing, Karlsruhe, Germany,* vol. 1707, pp. 304-307, 1999.

[36] C. Feng, W.S.A. Au, S. Valaee, Z. Tan, "Received-Signal-Strength-Based Indoor Positioning Using Compressive Sensing," *IEEE Transactions on Mobile Computing,* vol. 11, no. 12, pp. 1983-1993, December 2012.

[37] M. Molina-García, J. Calle-Sánchez, J.I. Alonso, A. Fernández-Durán, F. B. Barba, "Enhanced in-building fingerprint positioning using femtocell networks," *Bell Labs Technical Journal,* vol. 18, no. 2, pp. 195-211, September 2013.

[38] K. Subbu, Jun Luo Chi Zhang, A. Vasilakos, "Analysis and status quo of smartphone-based indoor localization systems," *IEEE Wireless Communications,* vol. 21, no. 4, pp. 106-112, August 2014.

[39] A. El-Mougy, H. Mouftah, "On resource management and context-awareness in LTE-based networks for Public Safety," *Local Computer Networks Workshops (LCN Workshops), 2013 IEEE 38th Conference on ,* pp. 972-979, 21-24 October 2013.

[40] C. Baladron, J.M. Aguiar, B. Carro, L. Calavia, A. Cadenas, A. Sanchez-Esguevillas, "Framework for intelligent service adaptation to user's context in next generation networks," *IEEE Communications Magazine,* vol. 50, no. 3, pp. 18-26, March 2012.

[41] A. Khanafer, W. Saad, T. Başar, "Self-organizing context-aware small cell networks: challenges and future opportunities," *Mechanisms and Games for Dynamic Spectrum Allocation,* pp. 373-395, 2013.

[42] BeFEMTO Project, "Deliverable D2.2 "The BeFEMTO system architecture," *Available http://www.ict-befemto.eu/publications/deliverables.html,* 2012.

[43] 3GPP TS 32.593, "Telecommunication management; Home enhanced Node B (HeNB) Operations, Administration, Maintenance and Provisioning (OAM&P); Procedure flows for Type 1 interface HeNB to HeNB Management System (HeMS)".

[44] 3GPP TR 23.829, "Local IP Access and Selected IP Traffic Offload (LIPA-SIPTO)".

[45] 3GPP TR 36.902, "Evolved Universal Terrestrial Radio Access Network (E-UTRAN); Self-Configuring and Self-Optimizing Network (SON) Use Cases and Solutions".

[46] C.C. Lee, "Fuzzy logic in control systems: fuzzy logic controller," *IEEE Transactions on Systems, Man and Cybernetics,* vol. 20, no. 2, pp. 404-435, April 1990.

[47] J. M. Ruiz-Avilés, S. Luna-Ramírez, M. Toril, F. Ruiz, I. de la Bandera, P. Muñoz, R. Barco, P. Lázaro, V. Buenestado, "Design of a Computationally Efficient Dynamic System-Level Simulator for Enterprise LTE Femtocell Scenarios," *Journal of Electrical and Computer Engineering,* vol. 2012, 2012.

[48] Dr. Rainer Mautz, "Indoor Positioning Technologies," *PhD. Thesis, Venia Legendi in Positioning and Engineering Geodesy Institute of Geodesy and Photogrammetry, Department of Civil, Environmental and Geomatic*

Engineering, ETH Zurich, February 2012.

[49] K. Wu, J. Xiao, Y. Yi, M. Gao, "FILA: Fine-grained indoor localization," *IEEE INFOCOM, 2012 Proceedings,* pp. 2210-2218, 25-30 March 2012.

[50] K. Wu, J. Xiao, Y. Yi, D. Chen, X. Luo, L. M. Ni, "CSI-Based Indoor Localization," *IEEE Transactions on Parallel and Distributed Systems,* pp. 1300-1309, 2012.

[51] Y. Chen, N. Crespi, L. Lv, M. Li, A.M. Ortiz, L. Shu, "Locating using prior information: wireless indoor localization algorithm," *ACM SIGCOMM Computer Communication Review,* vol. 43, no. 4, pp. 463-464, August 2013.

[52] K. Chawla, G. Robins, L. Zhang, "Object localization using RFID," *5th IEEE International Symposium on Wireless Pervasive Computing (ISWPC), 2010,* pp. 301-306, May 2010.

[53] S.L. Ting, S.K. Kwok, A.H. Tsang, G.T. Ho, "The study on using passive RFID tags for indoor positioning," *International Journal of Engineering Business Management,* pp. 9-15, 2010.

[54] Z. Han, W. Hengtao, X. Lihua, J. Qing-Shan, "An RFID indoor positioning system by using weighted path loss and extreme learning machine," *IEEE 1st International Conference on Cyber-Physical Systems, Networks, and Applications (CPSNA), 2013 ,* pp. 66-71, 19-20 August 2013.

[55] M. Scherhäufl, M. Pichler, A. Stelzer, "UHF RFID Localization Based on Phase Evaluation of Passive Tag Arrays," *IEEE Transactions on Instrumentation and Measurement,* vol. 64, no. 4, pp. 913-922, April 2015.

[56] Songmin Jia, Jinbuo Sheng, Kunikatsu Takase, "Improvement of performance of localization ID tag using multi-antenna RFID system," *SICE Annual Conference, 2008,* pp. 1715-1718, 20-22 August 2008.

[57] S. Hamdoun, A. Rachedi, A. Benslimane, "Comparative analysis of RSSI-based indoor localization when using multiple antennas in Wireless Sensor Networks," *International Conference on Selected Topics in Mobile and Wireless Networking (MoWNeT), 2013,* pp. 146-151, 19-21 August 2013.

[58] S. Hara, D. Anzai, "Comparison of Three Estimation Methods for RSSI-Based Localization with Multiple Transmit Antennas," *IEEE International Conference on Mobile Adhoc and Sensor Systems, 2007. MASS 2007,* pp. 1-3, 8-11 October 2007.

[59] K. Kleisouris, Y. Chen, J. Yang, R. P. Martin, "Empirical Evaluation of Wireless Localization when Using Multiple Antennas," *IEEE Transactions on Parallel and Distributed Systems,* vol. 21, no. 11, pp. 1595-1610, November 2010.

[60] A. Rodriguez-Carrion, C. Campo, C. Garcia-Rubio, E. Garcia-Lozano, A.

Cortés-Martín, "Characterizing Mobile Telephony Signals in Indoor Environments for Their Use in Fingerprinting-Based User Location," *International Conference on Ubiquitous Computing and Ambient Intelligence,* pp. 223-230, December 2013.

[61] F.B. Barba, A.G. Martin, A.Fernández-Durán, "Wireless Indoor Positioning: Effective Deployment of Cells and Auto-Calibration," *Bell Labs Technical Journal,* vol. 18, no. 2, pp. 213-235, 2013.

[62] D. Karali, "Integration of RFID and cellular technologies.," *Wireless Internet for The Mobile Enterprise Consortium (Winmec), UCLA Anderson School of Management, Technical Report/White Paper UCLA-WINMEC-2004-205-RFID-M2M,* 2004.

[63] A.M. Vegni, F. Esposito, "Location aware mobility assisted services for heterogeneous wireless technologies," *IEEE MTT-S International Microwave Workshop on Wireless Sensing, Local Positioning, and RFID. IMWS 2009,* pp. 1-4, 24-25 September 2009.

[64] S. Sand, C. Mensing, Y. Ma, R. Tafazolli, X. Yin, J. Figueiras, J. Nielsen, B. H. Fleury, "Hybrid Data Fusion and Cooperative Schemes for Wireless Positioning," *VTC 2008-Fall. IEEE 68th Vehicular Technology Conference, 2008.,* pp. 1-5, 21-24 September 2008.

[65] S. H. Fang, T. N. Lin, "Cooperative multi-radio localization in heterogeneous wireless networks," *IEEE Transactions on Wireless Communications,* vol. 9, no. 5, pp. 1547-1551, May 2010.

[66] A. Papapostolou, H. Chaouchi, "Simulation-Based Analysis for a Heterogeneous Indoor Localization Scheme," *7th IEEE Consumer Communications and Networking Conference (CCNC), 2010,* pp. 1-5, 9-12 January 2010.

[67] Xingchuan Liu, Qingshan Man, Henghui Lu, Xiaokang Lin, "Wi-Fi/MARG/GPS integrated system for seamless mobile positioning," *IEEE Wireless Communications and Networking Conference (WCNC), 2013,* pp. 2323-2328, 7-10 April 2013.

[68] Sen Zhang, Wendong Xiao, Baoqiang Zhang, Boon Hee Soong, "Wireless indoor localization for heterogeneous mobile devices," *International Conference on Computational Problem-Solving (ICCP), 2012,* pp. 96-100, 19-21 October 2012.

[69] B. Denis, R. Raulefs, B. H. Fleury, B. Uguen, N. Amiot, L. de Celis, J. Dominguez, M. B. Koldsgaard, M. Laaraiedh, H. Noureddine, E. Staudinger, G. Steinboeck, "Cooperative and heterogeneous indoor localization experiments," *IEEE International Conference on Communications Workshops (ICC), 2013,* pp. 6-10, 9-13 June 2013.

[70] A. Z. Broder, "Some applications of Rabin's fingerprinting method," *In*

Sequences II: Methods in Communications, Security, and Computer Science. Springer-Verlag, pp. 143--152, 1993.

[71] Klaus Finkenzeller, "RFID Handbook: Fundamentals and Applications in Contactless Smart Cards, Radio Frequency Identification and Near-Field Communication, 3rd Edition," *Wiley,* pp. 47-48, June 2010.

[72] I. Kharrat, Y. Duroc, G. Andia Vera, M. Awad, S. Tedjini, T. Aguili, "Customized RSSI Method for Passive UHF RFID Localization System," *Journal of Telecommunications,* vol. 10, no. 2, September 2011.

[73] A. Moretto, E. Colin, C. Ripoll, S. Abou-Chakra, "Shunt Behavior in RFID UHF Tag According to ISO Standards and Manufacturer Requirements," *Proceedings of the IEEE, Special Issue: RFID - A Unique Radio Innovation for the 21st Century,* September 2010.

[74] H. Liu, H. Darabi, P. Banerjee, J. Liu, "Survey of wireless indoor positioning techniques and systems," *IEEE Transactions on Systems, Man, and Cybernetics, Part C: Applications and Reviews,* vol. 36, no. 6, pp. 1067-1080, 2007.

[75] C.D. Manning, P. Raghavan, M. Schütze, "Introduction to Information Retrieval," *Cambridge University Press,* p. 260, 2008.

[76] L. M. Ni, Yunhao Liu, Yiu Cho Lau, A. P. Patil, "LANDMARC: indoor location sensing using active RFID," *Proceedings of the First IEEE International Conference on Pervasive Computing and Communications, 2003. (PerCom 2003).,* pp. 407-415, 26 March 2003.

[77] Ela Innovation SA, "Ela Innovation active RFID tag and reader manufacturer," *Available: http://www.rfid-ela.eu,* 2014.

[78] G-MoN Application, *Available: https://www.wardriving-forum.de/wiki/G-MoNgmon.*

[79] 3GPP TS 36.331, "Evolved Universal Terrestrial Radio Access (E-UTRA); Radio Resource Control (RRC); Protocol specification".

[80] J. B. Eom, S. B. Yim, T. J. Lee, "An Efficient Reader Anticollision Algorithm in Dense RFID Networks With Mobile RFID Readers," *IEEE Transactions on Industrial Electronics,* vol. 56, no. 7, pp. 2326-2336, July 2009.

[81] J. Maneesilp, Wang Chong, "RFID Support for Accurate 3D Localization," *IEEE Transactions on Computing,* vol. 62, no. 7, pp. 1447-1459, July 2013.

[82] S. Chatrati, S. Naidu, C.R. Prasad, "RFID based student monitoring and attendance tracking system," *Fourth International Conference on Computing, Communications and Networking Technologies (ICCCNT),2013,* pp. 1-5, July 2013.

[83] V. Oruganti, V. Gharat, E. Colin, A. Moretto, "Location Performance Law According to the Dimensions of the Corridor Using Tri/Multilateration," *IEEE GRSS Proceedings Fifth International Conference on Indoor Positioning and Indoor Navigation,* October 2014.

[84] 3GPP TS 23.271, "Technical Specification Group Services and System Aspects; Functional stage 2 description of Location Services (LCS)".

[85] D. Lopez-Perez, X. Chu, A. Vasilakos, H. Claussen, "Minimising cell transmit power: towards self-organized resource allocation in OFDMA femtocells," *Special Interest Group on Data Communications (SIGCOMM),* pp. 410-411, August 2011.

[86] D. Xenakis, N. Passas, L. Merakos, C. Verikoukis, "Mobility management for femtocells in LTE-advanced: key aspects and survey of handover decision algorithms," *IEEE Communications Surveys & Tutorials,* vol. 16, no. 1, pp. 64-91, 2014.

[87] H. Claussen, F. Pivit, «Femtocell coverage optimization using switched,» *IEEE International Conference on Communications,* pp. 1-6, June 2009.

[88] H. Zhang, X. Wen, B. Wang, W. Zheng, Y. Sun, «A novel handover mechanism between femtocell and macrocell for LTE based networks,» *Second International Conference on Communication Software and Networks,* pp. 228-231, 2010.

[89] BeFemto. Broadband Evolved FEMTO Networks, *Available: http://www.ict-befemto.eu/.*

[90] SEMAFOUR. Self-Management of Unified Heterogeneous Radio Access Networks, *Available: http://www.fp7-semafour.eu/.*

[91] P. Muñoz, R. Barco, I. de la Bandera, "On the Potential of Handover Parameter Optimization," *IEEE Transactions on Vehicular Technology,* vol. 62, no. 5, pp. 1895-1095, 2013.

[92] P. Muñoz, D. Laselva, R. Barco, P. Mogensen, "Adjustment of mobility parameters for traffic steering in multi-RAT multi-layer," *EURASIP Journal on Wireless Communications and Networking 2013:133,* 2013.

[93] M. Sheng, C. Yang, Y. Zhang, J. Li, "Zone-based Load Balancing in LTE Self-Optimizing Networks: A Game Theoretic," *IEEE Transactions on Vehicular Technology,* vol. 63, no. 6, pp. 2916-2925, 2013.

[94] S. Donghoon, C. Sunghee, "Dynamic power control for balanced data traffic with coverage in femtocell networks," *Wireless Communications and Mobile Computing Conference (IWCMC), 2012 8th International,* pp. 648-653, 27-31 August 2012.

[95] H. Zhang, X. Qiu, L. Meng, X. Zhang, "Design of distributed and autonomic load balancing for self-organization LTE," *IEEE 72nd Vehicular Technology*

Conference Fall (VTC 2010-Fall), pp. 1-5, 6-9 September 2010.

[96] B. Yu, L. Yang, H. Ishii, X. Cheng, "Load Balancing with Antenna Tilt Control in Enhanced Local Area Architecture," *IEEE 79thVehicular Technology Conference (VTC Spring),* pp. 1-6, 2014.

[97] N. Papaoulakis, D. Nikitopoulos, S. Kyriazakos, "Practical radio resource management techniques for increased mobile network performance," *12th IST Mobile and Wireless Communications Summit,* June 2003.

[98] H. Li, S. Habibi, G. Ascheid, "Handover prediction for long-term window scheduling based on SINR maps," *Personal Indoor and Mobile Radio Communications (PIMRC), 2013 IEEE 24th International Symposium on,* pp. 917-921, 8-11 September 2013.

[99] N.A Amirrudin, S.H.S. Ariffin, N.N.N.A Malik, N.E. Ghazali, "User's mobility history-based mobility prediction in LTE femtocells network," *RF and Microwave Conference (RFM), 2013 IEEE International,* pp. 105-110, 9-11 December 2013.

[100] A. Freedman, D. Dilmon, A. Assayag, E. Deutscher, "Prediction based RSS fingerprinting for positioning and optimization in cellular networks," *Electrical & Electronics Engineers in Israel (IEEEI), 2012 IEEE 27th Convention of,* pp. 1-4, 14-17 November 2012.

[101] J. Moon, D. Cho, "Efficient handoff algorithm for inbound mobility in hierarchical macro/femto cell networks," *IEEE Communications Letters,* vol. 13, no. 10, pp. 755-757, October 2009.

[102] J. Moon, D. Cho, "Novel Handoff Decision Algorithm in Hierarchical Macro/Femto-Cell Networks," *Wireless Communications and Networking Conference (WCNC), 2010 IEEE ,* pp. 1-6, 18-21 April 2010.

[103] P. Xu, X. Fang, R. He, Z. Xiang, "An efficient handoff algorithm based on received signal strength and wireless transmission loss in hierarchical cell networks," *Telecommunication Systems,* vol. 52, no. 1, pp. 317-325, January 2013.

[104] 3GPP TSG-RAN WG2 meeting #85 R2-140089, «Mobility performance in real network,» *Qualcomm Incorporation,* 10-14 Februay 2014.

[105] P. Muñoz, "Optimization of Mobility Parameters using Fuzzy Logic and Reinforcement Learning in Self-Organizing Networks," *PhD. Thesis, University of Málaga,* June 2014.

[106] Y. Zhao, B. Le, J.H. Reed, "Chapter 11 Network Support - The Radio Environment Map," *Cognitive Radio Technology, Elsevier,* 2006.

[107] C. Tao, J. van de Beek, B. Sayrac, S. Grimoud, J. Nasreddine, J. Riihijarvi, P. Mahonen, "Design of layered radio environment maps for RAN optimization in

heterogeneous LTE systems," *IEEE 22nd Int. Symp. on Personal Indoor and Mobile Radio Communications,* pp. 172-176, 11-14 September 2011.

[108] H.B. Yilmaz, T. Tugcu, F. Alagöz, S. Bayhan, "Radio environment map as enabler for practical cognitive radio networks," *IEEE Communications Magazine,* vol. 51, no. 12, pp. 162-169, December 2013.

[109] K. E. Brassel, D. Reif, "A procedure to generate Thiessen polygons," *Geographical Analysis,* vol. 11, no. 3, pp. 289-303, 1979.

[110] X. Gelabert, B. Sayrac, S. Ben Jemaa, "A Heuristic Coordination Framework for Self-Optimizing Mechanisms in LTE HetNets," *IEEE Transactions on Vehicular Technology,* vol. 63, no. 3, pp. 1320-1334, March 2014.

[111] T. Takagi, M. Sugeno, "Fuzzy identification of systems and its applications to modeling and control," *IEEE Transactions on Systems, Man and Cybernetics,* Vols. SMC-15, no. 1, pp. 116-132, Febreary 1985.

[112] WINNER II IST project, "D1.1.2. WINNER II channel models. part II. radio channel measurement and analysis results," *WINNER II IST project, Tech. Rep.,* 2007.

[113] T. Sorensen, P. Mogensen, F. Frederiksen, "Extension of the ITU channel models for wideband (OFDM) systems," *Vehicular Technology Conference, 2005. VTC-2005-Fall. 2005 IEEE 62nd,* pp. 392-396, 25-28 September 2005.

[114] C. Bettstetter, C. Wagner, "The spatial node distribution of the random waypoint mobility model," *In Proceedings of German Workshop on Mobile Ad Hoc networks (WMAN),* March 2002.

[115] C. Feng, W. S. A. Au, S. Valaee, Z. Tan, "Received-Signal-Strength-Based Indoor Positioning Using Compressive Sensing," *IEEE Transactions on Mobile Computing,* vol. 11, no. 12, pp. 1983-1993, October 2012.

[116] A. Rai, K.K. Chintalapudi, V.N. Padmanabhan, R. Sen, "Zee: Zero-Effort Crowdsourcing for Indoor Localization," *Proceedings of the 18th annual international conference on Mobile computing and networking,* 2012.

[117] P. V. Nikitin, K. V. S. Rao, "Performance limitations of passive UHF RFID systems," *IEEE Antennas and Propagation Society International Symposium 2006, Albuquerque, NM,* pp. 1011-1014, 9-14 July 2006.

[118] S. Y. Seidel, T. S. Rappaport, «914 MHz path loss prediction models for indoor wireless communications in multifloored buildings,» *IEEE Transactions on Antennas and Propagation,* vol. 40, nº 2, pp. 207-217, August 2002.

[119] European Cooperation in the Field of Scientific and Technical Research, EURO-COST 231, "Digital Mobile Radio Towards Future Generation Systems," *COST 231 Final report.*

[120] M. Sugeno, "An introductory survey of fuzzy control," *Information sciences,* vol. 36, no. 1, pp. 59-83, 1985.

[121] "Fuzzy control programming. Technical report," *International Electrotechnical Commision,* 1997.

[122] J.G. Andrews, H. Claussen, M. Dohler, S. Rangan, M.C. Reed, "Femtocells: Past, Present, and Future," *IEEE Journal on Selected Areas in Communications,* vol. 30, no. 3, pp. 497-508, April 2012.

[123] S. Fortes, A. Aguilar-García, R. Barco, F. Barba, J. Fernández-Luque, A. Fernández-Durán, "Management architecture for location-aware self-organizing LTE/LTE-A small cell networks," *IEEE Communications Magazine,* vol. 53, no. 1, pp. 294-302, January.

[124] 3GPP TR 23.829, "Technical Report 3rd Generation Partnership Project; Technical Specification Group Services and System Aspects; Local IP Access and Selected IP Traffic Offload (LIPA-SIPTO) (Release 10)".